THESIS AND ABSTRACT

Cellular iron governs the host response to malaria infection and vaccination

by Sarah Karin Wideman



St Edmund Hall &

MRC Weatherall Institute of Molecular Medicine,

University of Oxford

Supervised by Hal Drakesmith

Thesis submitted in fulfilment of the requirements for the degree of Doctor of Philosophy, University of Oxford

Hilary Term 2022

Statement of authorship

The majority of the work in this thesis was developed and performed by myself, under the supervision of Prof Hal Draksmith and co-supervision of Prof Simon Draper, at the University of Oxford. The data in Figure 3.4 was acquired and analysed by two other members of the Drakesmith group, Dr Joe Frost and Natasha White. No part of this thesis has been submitted in fulfilment of the requirements for a degree, at this or any other university.

Sarah Karin Wideman

25th April 2022

Acknowledgements

I am incredibly grateful to all the people who gave me the opportunity to pursue this DPhil and that supported me throughout the journey. Here I would like to acknowledge some of those people.

Firstly, **Wellcome** and the **DPhil in Infection, Immunology and Translational Medicine** programme for the financial and administrative support. I am grateful to the directors and administrators for all their hard work and it has been great to be a part of the IITM student community. My rotation supervisors: **Dr Sarah Hollingshead**, **Prof Chris Tang**, **Dr Anne Chauveau**, **Prof Tal Arnon** and all the **Tang and Arnon lab members**, for teaching me and allowing me to be a part of your lab for a short time.

My DPhil supervisor **Prof Hal Drakesmith**, thank you for taking me on, for giving me freedom to pursue my scientific interests and for always making room for fun. **Dr Joe Frost**, you laid the foundation for this project and have provided endless helpful input, I'm very grateful for all of it and I couldn't have done it without you. **Dr Caitlin Naylor**, for being my partner in commiseration and celebration, through various malaria related woes and discoveries. **Ali Preston**, my fellow lab middle-child, looking back now I can't imagine doing this DPhil journey side by side with anyone else and I'm very grateful for the vinos. **Megan Teh,** for being such an inspiration and a joy to work with. **Dr Andy Armitage**, thanks for all your valuable advice and for sharing my passion for lab-admin. All the other amazing Drakesmith lab member that I have been fortunate to cross paths with (in order of appearance): **Kate Wray, Dr Pei Jin Lim, Dr Joao Arezes, David Ahern, Shamsideen Knowlton, Natasha White, Izzy Dale-Harris** - thanks for the spleen crushing, the coffees and the puns.

My co-supervisor **Prof Simon Draper**, thank you for all your insightful advice on malaria vaccines and for always being very generous. I am also very grateful to **Sarah Silk**, **Jordan Barrett** and **Dr Lloyd King** from the Draper lab for letting me pester you with questions and for lending a helping hand whenever I've needed it.

All the staff at the JR BMS animal facility, in particular Roo Bhasin and Jonathon Merrill, thanks for always letting me ask stupid questions, for all the i.v. injections and for the fun banter. I would also like to thank all the staff at the MRC WIMM Flow Cytometry facility for always providing excellent help.

I wouldn't have made it through this DPhil without the support of my amazing friends. All my friends from back home, especially **Annina, Oona, Ulle** and **Goggo**, thank you for always being my saving grace. My friends from the Karolinska Institute, **Anna, Armin, Jack, Lucia, Manon, Sara and Therese**, you are all such inspiring and amazing people and I wouldn't be

here without you. The ‘Brunch Club’, **Athena**, **Johannes**, **Jonny** and **Juli**, thanks for being there to share all the highs and lows of this DPhil. The ‘Oxfam’, **Alina, Alice, Anne, David x 3, Giorgio, Lilian, Lion, Luca, Mathilde, Matthias, Pablo** and **Sara**, thank you for all the fun we’ve had in between the struggles and for making this strange place a home.

I also couldn’t have done this without the support of my family. My **Mom**, who taught me everything that really matters, long before I ever held a pipette. My **Dad** and **Solveig**, for the endless rides to town, homecooked dinners, loads of laundry and all the rest, I’m truly grateful for all of it. My grandparents, **Olle** and **Dolores**, for always supporting me and believing in me. My sister **Petra**, thanks for always lending a listening ear and for being such a great big sister and role model. To the village that raised me, **Gerts**, **Mervi**, **Mia** and **Peter**, thank you for being there for me. Last but not least, **Dr Felix Richter**, you have supported me throughout my DPhil in more ways than I could possibly list here and I am so grateful that I get to go through life with you by my side.

Abstract

Iron deficiency and malaria are two major public health problems with largely overlapping epidemiology, and there is a complex relationship between iron and malaria. Iron deficiency can protect from malaria infection, whereas iron supplementation can increase the risk, and tissue iron loading can disrupt disease tolerance. Immune cells also need iron to support their function and iron deficiency can disrupt immunity. However, it is not known how tolerance or the immune response to malaria infection and vaccination is affected by iron deficiency.

In this thesis, the effects of cellular iron deficiency on the host's response to malaria infection and vaccination were investigated. Recently mosquito transmitted *P. chabaudi* parasites were used to infect mice with a mutation in transferrin receptor 1 ($Tfrc^{Y20H/Y20H}$ mice), which causes decreased cellular iron uptake. We discovered that $Tfrc^{Y20H/Y20H}$ mice had higher *P. chabaudi* parasite burden, but comparable malaria induced anaemia. The disease phenotype of $Tfrc^{Y20H/Y20H}$ mice was also altered, as they had increased weight loss and exacerbated kidney damage, but attenuated liver damage compared to wild-type mice. In addition, disrupted cellular iron uptake had a range of inhibitory effects on the immune response to *P. chabaudi*. The expansion of key effector cells was reduced during the acute stage of infection and the germinal centre response was impaired in $Tfrc^{Y20H/Y20H}$ mice. Moreover, $Tfrc^{Y20H/Y20H}$ lymphocytes cultured *in vitro* had impaired proliferation and effector function, which could be completely rescued by iron supplementation. We also demonstrated that decreased cellular iron uptake weakened the immune response to blood-stage malaria vaccine RH5.1 and that mini-hepcidin induced hypoferremia disrupted the response to experimental liver-stage vaccine AdHu5-*Py*9.

Hence, we have demonstrated for the first time that cellular iron deficiency has the potential to alter malaria disease tolerance and to impair the immune response to malaria infection and vaccination.

Contents

STATEMENT OF AUTHORSHIP I
ACKNOWLEDGEMENTS II
ABSTRACT IV
CONTENTS V
ABBREVIATIONS VIII
1. BACKGROUND AND INTRODUCTION 1
1.1. Iron physiology 1
1.1.1. Systemic iron regulation 1
1.1.2. Cellular iron regulation 4
1.1.3. Iron deficiency 7
1.1.4. Nutritional immunity 8
1.1.5. Iron deficiency and immunity 9
1.1.6. Iron deficiency and vaccination 13
1.2. Malaria 14
1.2.1. *Plasmodium falciparum* life cycle and biology 14
1.2.2. Malaria pathophysiology and treatment 18
1.2.3. Malaria immunity 20
1.2.4. Malaria vaccination 25
1.2.5. Experimental models of malaria 28
1.3. Iron and malaria 30
1.4. Aims and hypothesis 31
2. MATERIALS AND METHODS 33
2.1. Mice and *in vivo* procedures 33
2.1.1. Mouse breeding and husbandry 33
2.1.2. Administration of substances 33
2.1.3. Immunisations 34
2.1.4. *P. chabaudi* infection 34
2.2. Analysis of blood samples 35
2.2.1. Blood processing 35
2.2.2. Serum measurements 36
2.2.3. Enzyme linked immunosorbent assay (ELISA) 36
2.3. Analysis of tissue samples 37
2.3.1. Tissue processing 37
2.3.2. Liver non-haem iron measurement 38
2.3.3. Gene expression analysis by quantitative real time PCR (qRT-PCR) 38
2.3.4. Flow cytometry 39
2.4. *In vitro* experiments 40

2.4.1. *In vitro P. chabaudi* invasion assay 40
2.4.2. *In vitro* culture of primary immune cells 41
2.5. Software and statistical analysis 42
3. MOUSE MODELS OF IRON DEFICIENCY 44
3.1. Introduction 44
3.1.1. Aim 45
3.2. Results 46
3.2.1. *Tfrc*$^{Y20H/Y20H}$ mice have decreased iron levels and microcytosis 46
3.2.2. *Tfrc*$^{Y20H/Y20H}$ mice have a predominantly normal immunophenotype at homeostasis 47
3.2.3. Mini-hepcidin treated mice have hypoferremia and mild anaemia 50
3.2.4. Mini-hepcidin treatment does not substantially alter peripheral immune cell frequencies 51
3.3. Discussion 52
3.3.1. Conclusion 54
4. DECREASED CELLULAR IRON UPTAKE ALTERS MALARIA INFECTION 55
4.1. Introduction 55
4.1.1. Iron bioavailability affects *Plasmodium* growth 55
4.1.2. Iron availability affects blood-stage malaria infection by altering red blood cell physiology 56
4.1.3. Iron and haem affect malaria disease tolerance 58
4.1.4. Aim 60
4.2. Results 60
4.2.1. Decreased cellular iron uptake increases *P. chabaudi* pathogen burden 60
4.2.2. Circulating iron levels do not affect *P. chabaudi* pathogen burden 62
4.2.3. Decreased cellular iron uptake partially alters red blood cell physiology during *P. chabaudi* infection 65
4.2.4. Decreased cellular iron uptake alters *P. chabaudi* disease tolerance 67
4.3. Discussion 71
4.3.1. Conclusion 76
5. DECREASED CELLULAR IRON IMPAIRS THE IMMUNE RESPONSE TO MALARIA 77
5.1. Introduction 77
5.1.1. Iron and the immune response to malaria 77
5.1.2. Aims 78
5.2. Results 79
5.2.1. Decreased cellular iron uptake impairs the immune response to *P. chabaudi* 79
5.2.2. *Tfrc*$^{Y20H/Y20H}$ lymphocyte impairment is caused by cellular iron deficiency and can be rescued by iron supplementation 90
5.3. Discussion 94
5.3.1. Conclusion 99
6. IRON AVAILABILITY ALTERS THE RESPONSE TO MALARIA VACCINATION 101

6.1. Introduction 101
6.1.1. RH5.1 - a leading blood-stage malaria vaccine candidate 102
6.1.2. AdHu5-*Py*9 - an experimental pre-erythrocytic malaria vaccine 103
6.1.3 Aim 105
6.2. Results 106
6.2.1. Decreased cellular iron attenuates the immune response to RH5.1 106
6.2.2. Transient hypoferremia does not affect the immune response to RH5.1 109
6.2.3. Transient hypoferremia impairs the primary response to AdHu5-*Py*9. 113
6.3. Discussion 115
6.3.3. Conclusion 118
7. SUMMARY AND GENERAL DISCUSSION 119
7.1. Summary and outlook 119
7.1.1. Summary of findings 119
7.1.2. Proposed model and open questions 121
7.2. General discussion 124
7.2.1. A brief history of iron and malaria 124
7.2.2. Iron in malaria tolerance and resistance – a high stakes balancing act 126
7.2.3. The potential and perils of correcting iron deficiency to boost immunity 129
7.3. Final statement 131
SUPPLEMENTAL DATA 132
REFERENCES 154

Abbreviations

ALT - alanine aminotransferase

AMA1 - apical membrane antigen-1

ASC – antibody secreting cell

AU – arbitrary units

BCL6 – B cell lymphoma 6

BMP – bone morphogenetic protein

CCL - Chemokine C-C motif ligand

cGAS - Cyclic GMP-AMP synthase

ChAd63 - simian adenovirus 63

CHMI – controlled human malaria infections

CSP - circumsporozoite protein

CXCL - Chemokine C-X-C motif ligand

CXCR - C-X-C motif chemokine receptor

DC – dendritic cell

DMT1 - divalent metal transporter 1

EMP1 - erythrocyte remodelling protein 1

FLT3L - FMS-like tyrosine kinase 3 ligand

Fpn KO - ferroportin knockout

G6PD – glucose-6-phosphatase

GC – germinal centre

G-CSF - granulocyte colony stimulating factor

GFP – green fluorescent protein

GM-CSF – granulocyte macrophage colony stimulating factor

GPI - glycosylphosphatidylinositol

HFE - hereditary hemochromatosis protein

ABBREVIATIONS

i.p. - intraperitoneally

i.v. - intravenously

ICOS - inducible T cell co-stimulator

IFN – interferon

IFU – infectious units

IL - interleukin

iRBC – infected red blood cell

IRE – iron response element

IRF - interferon regulatory factor

IRP – iron regulatory protein

JAK – janus kinase

LDH - lactate dehydrogenase

LMIC - low- and middle-income countries

LN – lymph node

LPS – lipopolysaccharide

M-CSF – macrophage colony stimulating factor

Mo/Mac – monocyte/macrophage

MSP – merozoite surface protein

mTOR - mechanistic target of rapamycin

MVA - modified Vaccinia virus Ankara

MYD88 - myeloid differentiation primary response 88

NAD - nicotinamide adenine dinucleotide phosphate

NADPH - reduced nicotinamide adenine dinucleotide phosphate

NK – natural killer

NLRP3 - NLR family pyrin domain containing 3

NRF2 - Nuclear factor (erythroid-derived 2)-like 2

ABBREVIATIONS

NTBI – non-transferrin bound iron

OD405 - optical density at 405 nm

OXPHOS – oxidative phosphorylation

PCB - poly-r(C)-binding protein

PD-1 – programmed death ligand

Pf - Plasmodium falciparum

Py – Plasmodium yoelii

RAS - radiation attenuated sporozoites

RBC – red blood cells

Redox – reduction-oxidation

RH – reticulocyte-binding protein homologue

RNS – reactive nitrogen species

ROS – reactive oxygen species

RT – room temperature

RTS,S – RTS,S/AS01

s.c. - subcutaneous

SMAD – mothers against decapentaplegic homolog

STAT - signal transducers and activators of transcription

STEAP3 - six-transmembrane epithelial antigen of the prostate 3

TBI - transferrin-bound iron

Tfh – T follicular helper

TfR1 – transferrin receptor 1

TfR2 – transferrin receptor 2

TGF - transforming growth factor

Th1 – T helper 1

TLR – toll-like receptor

ABBREVIATIONS

TNF – tumour necrosis factor

Tr1 – T regulatory type I

TRAP - thrombospondin-related protein

Treg – regulatory T cell

Trf – T regulatory follicular

ZIP - ZRT/IRT-like protein

1. Background and introduction

1.1. Iron physiology

Iron is vital for biochemical and physiological processes, and consequently, iron is essential to almost all living organisms (1). Remarkably, 2% of human genes are predicted to encode iron-proteins, which includes proteins that contain iron ions, haem and iron-sulphur-clusters (2). More than half of all human iron-proteins have catalytic activity and they often function as enzymes, with 6.5% of all human enzymes predicted to be iron dependent (2). Iron's ability to act as an electron donor and acceptor makes it a common co-factor for reduction-oxidation (redox) reactions and oxygen binding (3). Important iron-proteins that perform redox reactions include cytochromes, ribonucleotide reductase and reduced nicotinamide adenine dinucleotide phosphate (NADPH) oxidase (4). Hence, iron-proteins are intricately involved in cellular metabolism and biosynthesis pathways, such as the citric acid cycle, oxidative phosphorylation (OXPHOS), nucleotide synthesis and DNA synthesis. Mitochondria are particularly iron rich organelles because they are the sub-cellular site of iron-sulphur-cluster and haem biogenesis, as well as, ATP generation through the complexes that mediate the electron transport chain and OXPHOS (5). Iron-proteins are also essential for oxygen transport and storage within the human body, as haemoglobin in erythrocytes and myoglobin in myocytes both utilise iron for oxygen binding (4). However, iron is also very reactive, and iron promotes the formation of reactive oxygen species (ROS) and reactive nitrogen species (RNS) that damage lipids, proteins and DNA (3). As a result, humans have tightly regulated systems for iron uptake, transport and storage that act at systemic and cellular levels.

1.1.1. Systemic iron regulation

Despite iron being the fourth most common element on earth, iron bioavailability is generally low because iron is poorly soluble in water when oxygen is present (4). Non-haem dietary iron is mostly ferric iron (Fe^{3+}) and must be converted to ferrous iron (Fe^{2+}) by ferrireductases (e.g. duodenal cytochrome B) to be absorbed in the duodenum (6). Fe^{2+} can be taken up by enterocytes through divalent metal transporter 1 (DMT1) (7). Haem is an important source of

dietary iron and it is absorbed through an unidentified DMT1-independent mechanism (3). Enterocyte haem oxygenases then convert haem into equal parts Fe^{2+}, carbon monoxide and biliverdin. Fe^{2+} is effluxed by ferroportin (encoded by *SLC40A1*) across the basolateral membrane and into circulation, after which the iron is re-converted to Fe^{3+} by ferroxidases (e.g. hephaestin) (8,9). Ferroportin is the only known cellular iron exporter in mammals. In the blood, transferrin chaperones Fe^{3+} until it is utilised by cells or deposited in the liver, which is the main storage site for excess iron (4).

The majority of an individual's daily systemic iron requirements are not met by dietary iron uptake (1-2 mg/day), but rather by iron recycling (20-25 mg/day) (4) (Figure 1.1A). Liver Kupffer cells and spleen red pulp macrophages phagocytose old and damaged erythrocytes and recycle haem iron from haemoglobin (10). Under stress conditions, monocytes can also be recruited and differentiated into iron-recycling macrophages (11,12). Damaged, deformed, stressed or aged erythrocytes can be detected by macrophage receptors (e.g. CD36, CD16) that bind ligands on the erythrocyte membrane (e.g. phosphatidyl serine, antibodies) to initiate phagocytosis (10). In addition, CD47 is displayed on intact erythrocytes and it is recognised as a "don't eat me" signal by splenic iron recycling macrophages (13). In response to systemic iron demands, the iron that is recycled by macrophages can either be stored or exported back into circulation by ferroportin (14). Iron excretion from the body is passive (e.g. via sloughing of dead skin cells) and therefore iron homeostasis is entirely controlled by absorption and recycling of iron.

Iron levels are regulated systemically by the iron-regulatory hormone hepcidin (Figure 1.1B). Hepcidin acts by binding directly to the extracellular side of ferroportin, occluding the iron efflux pathway and targeting ferroportin for internalisation and lysosomal degradation (15,16). Through this mechanism, hepcidin decreases both dietary iron absorption and cellular iron export. Hence, an increase in hepcidin leads to decreased serum iron levels and increased iron loading of macrophages and hepatocytes. Hepcidin is mainly produced and secreted by

hepatocytes and its expression is regulated by iron levels, erythropoietic demand and inflammation (4).

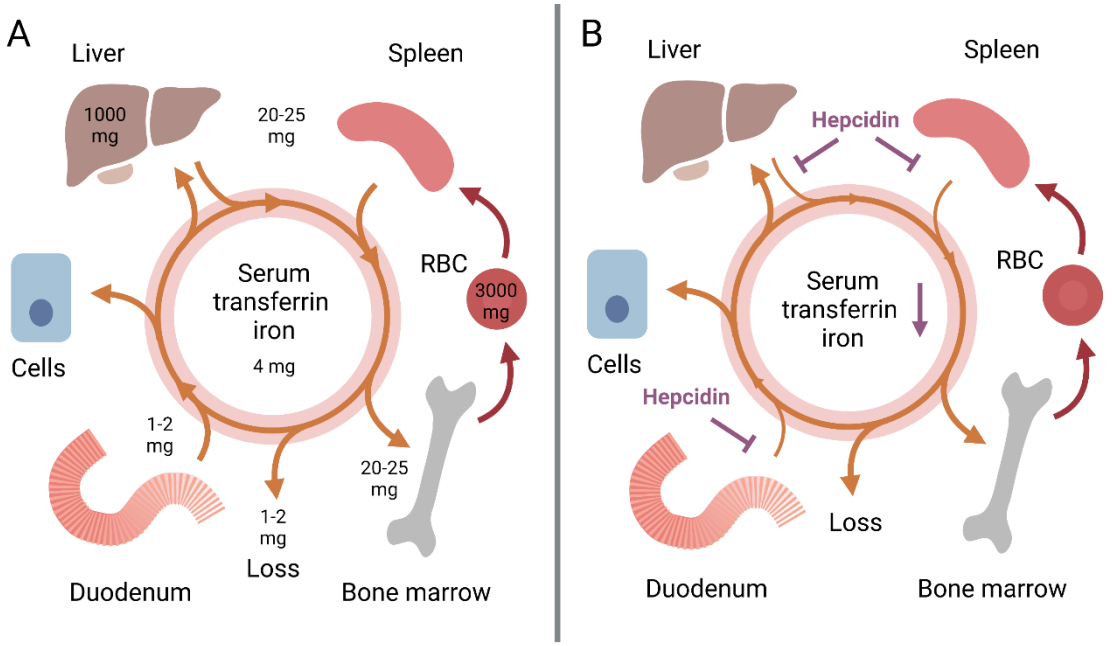


Figure 1.1. **Systemic iron homeostasis and regulation. A**) Dietary iron (~1-2 mg/day) is taken up in the duodenum and transported into circulation, where it is chaperoned by transferrin. This pool of transferrin iron (~4 mg) can be drawn upon by cells to meet their iron needs. Iron is primarily used for erythropoiesis in the bone marrow (~20-25 mg/day) and most iron is found within red blood cells (RBC, 3000 mg). Macrophages in the liver and spleen recycle iron from RBCs (~20-25 mg/day) and excess iron is primarily stored in in the liver (~1000 mg). Passive iron loss is approximately equal to dietary uptake (~1-2 mg/day). **B)** Hepcidin acts to decrease serum iron levels and increase iron loading of hepatocytes and macrophages by preventing the release of stored iron and decreasing dietary uptake.

HAMP (encodes hepcidin) gene expression is primarily modulated through the bone morphogenic protein (BMP) / mothers against decapentaplegic homologue (SMAD) signalling pathway. BMPs signal through a dimeric BMP receptor complex, which phosphorylates SMAD1/5/8 proteins causing them to associate with SAMD4 and translocate to the nucleus (5) (Figure 1.2.). This SMAD complex functions as a transcription factor that binds to BMP responsive elements in the hepcidin promoter (17). Liver sinusoidal endothelial cells produce BMP2 and BMP6, and they are both indispensable for iron homeostasis (3). *BMP2* and *BMP6* gene expression is altered in response to systemic iron availability, but the molecular mechanisms through which iron is sensed to control their expression have not been fully elucidated. However, Lim *et al.* recently showed that high cellular iron levels generate ROS that is sensed by nuclear factor (erythroid-derived 2)-like 2 (NRF2) to induce the expression of

BMP6 (18). In addition, BMP/SMAD signalling in hepatocytes is modulated in response to serum iron levels by transferrin receptor 1 (TfR1), transferrin receptor 2 (TfR2), hereditary hemochromatosis protein (HFE) and the BMP co-receptor hemojuvelin. TfR1 associates with HFE but if serum iron increases, HFE is displaced as TfR1 binds holo-transferrin. This enables HFE to form a complex with TfR2, hemojuvelin and the BMP receptor complex to promote hepcidin transcription (3). BMP6 and iron loading also induce hepatic expression of *TMPRSS6* that encodes matriptase-2, which interacts with the aforementioned complex to inhibit hepcidin expression in a negative feedback loop (19).

Most of the iron within the human body is found in erythrocyte haemoglobin, and therefore, it is unsurprising that erythropoietic demand affects hepcidin. Erythropoietin is synthesised in the kidneys in response to hypoxia and anaemia, and it promotes erythropoiesis by bone marrow erythroblasts (5). Erythropoietin also induces erythroblasts to produce erythroferrone (encoded by *FAM132b*), which in turn, regulates hepcidin production by binding to BMP6 and inhibiting its signalling (20). Thereby, hepcidin expression is decreased so that iron stores are mobilised to be utilised for erythropoiesis.

Hepcidin production is increased in response to pro-inflammatory cytokines, such as IL-6 and IL-22 (21,22). They bind to their cognate receptors to induce signalling through the janus kinase (JAK) / signal transducers and activators of transcription (STAT) pathway, which causes STAT3 to upregulate expression of *HAMP* (23). In response to an infection or injury, this results in a transient decrease in serum iron, which restricts iron availability to some pathogens (see section 1.1.4. Nutritional immunity). However, under conditions of chronic inflammation it can interfere with erythropoiesis and cause anaemia of inflammation (1). In summary, hepcidin regulation is complex and multi-faceted, highlighting the importance of maintaining systemic iron homeostasis.

1.1.2. Cellular iron regulation

On a cellular level, iron homeostasis is maintained by regulating iron uptake, storage and export. Cells primarily acquire iron through receptor-mediated endocytosis of the transferrin–

TfR1 complex (3). Transferrin has two iron binding sites, and can therefore exist in three different iron occupancy states: non-ferric apo-transferrin, mono-ferric transferrin and di-ferric holo-transferrin. TfR1 internalisation is induced by transferrin binding, regardless of its iron occupancy, although transferrin's affinity for TfR1 increases with iron occupancy (24). Transferrin has a very high affinity for iron at neutral pH, however, in the acidic endosome, iron is released from its carrier protein, converted to Fe^{2+} by ferrireductases (e.g. six-transmembrane epithelial antigen of the prostate 3 (STEAP3)), and transported to the cytosol by DMT1 (5). Apo-transferrin and TfR1 are subsequently recycled to the surface of the cell.

In a healthy human, transferrin saturation is between 20-50%, and as a consequence, non-transferrin bound iron (NTBI) levels are very low. However, in the context of haemolysis or iron overload disorders NTBI is present in circulation. In these conditions, trans-membrane NTBI transporters, such as ZRT/IRT-like protein (ZIP) 14, are able to facilitate cellular NTBI uptake from plasma (3). In addition, cells can take up soluble ferritin through ferritin receptors (e.g. scavenger receptor class A member 5) (25). Specialised cells, such as hepatocytes and macrophages, can take up iron in the form of cell-free haemoglobin bound to haptoglobin and haem bound to haemopexin, via scavenger receptors CD163 and CD91, respectively (5).

Inside cells, iron can be stored in a redox safe non-reactive form in ferritin. Ferritin is a polymer made up of ferritin heavy and light chain, where the heavy chain acts as a ferrioxidase (4). To release iron from ferritin, it is degraded and recycled through a specialised form of autophagy termed ferritinophagy (3). There is also an intracellular pool of loosely-bound redox-reactive iron, known as the labile iron pool, which can be drawn upon to synthesise iron-proteins or by the mitochondria (5). This cytosolic Fe^{2+} can be chaperoned and transported to specific subcellular locations by proteins belonging to the poly-r(C)-binding protein (PCB) family (3,26).

Intracellular iron levels are sensed and post-transcriptionally regulated by iron regulatory proteins (IRP) 1 and 2 (5). They bind iron response elements (IRE), a conserved nucleotide structure that forms a hairpin structure in the 3' or 5' untranslated regions of target mRNA, to

promote or inhibit translation. In low iron conditions, IRP1/2 binds to TfR1 and DMT1 mRNA to stabilise it for translation, while binding of ferritin and ferroportin mRNA blocks translation. Hence, cellular iron uptake is increased and iron storage and export are decreased. When iron is abundant, however, iron-sulphur clusters are synthesised within the cell and bind directly to IRP1, which prevents it from binding IREs but allows it to function as a cytosolic aconitase (27). In iron replete cells IRP2 and apo-IRP1 are also targeted for proteasomal degradation by F-box and leucine-rich repeat protein 5, which is stabilised by cytosolic iron (28,29). In this manner, the translation of proteins that mediate cellular iron uptake, storage and export are post-transcriptionally regulated in response to intracellular iron levels.

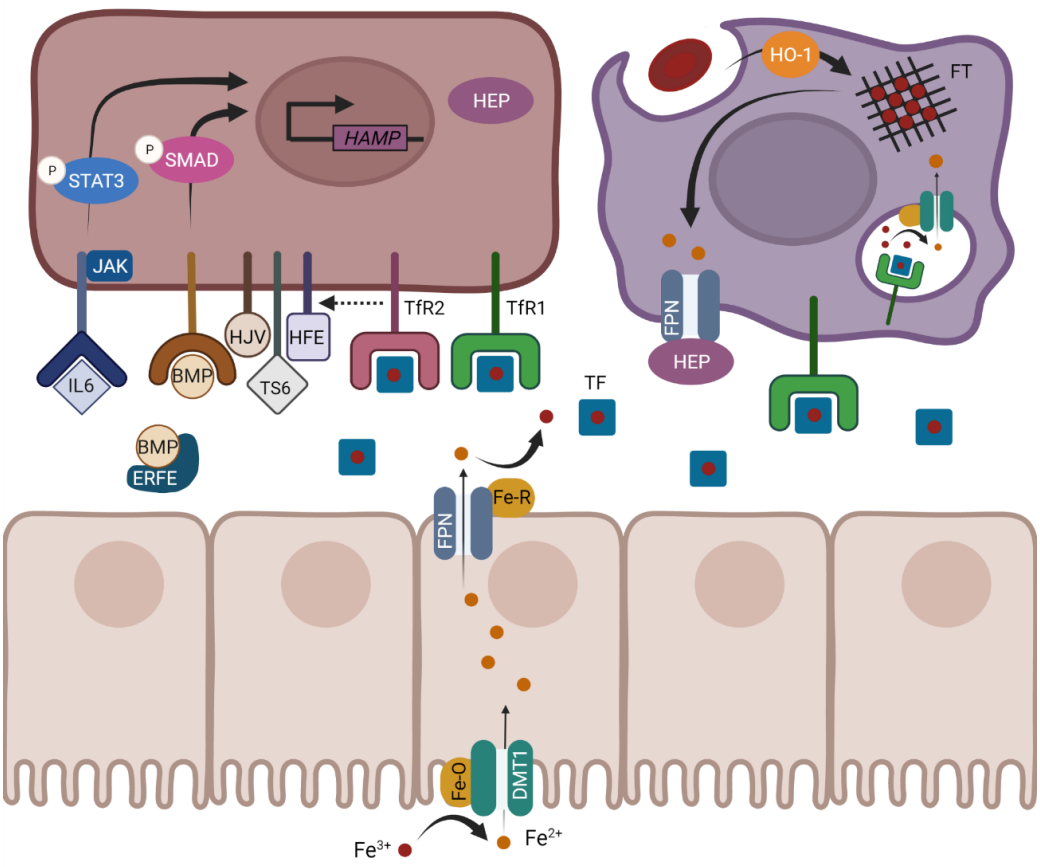


Figure 1.2. **Cellular iron handling and hepcidin regulation.** Ferroxidases (Fe-O) and ferrireductases (Fe-R) convert Fe^{2+} to Fe^{3+} and *vice versa*. Divalent metal transporter 1 (DMT1) and ferroportin (FPN) transport iron across cell membranes. Iron is chaperoned by transferrin (TF) in the blood and cells take up iron via transferrin receptor (TfR) 1 mediated endocytosis. Inside cells iron can be stored in ferritin (FT). Macrophages can recycle iron from erythrocyte derived haem, which is metabolised by haemoxygenase-1. Hepcidin can inhibit ferroportin mediated cellular iron efflux and *HAMP* expression is regulated through BMP/SMAD in response to iron levels and through JAK/STAT in response to inflammation. Serum iron levels are sensed by TfR1 and TfR2, and through interactions with HFE, hemojuvelin (HJV)

and matriptase-2 (TS6) signalling through the BMP receptor is altered. Erythroferrone inhibits hepcidin transcription by sequestering BMP proteins.

1.1.3. Iron deficiency

Human iron homeostasis is usually tightly regulated, but despite this, iron disorders are surprisingly common in humans. Iron deficiency is the most prevalent micronutrient deficiency and there are rare genetic disorders that cause iron deficiency anaemia (30). Diseases that cause iron overload are also common and include hereditary haemochromatosis, thalassemia and chronic liver disease (4). This section will focus on the most common iron disorder, acquired iron deficiency.

When nutritional iron uptake is not sufficient to meet tissue iron requirements or to compensate for physiological or pathological iron losses, body iron stores are depleted and absolute iron deficiency ensues (30). It is commonly caused by blood loss, growth, low iron diet or poor absorption of dietary iron. However, iron deficiency can also occur when iron stores are replete but persistent elevated hepcidin suppresses serum iron to the extent that erythropoietic and tissue iron demands are not met. This functional iron deficiency is generally caused by chronic inflammation, due to infection or long-term illness, such as cancer, severe physical trauma, chronic kidney disease or autoimmunity (30). As most of the iron within the human body is contained within erythrocytes, anaemia is generally the primary and most profound consequence of iron deficiency. The most common symptoms of iron deficiency anaemia are headache, fatigue, paleness and dyspnoea (31). However, iron deficiency also has negative impacts beyond and in the absence of anaemia, and iron deficiency may affect metabolic, myocardial, immune, neuronal and thyroid function (32).

Iron deficiency has a major public health impact, as iron deficiency anaemia affects approximately a sixth of the world's population and it is the fifth leading cause of years lived with disability (33). Iron deficiency anaemia primarily affects children and pre-menopausal women, in particular pregnant women. In addition, people living in low- and middle-income countries (LMIC) are disproportionately affected (30). In children, iron deficiency can impair development and it is likely caused by rapid growth and high infectious disease burden (30,34).

In pre-menopausal women, the menstrual cycle is thought to be the main cause of iron deficiency, although it is unclear whether it is mediated entirely by blood loss or whether hormonal factors contribute (35). During pregnancy, a woman's red blood cell mass needs to increase by 30%, and in addition, the growth of the placenta and the foetus requires iron. This results in greatly increased iron requirements, and 40% of pregnant women become anaemic (30). Anaemia during pregnancy can also affect the foetus, and it is associated with pre-term births, low birth weight and increased neonatal mortality (33).

Iron deficiency is generally diagnosed through a combination of blood markers, including serum/plasma iron, ferritin, soluble TfR1 and transferrin saturation (31). However, diagnosis is complicated by a lack of agreed upon measures and thresholds, as well as, by inflammation that affects serum iron and ferritin measurements (30). Additionally, anaemia can be determined through erythrocyte measurements, such as haemoglobin content and cell volume, and hepcidin measurements can help distinguish between absolute and functional iron deficiency (30). On a population level, preventative measures such as improving access to iron rich food, iron fortification of widely consumed foods, and reducing and preventing infection (e.g. deworming, insecticides) can decrease iron deficiency (31). On an individual level, oral iron supplementation is the first line of treatment but it can cause gastrointestinal side-effects and may not be efficiently absorbed, either due to pre-existing high hepcidin or because oral iron can induce hepcidin (30). Parenteral iron may be better tolerated and absorbed but it requires administration in a clinical setting and is therefore more expensive and complex to implement. In some settings, iron supplementation may also increase the risk of certain infections, including malaria (see section 1.3. Iron and malaria) and diarrhoea (36).

1.1.4. Nutritional immunity

Iron is an essential micronutrient that is needed by humans, fungi, parasites, and bacteria to maintain normal cellular functions, and possibly by viruses to facilitate replication (1). Consequently, humans have developed strategies to prevent pathogens from acquiring iron within the body (37). Hence, iron and haem are tightly chaperoned and sequestered by proteins

such as transferrin, lactoferrin, ferritin, haemopexin, haptoglobin and lipocalin-2, all of which are modulated by inflammation (1). Furthermore, iron is sequestered in macrophages and hepatocytes in response to hepcidin during infection and inflammation. This significantly decreases serum iron levels and restricts iron from extracellular pathogens (37,38). However, the redistribution of iron into macrophages can favour some intracellular pathogens. To restrict iron from intracellular pathogens, the iron transporter natural resistance associated macrophage protein 1 transports iron out of the phagosome (37). Together these mechanisms constitute an innate immune response that attempts to restrict iron from pathogens and form a prototypical example of `nutritional immunity' (37). Consequently, patients with iron overload disorders are more susceptible to infection by siderophilic bacteria and iron deficiency can protect against certain infections, such as malaria (1).

In response to these host-mediated defence mechanisms, many microbes have developed counterstrategies to subvert nutritional immunity and acquire iron within the host. Both extracellular and intracellular microbes often produce iron chelators known as siderophores, and some have developed mechanisms to acquire haem, ferritin iron or transferrin-bound iron (TBI) (37). Microbial proteins involved in iron acquisition are often encoded by genes that are key mediators of virulence, and which have been subject to repeated evolutionary selection (37,39), demonstrating the critical role of iron in host-pathogen relationships.

1.1.5. Iron deficiency and immunity

Like all cells, immune cells require iron to sustain cellular functions, and because immune cells are often highly proliferative and anabolic, they may be particularly sensitive to iron deficiency. It is well known that iron is required to maintain erythropoiesis but it is also required for immune cell development, especially via transferrin mediated iron uptake. Mice with a haematopoietic specific TfR1 knockout die shortly after birth, however, embryonic stem cells can be used to generate chimeric mice with mixed TfR1 deficient and wild-type bone marrow (40,41). TfR1 deficient haematopoietic lymphoid and myeloid precursors fail to expand or produce mature myeloid cells, T cells or B cells (40,41). The development of T cells lacking

TfR1 is blocked at an early double-negative stage of thymocyte development ($CD3^-$ $CD4^-$ $CD8^-$ $CD44^-$ $CD25^+$) and bone marrow B cells likely arrest at the highly proliferative pre-B cell (IgM^+) stage of development (40,42). Additionally, bone marrow neutrophils fail to proliferate and mature under conditions of low serum iron (hypoferremia), leading to a decrease in peripheral neutrophils (43).

Phagocytic innate immune cells, such as neutrophils and macrophages, generate ROS and RNS to kill phagocytosed microbes, in a process termed respiratory burst. Respiratory burst is initiated by the iron-dependent enzyme NADPH oxidase, which sets of a chain reaction of ROS formation inside the phagolysosome (44). In addition, macrophage TLR activation increases iron-dependent mitochondrial ROS formation that promotes microbial killing (45). Neutrophils also produce large quantities of the iron-dependent protein myeloperoxidase, which is stored in granules and can be released to kill extracellular pathogens (44). Consequently, limiting iron availability inhibits ROS formation and decreases the antimicrobial properties of neutrophils (43,46,47). Furthermore, iron-dependent NADPH oxidase activity is required to control leishmaniasis and salmonellosis in mice (48,49).

Tissue macrophages and monocyte-derived macrophages can be polarised to support a wide range of functions, by cytokines or other mediators, and their polarisation has been linked to iron metabolism (50). Iron is processed differently by *in vitro* polarized M1 and M2 macrophages, with M2 macrophages predisposed to import and export iron, and M1 macrophages predisposed to accumulate iron (51,52). Hence, inflammatory (M1) macrophages sequester iron from pathogens and their high intracellular iron levels promote the production of pro-inflammatory cytokines. In contrast, alternatively activated (M2) macrophages express high levels of HO-1 and can release iron to support tissue repair (50). Although it is clear that polarised macrophages process iron differently it is unclear precisely how iron exposure affects polarisation. *In vivo* studies have found that macrophages from both iron deficient (53,54) and iron loaded (55,56) mice are more pro-inflammatory than those from control mice. It is also

important to note that an *in vitro* polarised macrophage is not directly comparable to macrophages found *in vivo*, which exist on a continuum.

Iron is also important for lymphocyte activation and proliferation. TfR1 is upregulated shortly after T cell and B cell activation (57,58), and remarkably, CD8 T cells make 1 million new copies of TfR1 in the first 24 h of activation (59). *In vitro* activated T and B cells that are deprived of iron, via iron chelators, low iron media or anti-TfR1 blocking antibodies, have decreased proliferation and disrupted effector functions (57–62). Accordingly, animal studies have demonstrated that iron deficiency has significant effects on the ability of lymphocytes to respond to immune challenge and to form immune memory. A study by Frost *et al*., showed that the response to vaccination was impaired in mice and piglets with low serum iron and that vaccine responses could be rescued by iron supplementation (59). Notably, transient hypoferremia at the time of ovalbumin immunisation in mice was sufficient to impair the CD8 T cell recall response five weeks later. In addition, they found that hypoferremia severely impaired the T and B cell response to influenza in mice, leading to increased pulmonary inflammation and a lack of neutralising antibodies. Jiang *et al*. additionally found that severe nutritional iron deficiency in mice attenuated B cell responses to both T cell dependent and independent antigens (60). Iron deprivation resulted in smaller germinal centres and depressed antibody titres for several weeks after immunisation. In contrast, iron deficiency has been associated with decreased inflammation and improved outcome in neuroinflammatory disorders (62,63).

It is still not fully understood through which precise mechanisms iron deficiency impairs lymphocyte function, but decreased protein kinase C (PKC) and mechanistic target of rapamycin (mTOR) activity, mitochondrial dysfunction, decreased OXPHOS, stalled cell cycle progression, and impaired histone and DNA demethylation have all been implicated (59–61,64–66). The PKC family of kinases have diverse and essential roles in lymphocyte activation and function, and PKC activity is decreased in T and B cells from iron deficient mice (64). The kinase mTOR is the linchpin of the mTOR signalling pathway, which integrates intracellular

and extracellular cues to regulate cell survival, growth, proliferation and metabolism. Accordingly, mTOR is also involved in cellular iron sensing (67,68). mTOR signalling also plays a key role in immune cell development, activation and differentiation (69,70). Naïve T and B cells are quiescent but upon activation their bioenergetic and anabolic needs increase greatly, and mTOR activity is increased to facilitate nutrient uptake (69). However, *in vitro* activated iron deficient CD8 T cells have diminished mTOR activity (59). Thus, mTOR is a potential sensor and regulator of immune cell function in response to iron deficiency. Although activated T and B cells primarily rely on glycolysis to meet their metabolic needs, both lymphocyte subsets also upregulate OXPHOS upon activation (69,70). This process is likely negatively affected by iron deficiency, as CD8 T cells cultured in low iron media have decreased OXPHOS and depolarised mitochondria, and iron chelator treated CD4 T cells have diminished mitochondrial mass (59,66). Additionally, tetrahydrobiopterin deficient CD4 T cells have decreased iron levels, which causes impaired OXPHOS and mitochondrial function (65). Upon activation, the epigenetic landscape of T cells and B cells is remodelled to enable transcription of genes required for effector functions. Many of the enzymes involved in epigenetic remodelling are iron-dependent, in particular the histone demethylases and DNA demethylases, so that epigenetic remodelling may be sensitive to iron availability (61). Consistent with this, T helper 17 cells cultured in low iron media have decreased H3K27 demethylation and impaired differentiation (61). Moreover, iron chelated B cells have decreased H3K9 demethylation at the cell cycle regulator cyclin E1 promoter, resulting in reduced proliferation (60).

Observational studies on iron deficiency and the immune system in humans are complicated by confounding factors such as general malnutrition, inflammation and infectious disease burden (71). Additionally, there are issues with study design, such as varying methods of detecting and defining of iron deficiency, and with ethical aspects, primarily that it would be unethical to not provide treatment for iron deficiency anaemia once it is diagnosed. Nevertheless, decreased circulating T cell and neutrophil numbers have often been reported in iron deficient individuals

(71). However, the recent discovery of a rare mutation in TfR1provides compelling evidence for the importance of iron in human lymphocyte function (72). The mutation causes decreased cellular iron uptake by impairing the internalisation of TfR1. Patients with this mutation present with mild anaemia and combined immunodeficiency, resulting in increased susceptibility to infection and failure to respond to vaccination. Surprisingly, the patients had predominantly normal circulating lymphocyte numbers, but reduced memory B cell numbers and circulating IgG levels. Furthermore, their T cells and B cells failed to proliferate upon *ex vivo* stimulation, demonstrating a failure to respond to immune challenge.

1.1.6. Iron deficiency and vaccination

Low vaccine efficacy has been reported in populations that have a high prevalence of iron deficiency or chronic inflammation, such as in malnutrition, obesity, autoimmune disease and chronic kidney disease (73). However, there are only a limited number of studies that have tried to investigate the direct effects of iron deficiency on vaccine responses in humans (71,73). A few early observational studies that assessed the response to diphtheria, tetanus and typhoid immunisation found no effect of iron deficiency anaemia (74–76), although these studies were very small (5-24 participants/arm) and likely underpowered. In contrast, a study of over 1,500 Ecuadorian children showed that anaemia is associated with reduced antibody titres to a range of antigens, including tetanus, diphtheria and lipopolysaccharide (LPS) (77). Notably, in this study a higher proportion of anaemic children did not have protective levels of anti-diphtheria toxin antibody, compared to non-anaemic children. A recent study of Kenyan infants receiving routine vaccinations has provided further evidence that iron deficiency affects vaccine responses (78). Stoffel *et al.* found that haemoglobin and anaemia were predictors of poor vaccine responses to diphtheria, pertussis, pneumococcal and measles vaccines, but not *Haemophilus influenzae* type B, tetanus or polio vaccines. Furthermore, iron supplementation improved the response to measles vaccination, in a follow-up trial (78).

Even if these studies point to a role for iron in vaccine responses, it is important to note that anaemia is not equivalent to iron deficiency. While iron deficiency is the most common cause of

anaemia it is not the only one (31), and arguably, serum iron is a better indicator of iron deficiency in the context of immune responses (73). One small but interesting study that examined influenza vaccine responses in elderly people found that non-responders had significantly lower serum iron at the time of vaccination (79). Iron deficient Chinese adolescents and adults that were immunised against measles also had an impaired vaccine response, and in this study there was a significant positive correlation between serum iron and anti-measles antibody levels (60). Similarly, a small study of patients with a rare form of iron-refractory iron deficiency anaemia, which causes hypoferremia, found that the patients had decreased antibody responses to *Haemophilus influenzae* type B and *Streptococcus pneumoniae* vaccination (59). Hence, while there is still much to learn there is growing evidence that iron deficiency can negatively impact vaccine responses, putatively due to an inability to provide sufficient iron to meet the requirements of activated lymphocytes.

1.2. Malaria

Malaria is a serious, potentially fatal, infectious disease that affects a large proportion of the world's population. Remarkable progress has been made in decreasing the number of infections and deaths from malaria in the last two decades, but in 2020, there were still an estimated 241 million clinical cases and 627,000 deaths from malaria around the world (80). Pregnant women and children are most vulnerable to malaria infection and the vast majority of malaria deaths occur in children under the age of five. Regions with high-transmission and high disease burden account for a majority of cases and deaths, and approximately 95% of all deaths occur in the WHO African Region (80).

1.2.1. *Plasmodium falciparum* life cycle and biology

Plasmodium species parasites are part of the apicomplexan family of parasites and are the disease-causing agent of malaria. The parasites are transmitted between hosts by female *Anopheles* mosquitoes, which consume blood meals to sustain egg production (81). Hundreds of species of *Plasmodium* have been described, but only five are known to cause infections in humans: *P. falciparum*, *P. knowlesi*, *P. malariae*, *P. ovale*, and *P. vivax* (82). The main focus of

this section will be *P. falciparum*, as it is the major cause of malaria related disease and death in humans (80). Rodent species *P. chabaudi, P. yoelii* and *P. berghei* will also be referred to as they are often used to experimentally model *P. falciparum* infection (see 1.2.5. Experimental models of malaria).

P. falciparum has a complex life cycle consisting of multiple developmental stages that take place in specific organs within the mosquito and human host (Figure 1.3.). As an *Anopheles* mosquito consumes a blood meal it can ingest sexual stage parasites (a.k.a. gametocytes), which enter the mosquito midgut (81). Subsequently, the male microgamete fuses with the female macrogamete to form a diploid zygote. The zygote matures into a motile ookinete that travels out of the gut lumen to the abdomen, where it develops into a sessile oocyte that undergoes mitosis to form multiple sporozoites. The sporozoites then travel to the mosquito salivary glands from where they have the potential to be transmitted to a human host (81). The development from gametocytes to sporozoites in the mosquito takes approximately two weeks and malaria transmission can be influenced by a number of factors that affect sporozoite development and survival, including temperature and mosquito immunity (81,83).

Sporozoites enter the human host at the dermis and are dependent on gliding motility to exit the dermis and enter the blood stream. Only about half of the inoculated sporozoites manage to enter circulation, the rest remain in the dermis or enter the lymph vessels, and hepatocyte invasion usually occurs within a few hours (82,84). To invade hepatocytes, sporozoites first need to traverse the liver sinusoidal barrier by migrating through endothelial and Kupffer cells in a transient vacuole (82). Subsequent hepatocyte invasion involves the release of specialised secretory organelles, the micronemes and rhoptries, which enable the formation of a moving junction and movement into the hepatocyte. Upon invasion, a parasitophorous vacuole is formed from an invagination in the host cell membrane to create a protective barrier around the parasite. The precise molecular mechanisms that underpin hepatocyte invasion by sporozoites have only been partially defined, but a number of sporozoite proteins and their host ligands have been identified (85). Some notable examples of important sporozoite proteins include

circumsporozoite protein (CSP), thrombospondin-related protein (TRAP) and apical membrane antigen 1 (AMA1).

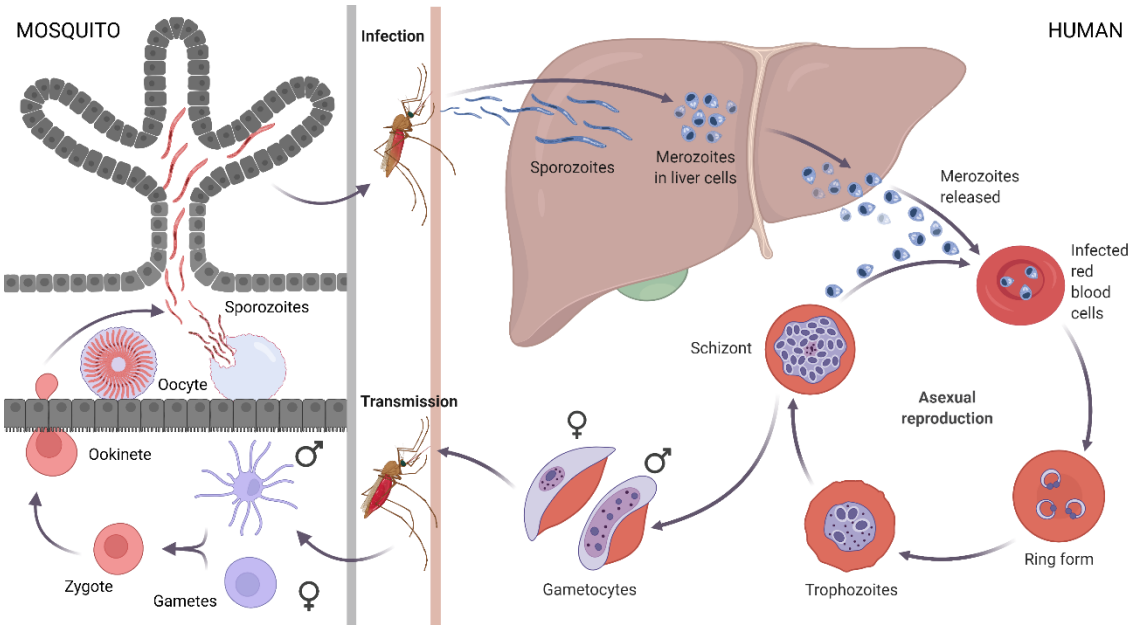


Figure 1.3. **The *Plasmodium falciparum* life cycle. Mosquito:** *P. falciparum* parasites undergo sexual replication inside the Anopheles mosquito midgut, where male and female gametes combine to form a zygote. The zygote develops into an ookinete which crosses the gut endothelium and matures into an oocyte. Sporozoites are released from the mature oocyte and travel to the mosquito salivary glands, from where they can be transmitted to a human host upon a mosquito blood meal. **Human:** Sporozoites enter the human body via the skin and travel to the liver, where they invade hepatocytes. In the liver the parasites undergo asexual replication to produce merozoites, which are released into circulation once they are mature. The merozoites invade red blood cells and undergo multiple cycles of asexual reproduction in the blood. Occasionally, gametocytes form and they can be taken up by feeding Anopheles mosquitos.

Once invasion has been completed, the sporozoites must execute major changes to transition from being motile invasive extracellular parasites to intracellular vacuole contained parasites (85). Moreover, liver stage *Plasmodium* undergoes rapid schizogony to produce tens of thousands of merozoites in just a few days. Hence, biosynthesis is increased, organelles are expanded, and the vacuole membrane is extensively modified to sustain its functions and facilitate host-parasite communication (85). Importantly, the liver stage parasites also directly alter hepatocyte functions to support themselves (85). Late in liver stage development schizonts differentiate into multiple individual merozoites, the parasitophorous vacuoles is broken down, and hepatocyte derived vesicles filled with merozoites, called merosomes, are released into circulation (82).

Merozoite invasion of erythrocytes is a swift multi-stage process that occurs in three stages: attachment, tight junction formation, and invasion (86). The initial attachment involves poorly characterised low affinity interactions between merozoite surface proteins (MSP) and the erythrocyte surface (87). MSP-1 is the largest and most abundant MSP, and it forms complexes with other MSPs to facilitate attachment (88). Subsequently, a higher affinity attachment is formed by erythrocyte binding antigen and reticulocyte binding protein homologue (RH) proteins, which are released from the micronemes (87). These proteins bind to receptors on the erythrocyte surface to enable adhesion and initiate signalling events that facilitate invasion. Additionally, these interactions deform the erythrocyte membrane and re-orient the merozoite so that the apical end is facing the host membrane. This process involves the non-canonical RH protein, RH5, which binds basigin and forms part of a protein complex that is essential for invasion (89,90). Tight junction formation is mediated by AMA1 and the merozoite invades the erythrocyte through the tight junction, propelled by its actinomyosin motor (87). Simultaneously, the rhoptries are released and a parasitophorous vacuole is formed around the merozoite. Invasion transiently induces echinocytosis in the erythrocyte, meaning it becomes smaller and forms spiky protrusions, potentially due to calcium influx (82).

There is considerable variation in parasite invasion ligands between different *Plasmodium* species, which contributes to vertebrate host tropism and erythrocyte tropism. For example, rodent erythrocytes do not express basigin, and thus the indispensable interaction between RH5 and basigin cannot occur, making *P. falciparum* invasion of rodent erythrocytes impossible. Host polymorphism in receptors used for invasion can also affect disease severity in different individuals of the same species (87). A preference for immature erythrocytes is observed in many *Plasmodium* species, including *P. falciparum* (91). It is most prominent in *P. vivax*, which exclusively infects immature red cells, putatively because of its reliance on receptors that are solely expressed on immature cells for invasion (92).

After invading an erythrocyte, the merozoite undergoes schizogony to produce dozens of new merozoites, which egress to infect further cells (82). In this manner, blood stage parasites go

through multiple 48 h cycles of asexual replication, resulting in the destruction of infected erythrocytes. Much like when a sporozoite invades a hepatocyte, the invading merozoite needs to extensively alter its function and remodel the host cell to support itself. To achieve this, it produces specialised proteins and organelles that enable nutrient scavenging, waste exchange and export of proteins across the parasitophorous vesicle membrane into the host cell (93). One of the most important proteins that are involved in erythrocyte remodelling is *P. falciparum* erythrocyte remodelling protein 1 (*Pf*EMP1). It locates to the erythrocyte surface where it facilitates adhesion to host cell receptors, resulting in sequestration within the microvasculature of various organs (82).

One to two weeks after the initiation of blood-stage infection, some parasites will commit to sexual development during schizogony and convert to gametocytes (81). The switch to sexual stage development is orchestrated by the transcription factor AP2-G, which can be spontaneously induced to activate the gametocyte conversion transcriptional programme (94). However, environmental factors such as parasitaemia, nutrient availability, drug treatment and the host immune response can also impact gametocyte formation. Gametocyte maturation occurs over approximately ten days and during this time the gametocytes are sequestered in the bone marrow to avoid clearance by the immune system (81). Mature gametocytes then re-enter circulation where they can be transmitted by mosquitos to re-start the cycle.

1.2.2. Malaria pathophysiology and treatment

Malaria can be classified into three main categories according to the severity of the disease (82,83). In asymptomatic malaria, parasites are present in circulation but the individual has no disease symptoms. This type of infection is the most common and it primarily affects adults in high-transmission areas that have developed immunity. Mild or uncomplicated malaria is characterised by non-life-threatening symptoms such as fever, malaise, headache, chills and anaemia, without any severe organ dysfunction. It is most often observed in young people or in areas with moderate-to-low transmission, i.e. in individuals that only have partial immunity. Severe malaria usually includes the same symptoms as mild malaria, but with the addition of

life-threatening complications, such as severe anaemia, coma, respiratory distress, hypoglycaemia or acute kidney injury. It primarily affects young children in high transmission areas, individuals in low transmission areas, and naïve adults, i.e. individuals that lack immunity.

Exponential parasite growth causes immune activation and many of the mild non-specific symptoms of malaria can be attributed to cytokines produced by the immune system, for example fever, chills, headache and malaise (82). Inflammation also causes endothelial activation that promotes adhesion and sequestration of infected red blood cells (iRBC), which in turn, causes microvascular obstruction. In severe malaria infection this can lead to disrupted metabolism and organ function (95). Severe malaria often manifests differently in children and adults, but it is unclear whether these differences are related to age or to other factors (82).

Hypoglycaemia and acidosis are both common metabolic features of severe malaria. Acidosis is thought to occur due to microvascular obstruction inducing hypoxia, which necessitates anaerobic glycolysis that produces lactic acid (95). Acidosis is intensified by severe anaemia, which is a common feature of malaria in children (95). In addition to erythrocyte destruction by parasites, it is exacerbated by a combination of factors, including a high prevalence of chronic anaemia, suppressed erythropoiesis and de-regulated removal of healthy erythrocytes from circulation (91,96). Liver dysfunction and acute kidney injury primarily occurs in adults, and it is likely caused by a combination of haemolysis, microvascular obstruction and dysregulated inflammation (95,97,98). Both children and adults can develop respiratory distress syndrome, which has a complex aetiology involving microvascular obstruction and acidosis (95). Cerebral malaria is a syndrome in which malaria infection results in neurological involvement with serious consequences such as brain swelling, seizures, coma and death (98). The mechanism of brain injury in malaria is not fully understood but it is thought to occur due to dysregulated cytokine responses, increased endothelial activation and sequestration of iRBCs in the brain.

A number of antimalarial drugs are available for the treatment of malaria. Chloroquine and other quinine antimalarials act by inhibiting the conversion of haem to hemozoin by intra-

erythrocytic *Plasmodium* parasites, causing a toxic build-up of ROS-generating free haem within the parasitophorous vacuole (99). However, *P. falciparum* has acquired mutations that enable it to effectively transport chloroquine out of the parasitophorous vesicle, thus making it resistant to chloroquine. Chloroquine used to be the most commonly used antimalarial, but due to widespread drug resistance the World Health Organisation no longer recommends its use for *P. falciparum* (80). The mechanism of action for artemisinin and its analogues is more poorly defined but the drug is dependent on reactive haem for its activation, and it causes parasite death via oxidative stress (83). Artemisinin resistance is mediated by mutations in the parasite protein Kelch13, which lead to decreased haemoglobin endocytosis and artemisinin activation (100). Because of the increase in drug resistance, artemisinin-based combination therapy (ACT) is now the first-line treatment for *P. falciparum* (80). One artemisinin derivative and one quinine derivative are administered together and this treatment strategy generally has a very high success rate (83). Concerningly, strains that are resistant to ACT have started to emerge in South East Asia (83).

It is important to understand that while efficient treatment for malaria is available, it is not always accessible to those who need it. One study showed that in 2015, 80% of children with malaria across sub-Saharan Africa did not receive ACT (101). Children living in poor or rural areas with limited access to healthcare were less likely to receive treatment (101), highlighting the disparities that underlie access to malaria treatment.

1.2.3. Malaria immunity

The immune response to malaria infection is, by necessity, as multi-faceted as the *Plasmodium* life-cycle. It involves a range of immune cell types, cytokines and chemokines that all need to be activated and inhibited at different times to mount an appropriate immune response. If this process fails, it can result in hyper-parasitaemia or immunopathology (102).

The importance of pre-erythrocytic immune responses in humans is unclear, as repeated infections do not result in sterile pre-erythrocytic immunity and infection-acquired immune responses are primarily directed against asexual blood-stage parasites (103–105). The minimal

immune response induced by pre-erythrocytic infection also means that it is clinically silent and does not cause symptoms like fever (106). However, sterilising pre-erythrocytic immunity can be induced through immunisation, and it is mediated by antibodies that target circulating sporozoites or via killing of infected hepatocytes (107).

The immune system can detect malaria parasites as soon as they enter the body, and sporozoites that end up in skin draining lymph nodes are taken up by DCs that prime CD8 T cells (108). Generally, DCs are a key component of the pre-erythrocytic immune response and DCs in the lymph nodes, liver and spleen can cross-present antigen to activate CD8 T cells (108,109). Hepatocytes can also present parasite antigens on MHC class I and sporozoite infection triggers a type I IFN response in hepatocytes, leading to the recruitment of lymphocytes (106,110). Liver stage immunity induced by vaccines is primarily mediated by CD8 effector T cells that kill infected hepatocytes. They are able to use a diverse, and potentially redundant, set of effector mechanisms, which includes an absolute requirement for IFNγ, and situation dependent involvement of TNFα, perforin, granzyme, and Fas ligand (106,111). Liver resident CD8 T cells can remain in the liver long after parasite exposure and they are indispensable for vaccine-acquired immunity in mice (112). Liver γδT, NK and NKT cells are also thought to contribute as early responders to liver stage infection that produce proinflammatory cytokines, such as TNFα and IFNγ (113). Furthermore, CD4 T cells have a supportive role during liver stage infection and IL-4 secretion supports CD8 T cell responses (114).

The immune response to blood stage infection consists of two distinct but complementary responses. To control exponential parasite growth a cell mediated response is required, whereas a shift to antibody mediated immunity is required to limit recrudescence and enable clearance (115). To prevent immunopathology, it is also vital to strike a balance between pro-inflammatory anti-parasite responses and anti-inflammatory tolerogenic and tissue protective responses (102).

The direct killing mechanisms that facilitate the clearance of *Plasmodium* parasites from circulation include phagocytosis, complement, cytotoxicity and antibodies (102). Phagocytes

can engulf iRBCs and merozoites, which are then killed by the acidic pH of the lysosome or by respiratory burst (116). The scavenger receptor CD36 interacts directly with iRBCs and can facilitate phagocytic clearance of *Plasmodium* parasites (117,118). In addition, iRBCs can be removed from circulation by macrophages through conventional erythrophagocytosis (10). Alternatively, phagocytosis is achieved via opsonisation, mediated by complement or antibodies (102). Complement activation can induce both phagocytosis and lysis of iRBCs. However, complement deficiency only results in a slight delay in the resolution of acute-phase parasitaemia in mice and thus likely only plays a minor role in parasite control (119). In contrast, complement confers protection during re-infection (119), perhaps due to a more decisive contribution of antibody-mediated complement activation. Similarly, platelet-mediated cytotoxic killing of iRBCs has been described (120) but platelet depletion does not affect parasite growth in mice (121). Furthermore, platelet mediated killing in humans is reliant on uptake via the Duffy antigen receptor, which is not present in the majority of people affected by *P. falciparum* (120). The role of cytotoxic lymphocytes, such as CD8 T cells, NK cells and γδT cells, in parasite clearance via direct cytotoxic mechanisms is a contested issue. They can kill infected cells *in vitro* and contribute to parasite clearance *in vivo*, however, their contribution may primarily be cytokine production rather than cytotoxicity (122–126). Antibodies facilitate parasite clearance via multiple mechanisms: neutralising antibodies that prevent invasion, antibody-mediated phagocytosis, antibody-mediated complement activation and antibody dependent cellular inhibition (102). The latter involves secretion of unknown soluble factors that inhibit parasite growth, upon engagement of Fc receptors on monocytes and NK cells (116,127) . Antibodies can also limit severe disease by decreasing sequestration of iRBCs through binding to parasite derived proteins that mediate cytoadherence (128).

Myeloid cells such as monocytes, macrophages, DCs and neutrophils are early responders in blood stage infection. They detect *Plasmodium* derived pathogen associated molecular patterns (e.g. haem, hemozoin & GPI anchors) via pattern recognition receptors (e.g. TLR2/4/9, cGAS & NLRP3) (110). This results in their activation, and subsequently, induction of effector functions

such as cytokine production and phagocytosis. However, these receptors may not be required for parasite control, or there may be substantial redundancy between different receptors, as knock-out mice (e.g. MyD88$^{-/-}$ & NLRP3$^{-/-}$ mice) are able to control parasitaemia (129,130). Early in infection, myeloid cells are mobilised from the bone marrow and infiltrate the spleen, where they differentiate into effector cells (131–133). This is dependent on the production of cytokines that stimulate myelopoiesis, such as G-CSF, GM-CSF and FLT3L, as well as, chemokines that direct migration, such as CCL2 and CCL7 (132,134–137). Interestingly, myelopoiesis in malaria also involves IFNγ signalling, and IFNγ can induce extramedullary myelopoiesis in the spleen of *P. chabaudi* infected mice (137,138).

T helper 1 (Th1) cells and IFNγ are both crucial for the immune response to malaria infection (139–142). Th1 cell polarisation and IFNγ production is promoted by interaction with *Plasmodium* exposed DCs and IL-12 production by myeloid cells (143,144). In turn, Th1 cell derived M-CSF and IFNγ promotes myeloid cell expansion and functions, such as cytokine production and antigen presentation (102,145). In addition to Th1 cells, other helper T cells, CD8 T cells, NKT cells, γδT cells, NK cells, endothelial cells and DCs can also produce IFNγ during malaria infection (113,115). Innate cells, like NK, NKT and γδT cells, are thought to be the main producers of IFNγ early in infection, while NK cells and CD4 T cells are the primary source of IFNγ at the peak of infection (113).

Efficient germinal centre (GC) responses are required to generate high affinity antibodies, and Tfh cells support the activation, differentiation and selection of high affinity GC B cells (146). T follicular helper (Tfh) cells expand during malaria infection and they are indispensable for GC B cell responses in malaria and for sustained control of parasitaemia (147,148). Tfh cells support B cell function through IL-21 production and co-stimulation via inducible T cell co-stimulator (ICOS) (149,150). A combination of transcription factors (e.g. IRF3), cytokines (e.g. IL-6 & IFNγ), and co-stimulatory (e.g. OX40) and inhibitory (e.g. LAG3 & PD-1L) receptors regulate Tfh function in malaria (115). Interestingly, Th1-polarised cytokine responses can

induce the formation of Th1-like Tfh cells, which have impaired B cell helper function (151,152).

In general, short-lived plasmablasts that produce low-affinity IgM antibodies are generated early in infection, whereas memory B cells and long-lived plasma cells that can produce high-affinity IgG antibodies are generated via slower germinal centre reactions (146). B cells are required to clear malaria infection and B cell deficient mice initially control peak parasitaemia but fail to clear the infection (153). The cytokines BAFF, IL-6 and IL-21 promote B cell function during malaria (150,154,155). In addition, production of IL-10 appears to support germinal centre responses and IFNγ promotes class-switching to IgG2 and IgG3 in malaria (156,157). Inefficient and short-lived antibody responses have been observed in malaria infection in both mice and humans, and the lack of sterile immunity to malaria in humans is sometimes attributed to impaired B cell function (105,158,159). There are several factors that potentially contribute to disrupted B cell function in malaria, including altered Tfh differentiation and function, excessive non-specific plasmablast responses, and the formation of atypical memory B cells (158,159). However, there is also evidence of strong long-lived B cell responses to malaria in some studies (158,159), and thus, the effect of *Plasmodium* infection on B cell function remains incompletely understood.

Immunoregulation is essential to preventing severe disease in malaria and anti-inflammatory cytokines such as IL-10, IL-27 and TGF-β have a central role. IL-10 deficient mice infected with *P. chabaudi* experience more severe pathology and higher lethality, however, anti-IL-10 antibody treatment in mice infected with a lethal strain of *P. yoelii* also increases lethality (160,161). Similarly, TGF-β appears to prevent severe pathology but it also inhibits the production of pro-inflammatory cytokines and prevents early parasite control in mice (162,163). Thus, appropriate temporal and spatial expression of anti-inflammatory cytokines is required to control parasitaemia while preventing tissue damage. Regulatory T cells (Tregs) are canonically key regulators of immune tolerance, but they have primarily been associated with poor disease outcomes in malaria (115,164). However, it remains to be seen if Tregs cause pathology in

malaria or if they are simply upregulated in more severe infections. Furthermore, Tregs are not the main producers of IL-10 in malaria, rather IL-10 is produced by T regulatory type I (Tr1) cells and T regulatory follicular (Trf) cells, originating from Th1 and Tfh cells, respectively (115).

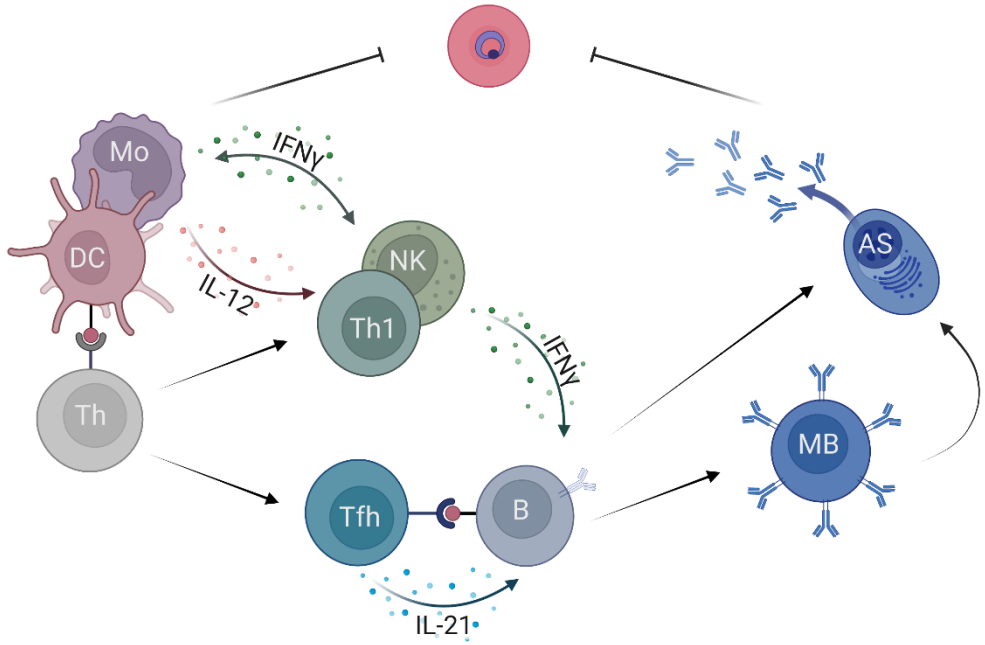


Figure 1.4. **The immune response to blood-stage malaria infection.** Phagocytic cells such as monocytes/macrophages (Mo) and dendritic cells (DC) can clear iRBCs from circulation and secrete pro-inflammatory cytokines (e.g. IL-12) to activate other immune cells. DCs also present malaria antigens to naïve CD4 T cells (Th), which primarily differentiate into T helper 1 (Th1) and T follicular helper (Tfh) cells. Th1 cells and natural killer (NK) cells produce interferon γ (IFNγ), which promotes the effector functions of phagocytic cells and B cells. Tfh cells promote the activation, differentiation and selection of high affinity GC B cells, through direct interactions and cytokine secretion (e.g. IL-21). Activated B cells (B) can differentiate into plasmablast (AS) or enter germinal centres. Germinal centre responses generate plasma cells (AS) and memory B cells (MB) that can produce high-affinity antibody, which promotes parasite clearance.

1.2.4. Malaria vaccination

Efficient immunisation against malaria is sorely needed, but has proven difficult to achieve. Despite more than 50 years of research, only one vaccine has reached the market, the recently approved RTS,S/AS01 vaccine (RTS,S). RTS,S induces immune responses against *Plasmodium falciparum* CSP (*Pf*CSP), generating sporozoite-targeting antibodies. The RTS,S, antigen consist of multiple repeats of the central and C-terminal regions of *Pf*CSP, fused to the hepatitis B surface antigen, which together form a virus-like particle. It is administered together with

AS01, a strong liposome adjuvant that includes immune enhancers MLP and QS21 and induces strong antibody responses in humans (107,165). It contains both B cell and T cell epitopes but immunity is primarily mediated by antibodies. However, RTS,S is not a very efficient vaccine, and four doses are required to achieve a 39% reduction in infections and a 29% reduction in severe disease over a median 48 month follow-up period (166). This can be compared to the Malaria Vaccine Technology Roadmap 2015 goal of >50% efficacy lasting longer than one year, and the 2030 goal of 75% efficacy lasting over two years (167). Although this vaccine and its implementation by the WHO is a major breakthrough, which will reduce loss of life due to malaria infection, it is clear that more efficient vaccines are still needed.

Malaria vaccines have generally been designed to target specific aspects of the *Plasmodium* life cycle. However, to completely prevent infection a multi-antigen vaccination strategy, targeting more than one stage, may ultimately be required. Most vaccine candidates (including RTS,S) are pre-erythrocytic vaccines and aim to prevent sporozoite invasion and/or to kill infected hepatocytes (107). A multitude of pre-erythrocytic subunit vaccines, utilising different vaccine platforms have been developed and trialled. R21 is a candidate malaria vaccine, which aims to improve on RTS,S by increasing the ratio of *Pf*CSP to HbS displayed on the viral particle (168). In a recent Phase IIb clinical trial in children in Burkina Faso the R21 vaccine, given together with Matrix-M adjuvant, showed an efficacy of 77%, one year after immunisation (169). This is a considerable improvement on RTS,S and may hold promise. However, it is important to note that the participants were fully immunised shortly before the high-transmission wet season and much of the follow-up took place during the malaria-free dry season. Consequently, it is unclear how the vaccine will fare in a region with year-round malaria transmission. It will also be necessary to do a side by side comparison with RTS,S to really compare the two vaccines. Vaccine candidates that utilise replication deficient viral vectors for vaccine delivery have also shown some promise in clinical trials (107). They generally induce quite strong CD8 T cell responses, and as such, they are ideal liver stage malaria vaccines. Researchers are also trying to devise strategies to stimulate resident memory T cells in the liver, through heterologous vector

and route of administration prime-boost strategies (112). The most advanced is an adenoviral vaccine expressing multiple *P. falciparum* epitopes, simian adenovirus 63 (ChAd63) ME-TRAP, although it recently failed to provide protection in a phase IIb trial in infants (170). However, the success of the adenoviral vectored ChAdOx1-S COVID-19 vaccine is likely to fuel further research and trials of viral vectored malaria vaccines.

A different type of pre-erythrocytic vaccine is whole sporozoite vaccines. The earliest malaria vaccines utilized live radiation attenuated sporozoites (RAS), which can infect hepatocytes but arrest at the liver stage (171). In pre-clinical and controlled human malaria infection (CHMI) settings, these vaccines can provide high-level sterile protection against infection. Immunity is primarily mediated via cytotoxic CD8 T cells, in particular liver resident CD8 T cells (172), but γδT cells and antibodies against *Pf*CSP likely also contribute (107). However, recent studies have shown that existing RAS vaccines may not be as protective in malaria-experienced individuals (173,174), and as of yet, no trials have been carried out in infants in malaria endemic regions. Genetically attenuated sporozoites and sporozoites administered together with antimalarials have also been used as whole sporozoite vaccines. Both approaches enable later parasite arrest (late liver-stage or early blood-stage) and consequently have the potential to induce more antigenically diverse immune responses (107). Pre-clinical and early clinical studies show promise, however, further studies are needed to confirm whether they will be more effective than RAS.

Pre-erythrocytic vaccines against malaria must be almost completely effective, as any parasites that escape from the liver, can still replicate exponentially in the blood and cause disease. For this reason, blood-stage vaccines that target the disease-causing stage of infection are beneficial. Blood-stage vaccines target merozoites or aim to prevent RBC invasion, and most candidate vaccines have focused on antigens that are targeted by infection-acquired antibodies (e.g. *Pf*AMA-1) (107). However, there are multiple challenges to this approach and it has been questioned because infection-acquired immunity does not provide sterile immunity or prevent malaria transmission (175). One challenge consists of the fact that merozoites are only exposed

in the bloodstream for a very short time and RBC invasion occurs in a matter of seconds (87). Consequently, a very high amount of high-quality antibody is required to prevent disease. Perhaps most importantly, there is high antigenic polymorphism and redundancy in merozoite and invasion proteins (107). To circumvent some of these issues, new antigens that are not subject to antigenic variation and redundancy have been identified. One such vaccine candidate is RH5.1 which is the first blood stage vaccine to reduce blood-stage parasite growth in a CHMI trial (176).

Transmission blocking vaccines (TBV) target gametocytes or one of the later mosquito stages. These vaccines are designed to prevent malaria transmission from vaccinated individuals, but do not prevent them from being infected or developing disease, if they are exposed to malaria (107). The aim is therefore to eradicate malaria from a community by generating herd immunity through mass-vaccination (177). Even so, TBV would likely need to be used together with other malaria vaccines or eradication measures (e.g. insecticides). The current leading vaccine candidates target proteins expressed on the surface of gametes, zygotes and/or ookinetes, including Pfs25, Pfs28, Pfs48/45 and Pfs230 (107,177). An advantage of TBV is that surface antigens on mosquito stage parasites are usually far more conserved, compared to other stages, as they are not subject to the same level of selective pressure by the human immune system (177). However, high antibody levels are required to ensure ingestion by the mosquito, and in early clinical trials transmission blocking vaccines have struggled with poor immunogenicity and suboptimal adjuvants. As a consequence, only one TBV has progressed to Phase II clinical trials (Pfs230) (177).

1.2.5. Experimental models of malaria

There are only a few experimental models available to study human malaria infection. *P. falciparum* can easily be cultured *in vitro* and this system has been used extensively. However, it does not enable the direct study of complex host-parasite interactions or of malaria vaccination (178). The use of animal models is complicated by the stringent host tropism of different *Plasmodium* species, and *P. falciparum* can only be used in host species such as

chimpanzees and New World monkeys (178). An alternative to animal models is CHMI, where subjects are intentionally infected with malaria in an experimental setting (179). Although both of these approaches continue to produce invaluable insights, their use is limited by the complex ethical, safety and logistical issues involved, as well as by financial constraints.

As a consequence, the most prevalent experimental models of malaria are rodent species of *Plasmodium,* where the most commonly used species are *P. chabaudi, P. yoelii* and *P. berghei.* They each replicate some, but not all, aspects of *P. falciparum* infection in humans (Table 1.2.1) (180). In addition, there are several strains of each of species, which have varying severity, organ involvement and immune responses (180). Furthermore, different inbred mouse strains have different susceptibility to infection. The use of mouse models for malaria research has been somewhat controversial, as some argue that they do not mimic human pathology closely enough to be useful (181). Meanwhile, others have argued that it is the only widely available model and that many discoveries initially made in mice have later been confirmed in humans (181). The truth likely lies somewhere in the middle, and while mouse models of malaria continue to be widely used, findings should be used to inform further studies in humans rather than directly applied.

Table 1.2.1. **Differences and similarities in the life cycle, biology and clinical presentation of human and murine *Plasmodium* species.**

Species	**Liver stage (days)**	**Blood Stage (h/cycle)**	**Synch-ronous**	**Seques-tration**	**Reticulo-cyte preference**	**Cerebral malaria**
P. falciparum	~7	48	Y	Y	Y	Y
P. chabaudi	~2	24	Y	Y	N	N
P. yoelii	~2	24	N	N	Y	N
P. berghei	~2	24	N	N	Y	Y

To enable the study of blood-stage malaria infection in mouse models, parasites have generally been maintained through serial blood passage of iRBCs. However, serial blood passage alters parasite gene expression, resulting in increased *P. chabaudi* virulence, whereas mosquito transmission resets gene expression, resulting in decreased virulence (182). Consequently, mice

infected by recently mosquito transmitted *P. chabaudi* have less severe disease symptoms and mount a more efficient immune response to infection (182). Considering that vector transmission affects the host's immune response to malaria, it is preferable to use sporozoites or recently mosquito transmitted iRBCs for immunological malaria studies in mice.

1.3. Iron and malaria

There is an intricate and complex relationship between iron and malaria. Both iron deficiency and malaria are major public health problems and they have a largely overlapping epidemiology (33,80). In part, because malaria is a major cause of iron deficiency in malaria endemic regions (183). Iron deficiency has been postulated as a protective factor in malaria while iron supplementation may be a risk factor (184).

There is a range of evidence indicating that iron deficiency can protect from malaria infection. Iron-chelating agents (e.g. desferrioxamine) can inhibit *P. falciparum* growth *in vitro* and in mice (185,186), indicating that the parasites are dependent on iron. However, iron chelators do not protect humans from malaria (187). Furthermore, nutritional iron deficiency has been associated with lower parasitaemia and improved survival in *P. yoelii, P. chabaudi* and *P. berghei* infected mice (188–190). Several observational studies in humans have also found an association between iron deficiency and decreased malaria risk. A cross-sectional study of children in Kenya found that the incidence of clinical malaria was lower among iron deficient children, and that plasma ferritin was associated with malaria incidence (191). In addition, two longitudinal studies in Tanzania and Malawi showed that iron deficiency decreased the incidence of parasitaemia and clinical malaria (192,193). Strikingly, mortality from malaria was also lower in iron deficient children in the high-transmission setting of the Tanzanian study (192). Furthermore, iron status may affect the risk of malaria in pregnant women but conclusive studies have not yet been performed (184).

Epidemiological connections have been made between iron supplementation and an increased risk of malaria since the 1970s (71). However, major concerns about iron supplementation and

malaria were first raised in 2006, when a large scale placebo controlled clinical trial on Pemba Island was interrupted due to increased mortality from malaria in children receiving oral iron supplements (194). This generated a number of follow up studies and initiated a debate about the safety of iron supplementation in malaria endemic regions that still continues today. Consequently, several Cochrane reviews have sought to determine whether iron supplementation increases the incidence or severity of malaria in children (195–197). The most recent review concluded that iron supplementation is safe and may even be beneficial in areas with malaria prevention and management services (197). Although, it also highlights that iron supplementation may be detrimental in areas where such services are not available. Hence, population level iron supplementation appears to be safe and may even reduce the malaria risk, if it is coupled with appropriate preventative, monitoring and treatment strategies. However, such strategies are not available in many areas and as a consequence iron interventions must be well designed and considered to prevent an increased risk of malaria.

1.4. Aims and hypothesis

Although it is clear that host iron status can affect malaria infection, the mechanisms through which this occurs remain poorly defined. Previous studies of iron deficiency and malaria have mainly focused on how anaemia and altered RBC phenotypes affect *Plasmodium* growth (91). There is some research indicating that extra-erythrocytic iron sources, such as serum iron, can affect *Plasmodium* growth and clear evidence that iron loading of tissues can disrupt malaria tolerance (91). However on the whole, we know very little about how cellular iron deficiency affects the host's response to malaria infection, beyond anaemia. At the same time, we are beginning to understand that iron deficiency can have a significant negative impact on immune responses to infection and vaccination (59,72,73). Yet, the effects of iron deficiency on the immune response to malaria infection and vaccination remain largely unexplored.

We hypothesised that host iron deficiency can impair the immune response to malaria infection and vaccination. Furthermore, we postulated that host cellular iron deficiency may affect

parasite growth or host tolerance. In the following chapters, we address these hypotheses by focussing on four main objectives:

1. Establish models to study host cellular iron deficiency in the absence of (severe) anaemia

2. Assess the effects of decreased cellular iron on the course and severity of malaria infection

3. Determine how decreased cellular iron affects the immune response to malaria

4. Investigate the effects of decreased cellular iron on malaria vaccine immunogenicity

Malaria remains a major cause of childhood mortality and both iron deficiency and malaria are leading global causes of disability (80,198). By gaining a greater understanding of the complex relationship between host iron status and malaria, we may be able to improve or identify new treatment strategies. Furthermore, in order to improve malaria vaccine efficacy it is important to understand how host factors like iron deficiency affect malaria vaccine immunogenicity.

2. Materials and methods

2.1. Mice and *in vivo* procedures

2.1.1. Mouse breeding and husbandry

All animal experiments were approved by the University of Oxford Animal Welfare and Ethical Review Board and performed in accordance with the U.K. Animals (Scientific Procedures) Act 1986. Wild-type BALB/cOlaHsd and C57BL/6JOlaHsd mice were purchased from Envigo. *Tfrc*$^{Y20H/Y20H}$ mice were kindly provided by Professor Raif Geha, Boston Children's Hospital/ Harvard Medical School, and were generated as previously described (72). They were bred at the University of Oxford by crossing homozygotes.

The mice were housed in individually ventilated cages under specific pathogen free conditions, fed standard chow *ad libitum* (SDS Dietex Services, diet 801161), and housed under natural light conditions (light 07:00–19:00, dark 19:00–07:00). Age matched, 6-13 week-old, female mice were used for all experiments, unless indicated otherwise. All animals were euthanised through suffocation by rising carbon dioxide concentrations, and death was confirmed by cervical dislocation.

2.1.2. Administration of substances

A previously described mini-hepcidin peptide PR73 (da-TH-Dpa-bhPro-RCR-bhPhe-Ahx-Ida(Hexadecylamine)-NH2) (199) was administered to suppress serum iron. It was custom synthesised by Chinese Peptide Company. To prepare mini-hepcidin for administration, an appropriate mass was dissolved in 80% ethanol and mixed with 60 mg of the vehicle substance 351 Purebright SL220/ Sunbright DSPE-020CN (NOF). The ethanol was subsequently evaporated using a vacuum concentrator set to 50º C, to produce a gel that was stored for up to 24 h at 4º C. Prior to injection, the mini-hepcidin/vehicle gel was dissolved in water for a final concentration of 1 mM mini-hepcidin. An anti-BMP6 monoclonal blocking antibody was administered to raise serum iron, as previously described (200). Anti-BMP6 IgG (KY1060) or a human IgG4 isotype control was diluted in PBS and administered at a dose of approximately 10

mg/kg body weight. Both substances were administered through intraperitoneal (i.p.) injection of 100 µL.

2.1.3. Immunisations

The RH5.1 and AdHu5-*Py*9 malaria vaccines were kindly provided by Professor Simon Draper, University of Oxford. The RH5.1 protein was produced as previously described (201). Prior to administration, RH5.1 was diluted (to the specified concentration x 2) in PBS and mixed 1:1 with the experimental adjuvant AddaVax (ac-adx-10, InvivoGen). AdHu5-*Py*9 is a recombinant human adenovirus serotype 5 (AdHu5) viral vector expressing the *P. yoelii* CSP CD8 T cell epitope SYVPSAEQI. AdHu5-*Py*9 was diluted in PBS to 5×10^9 infectious units (IFU)/mL, before administration. For both vaccines, the mice were immunised by subcutaneous (s.c.) injection of 100 µL vaccine into the flank. Controls were sham immunised with adjuvant alone (for RH5.1) or PBS (for AdHu5-*Py*9).

2.1.4. *P. chabaudi* infection

Transgenic recently mosquito transmitted *P. chabaudi chabaudi* AS parasites expressing GFP (hereafter referred to as *P. chabaudi*) were used for all malaria experiments in this thesis and were generated as previously described (202,203). The *P. chabaudi* iRBC stabilates were a kind gift from Professor Joanne Thompson, University of Edinburgh/European Malaria Reagent Repository.

Additional stabilates were prepared by propagating the parasites in donor mice. Approximately 100 µL of the stabilate was injected i.p. into a donor mouse, and blood was collected by cardiac puncture once parasitaemia reached 0.5-1%. A second set of donor mice were then infected by i.p. injection of 10^5 donor-derived iRBC. The second donor infection was allowed to proceed until parasitaemia reached 0.5-2%, at which point blood was collected, mixed 1:4 with *Plasmodium* freezing media: RPMI-1640 (R8758, Merck) with 15% FBS (F9665, Merck) and 10 units/mL heparin (H3149, Merck). The new stabilates were snap frozen and stored in liquid nitrogen until needed.

Experimental mice were infected with *P. chabaudi* using iRBCs from a donor mouse, and donor infection was initiated by i.p. injection of ~100 µL stabilate. Donor parasitaemia was monitored and once parasitaemia reached 0.5-2%, donor iRBCs were collected and used for infection. For the subsequent experimental infections, donor mouse blood was diluted into Alsever's solution (A3551, Merck) for a concentration of $1 \cdot 10^6$ iRBC/mL, and 100 µL was injected intravenously (i.v.). Uninfected control mice were injected with 100 µL Alsever's solution. All donor iRBC were exclusively collected during the ascending phase of parasitaemia.

To monitor *P. chabaudi* infection, weight, RBC and parasite measurements were taken regularly at ~9:00 am. Parasitaemia, parasite load and RBC counts were monitored by micro-sampling of blood (2 µL) from the tail vein of infected mice (see 2.3.4. Flow cytometry).

2.2. Analysis of blood samples

2.2.1. Blood processing

Blood was collected by tail vein sampling in live mice or by cardiac puncture immediately after euthanasia. BD Microtainer K2EDTA (BD) blood collection tubes were used for whole blood to prevent clotting. Serum was prepared by centrifugation at 10,000 x g for 5 min in BD Microtainer SST (BD) or Microvette 100 Serum (Sarstedt) collection tubes, and stored in aliquots at -80° C.

Red blood cell parameters, including RBC count, haemoglobin and mean cell volume, were measured in whole blood, using a KX-21N Haematology Analyser (Sysmex).

To prepare immune cells from blood for flow cytometry, 50-100 µL whole blood was diluted in 1 mL tris-buffered ammonium chloride buffer (0.017 M Tris / 0.14 M NH_4Cl, adjusted to pH 7.2 with HCl) to lyse RBCs. The blood was incubated with RBC lysis buffer for 20-30 min at room temperature, washed once in PBS, and resuspended in PBS for flow cytometry staining (see 2.3.4. Flow cytometry).

2.2.2. Serum measurements

Serum iron measurements were performed on an Abbott Architect c16000 automated analyser using a MULTIGENT Iron Kit (Abbott) by Oxford University Hospitals Clinical Biochemistry, or on a Pentra C400 automated analyser using an Iron CP ABX Pentra kit (HORIBA Medical). Serum alanine aminotransferase (ALT), lactate dehydrogenase LDH and creatinine levels were also analysed on a Pentra C400 automated analyser using ALT CP, LDH IFCC CP and Enzymatic Creatinine CP ABX PENTRA kits (HORIBA Medical).

Serum cytokines were measured using a LEGENDplex Mouse Inflammation Panel (740446, BioLegend) bead-based immunoassay, according to the manufacturer's instructions. The protocol was adapted to use half volumes.

2.2.3. Enzyme linked immunosorbent assay (ELISA)

Anti-mouse RH5 IgG standardised ELISAs were performed as previously described (201,204). NUNC MaxiSorp 96-well plates (Thermo Fisher Scientific) were coated with 2 µg/mL RH5.1 protein overnight at 4° C. The plates were washed five times, using PBS with 0.05% Tween-20, between each of the following experimental steps. Blocking in 5% skim milk powder (Marvel) in PBS was performed for 1-1.5 h at room temperature (RT). Experimental serum samples from immunised mice were diluted to fit within the linear portion of the standard curve, added in (50 µL) triplicate to the plate, and incubated at RT for 2-2.5 h. A reference serum sample with a known dilution corresponding to an optical density at 405 nm (OD_{405}) = 1 was used for the standard curve, and as an internal control. A secondary goat-anti-mouse alkaline phosphatase (A3562, Sigma) antibody was added for 1-1.5 h at RT, before developing with 4-nitrophenyl phosphate (N2765, Sigma), according to the manufacturer's instructions. The OD_{405} was read on an ELx800 (GenTek) plate reader and each individual test sample was converted into arbitrary units (AU) using the standard curve and Gen5 software (BioTek).

2.3. Analysis of tissue samples

2.3.1. Tissue processing

Organs were harvested shortly after euthanasia, and livers and spleens were weighed to determine the liver and spleen index. Liver samples were collected and frozen, for non-haem iron measurement. Equally sized liver and spleen pieces were also preserved in RNAlater Stabilization Solution (AM7020, Thermo Fisher Scientific) for gene expression analysis.

Single cell suspensions were prepared for flow cytometry in R10 media: RPMI-1640 with 10% FBS, 2 mM glutamine (G7513, Merck), 1% penicillin-streptomycin (P0781, Merck). Spleens and lymph nodes were mechanically dissociated by passing them through 40 µM cell strainers, to prepare single cell suspensions. Spleens from *P. chabaudi* infected animals were first passed through 70 µM cell strainers and incubated with 120 Kunitz U/mL deoxyribonuclease I (DN25, Merck) for 15 min with agitation, before being passed through 40 µM cell strainers. The cells were pelleted and resuspended in R10 or red blood cell lysis buffer. Splenocyte red blood cells were lysed by incubating with RBC lysis buffer for 3-5 min on ice, and the lysis was stopped by adding RPMI-1640. The cells were washed and resuspended in R10.

For bone marrow, femurs and tibias were collected and cleaned of muscle and connective tissue. The bones were crushed in media with a pestle and mortar, and the resulting cell suspension was passed through a 40 µM cell strainer. Red blood cell lysis was performed as for splenocytes.

Immune cells were isolated from livers by Percoll (17-08-91, GE Healthcare) separation. Livers were perfused with PBS with 10% FBS, and mechanically dissociated using a 70 µM cell strainer to produce a single cell suspension. The liver cells were resuspended in 40% buffered Percoll and centrifuged for 25 min at 2000 rpm with 80% buffered Percoll. After centrifugation, leukocytes were collected by aspirating the interphase. The cells were washed in R10 to remove the Percoll, and red blood cell lysis was performed as for splenocytes.

The cells were counted using a CASY Cell Counter and Analyser (BIOKE) or Precision Count Beads (424902, BioLegend), according to the manufacturers' instructions.

For intracellular cytokine staining, splenocytes were cultured *ex vivo* in R10 at 5-20·10^5 cells/mL, in round-bottom tissue culture treated 96-well plates, with protein transport inhibitor Brefeldin A for 4-6 h at 37° C, 5% CO_2. To activate T cells, 0.5 µg/mL anti-mouse CD3 (100201, BioLegend) was added to splenocytes from *P. chabaudi* infected mice, and 1 µg/mL *Py*9 peptide (SYVPSAEQI, GenScript) was added to splenocytes from AdHu5-*Py*9 immunised mice.

2.3.2. Liver non-haem iron measurement

Liver non-haem iron measurements were performed as previously described (205). Liver pieces were dried at 100º C in a heat block for ~6 h and subsequently weighed. The dried liver pieces were then digested in 10% trichloroacetic acid / 30% hydrochloric acid in water for ~20 hours at 65ºC. A chromogen reagent containing 0.1% bathophenanthrolinedisulphonic acid (Sigma, 146617) / 0.8% thioglycolic acid (Sigma, 88652) / 11% sodium acetate in water was added to the digested liver supernatant. The iron content was determined colourimetrically by measuring the absorbance at 535 nm, and comparing it against a standard curve of serially diluted ammonium ferric citrate (F5879, Merck).

2.3.3. Gene expression analysis by quantitative real time PCR (qRT-PCR)

Total RNA was extracted from homogenised liver and spleen samples using RNeasy Plus Mini Kit (74136, QIAGEN) and cDNA was synthesised using High-Capacity RNA-to-cDNA Kit (4387406, Thermo Fisher Scientific), according to the manufacturers' protocols. Gene expression analysis was performed on 1-5 ng/mL cDNA, using TaqMan Gene Expression Master Mix (4369016, Thermo Fisher Scientific) and the TaqMan Gene Expression Assays (Thermo Fisher Scientific) listed in Table 2.1. The qRT-PCR samples were run on an Applied Biosystems 6500 Fast Real-Time PCR System (Thermo Fisher Scientific) instrument and the relative gene expression was determined by normalising to housekeeping gene *Hprt*, according to the $2^{-\Delta CT}$ method (206).

Table 2.1. **List of TaqMan Gene Expression Assays.**

Protein	Gene	Assay code
Bone morphogenetic protein 6	*Bmp6*	Mm01332882_m1
Erythroferrone	*Fam132b*	Mm00557748_m1
Fibrinogen alpha chain	*Fga*	Mm00802584_m1
Ferritin heavy chain	*Fth1*	Mm00850707_g1
Glutamate-cysteine ligase catalytic subunit	*Gclc*	Mm00802655_m1
Hepcidin	*Hamp1*	Mm04231240_s1
Haem oxygenase 1	*Hmox1*	Mm00516005_m1
Hypoxanthine-guanine phosphoribosyltransferase	*Hprt*	Mm01545399_m1
Interferon γ	*Ifng*	Mm01168134_m1
Interleukin 1β	*Il1b*	Mm00434228_m1
Interleukin 6	*Il6*	Mm99999064_m1
NAD(P)H dehydrogenase, quinone 1	*Nqo1*	Mm01253561_m1
Serum amyloid A1	*Saa1*	Mm00656927_g1
Ferroportin	*Slc40a1*	Mm01254822_m1
Tumour necrosis factor α	*Tnf*	Mm00443258_m1

2.3.4. Flow cytometry

P. chabaudi infection was monitored by flow cytometry, as previously described (203). In brief, 2 µL of blood was diluted in 500 µL Alsever's solution to prevent clotting. The samples were further diluted 1:10 in PBS immediately before acquisition on an Attune NxT Flow Cytometer (Thermo Fisher Scientific). RBCs were defined by forward scatter and side scatter and infected cells were gated using an uninfected control (see Supplementary figure S2A). A fixed volume of each sample was acquired, thus allowing for the enumeration of total RBCs and iRBCs per µL of blood.

For analysis of immune cells, $1\text{-}5 \cdot 10^6$ cells from splenocyte, liver, lymph node or bone marrow single cell suspensions were stained for flow cytometry in round-bottom 96-well plates. The cells were washed in PBS and incubated with TruStain FcX (101319, BioLegend) block and a viability dye: Zombie Aqua/NIR Fixable Viability Kit (42301/5, BioLegend) or LIVE/DEAD Fixable Near-IR Dead Cell Stain Kit (L34975, Thermo Fisher Scientific), for ~10 min at 4° C in the dark. A cocktail of fluorophore conjugated antibodies (see Supplemental data) was added

and the cells were incubated for a further ~20 min. The cells were washed twice in PBS with 2.5% FBS and fixed by incubating with Fixation Buffer (420801, BioLegend) for ~10 min at 4° C in the dark.

Alternatively, the cells were fixed and permeabilised using eBioscience FOXP3/Transcription Factor Staining Buffer Set (00-5523-00, Thermo Fisher Scientific) and transcription factor staining was performed, according to the manufacturer's instructions. Intracellular cytokine or antibody staining was performed after permeabilization with Intracellular Staining Permeabilization Wash Buffer (421002, BioLegend) for ~30 min, according to the manufacturer's protocol. To detect antigen specific CD8 T cells in AdHu5-*Py*9 immunised mice, tetramer staining was performed prior to surface staining. Cells were incubated with PE labelled tetramers specific for the H-2K^{d} restricted *P. yoelii* CSP epitope SYVPSAEQI (NIH Tetramer Core Facility) in PBS with 2% FBS and 0.04% sodium azide, for ~30 min at room temperature.

All samples were acquired on Attune NxT or BD LSR Fortessa X-20 (BD) flow cytometers. Example gating schemes are included as supplementary figures (see Supplementary data).

2.4. *In vitro* experiments

2.4.1. *In vitro P. chabaudi* invasion assay

RBCs from wild-type and *Tfrc*$^{Y20H/Y20H}$ mice, and iRBCs from a *P. chabaudi* infected donor mouse were collected by tail vein blood sampling and cardiac puncture, respectively. The blood was filtered to remove leukocytes, using a cellulose (C6288, Merck) packed column as previously described (207). The uninfected RBCs were fluorescently labelled with 1 µM CellTrace Far Red (C34572, Thermo Fisher Scientific) in PBS for 15 min at 37° C. The cells were washed twice in R10 and resuspended in R10 media with 0.5 mM sodium pyruvate (1136007050, Thermo Fisher Scientific) and 50 µM 2-Mercaptoethanol (31350, Thermo Fisher Scientific). The RBCs were counted using the Attune NxT flow cytometer, and $2{\cdot}10^{7}$ iRBCs and $2{\cdot}10^{7}$ fluorescently labelled wild-type or *Tfrc*$^{Y20H/Y20H}$ RBCs were plated together in the same

well of a 96-well plate. The cells were cultured overnight (~16 h) in a candle jar at 37° C, to allow sufficient time for schizonts to develop and release merozoites. Invasion was measured as iRBC (see 2.3.4. Flow cytometry) and compared by calculating the susceptibility index:

$$SI = \frac{\frac{X\ RBC}{X\ iRBC}}{\frac{Y\ RBC}{Y\ iRBC}}$$

X = fluorescently labelled wild-type or *Tfrc*$^{Y20H/Y20H}$ RBCs

Y = donor derived wild-type RBCs

2.4.2. *In vitro* culture of primary immune cells

B cells were isolated from splenocyte single cell suspensions using EasySep Mouse B Cell Isolation Kit (19854, STEMCELL) and naïve CD4 T cells were isolated from mixed splenocyte lymph node single cell suspensions using EasySep Mouse Naïve CD4+ T Cell Isolation Kit (19765, STEMCELL), according to the manufacturer's instructions. The isolated B and CD4 T cells were fluorescently labelled with 5 µM CellTrace Violet (C34571, Thermo Fisher Scientific) in PBS for 8 min at 37° C, as prescribed by the manufacturer. The labelling was stopped by washing twice in 10 mL R10 media. The cells were counted using a CASY cell counter.

The isolated B cells were cultured at $7.5 \cdot 10^5$ cells/mL in flat-bottom tissue culture treated 96-well plates, in R10 media with 1% MEM amino acids (11130, Thermo Fisher Scientific) and 50 µM 2-Mercaptoethanol. To activate the B cells 2 µg/mL LPS (tlrl-peklps, InvivoGen), 10 ng/mL IL-4 (574302, BioLegend) and 10 ng/mL IL-5 (581502, BioLegend) was added. Ammonium ferric citrate was added at the specified concentrations to modify the iron content of the media. The B cells were cultured for 72 h at 37° C, 5% CO_2 and subsequently analysed by flow cytometry.

The CD4 T cells were plated at $5 \cdot 10^5$ cells/mL in flat-bottom tissue culture treated 96-well plates that had been pre-coated with 5 µg/mL anti-mouse CD3, in R10 media with 50 µM 2-Mercaptoethanol. To activate the CD4 T cells and polarise them to Th1 cells, 1 µg/mL anti-

mouse CD28 (102101, BioLegend), 5 µg/mL anti-mouse IL-4 (504102, BioLegend), 10 ng/mL IL-12 (505201, BioLegend) and 25 U/mL IL-2 (575404, BioLegend) was added. Iron sulfate heptahydrate (F8633, Merck) was added at the specified concentrations to modify the iron content of the media. To improve viability, the media was replaced with fresh media after 48 h of culture. The CD4 T cells were cultured for a total 96 h at 37° C, 5% CO_2, before flow cytometry analysis.

2.5. Software and statistical analysis

All flow cytometry data analysis was performed using FlowJo analysis software (BD). Graphs were generated using GraphPad Prism (GraphPad Software) and illustrations were created with BioRender.com (BioRender). Figure 1.3. was adapted from the "Malaria Transmission Cycle" BioRender template (retrievable from https://app.biorender.com/biorender-templates).

Statistical analysis was also performed in GraphPad Prism and differences were considered statistically different when $p<0.05$ (* $p<0.05$, ** $p<0.01$, *** $p<0.001$, **** $p<0.0001$). Analysis was performed with the baseline assumption that most parameters measured were normally distributed, as most biological parameters have a Gaussian distribution. However, where the visual appearance of data deviated from this assumption, the D'Agostino-Pearson omnibus normality test was used to determine normality/lognormality. For lognormal distributions, the data was log transformed prior to statistical analysis. Where data did not have a normal or lognormal distribution, or too few data points were available for normality testing, a nonparametric test was applied.

A t-tests (or a comparable nonparametric test) was used to compared the means of two groups. As a rule, t-tests were performed with Welch's correction, as it corrects for unequal standard deviations but does not introduce error when standard deviations are equal. Multiple t-tests with multiple test correction (m.t.c.) was performed when two groups were compared across several parameters (e.g. several cell populations). Two-way ANOVA was used for analysis with two categorical variables and one continuous variable (e.g. the effect of iron supplementation and

genotype on T cell proliferation). While the use of two-way ANOVAs for time course (a.k.a. repeated measures) analysis is controversial, it is commonly used within the field of biology and can be useful when used with caution and understanding of what the statistical test. For example, to determine at which (multiple) time points there is a difference between the means of two groups (e.g. parasitaemia). Hence, it has been applied to time course analysis in this thesis.

The applied statistical test, sample size (n) and number of independent experimental repeats (N) is indicated in each figure legend.

3. Mouse models of iron deficiency

3.1. Introduction

Iron homeostasis is a complex process that is regulated on both the systemic and cellular level, and which is affected by nutritional input, growth, infection and other stimuli (1,4,5) . As a consequence, it is difficult to establish murine models of human iron deficiency that replicate all aspects of the human condition. A common approach is to alter the iron content of murine diet, however, our lab has found that there are drawbacks to this approach. Although liver iron stores are quickly depleted in mice fed a low iron diet, circulating iron levels are often maintained for several weeks (59). In contrast, iron deficient infants have strikingly low serum iron levels (34), thus underlining the limitations of diet-based approaches in studying iron deficiency in mice. Because immune cells rely primarily on acquiring circulating iron, low iron diets are not ideal to study acute effects of iron deficiency on the immune system in mice.

Numerous mutant and genetically engineered mouse models of iron deficiency have been identified or generated over the years, which has helped to increase our understanding of iron biology. For example, *Tmprss6* mutant mice with disrupted BMP/SMAD signalling that results in elevated hepcidin levels, and consequently, low serum iron (208). Another example is DMT-1 mutant mice that have disrupted iron uptake and transport, with resulting microcytic anaemia (209). The primary phenotype in most of these mice is a characteristic anaemia (210). However, since *Plasmodium* growth is affected by anaemia (211), these models are sub-optimal for studying malaria. One model that partially circumvent this issue is the $Tfrc^{Y20H/Y20H}$ knock-in mutant mouse, which has a hypomorphic *Tfrc* allele (212). The mutation results in a tyrosine to histidine substitution in the internalisation motif of TfR1, which in turn, reduces internalisation of the TfR1-holotransferrin complex and decreases cellular iron uptake, resulting decreased iron availability within cells. Interestingly, these mice don't present with severe anaemia, likely due to a compensation mechanism observed in erythroid precursor cells. Erythroid precursor cells express high levels of ferrireductase STEAP3, which colocalizes with TfR1 and is presumed to facilitate TfR1 endocytosis (212). In addition, this model of iron deficiency is particularly

interesting as this *Tfrc* mutation results in combined immunodeficiency in both humans and mice (212).

Pharmacological intervention can also be used to model iron deficiency in mice. Substances that mimic the effects of hepcidin or induce endogenous hepcidin expression can be administered to achieve this. For example, small molecule ferroportin inhibitors that prevent the release of stored iron (213), or antisense oligonucleotides that target *Tmprss6* mRNA for degradation *in vivo* to increase endogenous hepcidin expression (214). A benefit of this type of experimental model is that iron deficiency can be temporally controlled and reversed. A drawback of these methods is that they requires continuous administration to maintain iron deficiency. Furthermore, in the short-term it is possible to pharmacologically replicate certain aspects of iron deficiency (e.g. hypoferremia) without significantly affecting other aspects (e.g. anaemia). One class of such iron modulating substances are mini-hepcidins, synthetic peptides, based on the biologically active N-terminal segment of hepcidin, which have been optimised to increase potency, bio-availability and half-life (215). When administered *in vivo*, mini-hepcidin mimics the action of hepcidin and induces hypoferremia by preventing cellular iron export. Hypoferremia peaks approximately 12-24 h post mini-hepcidin administration, and recovers completely within 48 h (216). As such, mini-hepcidin treatment rapidly and transiently decreases circulating iron levels, and thus, cellular iron availability. Mini-hepcidin treatment has also been shown to decrease iron availability sufficiently to impair immune cell function (59).

3.1.1. Aim

In this chapter, we characterise the iron status, RBC parameters and immune compartment in two experimental mouse models of iron deficiency ($Tfrc^{Y20H/Y20H}$ mice and mini-hepcidin treatment), which are used in this thesis. While some of this data has been previously described, we validated the mouse models in our own hands and aim to provide all relevant information that is required to understand subsequent result chapters.

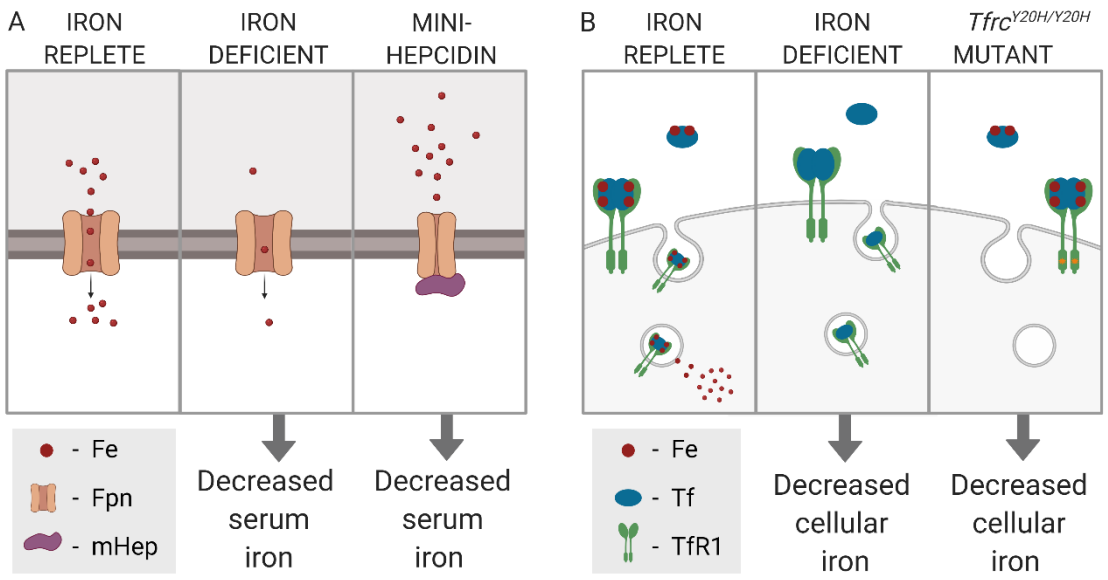


Figure 3.1. **The mechanism of action for mini-hepcidin and *Tfrc*$^{Y20H/Y20H}$ mice. A)** Iron (Fe) is exported from cells by ferroportin (Fpn) to maintain appropriate serum iron levels. In iron deficiency, serum iron levels are low due to an absolute deficiency, but with mini-hepcidin (mHep) treatment iron is locked into cells, resulting in a transient decrease in serum iron. **B)** Transferrin (Tf) bound Fe is acquired by cells via transferrin receptor 1 (TfR1) mediated endocytosis. In iron deficiency this process continues to function but Tf bound iron is scarce, resulting in low cellular iron levels. In *Tfrc*$^{Y20H/Y20H}$ mice, Tf bound Fe is available but TfR internalisation is impaired, leading to decreased cellular iron levels.

3.2. Results

3.2.1. *Tfrc*$^{Y20H/Y20H}$ mice have decreased iron levels and microcytosis

In this thesis, *Tfrc*$^{Y20H/Y20H}$ mice are used as a model of constitutive cellular iron deficiency. Although the strain has previously been described by Jabara et al. (212), we confirmed their results in our animal facility and further characterised the strain. *Tfrc*$^{Y20H/Y20H}$ mice displayed no visual signs of disease and were phenotypically similar to C57BL/6 wild-type mice such as having comparable body weight and spleen index (Figure 3.2A). To determine the effects of the *Tfrc* mutation on systemic iron status, we measured liver and serum iron. We found that *Tfrc*$^{Y20H/Y20H}$ mice had significantly lower liver and serum iron levels compared to wild-type mice (Figure 3.2B). However, their iron levels were only slightly diminished, and are unlikely to result in any meaningful biological impairment (59,217).

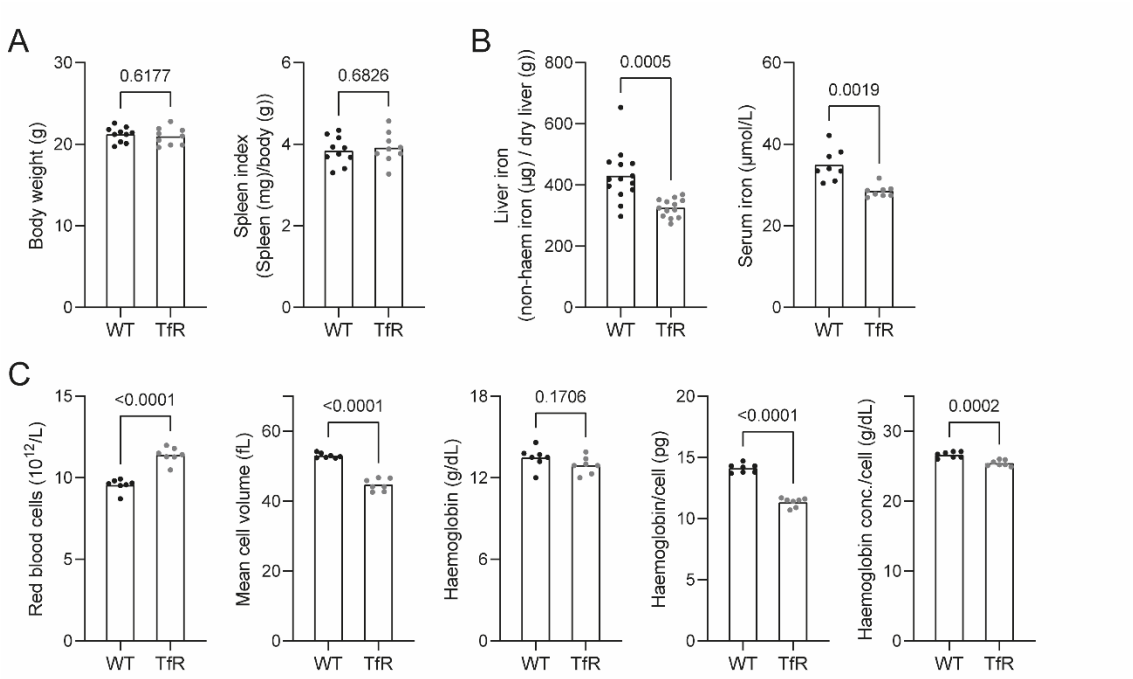


***Figure 3.2. Tfrc$^{Y20H/Y20H}$* mice have decreased iron levels and microcytosis.** The phenotype of untreated, 8–12-week-old, female C57BL/6 (WT) and *Tfrc$^{Y20H/Y20H}$* (TfR) mice was compared. **A)** Body weight and spleen index. **B)** Serum iron and liver iron levels. **C)** Red blood cell parameters. Mean, Welch's t-test, n = 7-14, N = 2.

To assess erythrocyte parameters, wild-type and *Tfrc$^{Y20H/Y20H}$* RBCs were analysed using an automated haematology analyser. *Tfrc$^{Y20H/Y20H}$* mice had an increased number of RBC, which were reduced in size, a typical feature of microcytic anaemia. Blood haemoglobin levels were not significantly different, however, both the per cell haemoglobin content and concentration was reduced in the *Tfrc$^{Y20H/Y20H}$* mice (Figure 3.2C). This suggests that *Tfrc$^{Y20H/Y20H}$* RBCs have lower haemoglobin content, which is compensated for by an increase in RBCs, resulting in normal blood haemoglobin concentrations. Taken together, *Tfrc$^{Y20H/Y20H}$* mice exhibit signs of microcytic and hypochromic RBCs at homeostasis but are not formally anaemic as defined by haemoglobin concentration.

3.2.2. *Tfrc$^{Y20H/Y20H}$* mice have a predominantly normal immunophenotype at homeostasis

As this thesis is focused on studying immune responses, it was of particular interest to characterise the immune compartment in *Tfrc$^{Y20H/Y20H}$* mice at homeostasis.

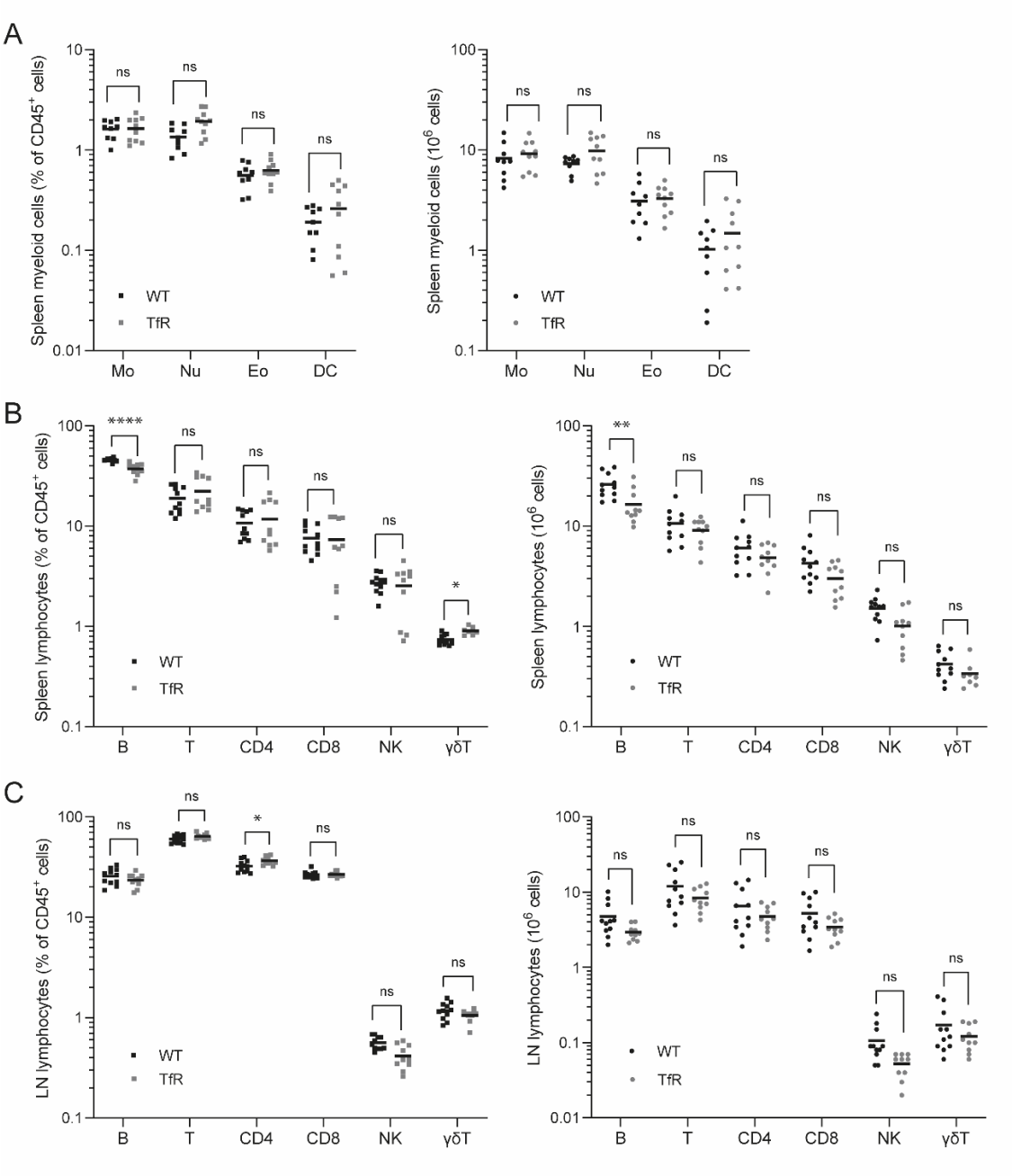


***Figure 3.3. Tfrc$^{Y20H/Y20H}$* mice have a predominantly normal immunophenotype at homeostasis.** The immunophenotype of untreated, 8–12-week-old, female C57BL/6 (WT) and *Tfrc*$^{Y20H/Y20H}$ (TfR) mice was compared. **A)** Spleen myeloid cell proportions and absolute numbers were analysed by flow cytometry, including monocytes/macrophages (Mo), neutrophils (Nu), eosinophils (Eo) and dendritic cells (DC). **B)** Spleen and **C)** lymph node (LN) lymphocyte proportions and numbers, including B cells (B), T cells (T), CD4 T cells (CD4), CD8 T cells (CD8), NK cells (NK) and γδT cells (γδT), were quantified. Mean, multiple t-tests, Holm-Sidak's m.c.t., n = 9-10, N = 2.

Consequently, the frequency of various peripheral immune cell types was analysed by flow cytometry and presented as a percentage of total leukocytes and as absolute numbers. No difference was observed in the frequency of splenic myeloid cells, including

monocytes/macrophages (CD11b^{hi} Ly6G^{-} Siglec-F^{-}), neutrophils (CD11b^{+} Ly6G^{+}), eosinophils (CD11b^{+} Siglec-F^{+}) and dendritic cells (CD11c^{+}) (Figure 3.3A). *Tfrc*$^{Y20H/Y20H}$ mice also had mostly normal frequencies of splenic lymphocytes, including total T cells (TCRβ^{+}), CD4 T cells (TCRβ^{+} CD4^{+}), CD8 T cells (TCRβ^{+} CD8^{+}) and NK cells (NK1.1^{+}) (Figure 3.3B).

Notably, *Tfrc*$^{Y20H/Y20H}$ mice had fewer splenic B cells (B220^{+}) compared to wild-type mice. For γδT cells (TCRγδ^{+}) in the spleen the percentage, but not the absolute number, was higher in the *Tfrc*$^{Y20H/Y20H}$ mice. However, this finding may be an arithmetic artefact resulting from the decrease in B cell numbers, which may disproportionally affect the rare γδT cell population. In the lymph nodes there were also few differences in lymphocyte frequencies between the two genotypes (Figure 3.3C). The only exception was a slight increase in the percentage of CD4 T cells in *Tfrc*$^{Y20H/Y20H}$ mice, which did not translate into an increase in absolute numbers.

To investigate whether the *Tfrc* mutation resulted in altered systemic inflammation, we measured circulating cytokine levels using a flow cytometry based multiplex cytokine assay. There was no difference between wild-type and *Tfrc*$^{Y20H/Y20H}$ mice for any of the measured cytokines (Figure 3.4). Thus, we concluded that homeostatic *Tfrc*$^{Y20H/Y20H}$ mice exhibit no signs of immune abnormalities or inflammation, and are comparable to wild-type mice under steady state conditions.

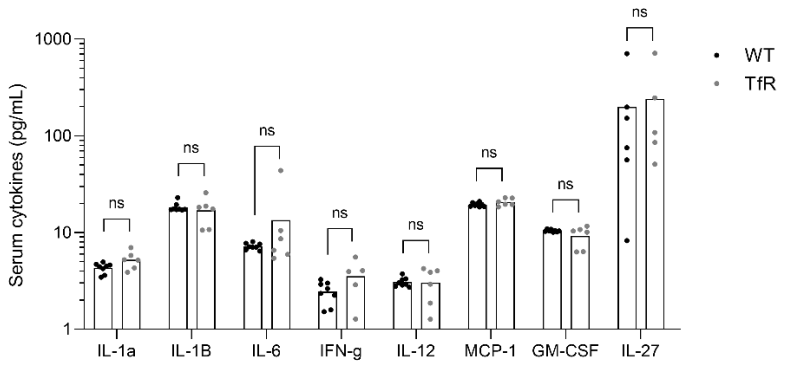


***Figure 3.4. Tfrc*$^{Y20H/Y20H}$ mice have a normal circulating cytokine levels.** Serum cytokine levels were measured in untreated, 8–12-week-old, female C57BL/6 (WT) and *Tfrc*$^{Y20H/Y20H}$ (TfR) mice using a flow cytometry based multiplex cytokine assay. Interleukin (IL)-1α, IL-1β, IL-6, interferon-γ (IFN-g), IL-12, monocyte chemoattractant protein 1 (MCP-1), granulocyte-macrophage colony stimulating factor (GM-CSF) and IL-27. Mean, multiple t-tests, Holm-Sidak's m.c.t., n = 4-6, N = 2.

To understand whether reduced peripheral B cells in the *Tfrc*$^{Y20H/Y20H}$ mice may be the consequence of impaired B cell differentiation, we subsequently analysed bone marrow B cell progenitors by flow cytometry. We observed no difference in the percentage of bone marrow B cells that were immature pro-B cells (CD43^{+}), pre-B cells (CD43^{-} B220^{lo}) or mature recirculating B cells (CD43^{-} B220^{hi}) (Figure 3.5A). Additionally, there was no difference in the frequency of transitional (CD93^{+}) and mature (CD93^{-}) B cells in the spleen (Figure 3.5B). Therefore, it is unlikely that B cell development is disrupted, but rather there appears to be a general B cell deficit in the *Tfrc*$^{Y20H/Y20H}$ mice.

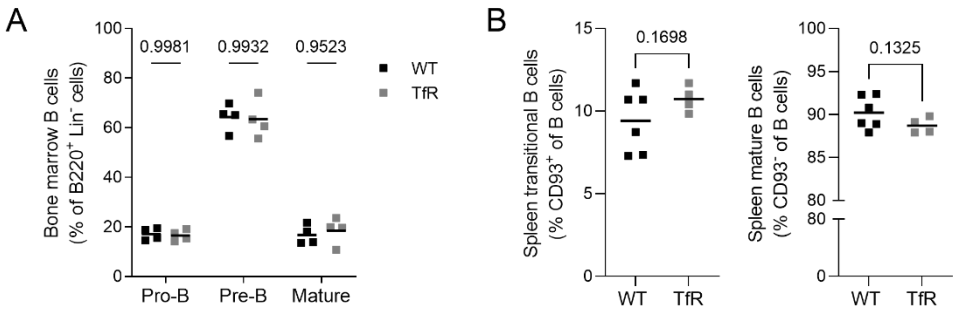


***Figure 3.5*. B cell development is not altered in *Tfrc*$^{Y20H/Y20H}$ mice.**
B cell development was compared in untreated, 8–12-week-old, female C57BL/6 (WT) and *Tfrc*$^{Y20H/Y20H}$ (TfR) mice. **A)** The percentage of bone marrow (BM) B cells that were Pro-B cells (Pro-B), Pre-B cells (Pre-B) and mature recirculating B cells (mature) was analysed by flow cytometry. Mean, two-way ANOVA, Sidak's m.c.t., n = 4, N = 1. **B)** Additionally, the frequency of spleen transitional and mature B cells was measured. Mean, Welch's t-test, n = 4-6, N = 1.

3.2.3. Mini-hepcidin treated mice have hypoferremia and mild anaemia

Mini-hepcidin treatment is used as an inducible and transient model of iron deficiency in this thesis. The efficacy of mini-hepcidin treatment was assessed by administering four daily doses of mini-hepcidin and analysing the iron status of the animals 24 h after the last dose (Figure 3.6A). Mini-hepcidin treated mice had three-fold lower serum iron levels and profoundly suppressed, 200-fold lower, endogenous expression of *Hamp*, the gene encoding hepcidin (Figure 3.6B). Four days of mini-hepcidin treatment was also found to cause mild anaemia (Figure 3.6C). Specifically, mini-hepcidin treated mice had fewer but larger RBCs compared to vehicle treated mice. They also had less total haemoglobin and lower per cell haemoglobin concentration (Figure 3.6C). Altogether, these features are characteristic of mild macrocytic

anaemia, and the increased RBC cell size is likely due to an increase in circulating immature RBCs (i.e. reticulocytes) .

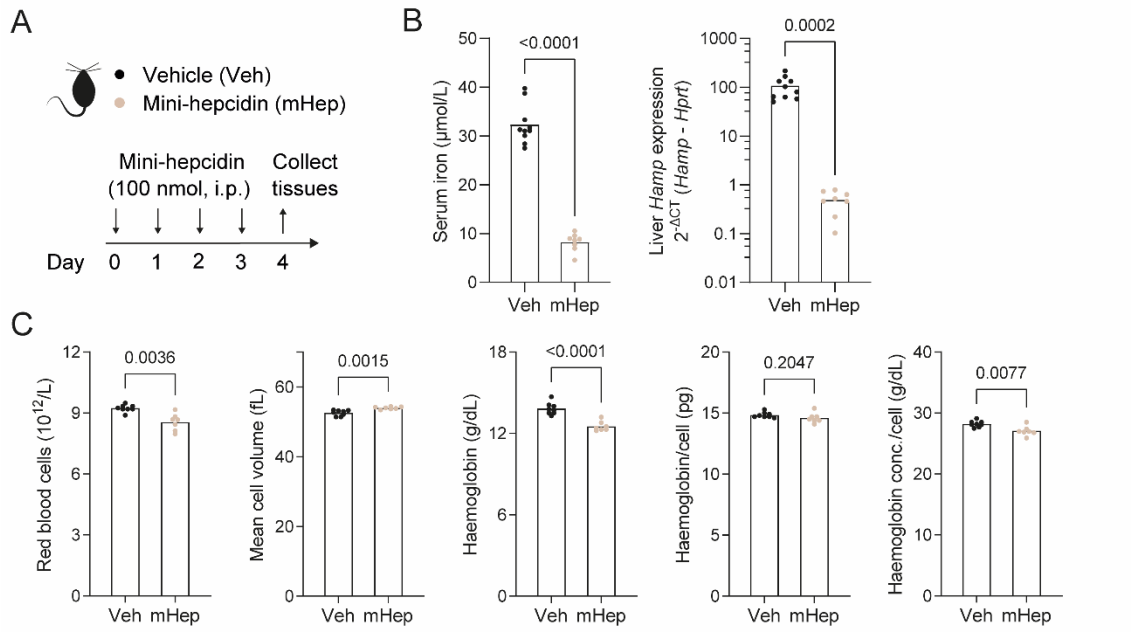


***Figure 3.6*. Mini-hepcidin treatment decreases serum iron and causes mild anaemia. A)** Female C57BL/6 mice were given four, once daily, intraperitoneal (i.p.) injections of 100 nmol mini-hepcidin (mHep) or vehicle (Veh). **B)** Serum iron and liver *Hamp* (encodes hepcidin) gene expression was measured using an automated clinical chemistry analyser and RT-qPCR, respectively. **C)** Red blood cell parameters were analysed using an automated haematology analyser. Mean, Welch's t-test, n = 7-10, N = 1.

3.2.4. Mini-hepcidin treatment does not substantially alter peripheral immune cell frequencies

To determine whether mini-hepcidin treatment alone is sufficient to perturb the composition of the immune system at steady state, the frequency of splenic immune cells was measured in wild-type mice given four doses of mini-hepcidin (as in Figure 3.6A). No differences were observed in the percentage or absolute number of splenic monocytes/macrophages, neutrophils or dendritic cells (Figure 3.7A). Similarly, splenic lymphocyte frequencies, including B cells, T cells and γδT cells, were unperturbed by mini-hepcidin (Figure 3.7B). However, the percentage of splenic eosinophils was reduced after mini-hepcidin treatment (Figure 3.7A). Overall, it appears that mini-hepcidin treatment does not have a substantial effect on peripheral immune cell frequencies at homeostasis.

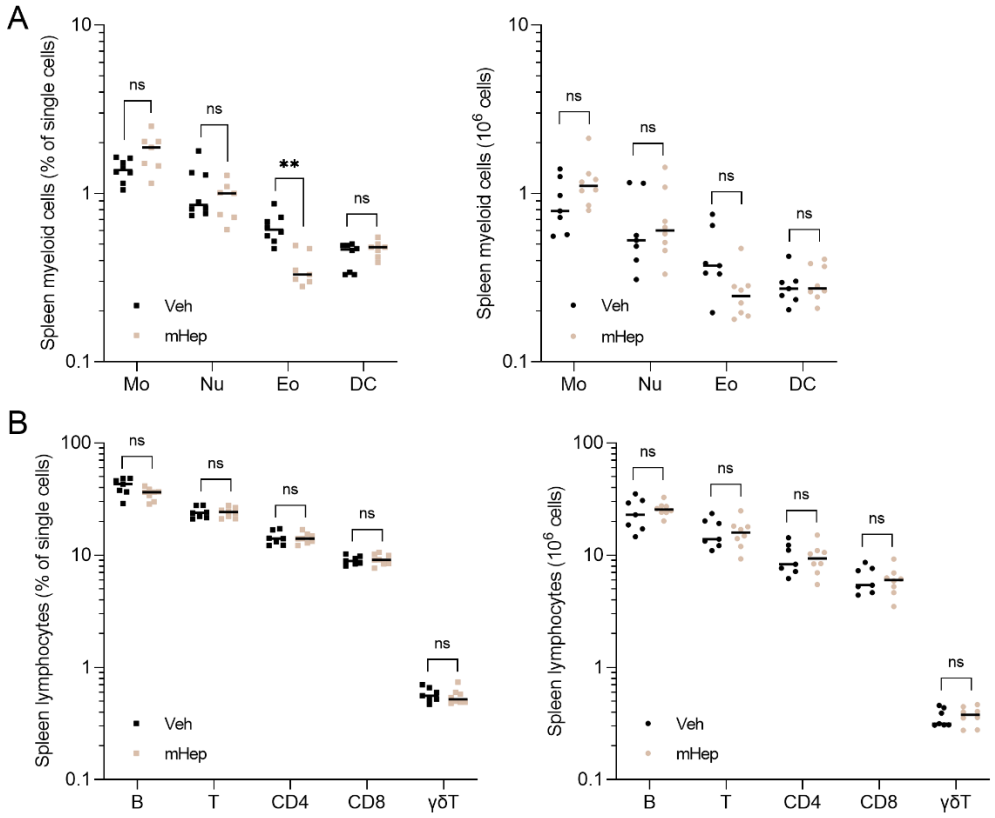


Figure 3.7. **Mini-hepcidin treatment does not substantially alter peripheral immune cell frequencies.** The immunophenotype of female C57BL/6 mice given four, once daily, i.p. injections of 100 nmol mini-hepcidin (mHep) or vehicle only (Veh) was assessed. **A)** Spleen myeloid frequencies were analysed by flow cytometry, including monocytes/macrophages (Mo), neutrophils (Nu), eosinophils (Eo) and dendritic cells (DC). **B)** In addition, spleen lymphocyte frequencies were measured, including B cells (B), T cells (T), CD4 T cells (CD4), CD8 T cells (CD8) and γδT cells (γδT). Mean, multiple t-tests, Holm-Sidak's m.c.t., n = 7-8, N = 1.

3.3. Discussion

In this chapter, two experimental mouse models of iron deficiency were characterised with regards to their iron and immune status. The transgenic *Tfrc*$^{Y20H/Y20H}$ mouse is a useful constitutive model for studying cellular iron deficiency in the absence of severe anaemia. We observed slightly decreased serum and liver iron levels, without evident anaemia, in the *Tfrc*$^{Y20H/Y20H}$ mice. This is in line with previous findings (212) and validates our model. We therefore concluded that the effect of the *Tfrc* mutation on RBCs and their homeostatic production is limited. Additionally, *Tfrc*$^{Y20H/Y20H}$ peripheral immune cell frequencies were predominantly normal at homeostasis. It is known that mice and humans with the *Tfrc*$^{Y20H/Y20H}$ allele have mostly normal blood lymphocyte profiles (212), however, here we expand this

characterisation and show for the first time that this also applies to secondary lymphoid organs and myeloid cells in mice. We did not observe any alterations in the systemic proinflammatory cytokine profile of *Tfrc*$^{Y20H/Y20H}$ mice at homeostasis. However, only a limited number of cytokines was measured and it is possible that other cytokines, e.g. ones that regulate haematopoiesis, chemotaxis or cell survival, are altered. It would be of particular interest to measure factors that regulate B cell development and survival, such as IL-7, BAFF and IL-4.

We found that *Tfrc*$^{Y20H/Y20H}$ mice have fewer peripheral B cells, but no clear B cell developmental defects. Potentially, the reduction in B cells is caused by a general proliferative defect, resulting in fewer B cells at each developmental stage, or by a defect in early B cell development (i.e. before the pro-B cells stage). Alternatively, the reduced B cell numbers could be the result of a decreased response to commensal microbes. This would be in line with the reduction in memory B cell frequencies that have previously been reported in children carrying the *Tfrc*$^{Y20H/Y20H}$ allele (212). To determine the cause would require further in-depth studies which are beyond the scope of this thesis. Whatever the cause, it is worth noting, as the B cell deficiency may be exacerbated under immunological challenge conditions.

Mini-hepcidin treatment is a reversible experimental model of profound hypoferremia (215). Four doses of mini-hepcidin treatment decreases serum iron to comparable levels to those seen in iron deficient Gambian infants and in adults during acute infection (34,38). Additionally, mini-hepcidin treatment caused mild anaemia. Despite this, short-term hypoferremia does not appear to substantially affect peripheral immune cell frequencies in the absence of any immunogenic stimuli. The mini-hepcidin treated mice did, however, have fewer splenic eosinophils, and our group has previously shown that hypoferremia impairs granulopoiesis (43). We believe this to be caused by a combination of high turnover rate and particularly high cellular iron demand of granulocytes. Nevertheless, it seems unlikely that impaired granulocytosis would significantly impact adaptive immune responses to vaccines investigated in this thesis.

3.3.1. Conclusion

This chapter has established two models of iron deficiency that both display mild effects on erythropoiesis and show no substantial changes in the composition of the peripheral immune cell compartment at homeostasis. Based on these findings, both models were determined to be suitable for the further explorations of iron-dependent immunological responses to malaria infection and vaccination outlined in this thesis.

4. Decreased cellular iron uptake alters malaria infection

4.1. Introduction

There is a complex relationship between iron and malaria infection that has not yet been fully elucidated. Malaria is a contributing cause of iron deficiency in children in malaria-endemic countries, and by reducing malaria episodes it is believed that iron deficiency could be profoundly decreased (183). A large number of studies, with different study designs, have investigated the effects of iron deficiency and iron supplementation on malaria infection. Although the results have varied, it is now generally accepted that iron deficiency is protective against malaria, whereas iron supplementation can increase the risk of malaria in some settings (1,184,218). However, it remains poorly understood precisely how these effects are mediated and how host iron status influences *Plasmodium* virulence.

4.1.1. Iron bioavailability affects *Plasmodium* growth

Iron is an essential nutrient for most organisms, including *Plasmodium* species, which require iron for anabolic processes, such as pyrimidine, deoxynucleotide and haem synthesis (91). Consequently, iron chelators can inhibit *Plasmodium* growth *in vitro* and *in vivo* (91). However, little is known about how *Plasmodium* imports, exports and stores iron. There are only two known putative *Plasmodium* iron transporters: ZIP domain containing protein (ZIPCO) and vacuolar iron protein (VIT). ZIPCO mediates iron, and possibly zinc, uptake and is essential for *P. berghei* liver stage growth (219). However, ZIPCO is not required during the blood or mosquito stages of infection, so *Plasmodium* parasites must also acquire iron via other mechanisms. VIT also mediates iron uptake, primarily of reactive Fe^{2+}, and VIT is thought to detoxify excess iron by sequestering it in organelles (220). Consequently, VIT is required for optimal *P. berghei* liver and blood stage growth. *Plasmodium* has no ferritin homologue, and to date, no other *Plasmodium* iron storage protein has been discovered (91).

Surprisingly, blood-stage malaria parasites do not appear to actively metabolise haemoglobin to acquire iron, despite it being readily available inside RBCs. The parasite does however break

down haemoglobin at high rates in order to acquire amino acids, while the remaining haem is converted into a non-reactive insoluble crystal form - hemozoin (91). *P. falciparum* lacks a canonical haem oxygenase-1 (HO-1) pathway and has no enzymatic haem oxygenase activity, indicating that haem is not actively metabolised by the parasite (221). However, haem can be non-enzymatically oxidised, e.g. by hydrogen peroxide inside the *Plasmodium* food vacuole, resulting in iron release (99,222). It follows that haem is a potential source of iron for the parasite, but it remains to be seen whether it is actually utilised or essential for parasite growth. It is also questionable whether host iron deficiency would limit this particular source of iron, as it is estimated that just 1% of the haemoglobin iron within one RBC is enough to satisfy the iron needs of *Plasmodium* (222). There are also several non-haem sources of iron within RBCs, including labile iron and ferritin, although it is unclear whether they are utilised by blood stage parasites (91).

There is conflicting evidence as to whether or not *Plasmodium* can acquire and utilise serum iron. It has been proposed that malaria parasites utilise transferrin-bound iron (TBI), as some studies show that iRBCs, but not uninfected RBCs, can take up TBI, and that *in vitro* supplementation of TBI increases iron levels in iRBCs (223,224). However, other studies have found that TBI is not taken up by iRBCs or utilised by the parasite to any meaningful extent (225,226). Furthermore, depriving *P. falciparum* culture media of TBI does not affect parasite growth (226). There are also conflicting studies regarding non-transferrin bound iron (NTBI). One study observed increased *in vitro* NTBI uptake in iRBCs, compared to uninfected RBCs (224), whereas another did not (226). Regardless, there is a consensus that NTBI can be taken up by iRBCs (91,224–226), and as such, it is a potential source of bioavailable iron for blood-stage *Plasmodium* parasites.

4.1.2. Iron availability affects blood-stage malaria infection by altering red blood cell physiology

A very large amount of iron (~20 mg/day) is required to maintain RBC haemoglobin synthesis, and consequently, iron deficiency can disrupt erythropoiesis, alter RBC physiology, and cause

anaemia (227). In turn, these factors have the potential to impact *Plasmodium* invasion and growth during the blood-stage of infection.

Clark *et al.* have shown that RBCs from individuals with iron deficiency anaemia are less amenable to *P. falciparum* invasion and growth *in vitro*, compared with RBCs from iron replete individuals (211). Furthermore, *P. falciparum in vitro* invasion and growth was increased in RBCs from iron deficient patients receiving iron supplementation, as a result of an increase in immature red cells during anaemia recovery. Some strains of malaria (e.g. *P. yoelii* but not *P. chabaudi*) preferentially invade immature RBCs (228). Hence, this study not only shows that iron deficient RBCs are unfavourable for *Plasmodium* growth (through an undetermined mechanism), but it also demonstrates that iron supplementation can increase malaria severity by increasing the frequency of immature RBC.

RBC labile iron and ROS levels have been proposed to affect blood-stage parasites. If RBC iron export is ablated through an erythroid-specific ferroportin knockout ($Fpn^{-/-}$), it increases labile iron and ROS, resulting in RBC fragility and haemolysis (229). Additionally, the $Fpn^{-/-}$ results in increased susceptibility to malaria infection (229). $Fpn^{-/-}$ mice infected with *P. chabaudi* have slightly higher parasitaemia, and when infected with *P. yoelii*, which preferentially infects immature RBCs, they display uncontrolled parasitaemia and decreased survival. Potentially, $Fpn^{-/-}$ mice are primarily more susceptible to malaria infection because they have more reticulocytes due to haemolysis, as the effect was much more pronounced with *P. yoelii*. It is worth noting that the $Fpn^{-/-}$ mice had decreased RBC counts (~15% fewer compared to wild-type) and Zhang *et al.* do not present absolute parasite numbers (229). Thus, it is possible that the difference in *P. chabaudi* parasitaemia may actually be primarily mediated by a difference in RBC counts. In addition, this study proposed that the Q248H ferroportin mutation, which renders ferroportin hepcidin resistant, could confer protection against malaria (229). However, a large scale study of 18,000 African children has since shown that the ferroportin Q248H variant does not affect parasite density in infected individuals and does not confer protection against mild or severe malaria (230).

Iron deficient RBCs have a shorter life-span, due to decreased deformability, higher rates of eryptosis and higher expression levels of markers associated with clearance, e.g. phosphatidylserine (91). In line with this, a few studies have found that iron deficient RBCs display higher levels of membrane phosphatidylserine and are cleared from circulation more quickly than iron replete RBCs during *Plasmodium* infection (189,190). The iron deficient RBCs are cleared through erythrophagocytosis (189,190), however, it is unclear if altered phagocyte function also affects the rate of clearance. In either case, it follows that increased clearance of infected iron deficient RBCs by phagocytes could have a protective effect during malaria infection.

4.1.3. Iron and haem affect malaria disease tolerance

Disease tolerance strategies limit the negative impact of pathogens on host health, without directly affecting the pathogen (231). Tolerance is often mediated by limiting and controlling tissue damage caused either by the pathogen or by the immune response to the pathogen (232). Haem and iron detoxification mechanisms have been identified as key aspects of malaria disease tolerance.

Haemolysis occurs extensively during blood-stage malaria infection, and it generates cell-free haemoglobin, which can be oxidised to release globin and proinflammatory and cytotoxic free haem. To prevent oxidative damage, the plasma glycoproteins haptoglobin and haemopexin sequester free haemoglobin and haem, respectively, and deliver them to cells for uptake (5). Additionally, the antioxidant enzyme HO-1 is required to break down and recycle haem inside cells. HO-1 catabolises haem to produce carbon monoxide (CO), iron and biliverdin. HO-1 confers disease tolerance to malaria, and mice lacking HO-1 have unaltered pathogen burden but substantially decreased survival (233–235). HO-1 prevents oxidative stress mediated liver failure, induced by a combination of haem and TNF, in *P. chabaudi* infected mice (234). Moreover, HO-1 prevents the onset of experimental cerebral malaria in mice infected with *P. berghei* by preventing the build-up of cytotoxic free haem, resulting in decreased blood brain barrier disruption and neuroinflammation (233). In line with this, sickle cell haemoglobin

confers protection from experimental cerebral malaria in mice, without reducing *P. berghei* pathogen load (236). Mice with sickle cell haemoglobin have higher expression of HO-1 at baseline and during infection, and thus, have improved malaria disease tolerance. However, it remains to be seen whether this mechanism contributes to the malaria protective effects of sickle cell haemoglobin in humans.

Similar to free haem, excess cellular iron can be pro-oxidant and cytotoxic. During malaria infection, tissue iron levels are likely to increase, due to a combination of haemolysis and inflammation mediated iron redistribution from circulation to tissues. Iron-mediated cell and tissue damage can be prevented by storing excess iron in ferritin (5), and this appears to be an important mechanism for malaria disease tolerance (235,237). Gozzelino *et al.* found that in the absence of ferritin heavy chain, mice infected with *P. chabaudi* succumb to infection even though pathogen burden is unaffected (237). During infection, ferritin acts as an antioxidant and prevents liver iron overload from causing liver failure. The same study found that patients infected with *P. vivax* that had higher liver damage scores also had lower levels of plasma ferritin (237). However, plasma ferritin does not necessarily reflect tissue ferritin levels and it is impacted by other factors such as inflammation (30). Interestingly, HO-1 is required for ferritin heavy chain upregulation during *Plasmodium* infection, so the protective mechanism of HO-1 may be partially mediated via ferritin (237).

While high tissue levels of free haem and iron in experimental malaria cause liver damage, high levels of circulating iron, haem and cell free haemoglobin can cause acute kidney injury (235,238,239). Renal proximal tubule cells in the kidney take up and metabolise cell free haemoglobin that is released because of haemolysis during malaria infection. Renal HO-1 and ferritin are required to process haem and to store the resulting iron, respectively (235). In the absence of either of these proteins, iron overload will cause oxidative stress and acute kidney injury (235). Expression of both HO-1 and ferritin heavy chain is induced by the transcription factor NRF2, in response to oxidative stress during malaria infection (235). The kidney may also be important for iron recycling in this context, as renal proximal tubule cells increase

ferroportin expression during infection (238). This iron recycling by the kidney provides iron to support compensatory extramedullary erythropoiesis in the spleen of *P. chabaudi* infected mice (238). None of these processes affect pathogen burden but they confer a host survival advantage, and therefore iron handling in the kidney is an important aspect of disease tolerance to malaria.

Finally, iron availability may affect malaria infection by influencing the immune response, which will be discussed in further detail in Chapter 5 of this thesis.

4.1.4. Aim

In this chapter the effect of decreased host cellular iron uptake on the course of malaria blood stage infection is examined using murine malaria strain *P. chabaudi* and the $Tfrc^{Y20H/Y20H}$ mouse model of iron deficiency. The aim is to investigate whether pathogen burden is affected, and if so, whether it is mediated by any of the known ways in which iron availability affects malaria infection. In addition, the disease severity of mice with decreased cellular iron uptake is assessed to investigate how changes in host iron distribution can alter malaria disease tolerance.

4.2. Results

4.2.1. Decreased cellular iron uptake increases *P. chabaudi* pathogen burden

To determine if host cellular iron availability affects the course of *P. chabaudi* infection $Tfrc^{Y20H/Y20H}$ mice and wild-type mice were infected by i.v. injection of 10^5 infected RBCs (iRBC) (Figure 4.1A). A transgenic strain of *Plasmodium chabaudi chabaudi* AS, which expresses GFP, was used for ease of tracking the infection (203). The iRBC were derived from recently mosquito transmitted parasites, so that the parasites used for the infection were five blood passages away from a mosquito transmitted inoculum. Recently mosquito transmitted parasites were used because mosquito transmission is known to alter parasite virulence, resulting in a model that mimics natural infection more closely (182) (see section 1.2.5. Experimental models of malaria).

Blood samples were collected and analysed by flow cytometry throughout the infection. Mice with decreased cellular iron uptake had significantly higher pathogen burden compared to wild-type mice, both in terms of the percentage of RBCs that were infected (parasitaemia) and in terms of the absolute number of iRBC (Figure 4.1B).

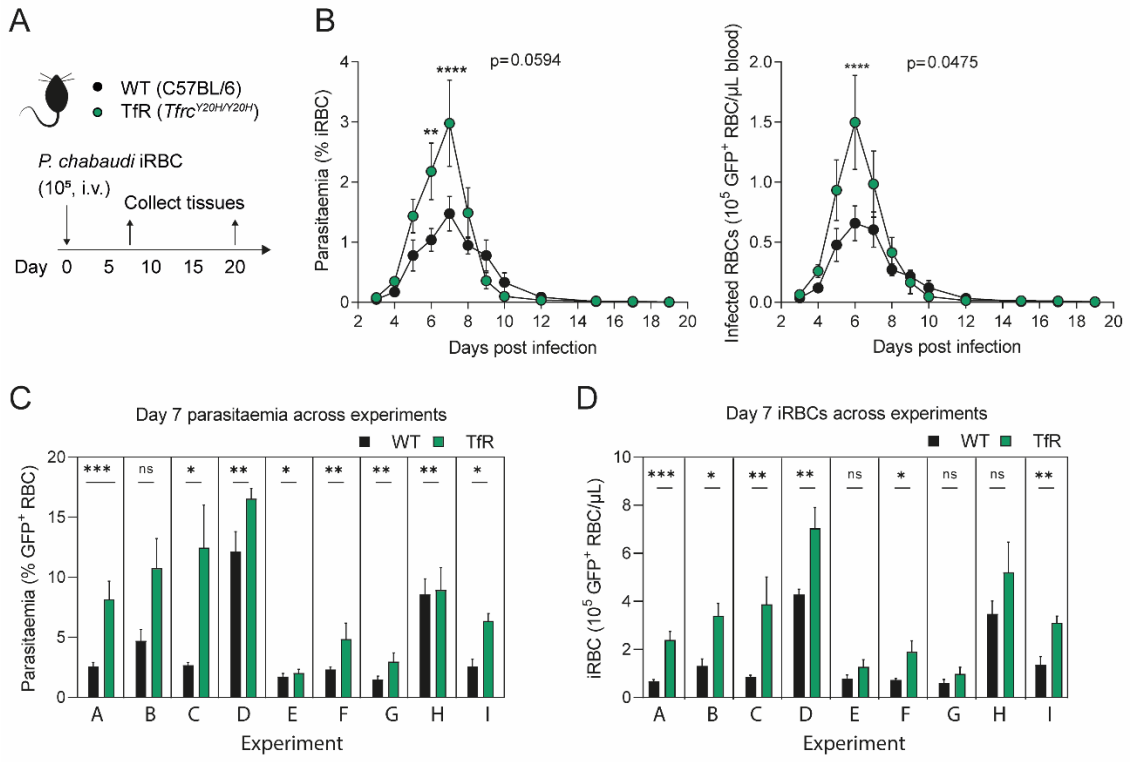


***Figure 4.1. Tfrc$^{Y20H/Y20H}$* mice have increased *P. chabaudi* pathogen burden. A)** C57BL/6 (WT) and *Tfrc*$^{Y20H/Y20H}$ (TfR) mice were infected by intravenous (i.v.) injection of 10^5 *P. chabaudi* infected red blood cells (iRBC). **B)** Blood was collected from the tail vein, and parasitaemia and parasite load was measured by flow cytometry. Mean ± SEM, two-way ANOVA with Sidak's m.c.t., n=7-8, representative of N=9. **C-D)** Parasitaemia on day 7 post infection was compared across all experiments, each individual experiment is separated by a vertical line. Mean ± SEM, Mann-Whitney test, n=6-11.

The inter-individual and inter-experimental variability in pathogen burden was quite high, likely due to subtle differences in infectious dose, parasite virulence and host response between individuals. This resulted in some experimental repeats being underpowered to detect significant differences in the parasitaemia and iRBC count. However, when comparing the peak parasitaemia and parasite load data across all experiments, it is clear that, overall, mice with decreased cellular iron uptake have higher peak pathogen burden (Figure 4.1C-D). In contrast, no difference in parasite clearance, to low-level chronic infection, was observed between the two genotypes (Figure 4.1B). Next, further investigations were performed to determine the

cause of the increased *P. chabaudi* peak pathogen burden in mice with decreased cellular iron uptake.

4.2.2. Circulating iron levels do not affect *P. chabaudi* pathogen burden

To assess whether altered *Plasmodium* iron bioavailability may have caused the increased pathogen burden, circulating iron levels were measured. Serum iron was increased compared to baseline in both wild-type and *Tfrc*$^{Y20H/Y20H}$ mice eight days after of *P. chabaudi* infection (Figure 3.1B & 4.2A). However, mice with decreased cellular iron uptake had significantly higher serum iron than wild-type mice (Figure 4.2A). To establish the cause of this increase in circulating iron, the expression of genes involved in iron regulation was measured. Hepcidin is the main regulator of circulating iron levels and it is primarily produced in the liver. Hence, *Hamp1* (encodes hepcidin) gene expression in the liver was measured and was found to be higher in mice with decreased cellular iron uptake (Figure 4.2B). As increasing hepcidin will decrease serum iron, hepcidin suppression was not the cause of the elevated serum iron in mice with decreased iron uptake.

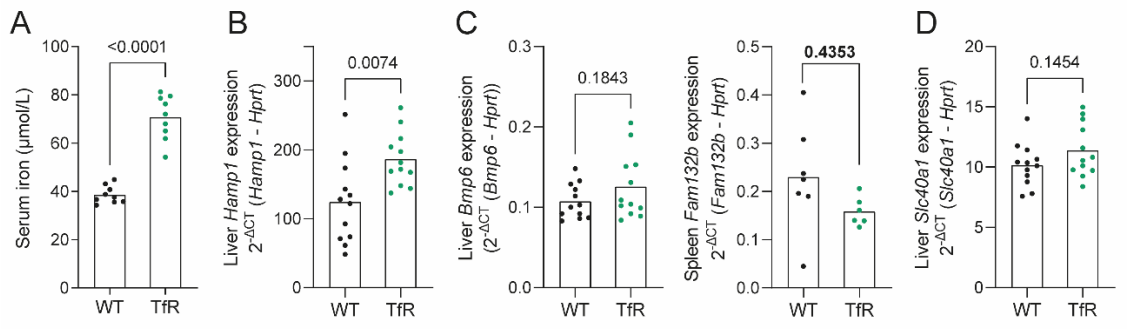


***Figure 4.2. Tfrc*$^{Y20H/Y20H}$ mice have increased serum iron during *P. chabaudi* infection.** Serum, spleen and liver samples were collected from C57BL/6 (WT) and *Tfrc*$^{Y20H/Y20H}$ (TfR) mice 8 days after *P. chabaudi* infection. **A)** Serum iron was measured using an automated clinical chemistry analyser. **B-D)** Gene expression of *Hamp1* (hepcidin), *Bmp6* (bone morphogenic protein 6) and *Slc40a1* (ferroportin) in the liver, and *Fam132b* (erythroferrone) in the spleen, was measured by qRT-PCR. Mean, Welch's t-test / **Welch's t-test on log transformed data**, n=7-15, N=1-2 (pooled).

However, we still sought to determine the cause of this increased hepcidin expression, and consequently, key regulators of hepcidin expression were examined. BMP-6 induces *Hamp1* expression, and *Bmp6* gene expression can be induced in response to excess cellular iron (18).

In addition, BMP6 signalling can be inhibited by erythroferrone (encoded by *Fam132b*) in response to high erythropoietic demand for iron (240). However, no difference was observed in the expression of *Bmp6* in the liver or *Fam123b* in the spleen, between mice with normal and decreased cellular iron uptake (Figure 4.2.C). Thus, it seems unlikely that varying cellular iron levels or erythropoietic demand was the reason for the difference in *Hamp1* expression. Preliminary data indicated that *Hamp1*, *Bmp6* and *Slc40a1* were not differentially expressed in $Tfrc^{Y20H/Y20H}$ and wild-type mice at homeostasis (data not shown).

Inflammation, in particular IL-6, can also induce *Hamp1* expression. Liver *Il6* expression was, however, below the limit of detection in both wild-type and $Tfrc^{Y20H/Y20H}$ mice eight days after infection (data not shown). As such, the increased hepcidin expression in $Tfrc^{Y20H/Y20H}$ mice is unlikely to be caused by BMP6, inflammation, or decreased erythroid demand. In addition, ferroportin can be transcriptionally regulated independently of hepcidin, resulting in altered cellular iron export and potentially changes in serum iron. However, no difference in the relative expression of liver *Slc40a1* (encodes ferroportin) was observed (Figure 4.2D). Taken together it seems likely that the increased serum iron levels in the $Tfrc^{Y20H/Y20H}$ mice are the result of increased haemolysis, due to the higher pathogen burden, combined with decreased uptake of TBI due to the *Tfrc* mutation. In turn, *Hamp1* expression is likely induced in response to the high levels of circulating iron, e.g. via TfR2 mediated signalling (241,242).

Regardless of what caused the elevated circulating iron in mice with decreased cellular iron uptake, it is possible that elevated serum iron could increase iron availability to *P. chabaudi*, and thereby promote parasite growth. We therefore experimentally induced hyperferremia during *P. chabaudi* infection in wild-type mice, using a recombinant monoclonal anti-BMP6 IgG antibody (αBMP6), which was administered 2, 12 and 16 days after infection (Figure 4.3A). αBMP6 treatment strongly suppresses hepcidin expression and elevates serum iron, as iron is liberated from cellular stores (200). Hence, serum iron was measured on day 9 and 21 after *P. chabaudi* infection to ensure that the treatment had worked. αBMP6-treated mice had increased serum iron compared to control mice given an isotype control antibody (Figure 4.3B).

Hyperferremia did not affect parasitaemia or body weight, however, a small increase in parasite load was observed at the peak of infection (Figure 4.3C-E). Mice treated with αBMP6 and isotype had similar frequencies of RBCs throughout *P. chabaudi* infection (Figure 4.3F). However, αBMP6 treated mice appeared to have recovered more fully from the malaria-induced anaemia three weeks after infection (Figure 4.3G). Altogether, this experiment clearly shows that supranormal serum iron does not affect *P. chabaudi* pathogen burden.

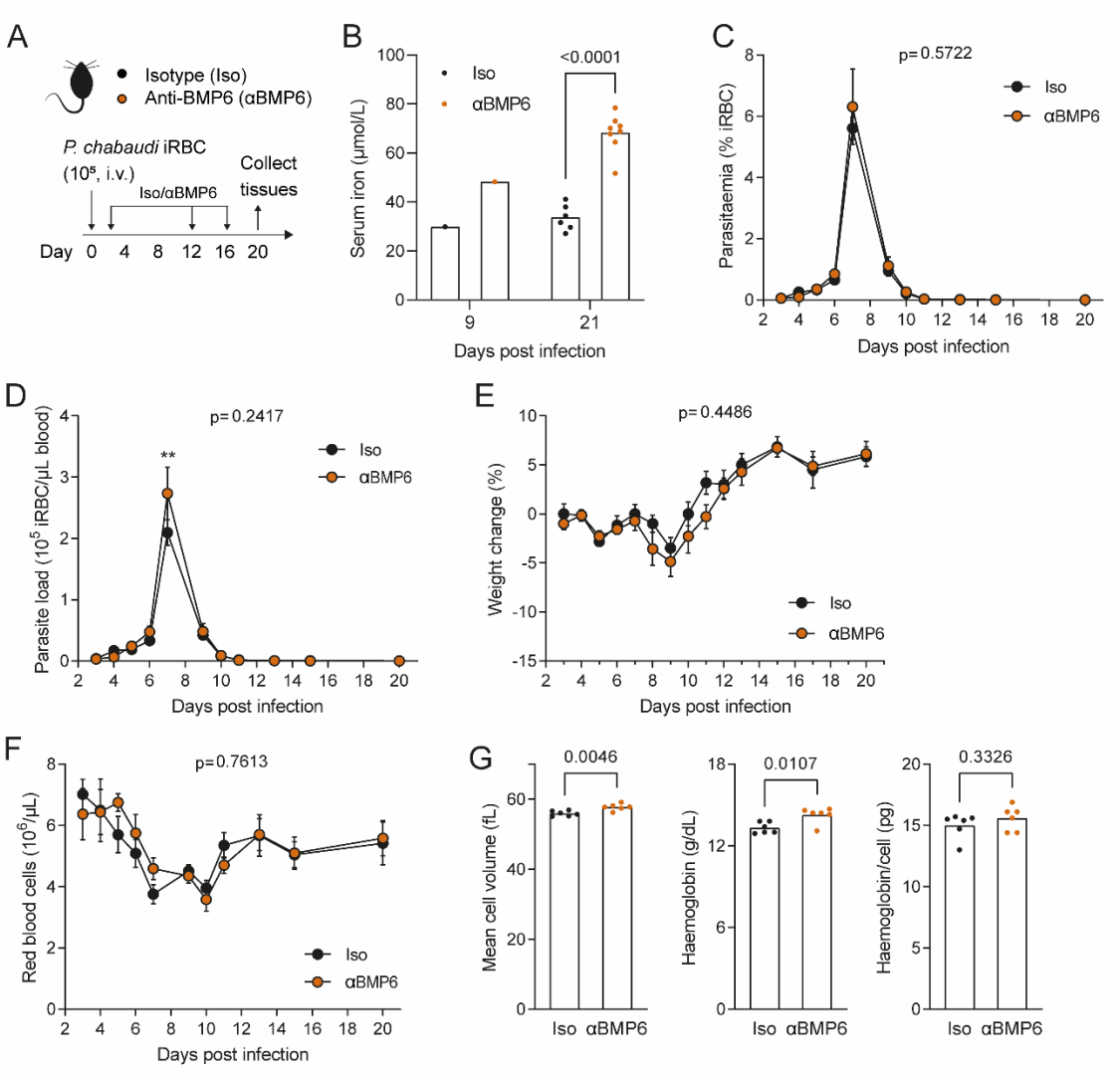


***Figure 4.3*. Hyperferremia does not substantially affect the course of *P. chabaudi* infection. A)** C57BL/6 mice were infected by intravenous (i.v.) injection of 10^5 *P. chabaudi* infected red blood cells (iRBC). Anti-Bmp6 IgG (αBMP6) or an isotype control (Iso) was administered 2, 12 and 16 days after infection. **B)** Serum iron was measured and pooled serum samples from 6-8 mice were used for the day 9 analysis. **C-F)** Blood was collected by micro-sampling from the tail vein, and parasitaemia, parasite load and red blood cell counts were measured by flow cytometry. Body weight was monitored throughout the experiment. **G)** Red blood cell parameters were measured 20 days post infection. Mean, Welch's t-test (B & G) or mean ± SEM, two-way ANOVA with Sidak's m.c.t. (C-F), n=6-8, N=1.

4.2.3. Decreased cellular iron uptake partially alters red blood cell physiology during *P. chabaudi* infection

During malaria infection a large number of RBCs are destroyed and must be replaced. In mice, the resulting increase in erythropoietic demand is compensated for by extramedullary erythropoiesis in the spleen. Mice with decreased cellular iron uptake may struggle to support this process, which could affect RBC physiology and consequently parasite growth. Extramedullary erythropoiesis was therefore assessed by performing flow cytometry on non-RBC-lysed splenocytes. Erythroid cells express TER119 but become smaller and downregulate expression of CD44 as they become more mature, and consequently, these markers can be used to assess RBC maturation (Figure 4.4A).

Eight days after infection with *P. chabaudi* there was an increase in immature red cells in the spleen, compared to uninfected mice (Figure 4.4A). However, mice with decreased cellular iron uptake had significantly fewer immature RBC precursors in the spleen eight days after *P. chabaudi* infection (Figure 4.4A-B). Three weeks after infection, lower but equal levels of extramedullary erythropoiesis were observed in both genotypes (Figure 4.4C). This indicates that $Tfrc^{Y20H/Y20H}$ mice had reduced erythropoietic capacity during the acute stage of infection, potentially affecting their RBC output at this point.

Due to the impaired extramedullary erythropoiesis observed in $Tfrc^{Y20H/Y20H}$ mice, we further monitored RBC counts throughout the course infection. Surprisingly, the loss and regeneration of RBCs during *P. chabaudi* infection was comparable between wild-type and $Tfrc^{Y20H/Y20H}$ mice (Figure 4.4D). This applied both to the total number of RBCs (Figure 4.4D) and the percentage change in RBCs, compared to baseline (data not shown). RBC phenotyping revealed that although mice with decreased cellular iron uptake had microcytic and hypochromic RBCs eight days after *P. chabaudi* infection, blood haemoglobin levels were equally low in both genotypes (Figure 4.4E). Three weeks after infection, RBC parameters were largely restored to pre-infection levels in both wild-type and $Tfrc^{Y20H/Y20H}$ mice, but the $Tfrc^{Y20H/Y20H}$ mice remained somewhat anaemic (Figure 4.4F). In conclusion, *P. chabaudi* induced comparable RBC loss and

anaemia in both genotypes, and while *Tfrc*$^{Y20H/Y20H}$ mice had reduced extramedullary erythropoiesis in the spleen, this only had a small effect on RBC and anaemia recovery.

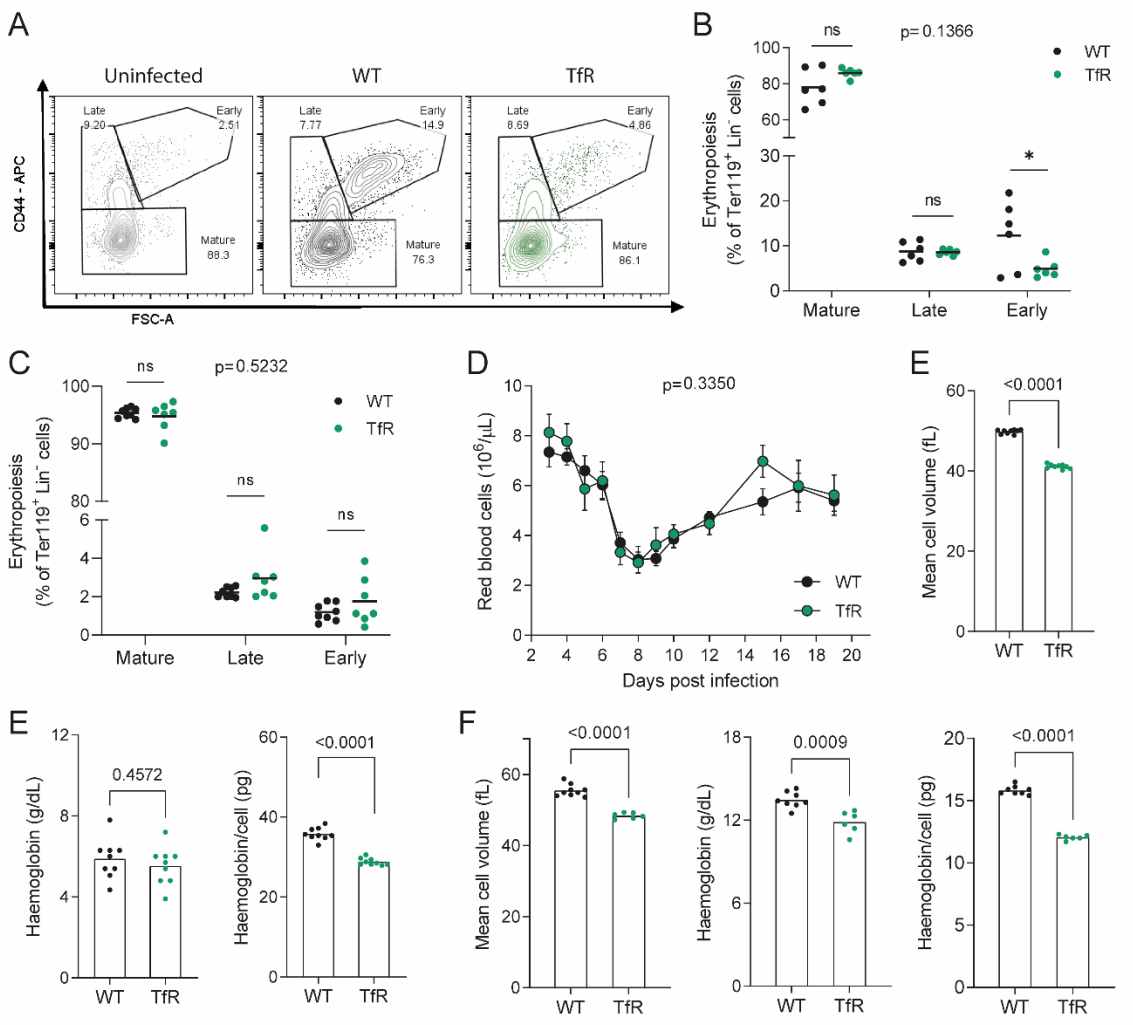


***Figure 4.4*. WT and *Tfrc*$^{Y20H/Y20H}$ mice have comparable *P. chabaudi* induced red blood cell loss and anaemia. A-C)** Splenic extramedullary erythropoiesis was assessed in *P. chabaudi* infected C57BL/6 (WT) and *Tfrc*$^{Y20H/Y20H}$ (TfR) mice, 8 (A-B) and 20 (C) days after infection. **D)** Blood was collected by micro-sampling from the tail vein and red blood cell counts were measured by flow cytometry. **E-F)** Red blood cell parameters were measured 8 (E) and 20 (F) days post infection. Mean ± SEM, two-way ANOVA with Sidak's m.c.t. (B-D) or Mean, Welch's t-test (E-F) n=6-9, N=1-3.

Keeping in mind that *Tfrc*$^{Y20H/Y20H}$ RBCs are microcytic and hypochromic, it is possible that they are qualitatively different from wild-type RBCs in ways that could affect parasite invasion and replication. Therefore, an *in vitro* invasion assay was performed to assess the susceptibility of wild-type and *Tfrc*$^{Y20H/Y20H}$ RBCs to invasion by *P. chabaudi*. Infected and uninfected RBCs donor were cultured together with fluorescently labelled RBCs from wildtype or *Tfrc*$^{Y20H/Y20H}$ mice. Upon completion of a blood cycle it was evaluated whether the merozoites preferentially

invaded wildtype or *Tfrc*$^{Y20H/Y20H}$ RBCs (Figure 4.5A). The assay revealed that *Tfrc*$^{Y20H/Y20H}$ and wild-type RBCs were equally susceptible to *P. chabaudi* invasion *in vitro* (Figure 4.5B).

In summary, mice with normal and decreased cellular iron uptake had partially disparate RBC phenotypes during *P. chabaudi* infection. Both genotypes had comparable malaria induced RBC loss and anaemia, and *P. chabaudi* did not preferentially invade *Tfrc*$^{Y20H/Y20H}$ or wild-type RBCs. However, mice with decreased iron uptake had microcytic and hypochromic RBCs, impaired erythropoiesis and delayed anaemia recovery. On the whole, these data suggest a limited direct effect of altered iron availability on the parasite itself and are unlikely to explain the differences in pathogen burden.

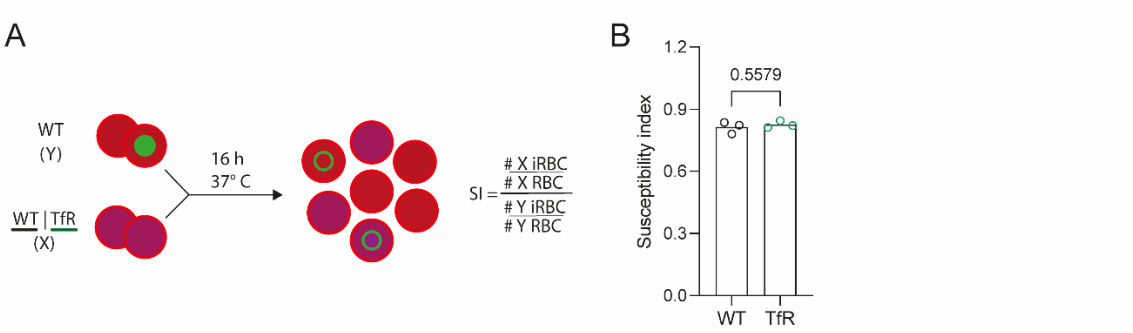


***Figure 4.5. Tfrc*$^{Y20H/Y20H}$ red blood cells are not more susceptible to invasion by *P. chabaudi*. A-B)** Unlabelled wild-type (WT) infected red blood cells (iRBC) were cultured overnight together with fluorescently labelled WT or *Tfrc*$^{Y20H/Y20H}$ (TfR) red blood cells (RBC). Invasion of donor and recipient cells was assessed by flow cytometry and the susceptibility index (SI) was determined. Mean, Welch's t-test, n=3, N=3.

4.2.4. Decreased cellular iron uptake alters *P. chabaudi* pathology

In addition to assessing the pathogen burden, the severity of disease was assessed in mice with decreased cellular iron uptake. Therefore, body weight was monitored in wild-type and *Tfrc*$^{Y20H/Y20H}$ mice infected by i.v. injection of 10^5 *P. chabaudi* iRBC (Figure 4.6A). Increased body weight loss was observed in mice with decreased cellular iron uptake (Figure 4.6B), which was sometimes accompanied by delayed weight regain (Figure 4.6C). Analogous to the parasitaemia data, weight change was often quite variable between individual mice and between different experiments. However, when the nadir of weight loss (8 days post infection) was

compared across experiments, it revealed that the *Tfrc*$^{Y20H/Y20H}$ mice generally experienced more severe weight loss compared to wild-type mice (Figure 4.6D).

Since weight loss is often associated with more severe pathology, markers of tissue damage were measured in serum samples collected eight days after infection (Figure 4.6E-F). Lactate dehydrogenase (LDH) is a metabolic enzyme which is expressed in most cells, and alanine aminotransferase (ALT) is a metabolic enzyme that is primarily expressed in the liver. When cells are damaged these enzymes are released into circulation, and blood levels of LDH and ALT can therefore be used as markers of general tissue damage or liver damage, respectively.

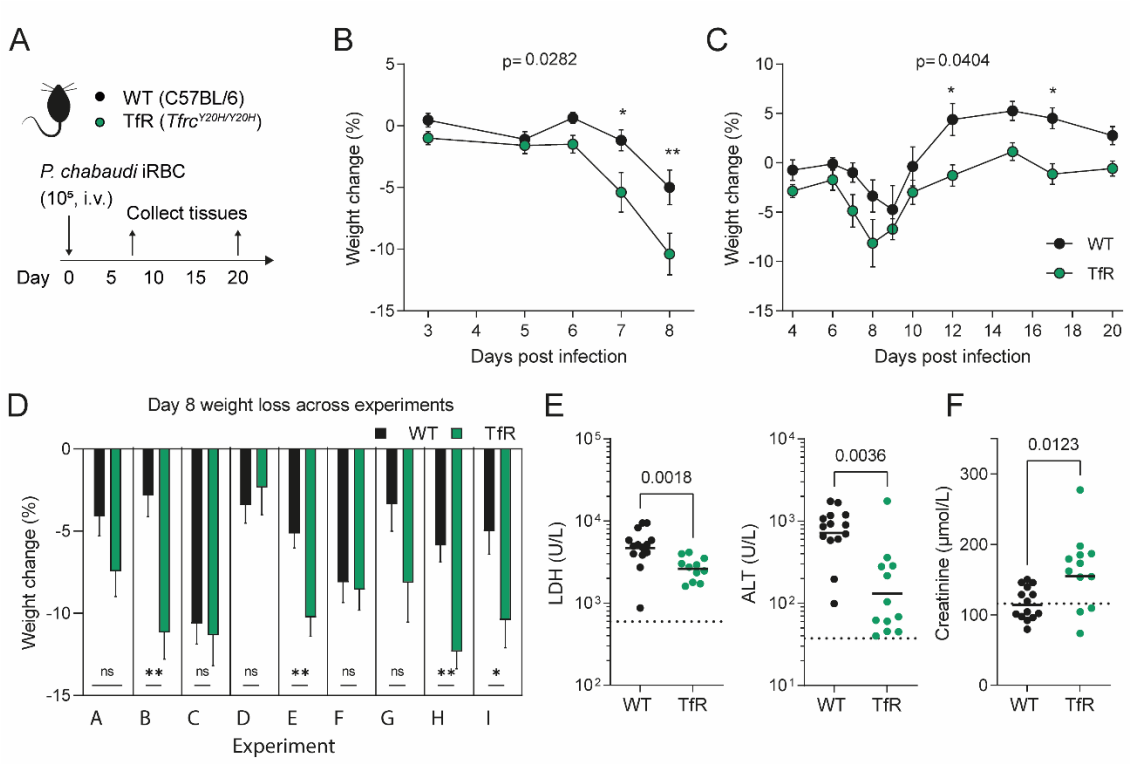


***Figure 4.6*. Decreased cellular iron uptake alters disease tolerance during *P. chabaudi* infection. A)** C57BL/6 (WT) and *Tfrc*$^{Y20H/Y20H}$ (TfR) mice were infected by intravenous (i.v.) injection of 10^5 *P. chabaudi* infected red blood cells (iRBC). **B-C)** Body weight was monitored throughout the course of infection. Mean ± SEM, two-way ANOVA with Sidak's m.c.t., n=7-11, N=9. **D)** Body weight change on day 8 post infection was compared across all experiments, each individual experiment is separated by a vertical line. Mean ± SEM, Mann-Whitney test, n=6-11. **E-F)** Serum lactate dehydrogenase (LDH), alanine aminotransferase (ALT) and creatinine levels were measured with an automated clinical chemistry analyser 8 days after infection. Geometric mean, Welch's t-test, n= 12-14, N=3 (pooled).

P. chabaudi infection raised LDH and ALT levels in both wild-type and *Tfrc*$^{Y20H/Y20H}$ mice, as can be expected during malaria infection (243). However, unexpectedly, LDH and ALT levels

were significantly higher in mice with normal iron uptake (Figure 4.6E), indicating that mice with decreased cellular iron uptake had reduced liver damage.

In addition, blood creatinine levels were measured in *P. chabaudi* infected wild-type and *Tfrc*$^{Y20H/Y20H}$ mice. Creatinine is a normal waste product, which builds up in the blood if the kidneys are damaged. Mice with decreased iron uptake had significantly higher serum creatinine levels, compared to wild-type mice (Figure 4.6F). There was no difference in ALT, LDH or creatinine levels between uninfected *Tfrc*$^{Y20H/Y20H}$ and wild-type mice (data not shown). Taken together, this indicates that mice with decreased cellular iron uptake have an altered disease phenotype during *P. chabaudi* infection, with markers suggesting relatively attenuated liver damage but aggravated kidney damage.

To investigate the disease phenotype further, livers were collected from wild-type and *Tfrc*$^{Y20H/Y20H}$ mice, eight days after infection with *P. chabaudi*. Both genotypes had hepatomegaly, although there was a trend towards less severe hepatomegaly in mice with decreased iron uptake (Figure 4.7A). Eight days after infection the non-haem liver iron content was elevated compared to uninfected mice in both wild-type and *Tfrc*$^{Y20H/Y20H}$ mice (Figure 3.1B & 4.7B). However, there was no difference in the non-haem liver iron content between the two genotypes after infection (Figure 4.7B). Genes that encode acute phase proteins are quickly induced to high expression levels in the liver in response to tissue damage and inflammation. Wild-type mice infected with *P. chabaudi* had higher relative expression of *Fga* and *Saa1*, the genes that encode acute phase proteins fibrinogen alpha chain and serum amyloid A1, compared to *Tfrc*$^{Y20H/Y20H}$ mice (Figure 4.7C). Preliminary data indicated that *Fga* and *Saa1* were not differentially expressed in *Tfrc*$^{Y20H/Y20H}$ and wild-type mice at homeostasis (data not shown). This is consistent with decreased cellular iron uptake ameliorating liver pathology during *P. chabaudi* infection.

There are multiple possibilities for how the hepatoprotective effect observed in mice with decreased iron uptake may be mediated. A likely explanation is that wild-type and *Tfrc*$^{Y20H/Y20H}$ mice differ in how they handle excess tissue haem and iron. HO-1 and ferritin confer a tissue

protective effect in malaria by limiting oxidative stress (237). The relative expression of *Hmox1* (encodes HO-1) was increased two-fold in mice with decreased iron uptake (Figure 4.7D), which is indicative of an improved ability to detoxify haem. However, the expression of *Fth* (encodes ferritin heavy chain) in the liver did not differ between genotypes (Figure 4.7E).

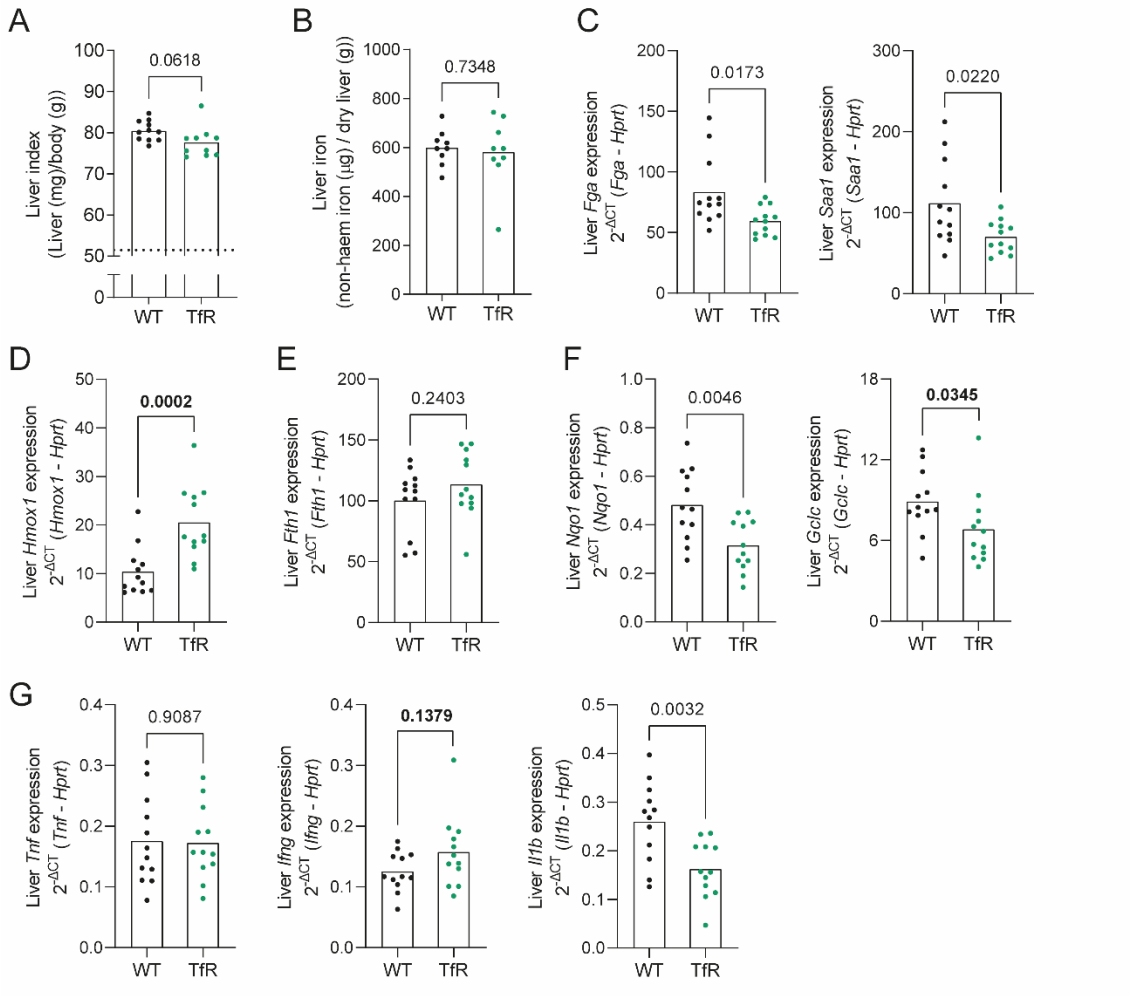


***Figure 4.7*. Decreased cellular iron uptake alters the hepatic response to *P. chabaudi* infection.** Livers were collected from C57BL/6 (WT) and *Tfrc*$^{Y20H/Y20H}$ (TfR) mice 8 days after *P. chabaudi* infection. **A)** The liver index and non-haem liver iron content was measured. **C-G)** Liver gene expression was measured by qRT-PCR. Mean, Welch's t-test / **Welch's t-test on log transformed data**, n=12-19, N=2 (pooled).

NRF2 is a sensor of intracellular iron and oxidative stress that induces the expression of oxidative stress response genes, including *Hmox1* (18). To assess if the NRF2-mediated oxidative stress response was activated, we measured the relative expression of NRF2 target genes *Nqo1* and *Gclc*. The relative expression of both genes was lower in mice with decreased cellular iron uptake during infection (Figure 4.7F). It is therefore unlikely that the increased

Hmox1 expression in mice with decreased iron uptake is mediated by NRF2, but in addition, these findings indicate that hepatic cellular oxidative stress may be lower in $Tfrc^{Y20H/Y20H}$ mice. Preliminary data indicated that at homeostasis *Fth* and *Gclc* was not differentially expressed in $Tfrc^{Y20H/Y20H}$ and wild-type mice, while *Hmox1* and *Nqo1* expression was lower in $Tfrc^{Y20H/Y20H}$ mice (data not shown).

Inflammation, mediated by cytokines such as TNFα and IL-1α, can exacerbate hepatocyte apoptosis during malaria infection (237,243). Consequently, the expression of genes that encode inflammatory cytokines was measured in the liver. There was no significant difference in the expression of *Tnf* or *Ifng* (encode TNFα and IFNγ), however, wild-type mice had higher relative expression of *Il1b* (encodes IL-1β). This further indicates that wild-type mice may have more severe liver inflammation during *P. chabaudi* infection than $Tfrc^{Y20H/Y20H}$ mice.

4.3. Discussion

There is an intricate and poorly understood relationship between malaria and iron. Iron deficiency can protect from malaria infection, while iron supplementation can increase the risk (see section 1.3. Aims and hypothesis). However, the exact relationship between host iron status and *Plasmodium* virulence remains incompletely understood .

Here the effects of cellular iron deficiency on the course of malaria infection were investigated. In contrast to what has been observed in several other murine models of iron deficiency (91), we found that mice with decreased cellular iron uptake have increased *P. chabaudi* pathogen burden. This was accompanied by elevated serum iron in the mutant mice during the peak of infection, likely as a result of decreased TfR1 mediated iron uptake. As it has been suggested that *Plasmodium* can acquire and utilise serum iron (223,224), the effect of increased serum iron levels on pathogen burden were investigated. However, experimentally-induced hyperferremia had little or no effect on parasite burden in wild-type mice. Furthermore, our lab has previously found that elevated serum iron does not affect *P. chabaudi* parasitaemia, in an inducible *Hamp1* knock-out mouse (unpublished). Even though studies have shown that *Plasmodium* can acquire serum iron (223,224), there is little evidence that it is actually utilised or essential for parasite

growth (225,226). Since uninfected *Tfrc*$^{Y20H/Y20H}$ mice only have slightly decreased serum iron levels, the effects of low serum iron on pathogen burden were not investigated here. In summary, fluctuations in serum iron appears to have a negligible effect on parasite burden during blood-stage malaria infection.

Extramedullary erythropoiesis was impaired in mice with decreased cellular iron uptake, during the acute stage of *P. chabaudi* infection. This did not appear to affect malaria induced anaemia, as it was comparable in both genotypes. However, it seems likely that impaired erythropoiesis caused delayed anaemia recovery in mice with decreased iron uptake. Perturbations in erythropoiesis can affect the frequency of immature RBCs in circulation and it is well established that immature RBCs are more susceptible to infection from multiple *Plasmodium* strains (91). In fact, *P. vivax* is thought to rely on molecules that are only expressed on immature RBCs (including TfR1) for invasion, and thus, exclusively invade immature RBCs (92). However, *P. chabaudi* does not have a preference for immature RBCs (228), and thus, it is unlikely that varying reticulocyte frequencies could affect pathogen burden in this model.

However, mice with decreased cellular iron uptake also had altered RBC physiology, which may have had an impact on pathogen burden. *Tfrc*$^{Y20H/Y20H}$ RBCs were microcytic and hypochromic, but did not appear to be more susceptible to *P. chabaudi* invasion. It remains unknow, however, how decreased cellular iron uptake affects parasite growth subsequent to invasion. The higher pathogen burden in mice with decreased cellular iron uptake is particularly interesting as multiple studies have found that iron deficient RBCs are unfavourable for *Plasmodium* growth (91,190,211) and that iron deficiency anaemia is associated with decreased pathogen burden in humans (184). Hence, there must either be an, as of yet unidentified, factor that makes *Tfrc*$^{Y20H/Y20H}$ RBCs more favourable for *P. chabaudi* growth than wild-type RBCs, or *Tfrc*$^{Y20H/Y20H}$ RBCs are less efficiently cleared from circulation. A study that utilised a mouse model with a different *Tfrc* mutation and a comparable RBC phenotype similarly observed increased *P. chabaudi* parasitaemia (244). However, it not known whether this phenotype was caused by increased *P. chabaudi* growth or decreased clearance.

One factor which could affect *Plasmodium* growth is RBC labile iron or ROS levels. ROS is generated as *P. falciparum* matures within RBCs (245) and excess ROS is harmful to the parasite, as the mechanism of killing for both artemisinin and chloroquine is via uncontrolled ROS formation (82,99). However, when RBC ferroportin is knocked out, labile iron and ROS increases, and this appears to benefit *Plasmodium* growth (229). Hence, it is possible that $Tfrc^{Y20H/Y20H}$ RBCs have altered ROS or labile iron levels that render them more amenable to *P. chabaudi* growth. If the phenotype is caused by reduced clearance, there are several potential factors that could disrupt clearance. RBC intrinsic factors such as size, density and membrane composition have the potential to affect sequestration in microvasculature, retention in the spleen, and recognition by erythrophagocytic macrophages (10,82). In addition, varying immune activation could affect the rate of iRBC clearance (see Chapter 5). Hence, further studies are needed to determine if RBCs are a factor in the higher *P. chabaudi* parasite burden observed in mice with decreased cellular uptake. Future work should be focused on characterising $Tfrc^{Y20H/Y20H}$ RBCs (e.g. ROS levels, phosphatidylserine expression) and defining their clearance rates (e.g. through adoptive transfer of labelled cells).

In addition, we have discovered that mice with decreased cellular iron uptake have an altered *P. chabaudi* pathology, characterised by increased weight loss, attenuated liver damage and exacerbated kidney damage. Although, at first glance, this phenotype appears quite contradictory, it can likely be explained by altered iron distribution in $Tfrc^{Y20H/Y20H}$ mice. Tissue haem and iron loading can cause organ damage and is associated with disrupted disease tolerance in malaria (234,235,237,238). $Tfrc^{Y20H/Y20H}$ mice have lower liver iron stores at homeostasis and decreased hepatic TfR1 mediated iron uptake during *P. chabaudi* infection. Hence, in wild-type mice liver macrophages will need to import, detoxify and store large amounts of TBI, haem and haemoglobin to prevent tissue damage during *P. chabaudi* infection, whereas hepatic TBI uptake will be lower in $Tfrc^{Y20H/Y20H}$ mice. This may suggest that $Tfrc^{Y20H/Y20H}$ mice are better poised to detoxify free haemoglobin and haem, which is supported by the observation that mice with decreased cellular iron uptake had higher hepatic expression

of *Hmox1*. Both genotypes had comparable non-haem liver iron levels during the peak of infection. However, this measurement does not take into account labile haem or differentiate between cytotoxic labile iron and innocuous ferritin-bound iron. If $Tfrc^{Y20H/Y20H}$ macrophages have lower iron levels they may also be more 'M2-like' and have higher expression of HO-1 (50), which would further promote their ability to detoxify haem. Interestingly, in mice monocytes are reprogrammed to promote tolerance after a single exposure to *P. chabaudi* (131). This involves monocytes acquiring an enhanced iron-recycling phenotype, further demonstrating the importance of iron for pathology in malaria.

Another possible explanation for the attenuated liver damage is that $Tfrc^{Y20H/Y20H}$ mice have less liver inflammation during *P. chabaudi* infection. If decreased cellular iron uptake dampens the immune response, $Tfrc^{Y20H/Y20H}$ mice may have lower levels of hepatic immune cell infiltration and pro-inflammatory cytokine production. The decreased hepatic expression of *Il1b* in $Tfrc^{Y20H/Y20H}$ mice would seem to support this hypothesis. However, since none of the other pro-inflammatory cytokines that were measured (*Ifng, Tnf,* and *Il6*) were increased, it is unclear whether hepatic inflammation was substantially altered. The effect of decreased cellular iron uptake on immune function will be explored further in Chapter 5. A third explanation, which could possibly explain both the higher parasitaemia and attenuated liver damage in mice with decreased cellular iron uptake, is that they have reduced hepatic parasite sequestration. It is know that the immune response can affect parasite sequestration in the liver (246), and hence, a decreased immune response could contribute to decreased parasite sequestration. This could, in turn, lead to attenuated liver damage and to more parasites being found in circulation.

Whereas the decrease in TfR1 mediated cellular iron uptake during *P. chabaudi* infection may result in less hepatic tissue iron loading, it also results in higher levels of serum iron, which exposes the kidneys to more iron. Serum iron and haem are filtered in the glomerulus of the kidney and then reabsorbed in the renal tubules. When serum iron or haem levels are very high, renal tubule cells need to handle large amounts of iron and can become damaged (97,239). Consequently, iron loading of renal tubule cells during malaria infection can cause acute kidney

injury and disrupt disease tolerance (235,238). While one might expect the decrease in TfR1 mediated cellular iron uptake to counteract tissue iron loading in the kidney (as in the liver), renal tubule cells have multiple redundant mechanisms to take up iron, and iron dissociates from transferrin at the low pH of tubular filtrate (239). Therefore, decreased TfR1 mediated iron uptake is unlikely to protect renal tubule cells from iron loading during *P. chabaudi* infection. Hence, the elevated serum iron in $Tfrc^{Y20H/Y20H}$ mice will increase the demand for iron filtration by the kidney and potentially cause acute kidney injury.

During *P. chabaudi* infection mice with decreased cellular iron uptake had more intense weight loss, which is often used as a readout for disease severity or disrupted tolerance. Weight loss during infection is usually multi-factorial and associated with altered behaviour (e.g. anorexia) and changes in metabolism (247). In malaria, mice enter a hypometabolic state during acute infection where physical activity and food intake is reduced and metabolism is shifted away from glycolysis to fatty acid oxidation and ketosis (248–250). Anorexia of infection is likely induced by haem exposure in malaria, as haem alone is sufficient to induce anorexia and suppress gluconeogenesis in the liver of uninfected mice (249). Anorexia can also cause dehydration, which can contribute significantly to weight loss. Additionally, kidney damage can disrupt fluid homeostasis to exacerbate weight loss from dehydration, and this could explain the increased wight loss observed in $Tfrc^{Y20H/Y20H}$ mice during *P. chabaudi* infection. Interestingly, iron supplementation prevents skeletal muscle loss in a mouse model of cancer associated cachexia (251), indicating that iron deficiency could potentially intensify lean body mass loss during infection.

Taken together, these findings highlight the importance of tissue iron homeostasis for malaria. However, additional experiments will need to be performed to fully understand the observed phenotype. It will be important to analyse the iron status and disease pathology at more time points and compare it to more extensive baseline data, to ensure that the observed effects are not confounded. In particular, histological analysis of the liver and kidney will need to be performed to confirm the altered organ damage phenotype, and to determine whether it is

mediated by iron loading or inflammation. Future work should also focus on characterising the kidney phenotype in greater detail, for example through functional urine readouts and by measuring kidney gene expression.

4.3.1. Conclusion

In this chapter we have discovered that mice with decreased cellular iron uptake have increased *P. chabaudi* pathogen burden and altered disease tolerance. We see a limited effect of serum iron levels or RBC parameters on parasite growth, and consequently, the next chapter will investigate if the immune response to *P. chabaudi* is impaired by decreased cellular iron uptake.

5. Decreased cellular iron impairs the immune response to malaria

5.1. Introduction

5.1.1. Iron and the immune response to malaria

Although the relationship between iron deficiency and malaria infection has been extensively researched, very few studies have examined how the immune response to malaria is affected by iron availability. There is no direct evidence on the effect of iron deficiency on immune cell function during malaria infection. However, one study found that iron sequestering protein lipocalin-2 may be important for the immune response to malaria. Lipocalin-2 levels increase during malaria infection in humans and mice, and mice lacking lipocalin-2 have increased *P. yoelii* parasitaemia and decreased survival (252). However, lipocalin-2 does not inhibit parasite growth *in vitro*, indicating that lipocalin-2 does not act directly on the parasite. In the absence of lipocalin-2, iron recycling appears to be disrupted and severe reticulocytosis occurs, which could explain the higher parasitaemia. Nevertheless, mice lacking lipocalin-2 also have altered macrophage and neutrophil function and an attenuated antibody response to *P. yoelii* (252), which may contribute to the higher pathogen burden. It remains to be seen precisely how lipocalin-2 affects immune cells in malaria and whether the effect of lipocalin-2 is mediated by decreased immune cell iron availability.

Iron supplementation may also affect the immune response to malaria. A study by Azcarate *et al.* found that extensive parenteral iron supplementation prior to infection with *P. yoelii* resulted in lower parasitaemia (253). The iron supplemented mice may have had more macrophages and dendritic cells in the spleen after infection, however, the applied statistical tests did not allow for a proper comparison. Moreover, iron supplementation suppressed reticulocytosis (253), which could explain the lower parasitaemia. Hence, these findings must be interpreted with caution. Iron overload in *P. berghei* infection may also prevent the development of cerebral malaria and improve survival (254). Parenteral iron supplementation increased systemic inflammation but decreased T cell chemotaxis. Consequently, iron supplemented mice had

fewer Th1 cells and more Tregs in the spleen, and decreased sequestration of T cells in the brain. The researchers thus proposed that excess iron makes T cells refractory to IFNγ signalling, resulting in decreased chemotaxis and neuropathology (254).

More recently, a study in humans found that iron deficiency is associated with attenuated antibody responses to malaria (255). The study showed that children in Kenya and Uganda with iron deficiency have lower anti-*P. falciparum* antibody titres to blood stage antigens MSP1 and AMA1, compared to iron replete children. This effect persisted even after the researchers accounted for potentially confounding factors such as previous malaria exposure, parasitaemia and study site. Furthermore, they discovered that iron deficiency has a greater impact on antibody levels in children with high malaria exposure, and that anti-*P. falciparum* antibody levels remained suppressed over the course of several years in iron deficient children (255). At least two other studies have also found an association between iron deficiency and reduced anti-*P. falciparum* antibody levels (191,256). However, these studies did not determine whether the decreased antibody levels are the result of altered immune function or decreased malaria exposure.

In summary, there are some indications that both iron deficiency and iron overload can affect the immune response to malaria, but many unknowns remain. Previous pre-clinical studies have primarily been focused on iron overload and they have often failed to take into account the confounding effects of iron on RBCs. Existing clinical studies demonstrate the importance of understanding how iron deficiency impacts on malaria immunity, but so far, they have not provided mechanistic insight. Hence, the effect of iron deficiency on different immune cell types and immune cell interactions in malaria remain to be elucidated.

5.1.2. Aims

In this chapter we aim to investigate how cellular iron deficiency affects the immune response to blood stage malaria infection. To this end, we use a mouse model with decreased cellular iron uptake, but no severe anaemia, and *P. chabaudi*, which does not preferentially infect reticulocytes. Thus, we hope to minimise the confounding effects of iron on RBCs. We also aim

to explore whether the higher pathogen burden observed in mice with decreased cellular iron uptake is caused by an impaired immune response.

5.2. Results

5.2.1. Decreased cellular iron uptake impairs the immune response to *P. chabaudi*

To investigate if decreased cellular iron uptake affects the immune response to malaria, wild-type and *Tfrc*$^{Y20H/Y20H}$ mice were infected with *P. chabaudi*, as previously described (see 4.2. Results). Serum cytokine levels were measured four, six and eight days after infection, using a flow cytometry based multiplex cytokine assay.

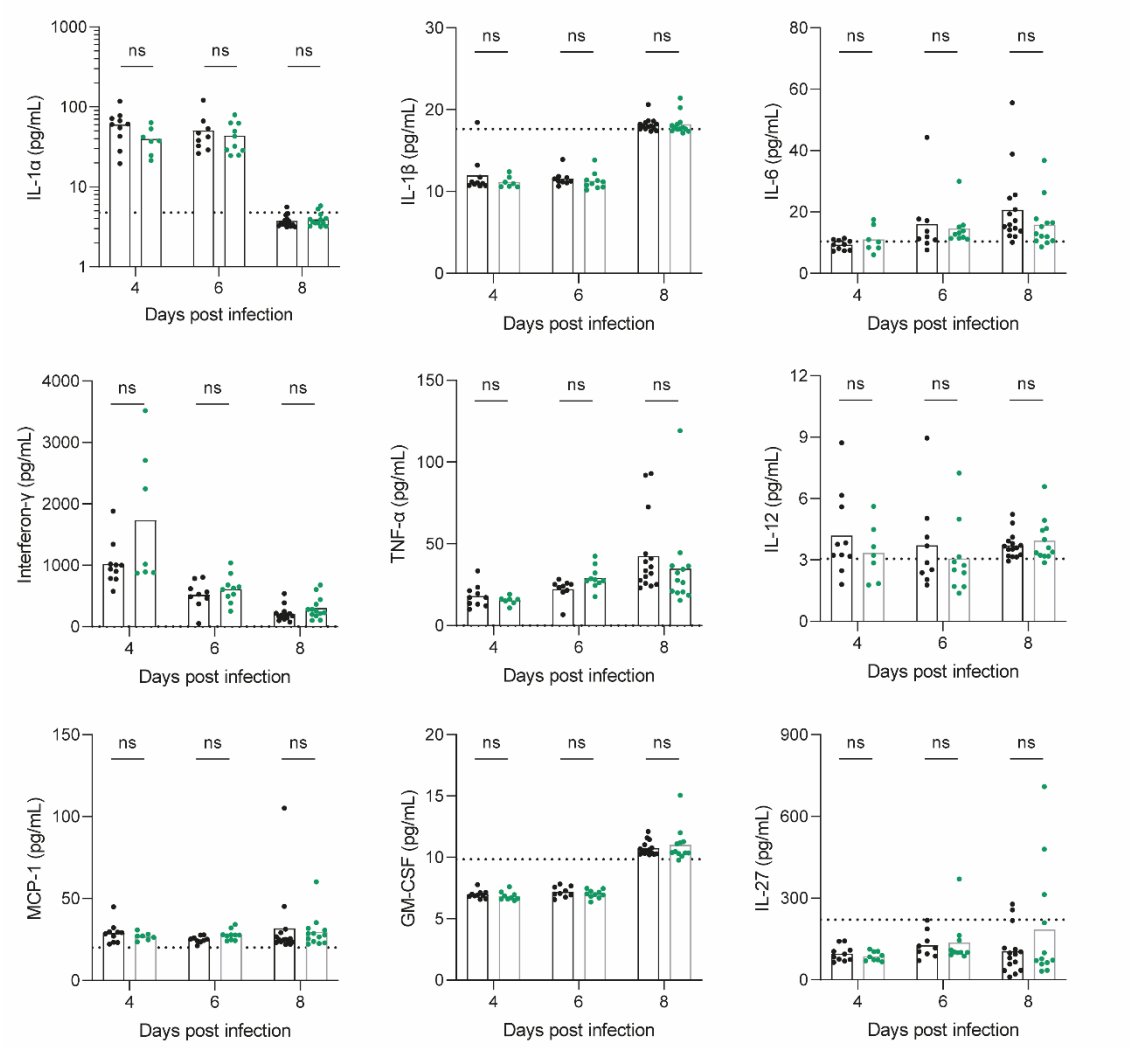


***Figure 5.1*. Decreased cellular iron does not substantially alter circulating cytokine levels during *P. chabaudi* infection.** Serum cytokine levels were measured in C57BL/6 (black) and *Tfrc*$^{Y20H/Y20H}$ (green) mice infected with *P. chabaudi*. Dotted line represents uninfected mice. Mean, multiple t-test's with Welch's correction and Holm-Sidak's m.c.t. on log transformed data, n=7-15, N=2 (pooled).

Out of the 13 cytokines measured, three were below the limit of detection (IL-10, IL-17 & IL-23) and one was excluded due to a technical issue (IFNβ). Only IL-1α, IFNγ and TNFα were substantially elevated above homeostatic levels during *P. chabaudi* infection (Figure 3.4 & 5.1). Additionally, the only significant difference in serum cytokines was that *Tfrc*$^{Y20H/Y20H}$ mice had higher circulating IFNγ levels on the fourth day of infection. Furthermore, there was a trend towards lower IL-1α levels in mice with decreased iron uptake, four days after infection. Taken together, it does not appear that cellular iron uptake substantially affects systemic inflammation during *P. chabaudi* infection.

The serum cytokine response may not, however, be representative of immunity in the key tissue sites of parasite clearance. It has previously been shown that systemic inflammation is not strongly induced in mice infected with recently mosquito transmitted *P. chabaudi*, compared to infection with serially blood passaged parasites (182,257). However, the host still mounts an efficient immune response and increased cytokine production can be detected in the spleen (182,257). As the spleen is the key site for the immune response to blood stage malaria, further investigations were focused on the splenic immune response (258). Notably, mice with decreased cellular iron uptake had attenuated splenomegaly compared to wild-type mice at the peak of infection, indicating that the splenic response may be disrupted (Figure 5.2A-B).

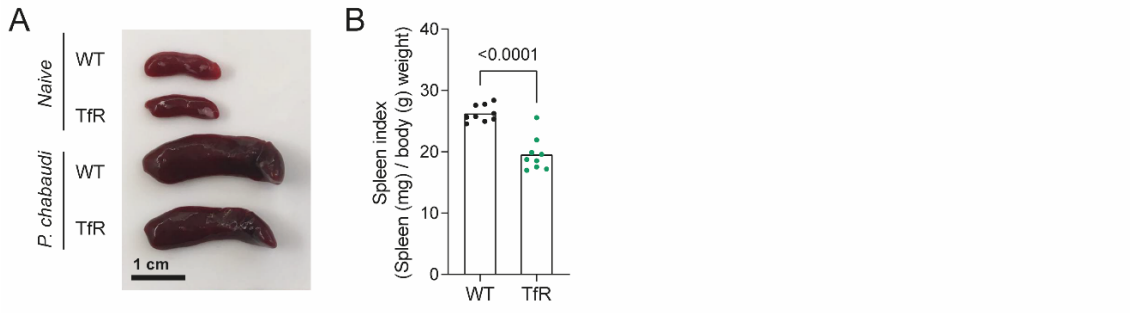


***Figure 5.2*. Decreased cellular iron uptake attenuates *P. chabaudi* induced splenomegaly. A)** Spleens from naïve and *P. chabaudi* infected C57BL/6 (WT) and *Tfrc*$^{Y20H/Y20H}$ (TfR) mice. **B)** Spleen index of WT and TfR mice eight days after *P. chabaudi* infection. Mean, Welch's t-test, n=9, N=4.

Malaria infection leads to an influx of myeloid cells into the spleen, where they are involved in cytokine production, antigen presentation and phagocytosis of iRBCs (131–133). Infiltrating monocytes, dendritic cells and resident macrophage populations are known to adopt highly

heterogeneous and context dependent cell states at inflammatory sites (259). Unfortunately there is no consensus for how to identify mononuclear phagocytes in murine malaria (260) and it can be difficult to identify specific populations due to autofluorescence and ambiguous surface marker expression during infection. In our study, we identified a putative mononuclear phagocyte (MNP) population by the absence of other characteristic cell type makers such as: TER119^{+} erythroid cells, B220^{+} B cells, CD90.2^{+} T cells, NK1.1^{+} NK cells, Siglec-F^{+} eosinophils and Ly6G^{+} neutrophils. Subsequently, two distinct MNP populations were identified: one was defined as CD11b^{hi} Ly6C^{hi} and likely consists of pro-inflammatory monocytes and monocyte-derived macrophages (Mo/Mac), and the other was defined as CD11c^{+} MHC-II^{+} and probably consists of inflammatory monocyte-derived and conventional DCs (supplementary Figure S5). However, the markers expressed by these MNP subsets should be considered more important than the labels that are used to refer to them here (i.e. Mo/Mac & DC). The number of Mo/Macs and DCs was increased in *P. chabaudi* infected mice, but this accumulation was significantly reduced in mice with decreased cellular iron uptake compared to wild-type mice (Figure 5.3A-B). To assess the effector function of these MNPs, intracellular cytokine staining was performed after *ex vivo* treatment with a protein transport inhibitor. We attempted to stain for multiple cytokines, but only IFNγ could be reliably detected. MNPs from uninfected mice did not produce IFNγ but 10-20% of MNPs from *P. chabaudi* infected mice produced IFNγ (Figure 5.3C). Furthermore, significantly fewer MNPs and DC from mice with decreased cellular iron uptake produced IFNγ (Figure 5.3C). The per cell IFNγ production, as measured by geometric mean fluorescence intensity (gMFI), did not differ between *Tfrc*$^{Y20H/Y20H}$ and wild-type mice (Figure 5.3D). Unfortunately, too few Mo/Macs were used for the intracellular cytokine staining assay to reliably measure their IFNγ production.

To further characterise the myeloid response to *P. chabaudi* in the spleen during the acute stage of infection, neutrophils (Ly6G^{+}) and eosinophils (Siglec-F^{+}) were assessed. Neutrophil numbers were increased during infection, however, cellular iron uptake did not affect splenic neutrophil frequencies (Figure 5.3E). Eosinophils numbers were not increased during infection,

and there was no difference in the frequency of eosinophils in infected wild-type and *Tfrc*$^{Y20H/Y20H}$ mice (Figure 5.3F). In summary, mice with decreased cellular iron uptake have an attenuated splenic MNP response to *P. chabaudi* infection, potentially resulting in impaired anti-parasite immunity.

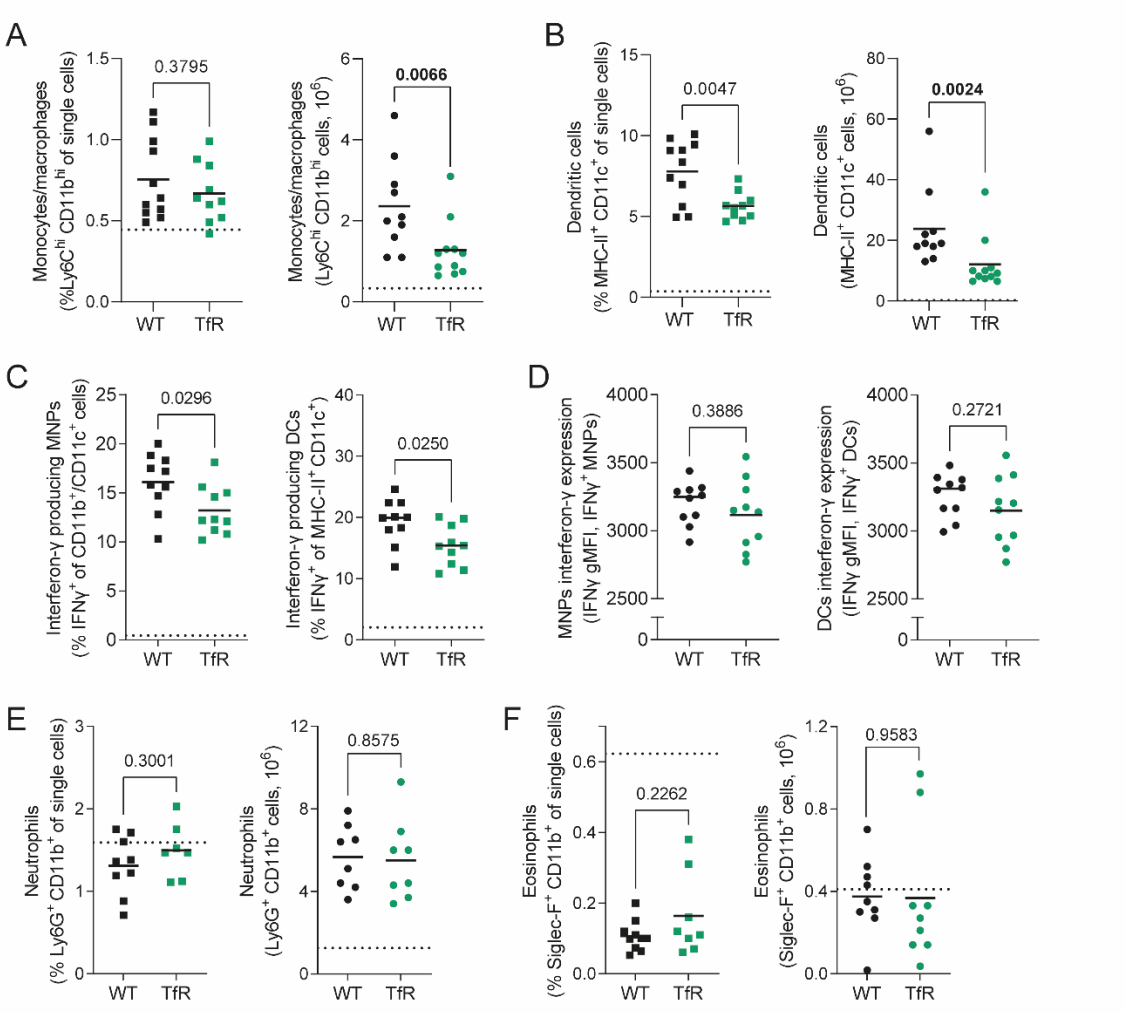


***Figure 5.3*. Decreased cellular iron impairs the mononuclear phagocyte response to *P. chabaudi* infection. A-B & E-F)** Percentages and absolute numbers of mononuclear phagocytes (MNPs) (A-B) and granulocytes (E-F) in the spleen of *P. chabaudi* infected C57BL/6 (WT) and *Tfrc*$^{Y20H/Y20H}$ (TfR) mice, eight days after infection **C-D)** Splenic MNP interferon γ (IFNγ) production, detected by intracellular cytokine staining. Dotted line represents uninfected mice. Mean, Welch's t-test / **Welch's t-test on log transformed data**, n=8-11, N=1-4.

T cells are a critical component of the immune response to malaria (115), and we therefore sought to assess the splenic T cell response to *P. chabaudi* eight days after infection. The total number of T cells (TCRβ$^+$) in the spleen was increased approximately three-fold in infected mice, but there was no difference in the number of T cells between mice with normal and

decreased cellular iron uptake (Figure 5.4A). However, T cells did represent a higher percentage of total splenocytes in *Tfrc*$^{Y20H/Y20H}$ mice (Figure 5.4A), likely due to the observed decrease in MNPs and erythroblasts (Figures 4.5 & 5.3). Similarly, CD8 T cell (CD8^{+}) numbers and the percentage of antigen experienced (CD44^{+}) CD8 T cells increased during *P. chabaudi* infection, although there was no difference between wild-type and *Tfrc*$^{Y20H/Y20H}$ mice (Figure 5.4B-C). The number of splenic CD4 T cells (CD4^{+}) increased almost three-fold in response to *P. chabaudi* infection in both genotypes (Figure 5.4D). Although, decreased cellular iron uptake did not affect the total number of CD4 T cells, it did reduce the percentage of antigen experienced (CD44^{+}) CD4 T cells (Figure 5.4E). As NK cells are important contributors to the immune response to malaria (124), splenic NK cells were also analysed eight days after infection.

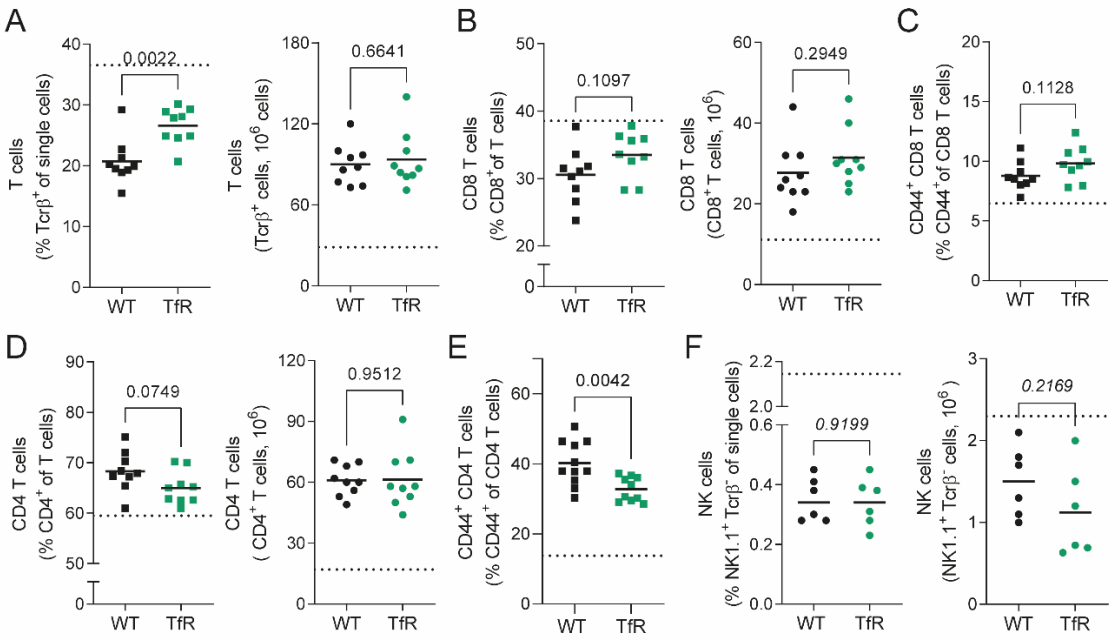


***Figure 5.4*. Decreased cellular iron attenuates the CD4 T cell response to *P. chabaudi* infection. A, B, D & F)** Percentages and absolute numbers of total, CD8 and CD4 T cells, and NK cells in the spleen of *P. chabaudi* infected C57BL/6 (WT) and *Tfrc*$^{Y20H/Y20H}$ (TfR) mice, eight days after infection. **C & E)** Percentage of antigen experienced (CD44^{+}) CD8 and CD4 T cells. Dotted line represents uninfected mice. Mean, Welch's t-test / Mann-Whitney test, n=8-11, N=1-4.

The number of splenic NK cells (NK1.1^{+}) was decreased compared to uninfected mice, but infected wild-type and *Tfrc*$^{Y20H/Y20H}$ mice had comparable NK cell frequencies (Figure 5.4F). In summary, *P. chabaudi* infection induced numerically comparable T cell responses in mice with

normal and decreased cellular iron uptake, however, CD4 T cell activation was impaired in mice with decreased iron uptake.

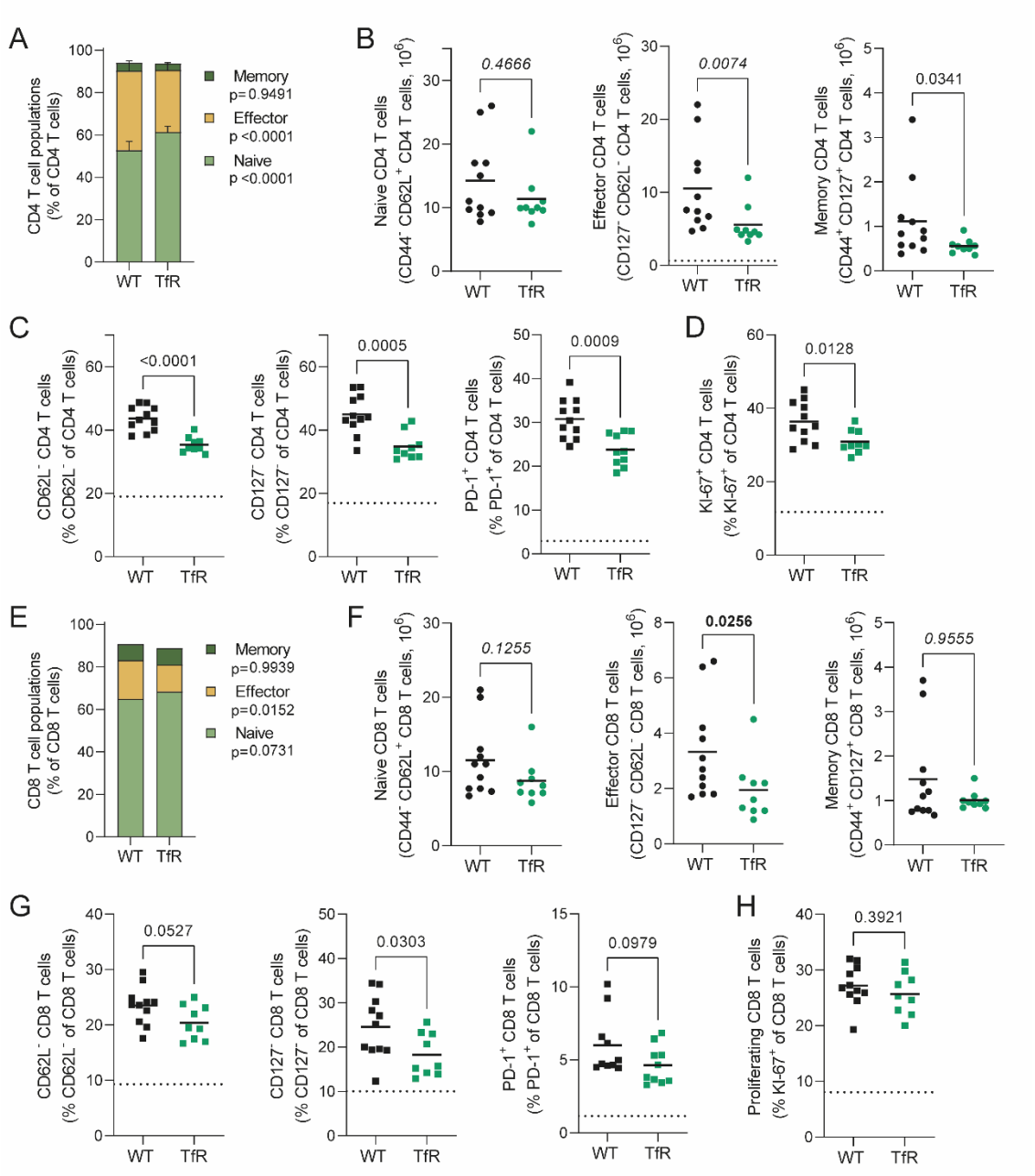


***Figure 5.5*. Decreased cellular iron impairs the effector T cell response to *P. chabaudi* infection. A-B & E-F)** Percentages and absolute numbers of naïve, effector and memory CD4 and CD8 T cells in the spleen of *P. chabaudi* infected C57BL/6 (WT) and *Tfrc*$^{Y20H/Y20H}$ (TfR) mice, eight days after infection. **C & G)** Percentage of CD4 and CD8 T cells expressing markers associated with naivety (CD127 & CD62L) and antigen experience (PD-1). **D & H)** Proliferating (KI-67^{+}) CD4 and CD8 T cells. Dotted line represents uninfected mice. **A & E)** Mean ± SD, two-way ANOVA, Sidak's m.c.t., n=8-11, N=1. **B-D & F-H)** Mean, Welch's t-test / **Welch's t-test on log transformed data** / *Mann-Whitney test*, n=8-11, N=1.

With this in mind, we further analysed the conventional (FOXP3$^-$) CD4 T cell phenotype during the acute stage of *P. chabaudi* infection. Mice with decreased cellular iron uptake had fewer effector (CD127$^-$ CD62L$^-$) CD4 T cells but comparable numbers of naïve (CD44$^-$ CD62L$^+$) and memory (CD44$^+$ CD127$^+$) CD4 T cells (Figure 5.5.A-B) (261). In addition, more CD4 T cells expressed markers associated with naivety (CD62L & CD127) and fewer expressed markers associated with antigen experience (CD44 & PD-1), in *Tfrc*$^{Y20H/Y20H}$ mice (Figure 5.4E & 5.5.C). Moreover, mice with decreased iron uptake had fewer conventional CD4 T cells that express proliferation marker KI-67, indicating that their CD4 T cells were dividing less (Figure 5.5.D). Altogether, these findings show that the effector CD4 T cell response is impaired in mice with decreased cellular iron uptake during *P. chabaudi* infection.

Although there was no difference in the percentage of CD44$^+$ CD8 T cells (Figure 5.4.C), their phenotype was also investigated in more depth. *Tfrc*$^{Y20H/Y20H}$ mice had fewer effector CD8 T cells, but there was no difference in the number of naïve or memory CD8 T cells (Figure 5.5E-F). There were more CD8 T cells expressing markers associated with naivety (CD62L & CD127) in mice with decreased iron uptake, however, it was not accompanied by a significant decrease in cells expressing markers associated with antigen experience (CD44 & PD-1) (Figure 5.4C & 5.5G). There was also no difference in the frequency of KI-67$^+$ proliferating CD8 T cells between the two genotypes (Figure 5.5.H). On the whole, it appears that the CD8 T cell response to infection is also attenuated in mice with decreased cellular iron uptake, albeit to a lesser degree than CD4 T cellsCD4 T cells can become polarised into T helper subsets with specialised functions (262). Given that the effector T cell response was suppressed by disrupted iron uptake, we wanted to investigate whether CD4 T cell differentiation was also affected. We focussed on two T helper subset that are known to be important during malaria infection: Th1 and Tfh cells. *Tfrc*$^{Y20H/Y20H}$ mice had fewer Th1 cells (T-BET$^+$) in the spleen, compared to wild-type mice, eight days after *P. chabaudi* infection (Figure 5.6A). Additionally, fewer CD4 T cells in mice with decreased cellular iron uptake expressed the IFNγ inducible chemokine receptor CXCR3 (Figure 5.6B), further demonstrating that the IFNγ mediated Th1 response was

attenuated. In line with this, mice with decreased cellular iron uptake had fewer IFNγ producing CD4 T cells, without affecting the amount of IFNγ produced per IFNγ^{+} cell (Figure 5.6C). Taken together, this data demonstrates a clear impairment of the Th1 effector cell response, which is known to be critical for parasite control during blood-stage infection, in mice with decreased cellular iron uptake.

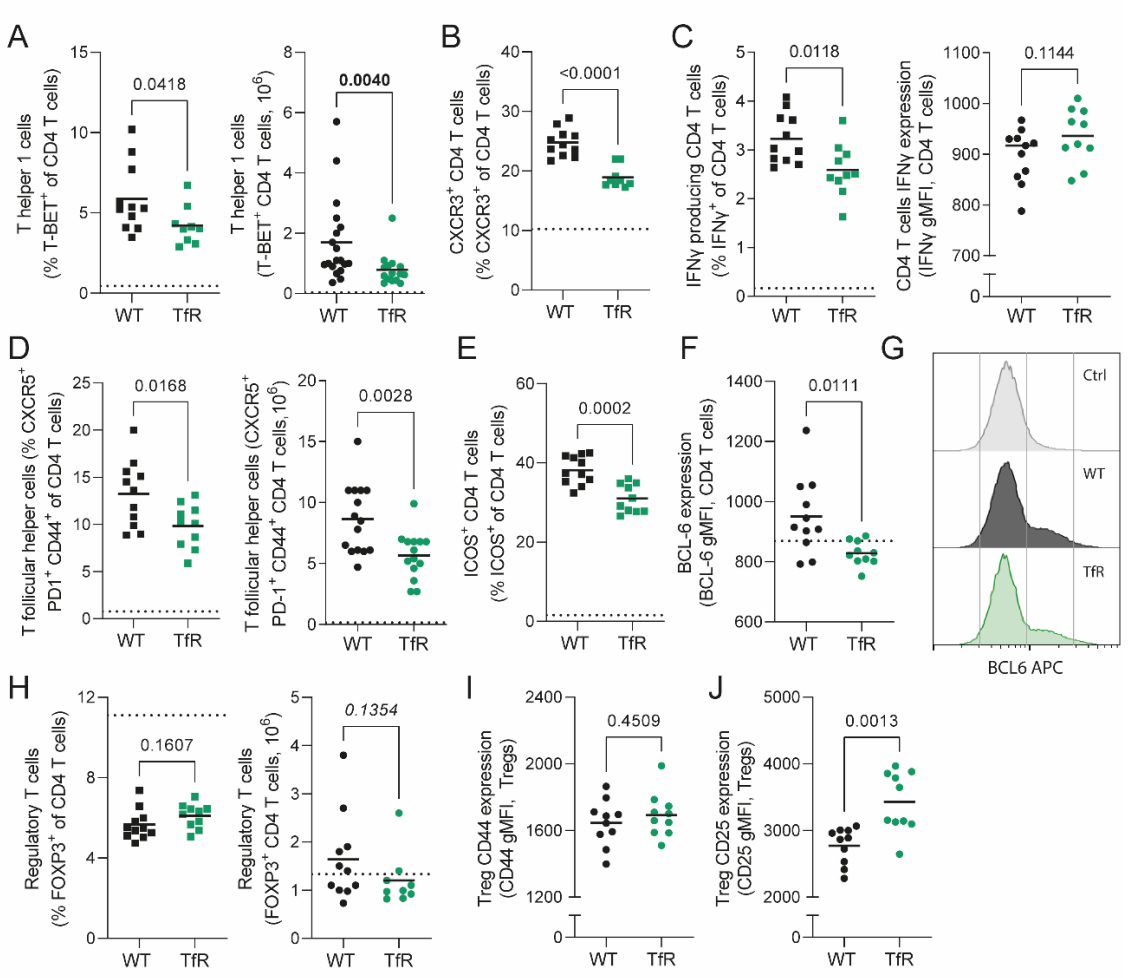


***Figure 5.6*. Decreased cellular iron alters CD4 T cell differentiation and effector function in *P. chabaudi* infection.** Conventional CD4 T cells in the spleen of *P. chabaudi* infected C57BL/6 (WT) and *Tfrc*$^{Y20H/Y20H}$ (TfR) mice, eight days after infection. **A)** Percentage and absolute number of T helper 1 cells. **B)** Percentage of CXCR3^{+} CD4 T cells. **C)** Interferon γ (IFNγ) producing CD4 T cells. **D)** Percentage and absolute number of T follicular helper (Tfh) cells. **E-F)** CD4 T cell expression of markers of Tfh function: ICOS and BCL-6. **G)** Flow cytometry plot of BCL-6 expression in CD4 T cells (normalised to mode). **H)** Percentage and absolute number of regulatory T cells (Tregs). **I-J)** Treg expression of markers of suppressive function: CD44 and CD25. Dotted line represents uninfected mice. Mean, Welch's t-test / **Welch's t-test on log transformed data** / *Mann-Whitney test*, n=9-11, N=2-4.

Next, we examined Tfh cells, which provide essential support to B cells to promote the formation of high affinity antibodies (146). Mice with decreased cellular iron uptake had

significantly fewer Tfh cells, eight days after *P. chabaudi* infection (Figure 5.6D). In addition, *Tfrc*$^{Y20H/Y20H}$ mice had significantly fewer CD4 T cells expressing co-stimulatory receptor ICOS and lower expression of the transcription factor BCL-6 in CD4 T cells (Figure 5.6E-G). Both ICOS and BCL-6 are key proteins involved in humoral immune responses in malaria (147,149). Overall, this data indicates that *Tfrc*$^{Y20H/Y20H}$ CD4 T cells may not be able to fully support B cell function and the formation of humoral immunity to *P. chabaudi.*

Tregs can modulate pro-inflammatory immune responses, and we wondered if an enhanced Treg response could be contributing to the suppressed effector T cell response in mice with decreased iron uptake. Tregs were decreased as a percentage of total splenocytes during acute *P. chabaudi* infection, but largely remained unaltered in terms of absolute numbers (Figure 5.6H). Additionally, there was no difference in Treg numbers between *Tfrc*$^{Y20H/Y20H}$ and wild-type mice (Figure 5.6H). Treg activation was further examined by measuring the surface expression of CD44 and CD25, two surface markers that are upregulated on more suppressive Tregs (263,264). *Tfrc*$^{Y20H/Y20H}$ and wild-type mice had equal expression of CD44 (Figure 5.6I). Notably, CD25 expression was increased on *Tfrc*$^{Y20H/Y20H}$ Tregs (Figure 5.6J), indicating that they might be more suppressive. The expression of CD25 was also higher on conventional T cells from *Tfrc*$^{Y20H/Y20H}$ mice (data not shown). In summary, it does not appear that the Treg response to *P. chabaudi* infection is substantially affected by decreased cellular iron uptake. At this point we cannot exclude that *Tfrc*$^{Y20H/Y20H}$ Tregs are more suppressive, however, further studies would be required to substantiate this.

We next sought to assess the B cell response to acute *P. chabaudi* infection. Eight days after infection, the frequency of splenic B cells was increased almost four-fold in both wild-type and *Tfrc*$^{Y20H/Y20H}$ mice, compared to uninfected mice (Figure 5.7A). There was no difference between the two genotypes in the absolute number of splenic B cells after infection (Figure 5.7A). However, mice with decreased cellular iron uptake had significantly fewer activated B cells (Figure 5.7B). In addition, *Tfrc*$^{Y20H/Y20H}$ mice had fewer antibody secreting cells (ASC, used here to collectively refer to plasmablasts and plasma cells) and GC B cells, indicating that

differentiation was impaired (Figure 5.7C-D). By analysing membrane-bound and intracellular immunoglobin expression, more information can be obtained about B cell function. B cells downregulate surface IgD but maintain IgM upon activation, and they can undergo class-switching to IgG, IgA or IgE before entering germinal centres (146,265). ASCs do not express membrane-bound Ig but produce and secrete large amounts of IgM, IgG, IgA or IgE antibodies, which can be detected intracellularly (266).

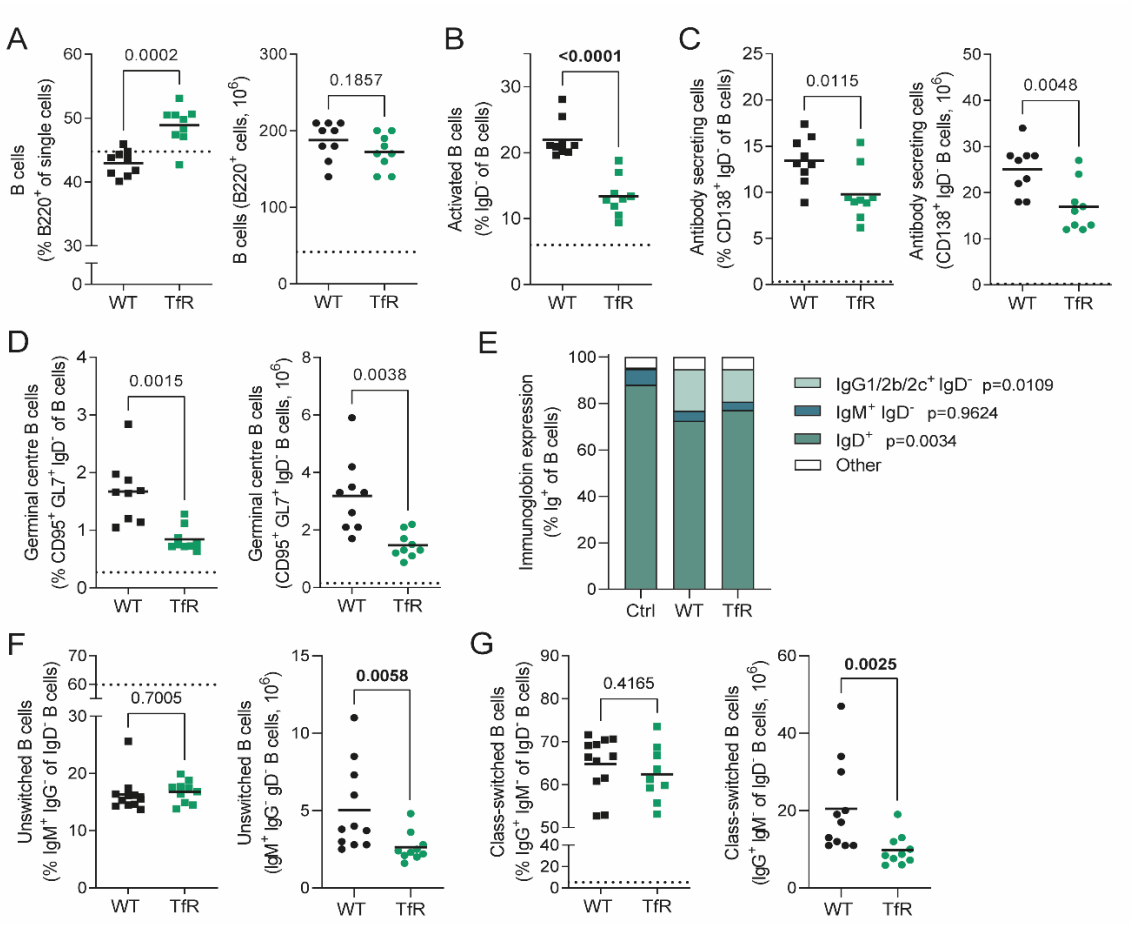


Figure 5.7. **Decreased cellular iron impairs the B cell response to *P. chabaudi* infection. A-D)** Percentages and absolute numbers of total, activated, antibody secreting and germinal centre B cells in the spleen of *P. chabaudi* infected C57BL/6 (WT) and *Tfrc*$^{Y20H/Y20H}$ (TfR) mice, eight days after infection. **E)** Percent IgD$^+$, IgM$^+$ and IgG$^+$ B cells. **F-G)** Percentages and absolute numbers of unswitched and class-switched activated B cells. Dotted line represents uninfected mice. **A-D & F-G)** Mean, Welch's t-test / **Welch's t-test on log transformed data**, n=9-11, N=1-4. **E)** Mean, two-way ANOVA with Sidak's m.c.t., n=9-11, N=2.

The frequency of resting (IgD$^+$) B cells was greatly reduced and the frequency of class-switched (IgG$^+$) B cells was increased upon *P. chabaudi* infection (Figure 5.7E). *Tfrc*$^{Y20H/Y20H}$ mice had a

lower percentage of class-switched and a higher percentage of naïve B cells, compared to wild-type mice (Figure 5.7E). However, among activated B cells the proportion of unswitched (IgM^+) and class-switched (IgG^+) B cells did not differ between wild-type and *Tfrc*$^{Y20H/Y20H}$ mice (Figure 5.7F-G). Thus, the overall decrease in class-switched B-cells is likely due to a failure of activation, rather than impaired class-switching *per se*. Taken together, the acute B cell response to *P. chabaudi* was disrupted in mice with decreased cellular iron uptake, which could potentially result in decreased protective immunity.

Finally, we wished to determine if the impaired immune responses observed during the acute stage of infection would persist to the chronic stage of infection. Therefore, the immune response to *P. chabaudi* was assessed 20 days after infection in wild-type and *Tfrc*$^{Y20H/Y20H}$ mice (Figure 5.8A). Mo/Mac and DC frequencies were still somewhat increased in the spleen compared to uninfected mice, although the DC response had largely contracted since day eight post infection (Figure 5.8B-C). Moreover, there were no longer any significant differences in the frequency of splenic MNPs between wild-type and *Tfrc*$^{Y20H/Y20H}$ mice, 20 days after infection (Figure 5.8B-C). The T cell response had also contracted, almost to pre-infection levels, and there was no difference in the absolute number of total T cells or CD4 T cells between the two genotypes (Figure 5.8D-E). Notably, the frequency of antigen experienced $CD44^+$ CD4 T cells was lower in mice with decreased iron uptake, indicating that they still had an impaired effector CD4 T cell response (Figure 5.8E). Correspondingly, *Tfrc*$^{Y20H/Y20H}$ mice still had significantly fewer Tfh cells 20 days after infection (Figure 5.8G). B cell frequencies remained elevated in the spleen of infected mice and the percentage of activated B cells was in fact higher compared to day eight (Figure 5.8H-1). Additionally, *Tfrc*$^{Y20H/Y20H}$ mice still had fewer activated B cells (Figure 5.7I). GC B cell frequencies were also increased compared to the acute stage of infection and mice with normal iron uptake had, on average, a two-fold greater GC B cell response than mice with decreased iron uptake (Figure 5.7J-K). Therefore, we can conclude that low cellular iron availability had persistent negative effects on the humoral immune response to *P. chabaudi*.

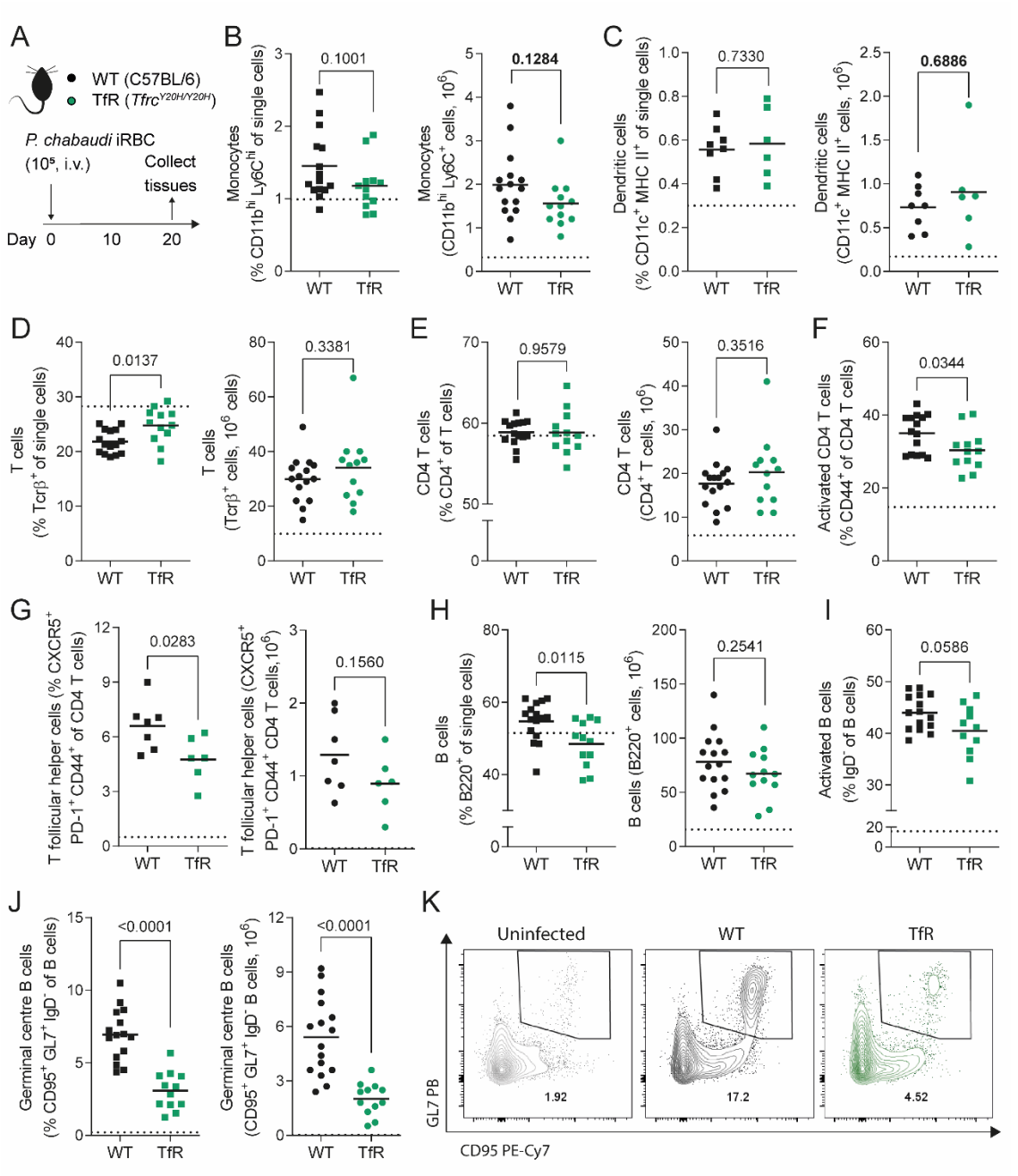


Figure 5.8. **Decreased cellular iron impairs the late germinal centre response to *P. chabaudi* infection. A-J)** Percentages and absolute numbers of indicated immune cell subsets in the spleen of *P. chabaudi* infected C57BL/6 (WT) and *Tfrc*$^{Y20H/Y20H}$ (TfR) mice, 20 days after infection. Mean, Welch's t-test / **Welch's t-test on log transformed data**, n=6-15, N=1-2 (pooled). **K)** Flow cytometry plot of germinal centre B cells, 20 days after *P. chabaudi* infection.

5.2.2. *Tfrc*$^{Y20H/Y20H}$ lymphocyte impairment is caused by cellular iron deficiency and can be rescued by iron supplementation

TfR1 is upregulated on activated lymphocytes and it has been proposed to have signalling functions in addition to its role in iron transport (267,268). We therefore sought to determine whether the immune impairment seen in *Tfrc*$^{Y20H/Y20H}$ mice was due to cellular iron deficiency or

another effect caused by the *Tfrc* mutation. Additionally, we intended to determine whether the *Tfrc*$^{Y20H/Y20H}$ mutation had immune cell-intrinsic effects.

To this end, naïve CD4 T cells were isolated from wild-type and *Tfrc*$^{Y20H/Y20H}$ mice, and cultured for five days *in vitro* in Th1 polarising media, with or without iron supplementation (Figure 5.9A). Cell viability of *Tfrc*$^{Y20H/Y20H}$ CD4 T cells was reduced compared to wild-type cells, but viability could be improved by iron supplementation (Figure 5.9B).

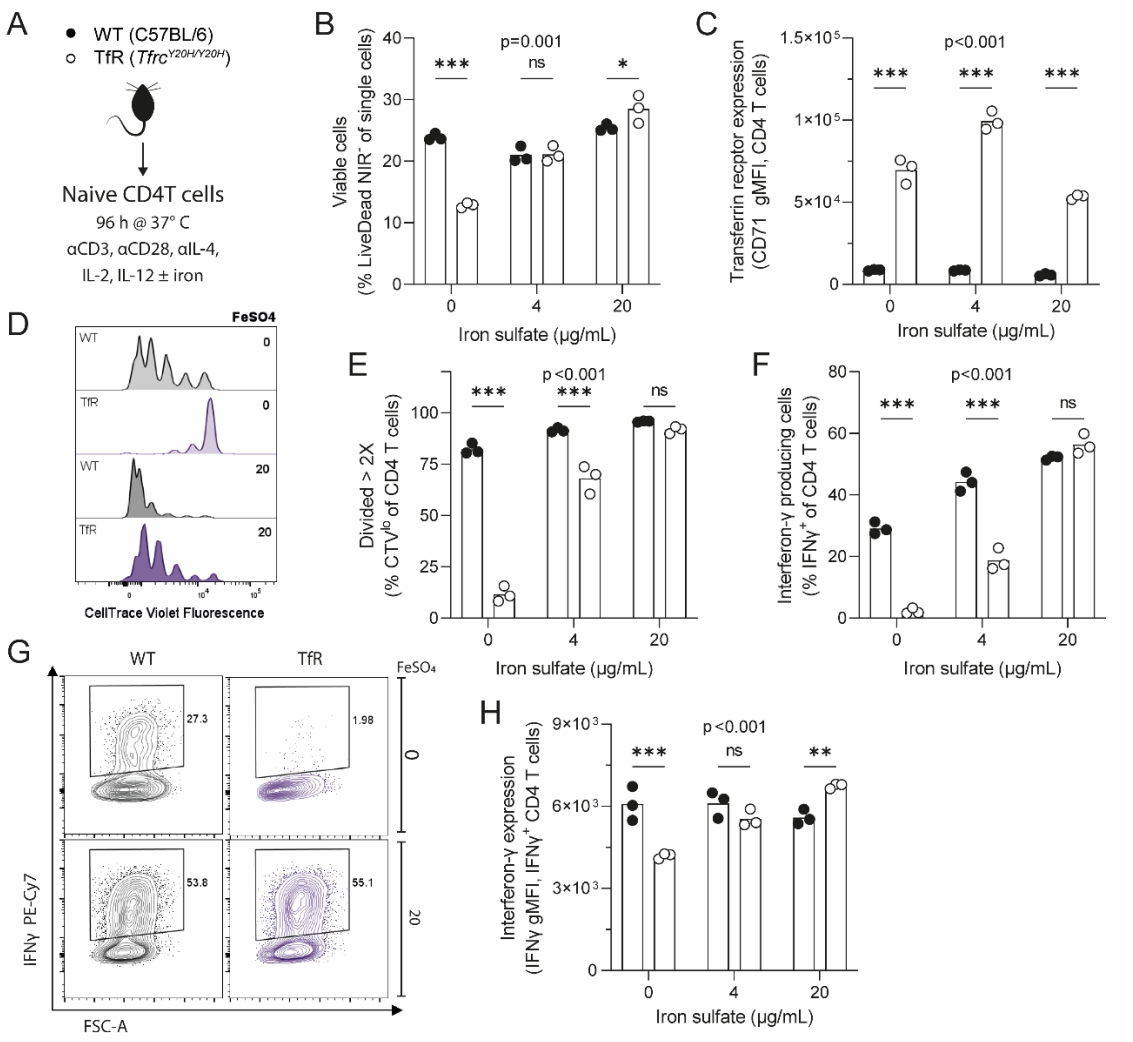


***Figure 5.9. In vitro* T helper 1 (Th1) polarised *Tfrc*$^{Y20H/Y20H}$ CD4 T cells have impaired proliferation and effector function, which can be rescued by iron supplementation. A)** Naïve CD4 T cells were isolated from C57BL/6 (WT) and *Tfrc*$^{Y20H/Y20H}$ (TfR) mice, and cultured for 96 h in Th1 polarising media, with varying concentrations of iron sulfate ($FeSO_4$). **B)** CD4 T cell viability. **C)** Transferrin receptor (CD71) expression. **D)** Flow cytometry plot of CD4 T cell CellTrace Violet dilution. **E)** Percentage of CD4 T cells that have divided more than two times (> 2X). **F & H)** Percentage of interferon γ (IFNγ) producing CD4 T cells and IFNγ production per cell. **G)** Flow cytometry plot of CD4 T cell IFNγ production. Mean, repeated measures two-way ANOVA with Sidak's m.c.t., n=3, N=3.

TfR1 surface expression on lymphocytes is regulated both by iron requirements and activation status, and as expected, all *Tfrc*$^{Y20H/Y20H}$ T cells had elevated TfR1 expression (Figure 5.9C). The varying TfR1 expression across iron supplementation conditions indicates that *Tfrc*$^{Y20H/Y20H}$ CD4 T cells were responsive to iron availability (Figure 5.9C). Proliferation, as measured by CellTrace Violet dilution, was substantially impaired in *Tfrc*$^{Y20H/Y20H}$ CD4 T cells, but could be completely rescued by iron supplementation (Figure 5.9D-E). Furthermore, *Tfrc*$^{Y20H/Y20H}$ CD4 T cells did not produce IFNγ, but iron supplementation increased the frequency of IFNγ expressing cells in a dose dependent manner (Figure 5.9F-G). Interestingly, iron supplementation also increased the percentage of IFNγ producing wild-type CD4 T cells (Figure 5.9F). The IFNγ production per IFNγ^{+} *Tfrc*$^{Y20H/Y20H}$ CD4 T cell was also decreased compared to wild-type, but increased with iron supplementation (Figure 5.9H). In summary, *Tfrc*$^{Y20H/Y20H}$ CD4 T cells cultured in Th1 polarising conditions had impaired proliferation and effector function, which could be completely rescued by iron supplementation.

To further investigate the effects of the *Tfrc*$^{Y20H/Y20H}$ mutation on lymphocytes, B cells from naïve wild-type and *Tfrc*$^{Y20H/Y20H}$ mice were isolated and activated *in vitro*, with or without iron supplementation (Figure 5.10A). *Tfrc*$^{Y20H/Y20H}$ B cells had slightly reduced viability after 72 h of culture, unless they were cultured in iron supplemented media (Figure 5.10B).The expression of TfR1 varied with iron supplementation, demonstrating that both *Tfrc*$^{Y20H/Y20H}$ and wild-type B cells were responsive to iron availability (Figure 5.10C). In addition, the expression of B cell activation marker large neutral amino acid transporter-1 (LAT-1) was lower on *Tfrc*$^{Y20H/Y20H}$ B cells, but its expression increased with iron supplementation (Figure 5.10D). Moreover, *Tfrc*$^{Y20H/Y20H}$ B cells had severely impaired proliferation, which was improved by iron supplementation, in a dose dependent manner (Figure 5.10E-F). Furthermore, *Tfrc*$^{Y20H/Y20H}$ B cells had disrupted T cell independent *in vitro* differentiation into CD138^{+} ASCs and class-switched surface IgG1^{+} B cells (Figure 5.10G-I). However, differentiation could be completely rescued by iron supplementation. Interestingly, in wild-type mice iron supplementation appeared to skew B cell differentiation, away from IgG1^{+} and towards CD138^{+} B cells (Figure

5.10H-I). In summary, this data shows that activation, proliferation and differentiation was impaired in *Tfrc*$^{Y20H/Y20H}$ B cells and that B cell function could be rescued by iron supplementation.

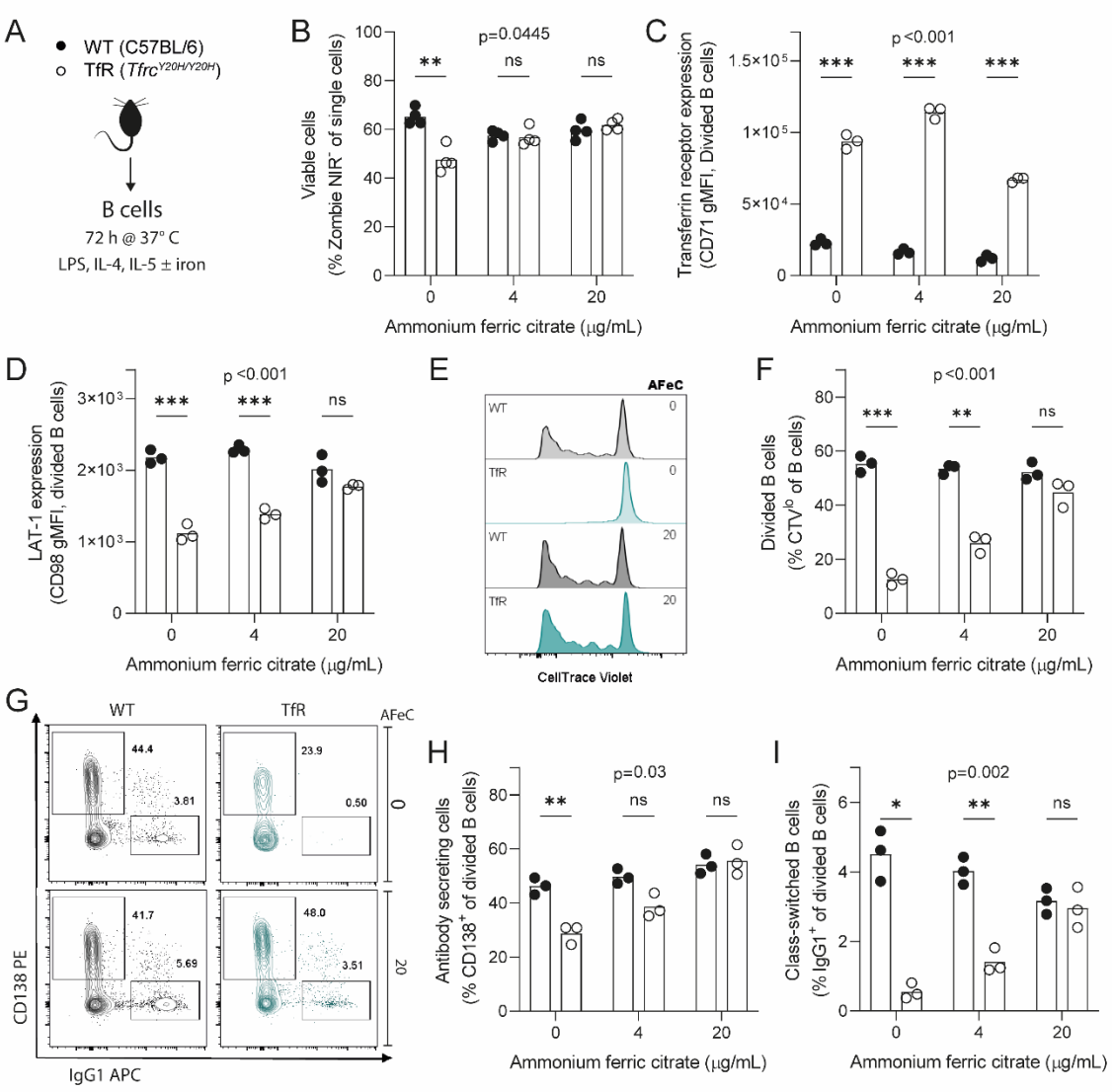


***Figure 5.9. In vitro* cultured *Tfrc*$^{Y20H/Y20H}$ B cells have impaired activation, proliferation and differentiation, which can be rescued by iron supplementation. A)** B cells were isolated from C57BL/6 (WT) and *Tfrc*$^{Y20H/Y20H}$ (TfR) mice, and cultured for 96 h in B cell activating media, with varying concentrations of ammonium ferric citrate (AFeC). **B)** B cell viability. **C-D)** Transferrin receptor (CD71) and large neutral amino acid transporter-1 (LAT-1/CD98) expression on divided B cells. **E)** Flow cytometry plot of B cell CellTrace Violet dilution. **F)** Percentage of divided B cells. **G-I)** Flow cytometry plot and percentage of antibody secreting and class-switched divided B cells. Mean, repeated measures two-way ANOVA with Sidak's m.c.t., n=3, N=3.

Taken together, it appears that *Tfrc*$^{Y20H/Y20H}$ immune cell impairment is primarily caused by cellular iron deficiency, as iron supplementation completely rescues lymphocyte function *in*

vitro. In addition, many of the lymphocyte defects observed *in vivo* in *Tfrc*$^{Y20H/Y20H}$ mice infected with *P. chabaudi* were recapitulated *in vitro.* Hence, we have shown that the *Tfrc*$^{Y20H/Y20H}$ mutation causes cell-intrinsic and iron-mediated lymphocyte impairment.

5.3. Discussion

It is well-known that iron deficiency can protect from malaria infection, but little is known about how iron deficiency affects the immune response to malaria. All cells need iron to maintain their cellular functions, especially activated immune cells that need iron to proliferate, differentiate and perform effector functions (73). As a consequence, iron scarcity can limit *Plasmodium* growth but it may also impair the immune response to infection.

In this chapter, a mouse model with disrupted cellular iron uptake was used to study the effects of cellular iron deficiency on the immune response to malaria. We have demonstrated that decreased iron uptake impairs both the cellular and humoral response to malaria infection (Figure 5.11). During acute *P. chabaudi* infection, the immune response of mice with decreased cellular iron uptake was characterised by attenuated effector cell responses, with fewer Mo/Macs, DCs, Th1 cells and ACSs in the spleen. In addition, cellular iron deficiency inhibited the production of IFNγ by MNPs and CD4 T cells in the spleen. Cellular iron deficiency also lead to impaired germinal centre responses, with fewer Tfh cells and GC B cells, both during the acute and chronic stage of infection. Hence, mice with decreased cellular iron uptake had a higher *P. chabaudi* pathogen burden and a weaker immune response, which is indicative of immune impairment.

The question of how decreased cellular iron uptake disrupts the immune response to malaria infection follows from these observations. Previous studies have found that the most profound effect of lymphocyte iron deficiency is reduced proliferation (59,60). In line with this, we found that CD4 T cells and B cells with decreased iron uptake have severely impaired proliferation *in vitro*. This was further supported by the reduction in K-I67^{+} proliferative CD4 T cells *in vivo.* Overall, the impaired proliferative potential may explain the decreased number of immune cells

in the spleen of *P. chabaudi* infected *Tfrc*$^{Y20H/Y20H}$ mice. In addition to proliferation, immune cell activation and differentiation was also disrupted by decreased cellular iron uptake. However, this could potentially also occur as a consequence of decreased proliferation. For example, proliferation is a requirement of ASC differentiation and it may be important for T helper cell differentiation (262,269). Although our data further substantiates that iron deficiency results in impaired immune cell proliferation, it is probably not the sole cause of the changes observed in our model. In the following paragraphs the effect of cellular iron deficiency on distinct immune cell subsets will be discussed.

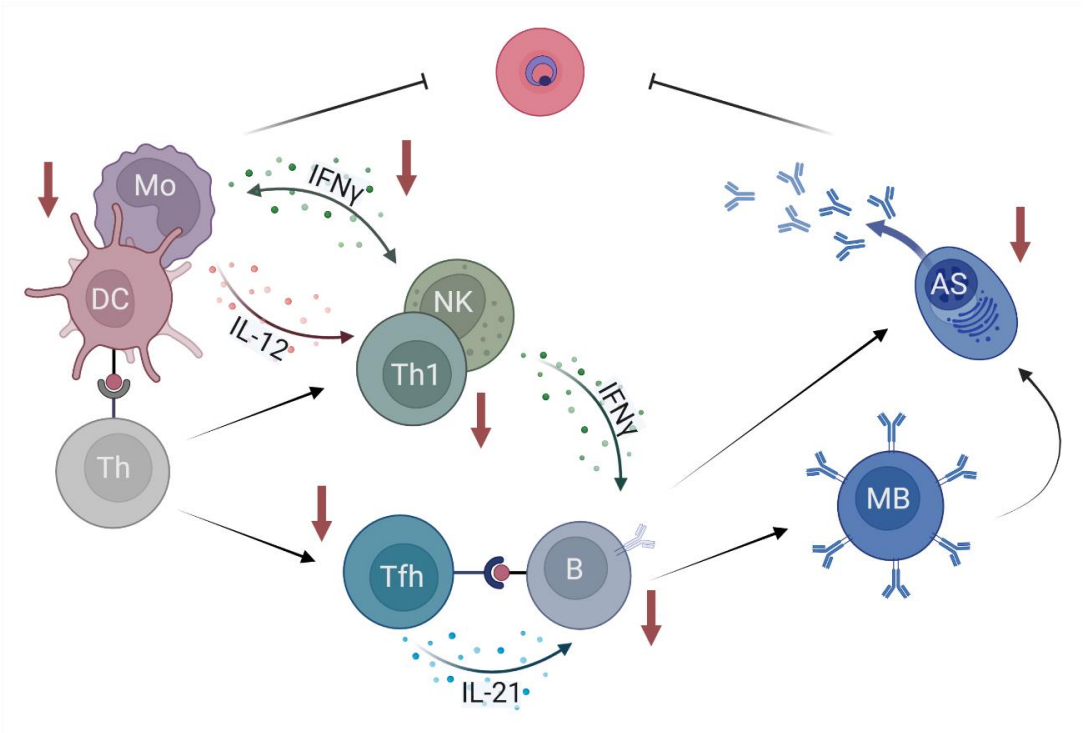


Figure 5.11. **Decreased cellular iron impairs the immune response to malaria.** *Tfrc*$^{Y20H/Y20H}$ mice infected with *P. chabaudi* have fewer splenic effector cells during the acute stage of infection, including fewer monocyte/macrophages (Mo), dendritic cells (DC) and T helper 1 cells (Th1). In addition, these cells produces less interferon γ (IFNγ). Mice with decreased cellular iron uptake also have impaired humoral immunity characterised by fewer T follicular helper cells (Tfh), activated B cells (B), germinal centre B cells and antibody secreting cells (AS). Taken together, the disrupted immune response caused by decreased cellular iron has the potential to impair parasite control.

The acute stage of *P. chabaudi* infection resulted in a large splenic influx of MNPs, especially DCs, but this accumulation was disrupted in mice with decreased cellular iron uptake. Such an influx is typically driven by inflammatory processes and achieved through recruitment and

differentiation of haematopoietic myeloid precursors from the bone marrow (259). TfR1 mediated iron uptake is required for myelopoiesis and hypoferremia impairs granulopoiesis (41,43). Therefore, the *Tfrc* mutation may directly disrupt myeloid progenitor proliferation and the MNP response to malaria infection. Alternatively, iron may play a role in the differentiation or the local expansion of DCs and Mo/Macs in the spleen. Although we did not observe any differences in systemic cytokine or chemokine levels, it is also possible that local differences in cytokine or chemokine levels in the bone marrow or spleen affected MNP activation, proliferation or migration. The impaired MNP response is also interesting in light of the attenuated liver damage observed in mice with decreased cellular iron uptake (see Chapter 4). Potentially, innate immune cell infiltration and activation is also reduced in the liver of $Tfrc^{Y20H/Y20H}$ mice, resulting in less liver inflammation and damage. On the other hand, the impaired MNP response may also lead to reduced parasite control, as these innate populations are crucial effector cells in malaria. In particular, the clear reduction in splenic IFNγ-producing MNPs could lead to decreased phagocytosis of iRBCs and reduced activation of adaptive immune cells (156,257,270). Understanding the role of iron in fuelling MNP function in malaria is an exciting future line of inquiry. Thus, future work should aim to determine if iron deficiency primarily affects emergency myelopoiesis in the bone marrow or MNP expansion and differentiation in the spleen, in malaria. Additionally, efforts should be made to further characterise the effect iron on MNP effector functions, for example through *in vitro* experiments that assess phagocytosis and antigen presentation.

We did not observe any effects of decreased cellular iron uptake on granulocytes or NK cells, eight days after *P. chabaudi* infection. In fact, NK cells appeared to be somewhat depleted in both genotypes at this time point, a feature that is also observed in uncomplicated human blood-stage malaria infection (271). NK cells are important early responders and neutrophils can contribute to immunopathology in malaria (272,273). Thus, they may still be of importance in our model, as iron deficiency is known to impair NK cell antiviral function and hypoferremia inhibits neutrophil production and effector functions (43,274). To gain a more complete picture,

future work should examine these immune cell subsets at earlier time points during infection and focus more on NK cell and neutrophil effector function.

The effector CD4 T cell response to *P. chabaudi* was also disrupted in mice with decreased cellular iron uptake. *Tfrc*$^{Y20H/Y20H}$ mice had fewer splenic Th1 cells and fewer IFNγ producing CD4 T cells eight days after *P. chabaudi* infection. The Th1 differentiation defect and impaired IFNγ production of *Tfrc*$^{Y20H/Y20H}$ CD4 T cells was recapitulated *in vitro*, and could be rescued by iron supplementation. Thereby suggesting that the Th1 impairment observed *in vivo* is cell-intrinsic and iron-dependent. This is in line with previous studies showing that iron deficiency can impair T helper cell differentiation and cytokine production (59,61,62,66). Th1 cells may be particularly sensitive to iron since they express the highest levels of TfR1 and NTBI uptake proteins of any T helper subset *in vitro* (275). Considering the essential role for IFNγ for parasite control (142,156,257), this data clearly indicates that cellular iron deficiency could negatively affect anti-parasite immunity in malaria. However, IFNγ has also been associated with immunopathology, such as experimental cerebral malaria and liver injury (276,277), and therefore, iron deficiency could potentially also decrease immunopathology.

In line with this, *Tfrc*$^{Y20H/Y20H}$ mice may have had an augmented Treg response. Although Tregs were not numerically different in mice with normal and decreased iron uptake, the increased ratio of Tregs to effector CD4 T cells and the enhanced expression of CD25 is consistent with a skewing of immunity towards a regulatory phenotype. However, the importance of bona fide Tregs in malaria infection is somewhat ambiguous. It appears that other T cell subsets are the primary producers of anti-inflammatory cytokines such as IL-10, and Tregs have mostly been associated with impaired immunity rather than tolerance in malaria (115,164,278).

It is known that Th1 responses can inhibit Tfh cell function and germinal centre responses in malaria (151). Therefore, an attenuated Th1 response could theoretically be beneficial for Tfh differentiation. However, we found that the Tfh response was repressed in *Tfrc*$^{Y20H/Y20H}$ mice, marked by fewer splenic Tfh cells and reduced CD4 T cell expression of ICOS and BCL-6 eight days after *P. chabaudi* infection. Both ICOS and BCL-6 are all key proteins involved in

humoral immunity to malaria. In the absence of BCL-6, CD4 T cells cannot differentiate into Tfh cells, resulting in a disrupted B cell response and a failure to produce IgG antibodies to *P. chabaudi* (147). While ICOS is not essential for Tfh cell induction it is required for the maintenance of Tfh cells, and thus for the generation of sustained high-affinity antibody responses (149). Tfh cells have higher levels of intracellular iron and cytosolic ROS compared to other conventional CD4 T cells, underlining the importance for iron in Tfh cell function (279). It follows that cellular iron deficiency has the potential to impair Tfh responses, and thereby, the humoral immune response to malaria.

CD4 T cells are an incredibly important immune cell subset in malaria, due to their ability to orchestrate both cellular and humoral immune responses. Hence, it will be important for future studies to continue exploring the effects of iron deficiency on CD4 T cells. In particular the mechanism(s) through which CD4 T cell function is impaired should be investigated, for example by characterising their metabolic, transcriptomic or proteomic profile. Further research should also aim to determine whether some CD4 subsets are more sensitive to iron deficiency than others.

The B cell response to *P. chabaudi* infection was considerably diminished in mice with decreased cellular iron uptake. *In vitro* $Tfrc^{Y20H/Y20H}$ B cell proliferation and differentiation was also impaired, and could be rescued by iron supplementation, indicating that B cell inhibition was cell-intrinsic and iron-dependent. However, it stands to reason that Tfh cell inhibition also contributed to the disrupted B cell response in mice with cellular iron deficiency. Eight days after *P. chabaudi* infection B cell activation was profoundly inhibited in $Tfrc^{Y20H/Y20H}$ mice, with the downstream consequence of fewer IgG class-switched B cells and fewer differentiated ASCs and GC B cells. This may have been caused by the previously described epigenetic inhibition of B cell proliferation that occurs during iron deficiency (60). Alternatively, iron deficient B cells may be unable to support the increase in mitochondrial activity and oxidative metabolism that is required for B cell activation (280,281), as both of these processes are highly iron dependent. Cellular iron deficiency could also impair mTOR signalling, which normally increases during B

cell activation (69). mTOR inhibition can lead to disrupted class-switch recombination, somatic hyper mutation, germinal centre formation and plasma cell differentiation (282,283). As LAT-1 is regulated by mTOR, the decreased expression of LAT-1 on *in vitro* cultured $Tfrc^{Y20H/Y20H}$ B cells indicate that cellular iron deficiency impairs mTOR signalling. Additionally, in *P. yoelii* infected mice, the expansion of plasmablast early in infection is detrimental to class-switching, germinal centre formation and parasite control, because the hyper-metabolic plasmablast act as a nutrient-sink, depriving other immune cells of nutrients (284). It remains to be seen if this effect also applies to iron, however if it does, the effect could be further compounded by iron deficiency.

Importantly, the germinal centre response to *P. chabaudi* remained attenuated three weeks after infection, in mice with decreased cellular iron uptake. The number of splenic GC B cells almost doubled from day 8 to day 20 post infection in wild-type mice, whereas there was only a slight increase in the $Tfrc^{Y20H/Y20H}$ mice. Hence, iron is required to induce and sustain the germinal centre B cell response to malaria. While we identified cells that express markers traditionally associated with Tfh cells and GC B cells, it is also known that the secondary structure of the spleen is disrupted during *P. chabaudi* infection, raising questions as to whether these are *bona fide* Tfh and GC B cells found in a germinal centre. Hence, it would be of great interest to perform histological analysis to determine if there are germinal centre structures and if they differ between mice with normal and decreased cellular iron uptake. Additional work aimed at understanding the B cell response should focus on characterising the antibody response and investigating whether protective immunity is altered by decreased cellular iron, for example through re-infection studies. Furthermore, the mechanism through which cellular iron deficiency disrupts B cell function should be explored further.

5.3.1. Conclusion

The immune characterisation presented in this study sheds light on the wide range of effects that cellular iron deficiency can have on immune cell function in malaria infection. Disrupted cellular iron uptake, caused by a mutation in *Tfrc*, reduced the expansion and effector function

of several immune cell populations that are essential for immune control in malaria. Since the model used in this study confers the *Tfrc*$^{Y20H/Y20H}$ mutation to all cell types, it remains to be seen which effector mechanisms or immune cells are most affected. It is clear from the presented data that there are cell-intrinsic inhibitory effect of cellular iron deficiency on lymphocytes. However, it is unclear if the effects on innate immune cells are cell-intrinsic and how stromal cells are affected. Additionally, it would of interest to investigate if iron deficiency primarily affects one cell type that causes impairments in other cell types, thus creating a 'domino effect'. Using genetic models that allow for cell type specific perturbation of immunity or iron may help to answer these outstanding questions. It will also be vital to analyse the immune response at more time points to determine whether there is a persistent inhibition of the immune response or just altered immune response kinetics. Although we observe disrupted immune cell expansion and effector function that could have an impact on parasite control, the impaired immune response and the higher pathogen burden remain to be causally linked. Understanding the effects of iron for immune cells in the context of malaria will be important for both therapeutic as well as vaccine approaches in the future.

6. Iron availability alters the response to malaria vaccination

6.1. Introduction

More efficient malaria vaccines are needed to reduce the global disease burden of malaria (see 1.2.4. Malaria vaccination). However, to enhance malaria vaccine efficacy it will be beneficial to not only improve the vaccines themselves, but also to gain a greater understanding of how host factors influence vaccine responses. As iron deficiency and malaria often affect the same regions (80,285), it is important to understand how iron deficiency might affect malaria vaccine responses. Moreover, some studies have indicated that iron status can affect the immune response to other vaccines (73). There are also indications that iron deficiency could affect the response to malaria vaccine RTS,S. A study that monitored the immune profile of children and infants in Tanzania and Mozambique given RTS,S or a comparator vaccine, hypothesised that iron deficiency anaemia attenuates the response to RTS,S (286). They based this on the observation that study participants from Mozambique have higher rates of anaemia and decreased IgG titres to RTS,S, compared to participants from Tanzania. Furthermore, they found that anaemia is associated with reduced frequencies of immune cells that are important to generate protective immunity, such as plasma cells and memory B cells. However, there were potential confounding factors in this study (e.g. study site), and to our knowledge, no studies have been performed that directly assess the effect of iron deficiency on malaria vaccine immunogenicity or efficacy.

Moreover, using vaccination models can provide further insight into which aspects of the immune response are most sensitive to iron availability. For example, in terms of the kinetics of specific types of immune responses, or the immune cell subsets that they involve. Having a greater understanding of these aspects is vital to inform decisions regarding iron interventions in the context of immunity.

6.1.1. RH5.1 - a leading blood-stage malaria vaccine candidate

The main malaria vaccine used in this thesis chapter is RH5.1, a blood-stage vaccine targeting *Plasmodium falciparum* reticulocyte binding homologue 5 (*Pf*RH5) (Figure 6.1). *Pf*RH5 is an essential merozoite protein, which binds host receptor basigin on the RBC surface (89,287). *Pf*RH5 forms a heteromeric complex together with cysteine-rich protective antigen and RH5-interacting protein, where each component is indispensable for invasion (89,90). Binding of the complex to the host RBC, directly or indirectly causes the formation of a pore in the RBC membrane, which allows calcium influx that is an important step in the invasion process (86,90). *Pf*RH5 is specific to *P. falciparum* but is highly conserved between different *P. falciparum* strains.

A study by Douglas *et al.* identified *PfR*H5 as a promising blood-stage vaccine target (288). They compared multiple merozoite antigens side-by-side, using a viral vector delivery system, and found that immunisation with *Pf*RH5 can induce robust antibody responses in rabbits. When isolated, these antibodies can inhibit the *in vitro* growth of multiple heterologous *P. falciparum* strains. Furthermore, malaria-experienced individuals in Kenya have low levels of anti-*Pf*RH5 antibodies, compared to other blood-stage antigens like *Pf*AMA1 and *Pf*MSP1, indicating that *Pf*RH5 is not subject to high levels of natural immune pressure (288). Thus, *Pf*RH5 is an ideal blood-stage vaccine target, as it is essential, highly conserved and antibody-susceptible.

Studies of *Pf*RH5 vaccines in non-human primates and humans have produced further evidence of strong *in vitro* growth neutralizing antibody responses against heterologous parasite strains (289,290). Moreover, non-human primates immunised with *Pf*RH5 are protected against *P. falciparum* challenge (289). A study of vaccinated *Aotus* monkeys showed that protection is primarily mediated by high anti-*Pf*RH5 IgG titres prior to challenge. The first human *Pf*RH5 vaccine trial utilised an adenoviral vector (ChAd63) prime and modified Vaccinia virus Ankara (MVA) boost regimen (290). Immunisation was shown to induce both B cell and T cell responses, but only resulted in a moderate antibody response.

In an attempt to improve antibody responses, focus was switched to a protein in adjuvant vaccine platform for use in humans, since the protein in adjuvant formulation induced stronger antibody responses and provided higher levels of protective immunity in non-human primates (289). This version of *Pf*RH5 is known as RH5.1 and three doses of RH5.1 in AS01 induced strong immune responses in mice (201). A controlled human malaria infection trial of RH5.1 formulated with AS01 followed, and showed improved IgG levels compared to the viral vectored *Pf*RH5 vaccine (176). The *in vitro P. falciparum* growth inhibition observed in this trial is the highest (70-75%) observed so far for any blood-stage vaccine in humans. Additionally, a delayed fractional third dose of RH5.1 was found to significantly improve antibody concentration, longevity and avidity. All subjects developed parasitaemia upon *P. falciparum* challenge, regardless of immunisation, but parasite multiplication rates were moderately reduced and time to diagnosis was delayed by approximately one day in individuals immunised with RH5.1.

Although, RH5.1 did not induce sterile immunity in its first clinical trial, it still holds promise as it appears to reduce pathogen growth, and a successful blood-stage malaria vaccine should primarily reduce clinical episodes and prevent severe malaria. As such, *Pf*RH5 remains a promising blood-stage vaccine target, but improvements will need to be made to improve vaccine efficacy.

6.1.2. AdHu5-*Py*9 - an experimental pre-erythrocytic malaria vaccine

The second vaccine used in this thesis is AdHu5-*Py*9, a pre-erythrocytic adenoviral vector vaccine, which targets the *P. yoelii* circumsporozoite protein (CSP) (Figure 6.1). The vaccine consists of recombinant human adenovirus serotype 5 (AdHu5) expressing the H-2K^{d} restricted *P. yoelii* CSP epitope SYVPSAEQI (*Py*9). Vaccines based on murine malaria strains like *P. yoelii* are often used for pre-clinical challenge studies, since it is not possible to infect rodents with *P. falciparum* (291). Murine malaria vaccination models are also used to gain insight into vaccine immunogenicity, and they are particularly useful for liver-stage vaccines, as they enable the study of liver-resident immune cells.

CSP is the predominant surface protein of *Plasmodium* sporozoites, and it plays a role in development and the early stages of infection (292). All *Plasmodium* CSPs have a similar structure, consisting of three functional regions, but the amino acid sequences vary between different *Plasmodium* species. The N-terminal region binds heparin sulphate proteoglycans and is involved in hepatocyte binding (292). The central region contains species-specific amino acid repeats (NANP in *P. falciparum* & QGPGAP *P. yoelii*), which are the major CSP B cell epitopes and the target of neutralising antibodies (293,294). The C-terminal region has a thrombospondin-like type I repeat and three T cell epitopes: a conserved CD4 T cell epitope, a polymorphic CD4 T cell epitope, and a polymorphic CD8 T cell epitope (*Py*9 in *P. yoelii*) (292,295,296).

CSP has been a key target for pre-erythrocytic malaria vaccines, ever since it was discovered that whole sporozoite immunisation generates protective antibodies against CSP, and later, that CSP is the immunodominant antigen of irradiated sporozoites (165). CSP is somewhat unusual, as a *Plasmodium* antigen that can be targeted by cytotoxic CD8 T cells. To be recognised by CD8 T cells, parasite antigens need to be presented by infected hepatocytes, but the parasites are protected by a parasitophorous vacuole during the liver-stage infection, which limits access to antigens. However, CSP is secreted from the vacuole into the hepatocyte cytoplasm during infection (297), and as a consequence it can be processed and presented on MHC class I to CD8 T cells. One approach to pre-erythrocytic malaria vaccines is to try to induce such CD8 T cell responses (107).

Recombinant replication-deficient viral vectored vaccines can induce strong CD8 T cell responses and have been used extensively for pre-clinical studies of liver-stage malaria vaccines. Viral vectored vaccines targeting CSP have been shown to induce protective immunity in mice. For example, a study by Rodrigues *et al*. found that immunisation with AdHu5 expressing the full length *P. yoelii* CSP induces strong CD8 T cell responses in the spleen and liver of mice after a single immunising dose (298). Additionally, immunisation inhibited *P. yoelii* liver stages and generated sterile immunity in a subset of mice. A few

controlled human malaria infection trials using viral vectored vaccines targeting *P. falciparum* CSP have also been conducted. One utilised an adenovirus prime, MVA boost regimen, and induced strong antigen specific IFNγ T cell responses, but only generated sterile immunity to *P. falciparum* infection in one out of fifteen study participants (299). Another study used a combination of *P. falciparum* CSP and AMA1 in a DNA prime-AdHu5 boost regimen (300). This immunisation only generated modest T cell responses but resulted in higher rates of sterile immunity (27%). However, protection was likely primarily mediated by anti-AMA-1 antibody levels in this study.

Overall, AdHu5-*Py*9 is not a direct analogue of a human malaria vaccine candidate, and it is unlikely to be directly adapted for use in humans. However, similar vaccines are well characterised in rodent models and are known to replicate many of the characteristics of a successful liver stage vaccine. Therefore, it remains a useful experimental vaccine for pre-clinical studies of viral vectored liver stage malaria vaccines.

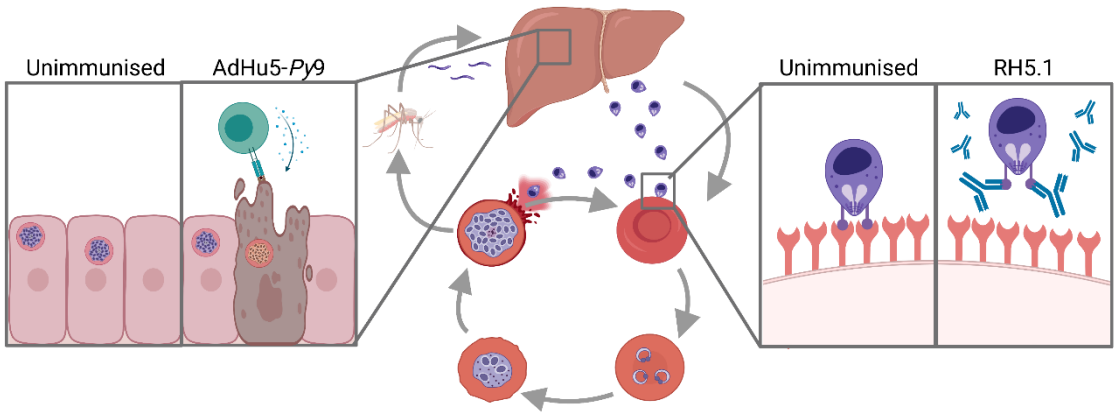


Figure 6.1. **Mechanism of action for malaria vaccines RH5.1 and AdHu5-*Py*9.** Immunisation with blood stage malaria vaccine RH5.1 generates antibodies that prevent merozoite invasion of erythrocytes. Immunisation with liver-stage malaria vaccine AdHu5-*Py*9 generates antigen specific cytotoxic CD8 T cells that recognise and kill infected hepatocytes.

6.1.3 Aim

The aim of this thesis chapter is to examine the effects of iron deficiency on malaria vaccine immunogenicity. To this end, two different malaria vaccines, RH5.1, a protein in adjuvant blood-stage malaria vaccine that induces a humoral immune response, and AdHu5-*Py*9, a viral

vectored pre-erythrocytic vaccine that induces a cytotoxic CD8 T cell response, were utilised. We also sought to elucidate which aspects of the immune response to these vaccines are sensitive to low iron availability, and if other factors that affect vaccine efficacy interact with iron availability to impact vaccine responses.

6.2. Results

6.2.1. Decreased cellular iron attenuates the immune response to RH5.1

To determine whether cellular iron availability affects the immune response to a malaria vaccination, wild-type and *Tfrc*$^{Y20H/Y20H}$ mice were immunised with malaria vaccine RH5.1. They were given a prime-boost regimen, consisting of two sub-cutaneous injections of 60 ng RH5.1 protein in AddaVax adjuvant, administered three weeks apart (Figure 5.2A). AddaVax is a squalene based oil-in-water adjuvant that was formulated to resemble MF59, which is a licensed influenza vaccine adjuvant that elicits both cellular and humoral immune responses (301).

The draining (inguinal) lymph node was collected, and the immune response was analysed by flow cytometry three-weeks after the boost. The T cell response to RH5.1 was altered in mice with decreased cellular iron uptake. There was a higher percentage of T cells and activated CD8 T cells, but a trend towards fewer activated CD4 T cells (Figure 6.2B). Importantly, fewer *Tfrc*$^{Y20H/Y20H}$ CD4 T cells had differentiated into Tfh cells (Figure 6.2C), indicating that they are less capable of providing support to GC B cells. Mice with decreased cellular iron uptake also had an impaired B cell response with fewer total B cells, fewer GC B cells and fewer IgG1 class-switched GC B cells (Figure 6.2D). Overall, the germinal centre response to RH5.1 in mice with decreased cellular iron uptake was attenuated compared to wild-type mice.

To monitor the antibody response to RH5.1, blood samples were collected three weeks post-prime and three weeks post-boost, and anti-RH5 IgG was measured by standardised ELISA. Before the boost, antibody levels were below the limit of detection (5 AU) in both genotypes. Three weeks after receiving a second dose of RH5.1, mice with decreased cellular iron had significantly lower anti-RH5 IgG titres (Figure 6.2E). Moreover, 36% of the *Tfrc*$^{Y20H/Y20H}$ mice

had no detectable IgG response, whereas all of the wild-type mice had detectable anti-RH5 IgG after the boost. Hence, the antibody response was impaired in mice with disrupted cellular iron uptake, demonstrating that cellular iron deficiency can impair B cell effector function in response to vaccination.

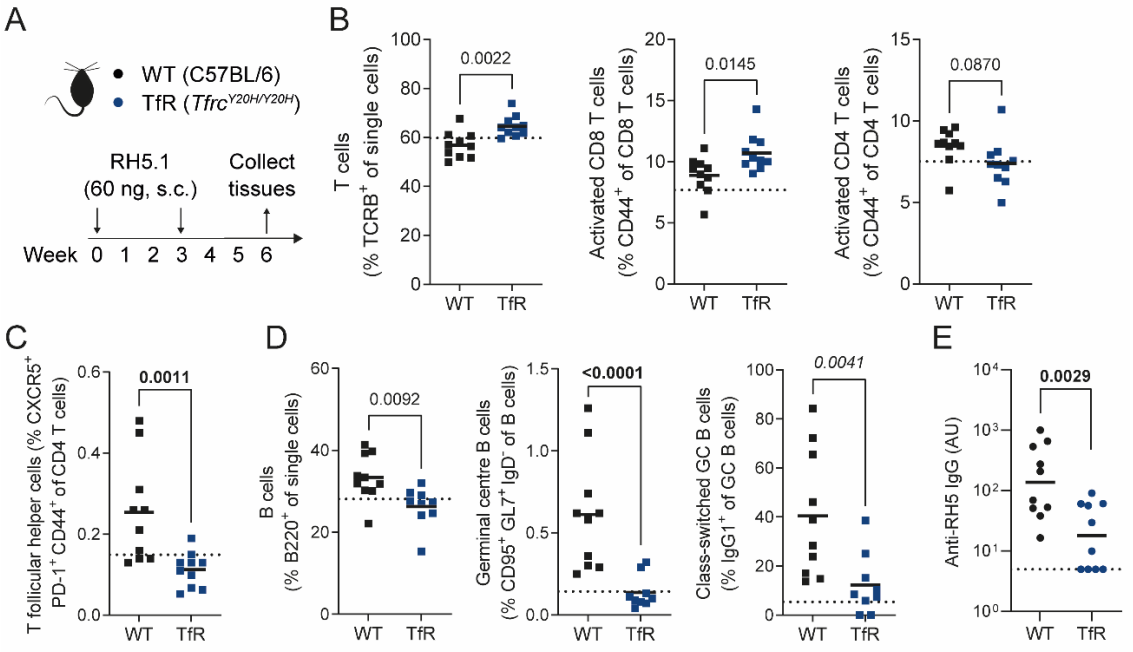


Figure 6.2. **Decreased cellular iron impairs the germinal centre response to malaria vaccine RH5.1**. **A)** C57BL/6 (WT) and *Tfrc*$^{Y20H/Y20H}$ (TfR) mice were immunised by sub-cutaneous (s.c.) injection of two doses of 60 ng RH5.1 in AddaVax, given three weeks apart. **B-D)** Draining lymph nodes were collected six weeks post-prime and immune cell frequencies were analysed by flow cytometry. Dotted line represents mice given adjuvant only. Mean, Welch's t-test/**Welch's t-test on log transformed data** /*Mann-Whitney test*, n=9-10, N=1.**E)** Circulating anti-RH5 IgG levels were measured by standardised ELISA six weeks post-prime. Dotted line represents the limit of detection (5 AU). Geometric mean, Welch's t-test on log transformed data, n=10-11, N=1.

Overall, the magnitude of the immune response to RH5.1 was quite small in both genotypes but increasing antigen exposure can often boost immunogenicity. Furthermore, we hypothesised that increasing antigen exposure could either exacerbate or override the effects of iron deficiency on the immune response. If the immune response is impaired due to an absolute cellular iron deficiency, then increasing antigen exposure would increase the magnitude of the response in wild-type but not *Tfrc*$^{Y20H/Y20H}$ mice. However, if iron availability is sensed and integrated with activation signals, then increasing antigen exposure could potentially improve

the response in both genotypes. In either case, such an observation would improve our understanding of immune cell iron requirements during vaccine responses.

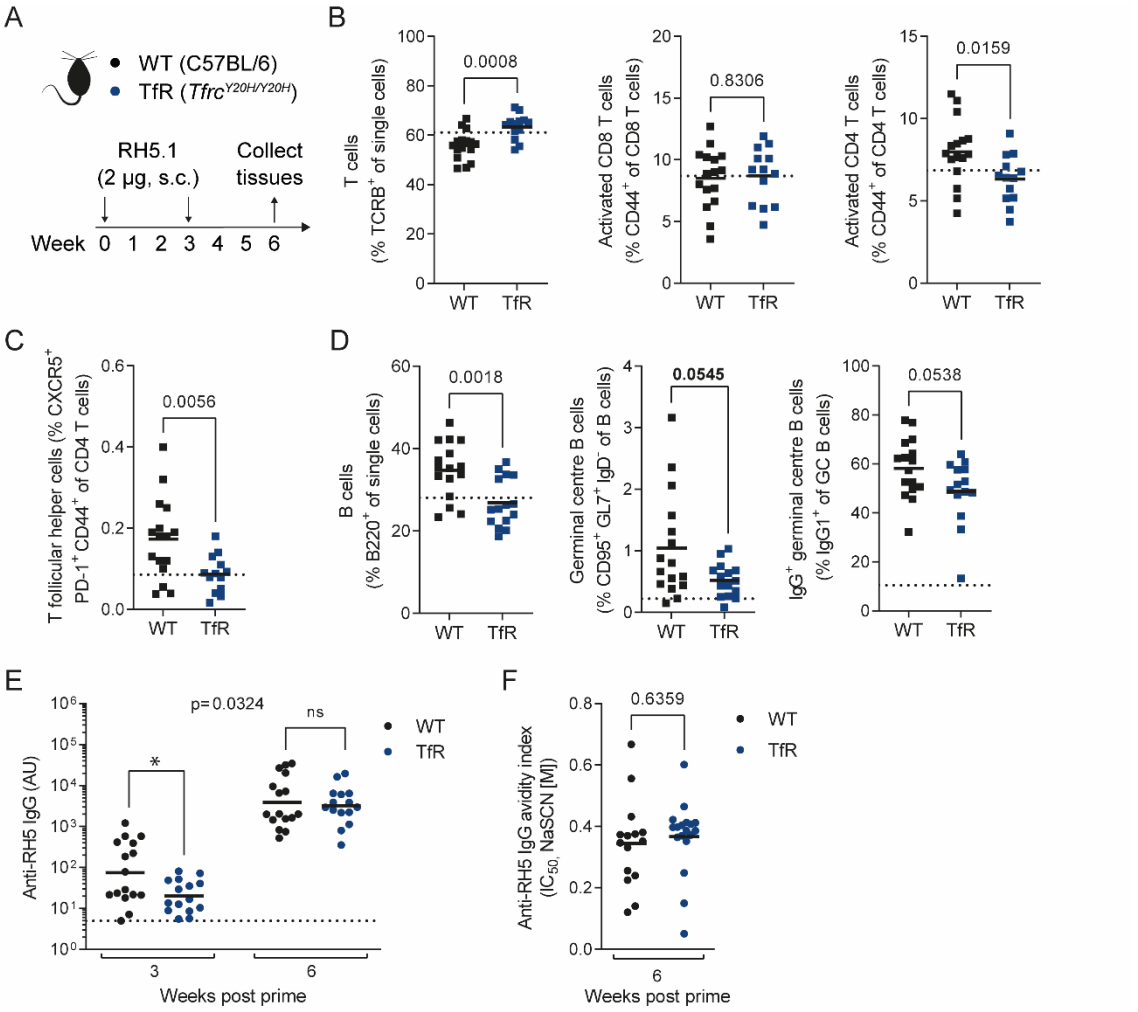


Figure 6.3. **Increasing antigen exposure can partially overcome the effects of cellular iron deficiency on the response to RH5.1. A)** C57BL/6 (WT) and *Tfrc*$^{Y20H/Y20H}$ (TfR) mice were immunised by sub-cutaneous (s.c.) injection of two doses of 2 µg RH5.1 in AddaVax, given three weeks apart. **B-D)** Draining lymph nodes were collected six weeks post-prime and immune cell frequencies were analysed by flow cytometry. Dotted line represents mice given adjuvant only. Mean, Welch's t-test/**Welch's t-test on log transformed data**, n=14-16, N=2 (pooled). **E)** Circulating anti-RH5 IgG levels were measured by standardised ELISA three and six weeks post-prime. Dotted line represents the limit of detection (5 AU). Geometric mean, two-way ANOVA on log transformed data, Sidak's m.c.t., n=14-16, N=2. **F)** Anti-RH5 IgG avidity was analysed six weeks post-prime by avidity ELISA based on sodium thiocyanate (NaSCN) displacement, presented as the half-maximal inhibitory concentration (IC_{50}). Mean, Welch's t-test, n=14-16, N=2.

Wild-type and *Tfrc*$^{Y20H/Y20H}$ mice were, therefore, immunised as previously described, but with a higher dose of 2 µg RH5.1 protein per immunisation (Figure 6.3A). The higher dose of RH5.1 led to a modest improvement in the immune response in both genotypes and reduced the

difference in immunogenicity between them (Figure 6.3). The T cell response to the low and the high dose of RH5.1 was comparable in both genotypes (Figure 6.2B & 6.3B). Accordingly, the Tfh response remained attenuated in *Tfrc*$^{Y20H/Y20H}$ mice given a high dose of RH5.1 (Figure 6.3C). Mice with decreased cellular iron still had a somewhat impaired B cell response, with marginally fewer GC B cells and class-switched GC B cells (Figure 6.3D).

Circulating IgG antibody titres were measured before, and three weeks after, the boost. Mice with decreased cellular iron uptake had lower anti-RH5.1 IgG titres pre-boost, but interestingly the antibody response was rescued after boosting (Figure 6.3E). Antibody avidity was also measured three weeks after the boost and no difference was detected between mice with normal and decreased iron uptake (Figure 6.3F). Thus, the initial antibody response to RH5.1 was weaker or slower to develop, but the maximum observed response was not inhibited in mice with decreased cellular iron uptake.

In summary, decreased cellular iron uptake has a negative effect on the immune response to blood-stage malaria vaccine RH5.1. However, it appears that it is possible to override some of the immune inhibition caused by cellular iron deficiency by increasing antigen exposure.

6.2.2. Transient hypoferremia does not affect the immune response to RH5.1

The mini-hepcidin model (described in chapter 3) was utilised to gain a better understanding of the kinetics of iron requirements during the immune response to a malaria vaccine. To this end, mini-hepcidin was administered to induce transient hypoferremia during different stages of the immune response to RH5.1.

To assess whether transient iron deficiency immediately after the prime or boost is sufficient to alter the memory response, BALB/c mice were immunised with RH5.1. BALB/c mice were used as RH5.1 is more immunogenic in BALB/c mice compared to C57BL/6 mice, and no transgenic mice were needed. The mice were given two sub-cutaneous doses of 2 µg RH5.1 in AddaVax, four weeks apart, and the draining LN was collected four weeks post-boost. Mini-

hepcidin was administered to induce low serum iron, either on day 4-7 post-prime or on day 3-6 post-boost (Figure 6.4A).

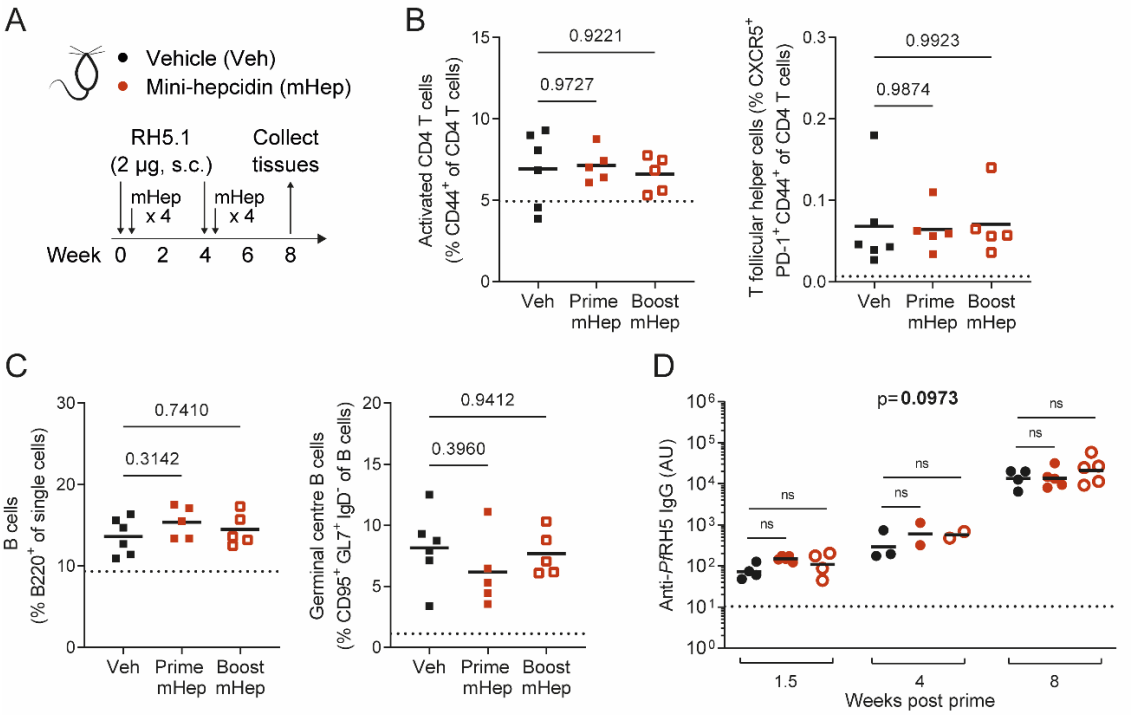


***Figure 6.4*. Transient hypoferremia does not affect the memory response to RH5.1. A)** BALB/c mice were immunised by sub-cutaneous (s.c.) injection of two doses of 2 µg RH5.1 in AddaVax, given four weeks apart. Mini-hepcidin (mHep) was injected intraperitoneally daily, either 4-7 days post-prime (prime mHep) or 3-6 days post-boost (boost mHep). Vehicle alone (Veh) was administered to control mice both post-prime and post-boost. **B-C)** Draining lymph nodes were collected eight weeks post-prime and immune cell frequencies were analysed by flow cytometry. Dotted line represents mice given adjuvant only. Mean, one-way ANOVA, Dunnett's m.c.t., n=4-5, N=1. **D)** Circulating anti-RH5 IgG levels were measured by standardised ELISA 1.5, 4- and 8-weeks post-prime. Dotted line represents the limit of detection (5 AU). Geometric mean, two-way ANOVA on log transformed data, Sidak's m.c.t., n=2-5, N=1.

Mini-hepcidin treatment, either post-prime or post-boost, did not alter the CD4 T cell or Tfh cell response to RH5.1 (Figure 6.4B). The B cell response to RH5.1 was also not affected by transient hypoferremia, and all groups had comparable B cell and GC B cell frequencies (Figure 6.4C). Anti-RH5 IgG titres were also measured throughout the course of the experiment. Although RH5.1 induced a robust antibody response, in particular after boosting, the antibody levels were not affected by mini-hepcidin treatment (Figure 6.4D). This data clearly shows that short-term transient hypoferremia is not sufficient to affect the memory response to RH5.1.

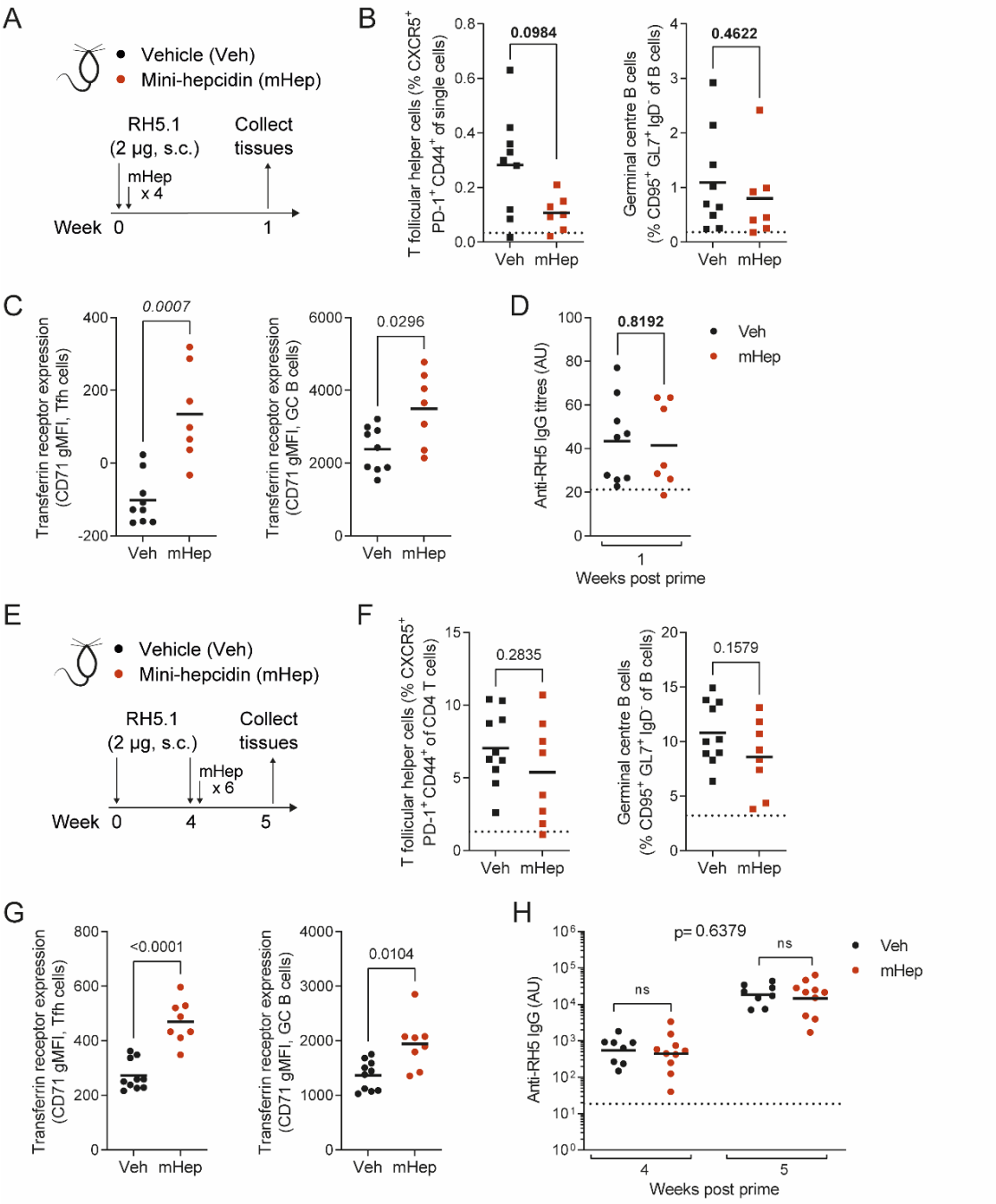


Figure 6.5. **Transient hypoferremia does not affect the immune response to RH5.1 prime or boost.** **A)** BALB/c mice were immunised by sub-cutaneous (s.c.) injection of 2 µg RH5.1 in AddaVax. Mini-hepcidin (mHep) or vehicle control (Veh) was administered intraperitoneally on day 3-6 post-prime. **B-C)** Draining lymph nodes were collected seven days post-prime and immune cells were analysed by flow cytometry. **D)** Circulating anti-RH5 IgG levels were measured by standardised ELISA one-week post-prime. **E)** BALB/c mice were immunised by sub-cutaneous (s.c.) injection of two doses of 2 µg RH5.1 in AddaVax, given four weeks apart. Mini-hepcidin (mHep) or vehicle control (Veh) was administered intraperitoneally on day 2-7 post-boost. **F-G)** Draining lymph nodes were collected eight days post-boost and immune cells were analysed by flow cytometry. **H)** Circulating anti-RH5 IgG levels were measured by standardised ELISA 4- and 5-weeks post-prime. Dotted line represents mice given adjuvant only (B-C & F-G) or the limit of detection (D & H). Mean, Welch's t-test/**Welch's t-test on log transformed data**/*Mann-Whitney test* (B-D & F-G) or geometric mean, two-way ANOVA on log transformed data, with Sidak's m.c.t., n=7-9 (B-D) or n=8-10 (F-H), N=1.

Nevertheless, it is unclear whether the immune response was initially impaired, but recovered once mini-hepcidin treatment was concluded, or whether the mini-hepcidin treatment had no effect. The immune response to RH5.1 was, therefore, evaluated shortly after immunisation and mini-hepcidin treatment. First, the immune response to prime was assessed in BALB/c mice given one dose of 2 µg RH5.1 in AddaVax, and mini-hepcidin or vehicle control on day 3-6 post-immunisation (Figure 6.5A). Mini-hepcidin treatment had no significant effect on the frequency of Tfh cells or GC B cells in the draining lymph node, seven days after immunisation (Figure 6.5B). However, this experiment was potentially somewhat underpowered, and there appears to be a trend towards an attenuated germinal centre response. Furthermore, GC B cells and Tfh cells from mini-hepcidin treated mice had increased expression of TfR1, indicating some degree of cellular iron deficiency (Figure 6.5C). Anti-RH5 IgG antibody levels were also evaluated, but they were very low at this early time point and were not affected by mini-hepcidin treatment (Figure 6.5D). Additionally, the immune response to boost was evaluated in BALB/c mice given two doses of 2 µg RH5.1 in AddaVax, and mini-hepcidin or vehicle control on day 2-7 post-boost (Figure 6.5E). No difference was observed in the frequency of Tfh cells or GC B cells, between mice given mini-hepcidin or vehicle eight days after the boost (Figure 6.5F). Similar to mice given mini-hepcidin after the prime, immune cells from mini-hepcidin treated mice had increased TfR1 expression after the boost (Figure 6.5F). Furthermore, although the anti-RH5 IgG titres increased substantially in the eight days after boosting, mini-hepcidin treatment had no effect on the antibody response (Figure 6.5H).

Taken together, it appears that short-term transient hypoferremia does not affect the immune response to RH5.1. The germinal centre response to RH5.1 takes place over several weeks, so it is likely that the immune system is able to recover once mini-hepcidin treatment is concluded and circulating iron levels are restored. However, this data also demonstrates that RH5.1 induces robust immune responses that are not very sensitive to transient hypoferremia.

6.2.3. Transient hypoferremia impairs the primary response to AdHu5-*Py*9.

Although transient hypoferremia does not affect the immune response to RH5.1, it is known that hypoferremia can affect other vaccine responses (59). To determine if the resistance to transient hypoferremia was specific to RH5.1, the effect of hypoferremia on a different malaria vaccine, AdHu5-*Py*9, was investigated.

BALB/c mice were immunised with 5×10^8 IFU of AdHu5-*Py*9 administered by s.c. injection and given mini-hepcidin or vehicle control on day 3-6 post-immunisation (Figure 6.6A). The primary immune response was evaluated by flow cytometry, including tetramer staining to identify antigen specific CD8 T cells, using a blood sample taken seven days post-immunisation. Although there was no difference in the overall frequency of circulating CD8 T cells, mice given mini-hepcidin had significantly fewer *Py*9-specific CD8 T cells, seven days after immunisation (Figure 6.6B-C). Hence, demonstrating that transient hypoferremia impaired the immune response to AdHu5-*Py*9.

In addition, the memory response to AdHu5-*Py*9 was evaluated 28 days after immunisation. At this time point, no difference was observed between mini-hepcidin and vehicle treated mice, in the frequency of circulating total CD8 T cells or *Py*9-specific CD8 T cells (Figure 6.6D). This observation is not entirely surprising, as the hypoferremia induced by mini-hepcidin treatment is transient, but antigen exposure from AdHu5 can persist for months (302). Therefore, it follows that an immune response that is suppressed by hypoferremia can recover, if serum iron is restored and antigen exposure is continued.

The immune response to AdHu5-*Py* was further characterised by measuring the T cell response in the liver and spleen 28 days post-immunisation. *Py*9-specific CD8 T cells were found in both the liver and spleen, however, mini-hepcidin treatment did not significantly alter the CD8 T cell response in either organ (Figure 6.6E-F). Furthermore, *ex vivo* restimulation of splenocytes with *Py*9 peptide, followed by ICS, was performed. Mini-hepcidin treatment did not significantly affect the percentage of TNFα, IFNγ, IL-2 or granzyme B producing splenic CD8 T cells.

However, there was a trend towards fewer IFNγ and IL-2 producing, and more granzyme B producing CD8 T cells in the mini-hepcidin treated mice.

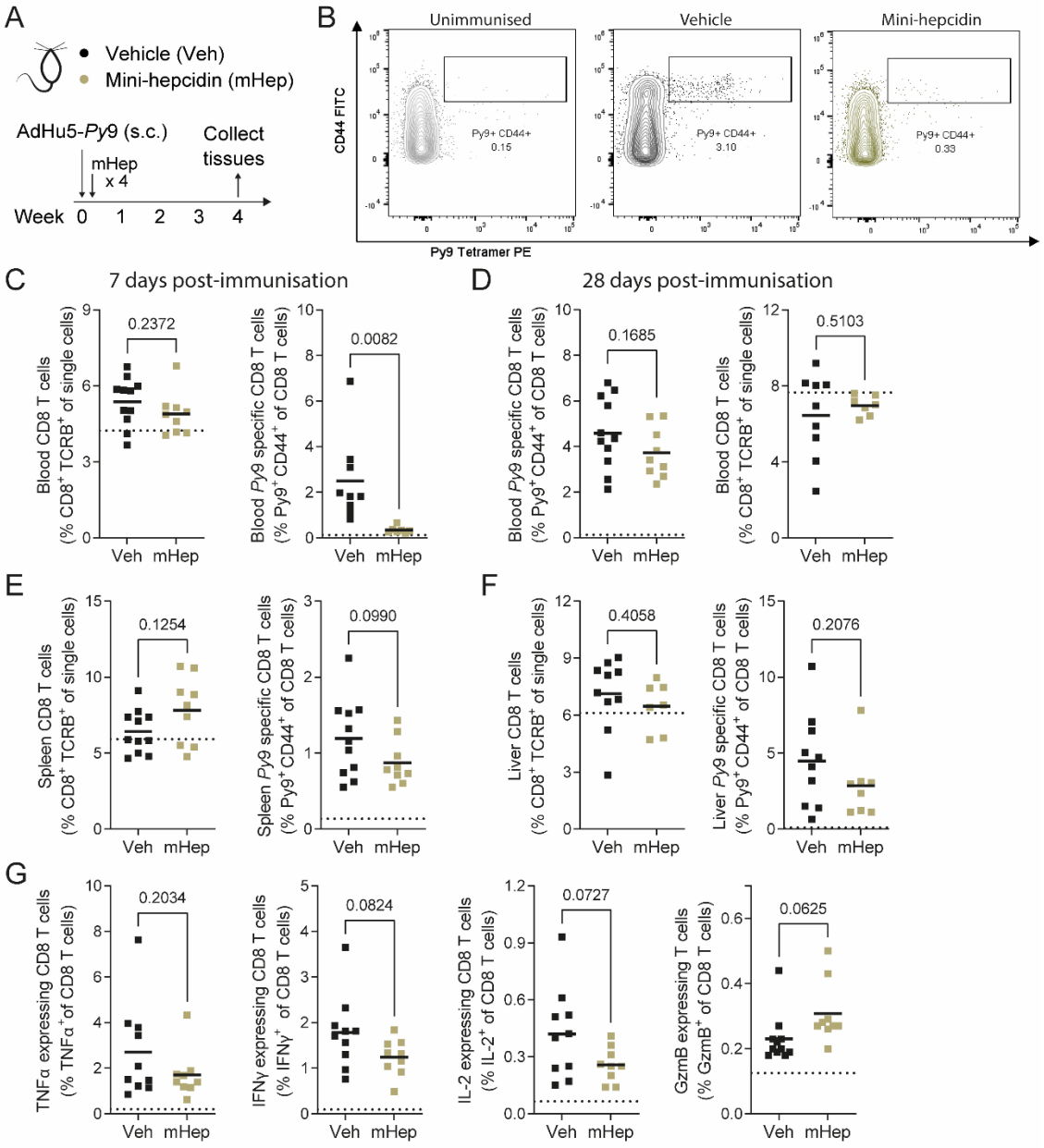


***Figure 6.6*. Transient hypoferremia impairs the primary response, but not the memory response, to AdHu5-*Py*9. A)** BALB/c mice were immunised by sub-cutaneous (s.c.) injection of 5×10^8 IFU of AdHu5-*Py*9, and mini-hepcidin (mHep) or vehicle control (Veh) was administered intraperitoneally on day 3-6 after immunisation. **B-C)** Blood samples were collected seven days after immunisation and antigen specific CD8 T cells were identified by flow cytometry, using *Py*9 specific tetramers. **D-F)** Antigen specific CD8 T cells were also identified in the blood, spleen and liver, 28 days after immunisation. **G)** Cytokine producing CD8 cells were identified by flow cytometry after *ex vivo* restimulation with *Py*9 peptide. Dotted line represents mice given adjuvant only. Mean, Welch's t-test, n=8-10, N=1.

In conclusion, the primary CD8 T cell response to AdHu5-*Py* was substantially impaired by hypoferremia. However, 28 days after immunisation there was no difference in the memory response to AdHu5-*Py*9. It follows that malaria vaccine immunogenicity can be impaired by hypoferremia, but once iron availability is restored, it is possible for the immune response to resume or recover.

6.3. Discussion

Iron deficiency is widespread in malaria endemic regions, and there is growing evidence to show that iron deficiency can affect immune responses to vaccination (73). However, there have been no studies to date that examine the effects of iron deficiency on malaria vaccine responses. Considering that more efficient malaria vaccines are needed, it is important to elucidate host factors that may influence vaccine efficacy.

Here the effects of iron deficiency on malaria vaccine immunogenicity were assessed using a mouse model of cellular iron deficiency. In line with previously published studies (59,60), we have show that cellular iron deficiency impairs the T cell and B cell response to immunisation. Mice with decreased cellular iron availability had disrupted germinal centre responses to malaria vaccine RH5.1, manifesting as fewer Tfh cells, fewer GC B cells and fewer class-switched GC B cells. Accordingly, cellular iron deficiency also impaired the antibody response to RH5.1. We thereby show for the first time that iron deficiency can impair the immune response to malaria vaccination

Some of the immune impairment caused by cellular iron deficiency could be overcome by immunising with a higher dose of RH5.1. In humans, the cellular and humoral response to RH5.1 was equivalent in participants receiving three doses of 2, 10 or 50 µg RH5.1, demonstrating that RH5.1 immunogenicity is not substantially affected by dose in iron replete humans (176). However, administering 2µg of RH5.1 instead of 60 ng, enhanced the germinal centre response in $Tfrc^{Y20H/Y20H}$ mice, although it still remained attenuated compared to wild-type mice. Cellular iron deficiency also impaired the early antibody response to a high dose of

RH5.1, but interestingly, the difference in antibody levels disappeared after the boost. This suggests that immune cell impairment does not occur as a consequence of absolute iron deficiency that completely blocks immune cell function. Rather it appears that iron availability is sensed and integrated together with other signals of activation and inhibition. As a result, the inhibitory effects of iron scarcity can be overcome by increasing activation signals, such as antigen exposure. However, it remains to be investigated precisely how cellular iron deficiency is sensed and signalled in this context, and how signalling interacts with immune cell activation cues.

A mouse model of mini-hepcidin mediated transient hypoferremia was also used to gain greater insight into which aspects of the immune response to malaria vaccination are most sensitive to iron deficiency. Our data shows that RH5.1 appears to be remarkably resistant to transient hypoferremia. Regardless of when short-term hypoferremia was induced it did not affect the T cell or B cell response to RH5.1. Notably, a ten-fold increase in anti-RH5 IgG in eight days was observed after boosting, and this response was completely unaffected by hypoferremia. It follows that memory B cell activation, differentiation into ASCs and subsequent antibody production, appears to be relatively resistant to hypoferremia. In particular, this result contrasts with the impaired germinal centre responses observed in mice with cellular iron deficiency caused by the *Tfrc* mutation. Nevertheless, the observation is congruous with the rapid and robust memory B cell responses that normally occur in response to infections, despite the inflammation mediated hypoferremia that infection induces (38,303). A putative variability in iron sensitivity between different types of B cell responses could possibly be explained by differences in B cell metabolism. Little is known about the metabolism of memory B cells, but mature ASCs are highly reliant on glycolysis and autophagy to meet the high metabolic demands of antibody production (304,305). In addition, proliferation is required for ASC differentiation, but once mature, they no longer proliferate (269,306). As a consequence, they could be more resistant to iron deficiency than cycling GC B cells with high proliferative demands and iron-dependent oxidative metabolism (304).

In contrast to RH5.1, the primary response to AdHu5-*Py*9 was substantially impaired by hypoferremia, perhaps as a result of the difference in vaccine platform and the type of immune response that is generated. A previous study by Frost *et al.* has shown that the response to both protein in adjuvant and viral vector vaccines are sensitive to hypoferremia, using an ovalbumin model (59). Hence, it is unlikely that the difference in vaccine platform alone can explain the different responses. However, the two vaccines induce responses that involve different immune cells and that have different kinetics. In humans, a refractory third dose of RH5.1 significantly improved the immune response, demonstrating that the kinetics of antigen exposure may be more important than the vaccine dose (176). AdHu5-*Py*9 induces a rapid cytotoxic CD8 T cell response, while RH5.1 induces relatively slow germinal centre responses that progress over several weeks. Upon activation, CD8 T cells proliferate quickly, greatly increase their protein content, and have very high iron demands (61,307). In comparison to CD8 T cells, CD4 T cells proliferate more slowly, increase their protein content to a lesser degree and have lower iron demands (61,307). Therefore, it is possible that AdHu5-*Py*9 induced CD8 T cell responses are more sensitive to short-term hypoferremia than RH5.1 induced CD4 T cell responses. It is also worth noting that once hypoferremia was resolved, the CD8 T cell response to AdHu5-*Py*9 could resume or recover, so that it was comparable to the response in iron replete animals, four weeks after immunisation. A similar process likely occurs in mice with cellular iron deficiency given RH5.1, although further studies would be required to confirm this.

Our findings may also have implications for vaccine design and implementation in areas with a high prevalence of iron deficiency. In terms of vaccine deign, vaccines with high levels of persistent antigen exposure may be preferred. In this context, short term hypoferremia, induced for example by a strong adjuvant or infection, does not appear to be a major concern. However, absolute and functional iron deficiency, where immune cell iron availability is persistently low, appears to be a bigger concern. Therefore, it may be beneficial to couple childhood vaccination programs with screening for and treatment of iron deficiency. However, further studies are still

needed to determine how iron deficiency and iron supplementation affects vaccine efficacy in humans, and whether vaccine design or implementation can minimise those effects.

6.3.3. Conclusion

In this chapter the effect of cellular iron deficiency on malaria vaccine immunogenicity was explored. We have found that cellular iron deficiency can impair the response to malaria vaccination, however, the vaccines studied here were also somewhat resistant to iron scarcity. Namely, the response to RH5.1 could be improved by increasing antigen exposure in mice with cellular iron deficiency and the response to AdHu5-*Py*9 recovered once iron availability was restored in mice that were hypoferremic at the time of immunisation. These findings highlight the importance of considering iron deficiency at the vaccine design stage. Furthermore, knowing that iron deficiency can disrupt malaria vaccine responses, it will be important for future studies to determine whether iron interventions can improve malaria vaccine efficacy.

7. Summary and general discussion

7.1. Summary and outlook

7.1.1. Summary of findings

Malaria is a leading cause of childhood mortality from infectious disease globally and there is a complex relationship between iron and malaria (80,91). Iron deficiency can protect from malaria infection while iron supplementation can increase the risk (184), but the mechanisms behind these effects are not well understood. In addition, iron is a vital nutrient that affects immune responses to infection and vaccination (59,72,73), but it is not known how iron availability affects the immune response to malaria infection and vaccination. In this thesis we have sought to elucidate the relationship between host iron status and malaria infection and vaccination.

We began by establishing two mouse models of iron deficiency in Chapter 3. We demonstrated that *Tfrc*$^{Y20H/Y20H}$ transgenic mice, with decreased TfR1 mediated cellular iron uptake, had microcytic and hypochromic RBCs but normal total haemoglobin. *Tfrc*$^{Y20H/Y20H}$ mice also had primarily normal peripheral immune cell frequencies at homeostasis, although splenic B cell numbers were reduced. Accordingly, we determined that *Tfrc*$^{Y20H/Y20H}$ mice are a suitable model to study the effects of host cellular iron deficiency on malaria infection and vaccination, in the absence of severe anaemia. In a second model, we showed that mice treated with the hepcidin mimetic peptide mini-hepcidin for four days had suppressed serum iron levels, very mild macrocytic anaemia and predominantly normal peripheral immune cell frequencies. Hence, this model could be used to acutely and transiently induce hypoferremia to study the effect of iron on specific temporal aspects of the immune response to malaria vaccination.

We went on to show that mice with decreased cellular iron uptake have higher parasite burden upon *P. chabaudi* infection, in Chapter 4. This finding was particularly noteworthy as it appears to contradict previous reports that iron deficiency protects against malaria (184). However, the protective effects of iron deficiency anaemia were likely minimised in our model. Indeed, uninfected *Tfrc*$^{Y20H/Y20H}$ mice were not anaemic and decreased cellular iron uptake did not appear

to affect malaria induced anaemia or RBC susceptibility to *P. chabaudi* invasion. Additionally, we determined that high serum iron, achieved via imposing hepcidin suppression, did not affect parasitaemia in wild-type mice, indicating that this form of iron may not be important for parasite growth. Interestingly, the disease tolerance phenotype of mice with decreased cellular iron uptake was also altered. On the one hand, eight days after *P. chabaudi* infection, $Tfrc^{Y20H/Y20H}$ mice had increased weight loss and indications of kidney damage, but on the other hand, they appeared to have less severe liver damage. We hypothesise that this phenotype is the result of altered tissue iron loading, caused by the *Tfrc* mutation. However, this finding demonstrates that the protective effect of iron deficiency in malaria could be partially mediated by decreased tissue iron loading, resulting in improved disease tolerance.

As we had not yet found a convincing explanation for the higher parasite burden in mice with decreased cellular iron uptake, we set out to investigate if the immune response to *P chabaudi* was altered, in Chapter 5. We discovered that disrupted cellular iron uptake had a wide range of effects on the immune response to *P. chabaudi*. The expansion of key effector cells, such as MNPs, ASCs and Th1 cells was decreased and there were fewer IFNγ producing cells in the spleen of $Tfrc^{Y20H/Y20H}$ mice. Furthermore, cellular iron deficiency severely impaired the germinal centre response to infection. While we have not formally shown that the impaired immune response caused the higher pathogen burden in mice with decreased cellular iron uptake, it is a likely cause. Going forward, it will be of great interest to determine how protective immunity is affected by cellular iron deficiency.

Vaccination is arguably the most effective way of preventing morbidity and mortality from infectious disease, but efficient malaria vaccines have proved difficult to generate. We hypothesised that the immune impairment caused by cellular iron deficiency could also impact on malaria vaccination. Therefore, we examined the effects of iron on malaria vaccine immunogenicity in Chapter 6. We showed that decreased cellular iron uptake weakened the immune response to blood-stage malaria vaccine RH5.1 and that hypoferremia disrupted the response to experimental liver-stage vaccine AdHu5-*Py*9. Hence, we have demonstrated that

iron deficiency has the potential to impair malaria vaccine efficacy, and consequently, it will be important to consider iron deficiency when designing and implementing malaria vaccines in the future.

7.1.2. Proposed model and open questions

In light of the findings in this thesis and previously published studies, we propose a model in which host iron status impacts on malaria infection on multiple levels:

I. Host iron status controls erythropoiesis and influences RBC physiology, which in turn, affects *Plasmodium* invasion and proliferation, and the clearance of iRBCs.

II. Host iron status may affect *Plasmodium* iron bioavailability and consequently its growth.

III. Host iron status affects disease tolerance by altering tissue and cellular iron levels, resulting in different capacities to store and detoxify excess labile haem and iron generated during malaria infection

IV. Host iron status affects immune cell function and iron deficiency may impair the formation of long-term protective immunity to *Plasmodium* infection.

This model suggests that iron deficiency could have beneficial and detrimental effects, for both the pathogen and the host. However, it remains to be seen to which degree each of these factors contribute to virulence, tolerance and immunity in a clinical setting.

I) The first part of the model has been established by previous research, which has shown that RBCs from iron deficient individuals are less amenable to *Plasmodium* growth and that immature RBCs are more susceptible to invasion and growth (91,211). Moreover, iRBCs from iron deficient individuals appear to be cleared more efficiently by macrophages (189,190). However, the mechanisms underlying these effects remain largely unknown, and as a consequence, future research should seek to elucidate those mechanisms.

II) The importance of various host iron stores for *Plasmodium* growth remains ambiguous. There is evidence that liver stage parasites need to acquire iron from the host and a liver-stage iron transporter (ZIPCO) has been identified (219,308). However, it is unclear whether blood-stage parasites need to acquire iron from the host. Our results indicate that serum iron is not of great importance as an iron source for *Plasmodium.* Hence, if and how *Plasmodium* acquires iron from the host during blood-stage infection remain key unanswered questions within the field.

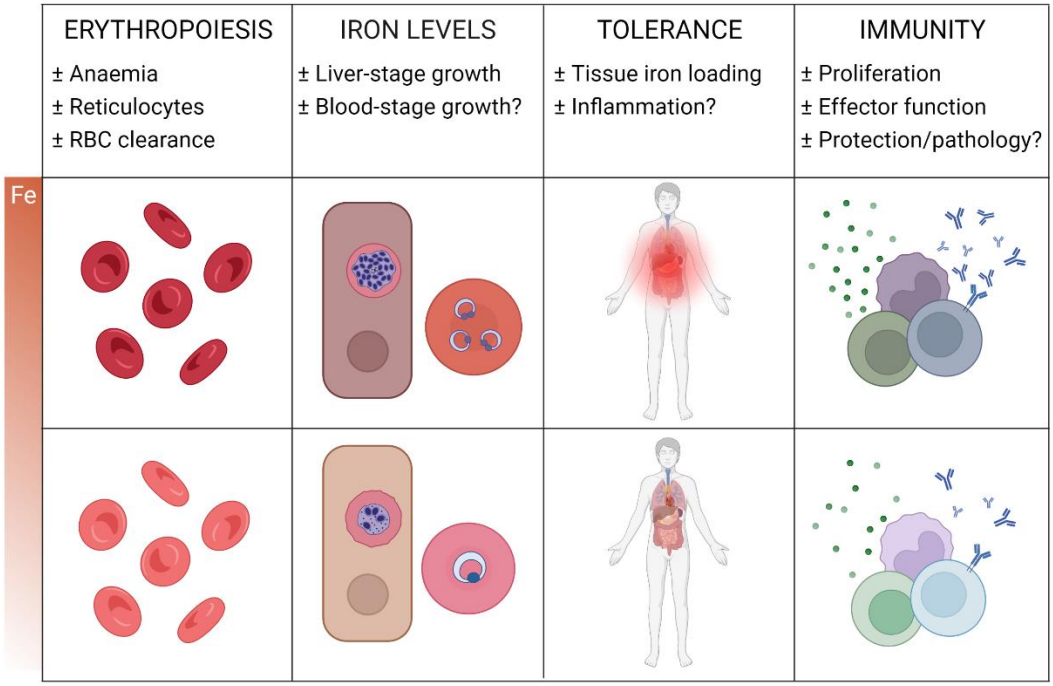


***Figure 7.1*. Proposed model of the effects of host iron status on malaria infection.** Host iron status affects erythropoiesis with downstream effects on red blood cell (RBC) physiology, *Plasmodium* growth and RBC clearance. The host's iron levels can impact on liver-stage growth and potentially also on blood-stage growth. The host's iron status affects tissue iron levels and tissue iron loading can disrupt tolerance in malaria. Possibly, immune cell iron availability also affects tissue level inflammation with effects on tolerance. Decreased iron availability impairs immune cell proliferation and effector function in malaria, but it remains to be seen whether this results in altered protective immunity or immunopathology.

III) Previous studies have shown the damaging effects of tissue iron loading on kidney and liver function during malaria (235,237). Here, we have shown for the first time that decreased tissue iron levels may also confer protection by improving malaria tolerance, specifically in the liver. Hopefully, this fascinating line of research will be expanded to determine whether it is mediated by immune or stromal and parenchymal cells, and whether it holds true in a clinical setting.

Furthermore, future studies should explore whether it is possible to pharmacologically target iron to improve malaria disease tolerance.

IV) Many questions still remain when it comes to the effect of iron deficiency on the immune response to malaria. We have discovered that disrupted cellular iron uptake has widespread inhibitory effects on immune cell expansion and effector function in malaria, with probable consequences for parasite control. However, it remains to be seen if malaria immunopathology and protective immunity is substantially altered by cellular iron deficiency. Consequently, research into this area should focus on answering these two questions, for example through antibody measurements, reinfection experiments and bone marrow transplant studies. In addition, cellular mechanisms and clinical implications should be identified.

The *Tfrc*$^{Y20H/Y20H}$ transgenic mice are a useful model to study the importance of cellular iron availability in the context of inflammation and immunity, and it could potentially be used to answer some of the questions posed here. In contrast to other models of iron depletion, such as iron deficient diet, the *Tfrc*$^{Y20H/Y20H}$ does not cause any severe anaemia which would also affect parasite physiology. Furthermore, this mutation may better mimic human conditions since it was first discovered in humans. However, the *Tfrc*$^{Y20H/Y20H}$ mutation occurs in all cells of our model, therefore it seems like a logical next step to use transplantation approaches of single immune subsets or the entire bone marrow to investigate the role of immune cell iron availability in malaria infection. Furthermore, the model can allow for transplantation of wild-type bone marrow to dissect the role of iron in the non-immune compartment in greater detail, but in the context of iron-sufficient immune cells. Therefore, it would be highly warranted to use these experimental approaches to further look at iron-dependent B cell and T cell responses to malaria, for instance in a lymphocyte-deficient mouse model or completely immunosuppressed mice. We would also be keen to investigate whether the effect observed in this thesis may be mainly derived from the non-immune compartment, which could be performed through wild-type bone marrow transplantation experiments. All together this model allows for greater insight into the role of cellular iron in a variety of immune cells and the

overall host and can further support specific aspects of iron biology in the context of malaria observed in this thesis.

7.2. General discussion

7.2.1. A brief history of iron and malaria

Iron is intricately linked with life on Earth, and iron has been proposed as a catalyst for early life and as a key driver of evolution (309). When early life-forms first appeared on Earth, soluble iron that could be used as a catalyst for biochemical reactions was abundant. However, as oxygen increased in the atmosphere over the last ~2.5 billion years, iron became increasingly oxidised making it less soluble and accessible. Consequently, life-forms developed strategies to acquire or recycle iron and these strategies were evolutionarily selected for (309). Indeed, today there are only two known organisms that do not require iron: *Lactobacilli* and *Borrelia burgdorferi* (310,311).

As a result, humans have tightly regulated systems to acquire, recycle and store iron, and to restrict iron from pathogens (see 1.1. Iron physiology). Human iron regulation has also been subject to evolutionary pressures, in particular during the Neolithic age, as humans shifted from living in a hunter-gatherer society to an agriculture-based society. At this time, their diet changed from meat and fish with plenty of bioavailable haem iron, to grains and dairy with low amounts of bioavailable iron (312). This shift in diet likely lead to an increase in iron deficiency among the population, and as a consequence, genetic polymorphisms that favour iron flux and iron storage appear around this time (312). For example, one of the most common mutations that causes iron overload, a single nucleotide substitution in *HFE*, likely originated in Europe during the Neolithic age (313). It was presumably selected for among the population because it confers a survival advantage to heterozygotes, by preventing iron deficiency through increased dietary iron absorption (312). Thus, human iron regulation has been shaped through interactions between shifts in human society and the evolutionary pressures of iron availability.

Malaria has probably had a greater impact on human evolution than any other pathogen. Genetic polymorphisms that result in altered RBC phenotypes are common in malaria endemic regions, because they confer a survival advantage against malaria infection (314). Three of the most common protective factors are sickle cell trait, thalassemia and glucose-6-phosphate dehydrogenase (G6PD) deficiency (315). Sickle cell anaemia is caused by a mutation in the gene that encodes the beta globin subunit of haemoglobin, and it results in the formation of sickle shaped RBCs, anaemia, and increased mortality. However, heterozygous carriers are protected from severe malaria (315). Individuals with thalassemia also have inherited mutations in the genes that encode alpha or beta globin, and both homozygous and heterozygous carriers are protected from severe malaria (315). Beyond haemoglobinopathies, mutations that cause G6PD deficiency result in a build-up of ROS inside RBCs, which can protect heterozygous carriers from severe malaria but causes haemolytic anaemia in homozygous carriers (315). Hence, some of the most well-known and prevalent mutations that protect humans from infectious disease are connected to iron, via haemoglobin, ROS and RBC survival.

Another astonishing example of human adaptation to malaria is the spread of a Duffy antigen "erythrocyte silent" mutation that has rendered the majority of Central and West African populations refractory to *P. vivax* infection (315). The Duffy antigen is a chemokine receptor that is essential for *P. vivax* merozoite invasion of RBCs (315). Heterozygotes that have the mutation still express Duffy antigen, albeit to a lesser degree, meaning that homozygosity is required to confer protection from *P. vivax* (314). The allele that confers Duffy negativity is almost at fixation in African populations, but very rare in other parts of the world. Hence, the Duffy mutation is thought to have arisen and spread after humans began migrating out of Africa, and as a result *P. vivax* is endemic in large areas of South America, Asia, and Oceania but not in Africa (315).

In turn, humans have affected the evolution of *Plasmodium* parasites. *P. falciparum* has surprisingly low genetic diversity and currently existing strains of *P. falciparum* likely emerged from a severe population bottleneck event ~10,000 years ago (316). This coincides with

growing human agricultural settlements, and thus it has been hypothesised that this bottleneck event represents adaptation to human infection (314). More recently, the extensive use of antimalarials has led to the spread of antimalarial resistance genes. Chloroquine resistance was first discovered in *P. falciparum* in South East Asia and South America in the late 1950s, and spread across much of Asia, South America and Africa through rapid selective sweeps of resistance genes (317). Within a few decades *P. falciparum* chloroquine resistance was essentially ubiquitous in many malaria endemic regions, causing a resurgence in cases (317). Concerningly, genes that confer resistance to artemisinin are now also becoming more widespread (83). The mechanism of action and resistance for both of these drugs is connected to the parasites ability to handle reactive iron and haem, and the resulting ROS (91,99). Consequently, the evolutionary pressure of antimalarials is having a major impact on *P. falciparum* iron regulation.

Looking into the future, humans, iron and malaria will inevitably remain entangled. Anthropogenic climate change is likely to increase both the risk of iron deficiency and malaria. Rising atmospheric CO_2 levels will decrease iron uptake by plants, and increase the risk of dietary iron deficiency for an estimated 1.4 billion people (318). Malaria transmission is largely dependent on time of mosquito stage and mosquito habitat, which is affected by temperature and humidity, respectively. Hence, global warming is predicted to increase malaria exposure (319). Hence, humans are having an impact on iron bioavailability and on malaria transmission, both of which will in turn affect human health.

7.2.2. Iron in malaria tolerance and resistance – a high stakes balancing act

Animals can employ three different strategies to protect themselves from infectious disease: avoidance, resistance and tolerance (231). Avoidance prevents or reduces exposure to infectious agents, primarily through the olfactory and gustatory sensory systems, which can trigger avoidant behaviours and reflexes. Resistance provides protection by decreasing pathogen burden, while tolerance limits damage to the host without affecting pathogen burden. Through

tolerance mechanisms the host can minimise both direct damage from the pathogen and collateral damage from the immune system (231).

Tolerance is particularly important in malaria infection. In fact, the discovery of tolerance to infectious disease in animals was made as a result of studies of malaria. A seminal study found that different inbred mouse strains had varying weight loss and anaemia (tolerance), despite having comparable parasite burden (resistance) (320). The importance of tolerance in malaria is also highlighted by the fact that high parasitaemia is not sufficient to cause severe disease and that anti-disease immunity precedes anti-parasite immunity (82,321,322).

As previously described in this thesis (see 4.1.3. Iron and haem affect malaria disease tolerance), a number of studies have identified the key role of iron and haem in malaria tolerance. Past studies have shown that tissue iron loading can disrupt malaria tolerance (234,235,237), but our findings additionally indicate that iron deficiency may improve malaria tolerance. *P. chabaudi* infected mice with decreased cellular iron uptake suffered less severe liver damage, putatively due to limited liver iron loading, and had increased serum iron levels that may have caused kidney damage. Although this particular pattern of altered iron distribution would not typically occur in an iron deficient individual, it provides valuable insight into how iron distribution affects malaria tolerance. Hence, we can hypothesise that an iron deficient person that has lower iron stores at the time of malaria infection may be able detoxify and store more iron without consequent tissue damage. However, the tissue protective effect of iron deficiency would likely come at the cost of erythropoiesis, as iron deficient individuals would be at greater risk of severe anaemia. In this context, it is interesting to consider whether iron deficiency might contribute to the varying severe malaria phenotypes seen in children and adults. Young children are more likely to be iron deficient and they often present with severe anaemia upon malaria infection (82,95). Adults on the other hand, are less likely to be iron deficient and in severe malaria they more often present with jaundice or acute kidney injury (82,95), which is consistent with a decreased ability to detoxify iron in the liver and kidney. Altogether, it appears to be vital for the host to maintain balanced iron levels during malaria

infection, which allow for normal physiological functions while preventing toxic tissue iron loading.

Our findings also suggest that iron is required to maintain the immune response to malaria infection. Mice with decreased cellular iron uptake have an attenuated pro-inflammatory immune response during the acute stage of *P. chabaudi* infection. Consequently, iron deficiency may increase the risk of uncontrolled *Plasmodium* growth, but it may also lower the risk of severe immunopathology. Both unrestrained parasite growth and an excessive pro-inflammatory immune response carry serious risks (102), although iron deficiency is usually accompanied by anaemia that likely limits parasite growth (211). Thus, the inhibitory effect of iron deficiency on the immune response to acute malaria may be protective on the whole, and it could be a contributing factor to the epidemiologically observed protective effect of iron deficiency in malaria.

However, in another trade-off, long term immunity may be impaired by iron deficiency, as the germinal centre response was inhibited in mice with decreased cellular iron uptake. Numerous factors (e.g. antigenic variation, complex life cycle) probably contribute to the slow pace at which immunity to non-severe malaria is acquired in humans, but it is possible that iron deficiency is a contributing factor in this regard. For example, the duration of antibody responses to *P. falciparum* appear to improve with age, and iron deficiency also becomes less prevalent with age in African children (96,323). Some argue that atypical memory B cells contribute to impaired immunity in malaria (158,159) and atypical memory B cells are associated with high malaria-transmission (324,325). As malaria is cause of iron deficiency (183), areas with high malaria transmission are also likely to have higher rates of iron deficiency. These are of course just observations that could be entirely coincidental. However, considering that we now know that decreased cellular iron can impair B cell function in mice, the effects of iron deficiency on B cells in human malaria infection warrant further investigation.

In summary, iron is inextricably linked to both malaria tolerance and resistance. Iron homeostasis during malaria infection appears to be vital to ensure balance between tissue damage and anaemia, and between immunity and immunopathology. However, it will be necessary to increase our understanding of the complex relationship between iron and malaria to intervene therapeutically.

7.2.3. The potential and perils of correcting iron deficiency to boost immunity

Nutrition is incredibly important for immune function, and malnutrition can have severe impacts on the immune system. This is highlighted by the striking fact that malnutrition is estimated to be an underlying cause of half of all deaths from infectious disease in children under the age of five (326). Furthermore, malnourished children may have altered responses to vaccination (327). Malnutrition is not equal to iron deficiency, however, iron deficiency, as the most common micronutrient deficiency, affects billions of people worldwide (30). Importantly, iron deficiency disproportionally affects areas with a high infectious disease burden, and frequent infections can lead to persistently raised hepcidin and cause iron deficiency (30,328). In addition, we are increasingly beginning to understand that iron is an important nutrient for immune function (44,73), a concept that is strengthened by the findings in this thesis. Taken together, these appear to be strong arguments for correcting iron deficiency to improve immunity. However, there is still limited evidence to support this approach and there are risks and complexities associated with iron supplementation.

Human observational studies that aim to assess the effects of iron deficiency and iron supplementation on infectious disease have generally been poorly controlled and have struggled with confounding factors, such as co-morbidities, socio-economic status and general malnutrition (71). Consequently, the effects of iron supplementation have varied across studies with some showing a protective effect, others an increased risk and others no effect at all. However, there is compelling evidence that iron supplementation increases the risk of sepsis in neonates, diarrhoea in children, and if no preventative measures are in place, malaria (71,329). When it comes to iron supplementation and vaccination, very little research has been conducted

so far. There is one study in piglets and one study in humans that have shown a positive effect of iron supplementation on vaccine responses (59,78). Hence, iron supplementation has the potential to be a simple and efficient way to improve vaccine efficacy, but additional well controlled and randomised clinical trials are needed to warrant implementation. This is particularly important when it comes to malaria vaccines, considering the safety concerns associated with iron supplementation in malaria endemic regions (194,197).

Nevertheless, in light of the findings in this thesis it is worth considering whether iron interventions could be used to improve infection- or vaccine-induced immunity to malaria. This would require finding ways to overcome the associated safety concerns. For example, in patients infected with malaria, iron supplementation could be administered together with antimalarials, with the aim of boosting immunity to decrease the risk of future clinical episodes. Alternatively, iron could be prescribed together with intermittent preventative antimalarial treatment, which is recommended to some groups in malaria endemic areas. Finally, it is worth considering if iron deficiency could be monitored and safely corrected as a part of routine childhood vaccination programmes.

Another challenge is that correcting iron deficiency through iron supplementation remains difficult in many situations. The children who are most at risk of dying from malaria may be frequently exposed to infection, and therefore have high hepcidin levels that can inhibit absorption of oral iron supplements (30,183). Potentially, this obstacle could be overcome through alternate day dosing of oral iron supplements, which appears to increase absorption compared to consecutive day dosing (330). Parenteral iron supplementation is unlikely to be a practical alternative in most settings, especially with children, although it is a highly efficient and well tolerated way of treating iron deficiency (30).

Whether or not iron supplementation can ultimately be used to boost immunity, it is still incredibly important that we understand the risks of iron supplementation so that we can mitigate them. Iron deficiency has a large socio-economic impact and can severely impact the health of those who are affected, causing disability, impaired development, and increased

maternal, foetal and perinatal mortality (30). Thus, we must aim to treat iron deficiency, and maintaining iron deficiency is not an ethical infectious disease prevention strategy, even if it reduces the risk of malaria infection. In fact, because malaria can cause iron deficiency, decreasing the malaria burden is also an important aspect of preventing iron deficiency anaemia in children (183). Hence, these two public health problems are closely entangled, and it is important that we increase our understanding of how they interact.

7.3. Final statement

In this thesis we have demonstrated that cellular iron deficiency results in higher *P. chabaudi* pathogen burden, altered pathology and an impaired immune response to infection. Additionally, we have shown that decreased immune cell iron availability can disrupt the response to malaria vaccination. These findings may have implications for malaria treatment strategies and malaria vaccine design and implementation in the future.

Supplemental data

Flow cytometry antibody panels

Table S1. Flow cytometry antibody panel for myeloid cells in Chapter 3.

Fluorophore	Marker	Dilution	Surface/ Intracellular	Clone	Supplier	Cat. no.
BUV395	SA	1:400	S		BD	564176
Biotin	CD71	1:400	S	RI7217	BioLegend	113803
BV421	CD11b	1:200	S	M1/70	BioLegend	101235
BV605	Ly6C	1:200	S	HK1.4	BioLegend	128035
FITC	CD45	1:400	S	30-F11	BioLegend	103107
PerCP Cy5.5	Ly6G	1:200	S	1A8	BioLegend	127615
PE	Siglec F	1:200	S	S17007L	BioLegend	155505
PE Cy7	CD11c	1:200	S	N418	BioLegend	117317
APC	I-A/I-E (MHC II)	1:200	S	M5/114.15.2	BioLegend	107613
APC Cy7	B220	1:200	S	RA3-6B2	BioLegend	103224
APC Cy7	CD90.2	1:200	S	30-H12	BioLegend	105327
APC Cy7	NK1.1	1:200	S	PK136	BioLegend	108723
APC Cy7	TER119	1:200	S	TER-119	BioLegend	116223
Zombie NIR Fixable Viability Kit		1:300			BioLegend	423105

Table S2. Flow cytometry antibody panel for lymphocytes in Chapter 3.

Fluorophore	Marker	Dilution	Surface/ Intracellular	Clone	Supplier	Cat. no.
BUV395	SA	1:400	S		BD	564176
Biotin	CD71	1:400	S	RI7217	BioLegend	113803
PB	CD45	1:200	S	30-F11	BioLegend	103125
BV605	B220	1:200	S	RA3-6B	BioLegend	103243
FITC	NK1.1	1:400	S	PK136	BioLegend	108705
PerCP Cy5.5	TCRβ	1:200	S	H57-597	BioLegend	109227
PE	CD8	1:200	S	53-6.7	BioLegend	100707
PE Cy7	TCRγδ	1:200	S	GL3	BioLegend	118123
APC	CD4	1:200	S	GK1.5	BioLegend	100411
APC Cy7	TER119	1:200	S	TER-119	BioLegend	116223
Zombie NIR Fixable Viability Kit		1:300			BioLegend	423105

Table S3. Flow cytometry antibody panel for bone marrow B cells in Chapter 3.

Fluorophore	Marker	Dilution	Surface/ Intracellular	Clone	Supplier	Cat. no.
BV421	CD127	1:200	S	A7R34	BioLegend	135023
BV605	B220	1:200	S	RA3-6B	BioLegend	103243

PerCP Cy5.5	IgD	1:200	S	11-26c.2a	BioLegend	405709
PE	CD3	1:200	S	17A2	BioLegend	100205
PE	CD4	1:200	S	GK1.5	BioLegend	100407
PE	CD8	1:200	S	53-6.7	BioLegend	100707
PE	CD11b	1:200	S	M1/70	BioLegend	101207
PE	Ly6G	1:200	S	1A8	BioLegend	127607
PE	Ter119	1:200	S	TER-119	BioLegend	116207
PE Cy7	CD71	1:200	S	RI7217	BioLegend	113811
APC	CD43	1:200	S	S11	BioLegend	143207
Zombie NIR Fixable Viability Kit		1:300			BioLegend	423105

Table S4. Flow cytometry antibody panel for transitional/mature splenic B cells in Chapter 3.

Fluorophore	Marker	Dilution	Surface/ Intracellular	Clone	Supplier	Cat. no.
BV421	CD71	1:200	S	RI7217	BioLegend	113813
BV605	B220	1:200	S	RA3-6B	BioLegend	103243
PerCP Cy5.5	CD23	1:200	S	B3B4	BioLegend	101617
PE	CD43	1:200	S	S11	BioLegend	143205
PE Cy7	CD5	1:200	S	53-7.3	BioLegend	100621
APC	CD93	1:200	S	AA4.1	BioLegend	136509
APC Cy7	CD11b	1:200	S	M1/70	BioLegend	101226
APC Cy7	CD90.2	1:200	S	30-H12	BioLegend	105327
Zombie NIR Fixable Viability Kit		1:300			BioLegend	423105

Table S5. Flow cytometry panel for erythroid cells in Chapter 4.

Fluorophore	Marker	Dilution	Surface/ Intracellular	Clone	Supplier	Cat. no.
BV421	Ter119	1:200	S			
PE	CD4	1:200	S	GK1.5	BioLegend	100407
PE	CD8	1:200	S	53-6.7	BioLegend	100707
PE	CD11b	1:200	S	M1/70	BioLegend	101207
PE	CD19	1:200	S	6D5	BioLegend	115507
PE	CD138	1:200	S	281-2	BioLegend	142503
PE Cy7	CD71	1:200	S	RI7217	BioLegend	113811
APC	CD44	1:200	S	IM7	BioLegend	103011
Zombie NIR Fixable Viability Kit		1:300			BioLegend	423105

Table S6. Flow cytometry panel for MNPs in Chapter 5.

Fluorophore	Marker	Dilution	Surface/ Intracellular	Clone	Supplier	Cat. no.
BUV395	SA	1:400	S		BD	564176

Biotin	I-A/I-E (MHC II)	1:200	S	M5/114.15.2	BioLegend	107603
BV421	CD11b	1:200	S	M1/70	BioLegend	101235
BV605	Ly6C	1:200	S	HK1.4	BioLegend	128035
PE	CD36	1:200	S	HM36	BioLegend	102605
PE Dazzle	SiglecF,	1:200	S	S17007L	BioLegend	155529
PE Dazzle	Ly6G	1:200	S	1A8	BioLegend	127647
PE Cy7	CD11c	1:200	S	N418	BioLegend	117317
APC	CD80	1:200	S	16-10A1	BioLegend	104713
APC Cy7	B220	1:200	S	RA3-6B2	BioLegend	103224
APC Cy7	CD90.2	1:200	S	30-H12	BioLegend	105327
APC Cy7	TER119	1:200	S	TER-119	BioLegend	116223
LIVE/DEAD Fixable Near IR (780) Viability Kit		1:1000			Invitrogen	L34992

Table S7. Flow cytometry panel for MNP cytokine production in Chapter 5.

Fluorophore	**Marker**	**Dilution**	**Surface/ Intracellular**	**Clone**	**Supplier**	**Cat. no.**
BUV395	SA	1:200	S		BD	564176
Biotin	I-A/I-E (MHC II)	1:200	S	M5/114.15.2	BioLegend	107603
BV421	CD11b	1:200	S	M1/70	BioLegend	101235
BV605	Ly6C	1:200	S	HK1.4	BioLegend	128035
FITC	TNFα	1:200	I	MP6-XT22	BioLegend	506303
PE	CD11c	1:200	S	N418	BioLegend	117307
PE Dazzle	SiglecF,	1:200	S	S17007L	BioLegend	155529
PE Dazzle	Ly6G	1:200	S	1A8	BioLegend	127647
PE Cy7	IFNγ	1:200	I	XMG1.2	BioLegend	505825
APC	IL-12	1:200	I	C15.6	BioLegend	505205
APC Cy7	B220	1:200	S	RA3-6B2	BioLegend	103224
APC Cy7	CD90.2	1:200	S	30-H12	BioLegend	105327
APC Cy7	TER119	1:200	S	TER-119	BioLegend	116223
LIVE/DEAD Fixable Near IR (780) Viability Kit		1:1000			Invitrogen	L34992

Table S8. Flow cytometry panel for granulocytes and NK cells in Chapter 5.

Fluorophore	**Marker**	**Dilution**	**Surface/ Intracellular**	**Clone**	**Supplier**	**Cat. no.**
BUV395	SA	1:200	S		BD	564176
Biotin	NK1.1	1:200	S	PK136	BioLegend	108703
BV421	CD11b	1:200	S	M1/70	BioLegend	101235
BV605	NKp46	1:200	S	29A1.4	BioLegend	137619
BV785	CD45.2	1:200	S	104	BioLegend	109839
PerCP Cy5.5	TCRβ	1:200	S	H57-597	BioLegend	109227
PE	Siglec F	1:200	S	S17007L	BioLegend	155505

PE Cy7	TCRγδ	1:200	S	GL3	BioLegend	118123
APC	Ly6G	1:200	S	1A8	BioLegend	127621
APC Cy7	B220	1:200	S	RA3-6B2	BioLegend	103224
APC Cy7	TER119	1:200	S	TER-119	BioLegend	116223
Zombie NIR Fixable Viability Kit		1:300			BioLegend	423105

Table S8. Flow cytometry panel for T cells in Chapter 5.

Fluorophore	**Marker**	**Dilution**	**Surface/ Intracellular**	**Clone**	**Supplier**	**Cat. no.**
BUV395	SA	1:200	S		BD	564176
Biotin	TCRβ	1:200	S	H57-597	BioLegend	109203
BUV805	CD4	1:200	S	RM4-5	Invitrogen	368-0042-82
BV421	TBET	1:200	I	4B10	BioLegend	644815
BV605	CD62L	1:200	S	MEL-14	BioLegend	104438
BV785	CD8	1:200	S	53-6.7	BioLegend	100749
FITC	KI67	1:200	I	SolA15	Invitrogen	11-5698-80
PerCP Cy5.5	CD44	1:200	S	IM7	BioLegend	103031
PE	CXCR3	1:200	S	CXCR3-173	BioLegend	126505
PE Cy7	FOXP3	1:200	I	FJK-16s	Invitrogen	25-5773-80
APC	CD127	1:200	S	A7R34	BioLegend	135011
APC Cy7	B220	1:200	S	RA3-6B2	BioLegend	103224
APC Cy7	CD11b	1:200	S	M1/70	BioLegend	101226
APC Cy7	TER119	1:200	S	TER-119	BioLegend	116223
LIVE/DEAD Fixable Near IR (780) Viability Kit		1:1000			Invitrogen	L34992

Table S9 . Flow cytometry panel for T cells in Chapter 5.

Fluorophore	**Marker**	**Dilution**	**Surface/ Intracellular**	**Clone**	**Supplier**	**Cat. no.**
BUV395	SA	1:200	S		BD	564176
Biotin	TCRβ	1:200	S	H57-597	BioLegend	109203
BUV805	CD4	1:200	S	RM4-5	Invitrogen	368-0042-82
BV421	CXCR5	1:200	S	L138D7	BioLegend	145511
BV605	ICOS	1:200	S	C398.4A	BioLegend	313537
BV785	CD8	1:200	S	53-6.7	BioLegend	100749
FITC	PD1	1:200	S	29F.1A12	BioLegend	135213
PerCP Cy5.5	CD44	1:200	S	IM7	BioLegend	103031
PE	CD25	1:200	S	PC61	BioLegend	102007
PE Cy7	FOXP3	1:200	I	FJK-16s	Invitrogen	25-5773-80
APC	BCL6	1:200	I	BCL-DWN	Invitrogen	17-5453-80
APC Cy7	B220	1:200	S	RA3-6B2	BioLegend	103224
APC Cy7	CD11b	1:200	S	M1/70	BioLegend	101226
APC Cy7	TER119	1:200	S	TER-119	BioLegend	116223

LIVE/DEAD Fixable Near IR (780) Viability Kit	1:1000			Invitrogen	L34992

Table S10 . Flow cytometry panel for T cell cytokine production in Chapter 5.

Fluorophore	**Marker**	**Dilution**	**Surface/ Intracellular**	**Clone**	**Supplier**	**Cat. no.**
BV421	TNFα	1:200	I	MP6-XT22	BioLegend	506328
BV605	CD44	1:200	S	IM7	BioLegend	103047
BV785	CD8	1:200	S	53-6.7	BioLegend	100749
FITC	CD4	1:200	S	GK1.5	BioLegend	100405
PerCP Cy5.5	TCRβ	1:200	S	H57-597	BioLegend	109227
PE	IL-10	1:200	I	JES5-16E3	BioLegend	505007
PE Cy7	IFNγ	1:200	I	XMG1.2	BioLegend	505825
APC	CD154	1:200	I	MR1	BioLegend	106509
APC Cy7	B220	1:200	S	RA3-6B2	BioLegend	103224
APC Cy7	CD11b	1:200	S	M1/70	BioLegend	101226
APC Cy7	TER119	1:200	S	TER-119	BioLegend	116223
Zombie NIR Fixable Viability Kit		1:1000			BioLegend	423105

Table S11. Flow cytometry panel for B cells in Chapter 5.

Fluorophore	**Marker**	**Dilution**	**Surface/ Intracellular**	**Clone**	**Supplier**	**Cat. no.**
BUV395	SA	1:200	S		BD	564176
Biotin	CD71	1:200	S	RI7217	BioLegend	113803
PB	GL7	1:200	S	GL7	BioLegend	144613
BV605	B220	1:200	S	RA3-6B2	BioLegend	103243
FITC	IgM	1:200	S & I	II/41	Invitrogen	11-5790-81
PerCP Cy5.5	IgD	1:200	S	11-26c.2a	BioLegend	405709
PE	CD138	1:200	S	281-2	BioLegend	142503
PE Cy7	CD95	1:200	S	Jo2	BD	557653
APC	IgG1	1:200	S & I	RMG1-1	BioLegend	406609
APC	IgG2a	1:200	S & I	RMG2a-62	BioLegend	407109
APC	IgG2b	1:200	S & I	RMG2b-1	BioLegend	406711
APC Cy7	CD11b	1:200	S	M1/70	BioLegend	101226
APC Cy7	CD90.2	1:200	S	30-H12	BioLegend	105327
APC Cy7	TER119	1:200	S	TER-119	BioLegend	116223
LIVE/DEAD Fixable Near IR (780) Viability Kit		1:1000			Invitrogen	L34992

Table S12. Flow cytometry panel for *in vitro* cultured CD4 T cells in Chapter 5.

Fluorophore	**Marker**	**Dilution**	**Surface/ Intracellular**	**Clone**	**Supplier**	**Cat. no.**
CellTrace Violet		1:1000			Invitrogen	C34571

FITC	TNFα	1:200	I	MP6-XT22	BioLegend	506303
PerCP Cy5.5	CD4	1:200	S	GK1.5	BioLegend	100433
PE	CD71	1:200	S	RI7217	BioLegend	113807
PE Cy7	IFNγ	1:200	I	XMG1.2	BioLegend	505825
APC	IL-12	1:200	I	C15.6	BioLegend	505205
Zombie NIR Fixable Viability Kit		1:1000			BioLegend	423105

Table S13. Flow cytometry panel for *in vitro* cultured B cells in Chapter 5.

Fluorophore	**Marker**	**Dilution**	**Surface/ Intracellular**	**Clone**	**Supplier**	**Cat. no.**
CellTrace Violet		1:1000			Invitrogen	C34571
FITC	CD71	1:400	S	RI7217	BioLegend	113805
PerCP Cy5.5	B220	1:200	S	RA3-6B2	BioLegend	103235
PE	CD138	1:200	S	281-2	BioLegend	142503
PE Cy7	CD98	1:200	S	RL388	BioLegend	128213
APC	IgG1	1:200	S	RMG1-1	BioLegend	406609
Zombie NIR Fixable Viability Kit		1:1000			BioLegend	423105

Table S14. Flow cytometry panel for T cells in Chapter 6.

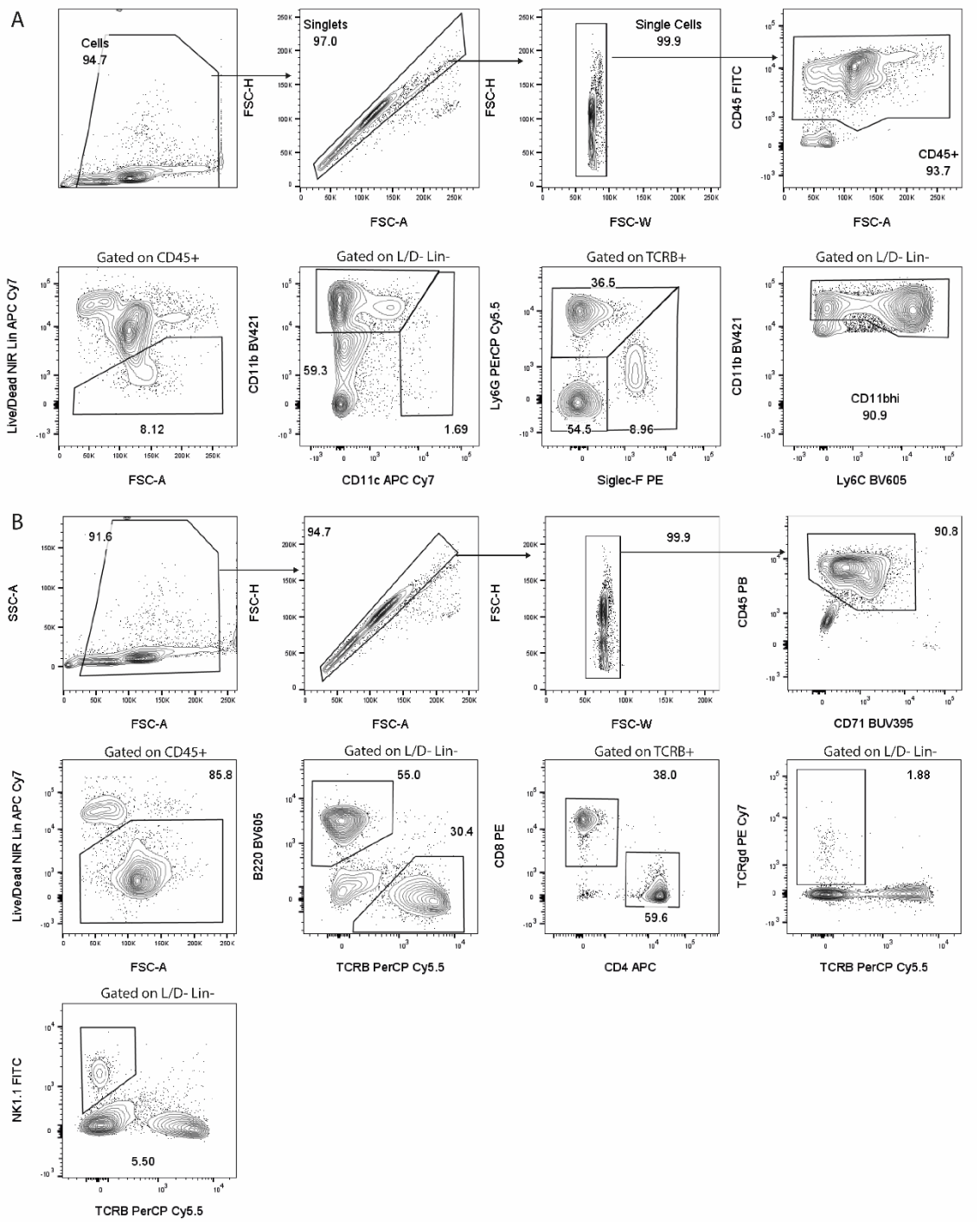
Fluorophore	**Marker**	**Dilution**	**Surface/ Intracellular**	**Clone**	**Supplier**	**Cat. no.**
BV421	CXCR5	1:200	S	L138D7	BioLegend	145511
BV605	CD8	1:200	S	53-6.7	BioLegend	100743
FITC	CD44	1:400	S	IM7	BioLegend	103005
PerCP Cy5.5	TCRβ	1:200	S	H57-597	BioLegend	109227
PE	CD71	1:200	S	RI7217	BioLegend	113807
PE Cy7	PD1	1:200	S	RMP1-3	BioLegend	109109
APC	CD4	1:200	S	GK1.5	BioLegend	100411
APC Cy7	B220	1:200	S	RA3-6B2	BioLegend	103224
APC Cy7	CD11b	1:200	S	M1/70	BioLegend	101226
Zombie NIR Fixable Viability Kit		1:300			BioLegend	423105

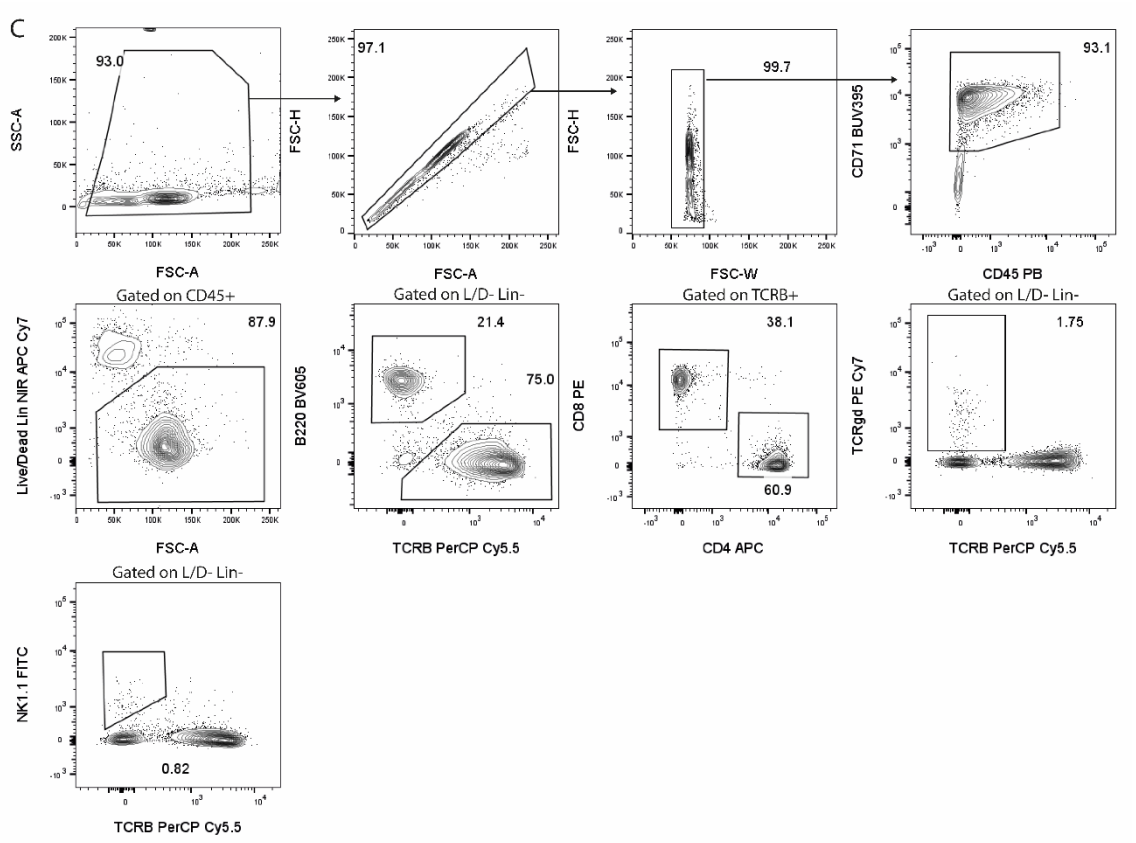
Table S15. Flow cytometry panel for B cells in Chapter 6.

Fluorophore	**Marker**	**Dilution**	**Surface/ Intracellular**	**Clone**	**Supplier**	**Cat. no.**
BV421	CD71	1:200	S	RI7217	BioLegend	113813
BV605	B220	1:200	S	RA3-6B2	BioLegend	103243
FITC	GL7	1:400	S	GL7	BioLegend	144603
PerCP Cy5.5	IgD	1:200	S	11-26c.2a	BioLegend	405709
PE	CD138	1:200	S	281-2	BioLegend	142503
PE Cy7	CD95	1:200	S	Jo2	BD	557653

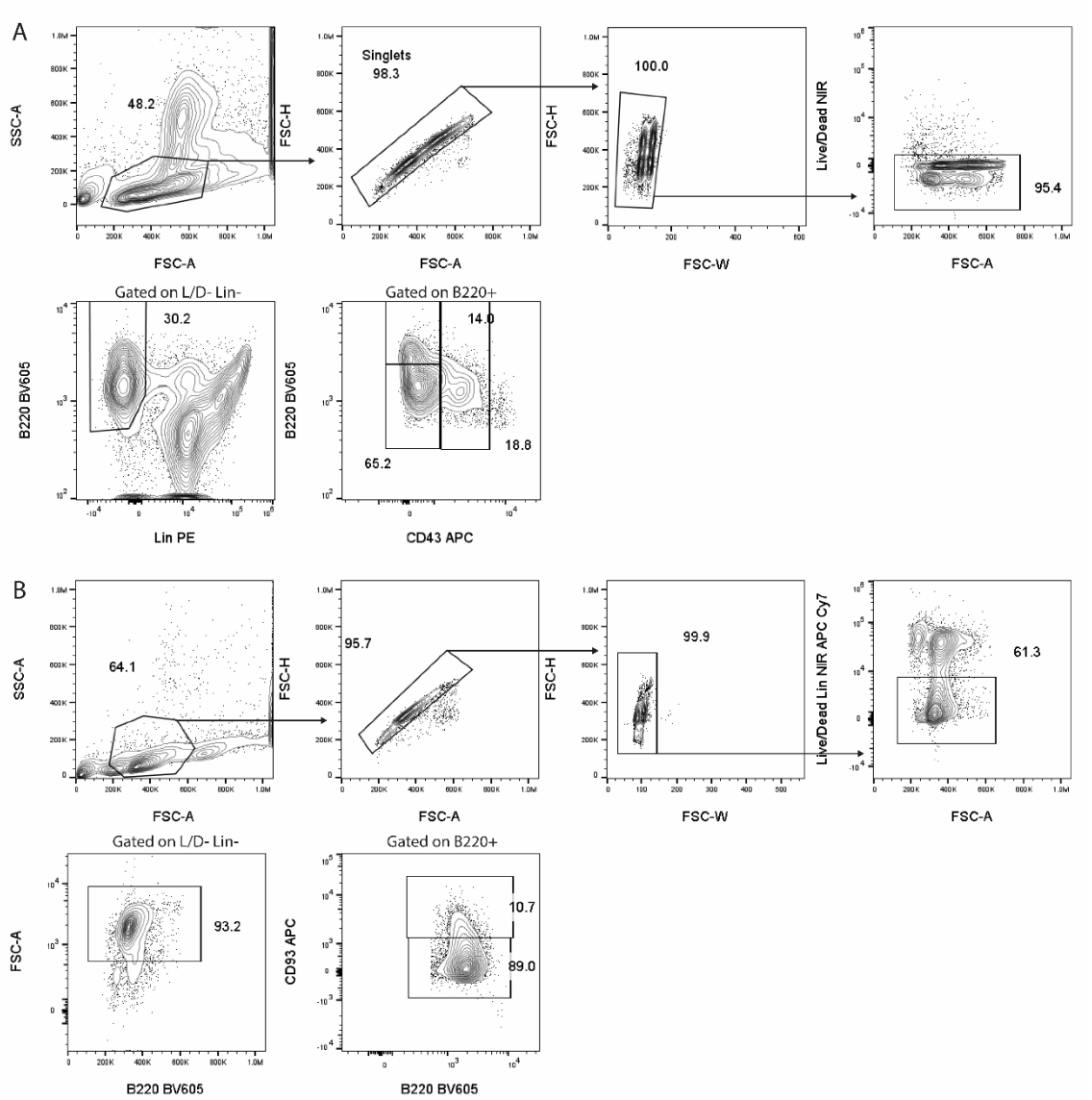
APC	IgG1	1:200	S	RMG1-1	BioLegend	406609
APC Cy7	CD11b	1:200	S	M1/70	BioLegend	101226
APC Cy7	CD90.2	1:200	S	30-H12	BioLegend	105327
Zombie NIR Fixable Viability Kit		1:300			BioLegend	423105

Flow cytometry gating schemes

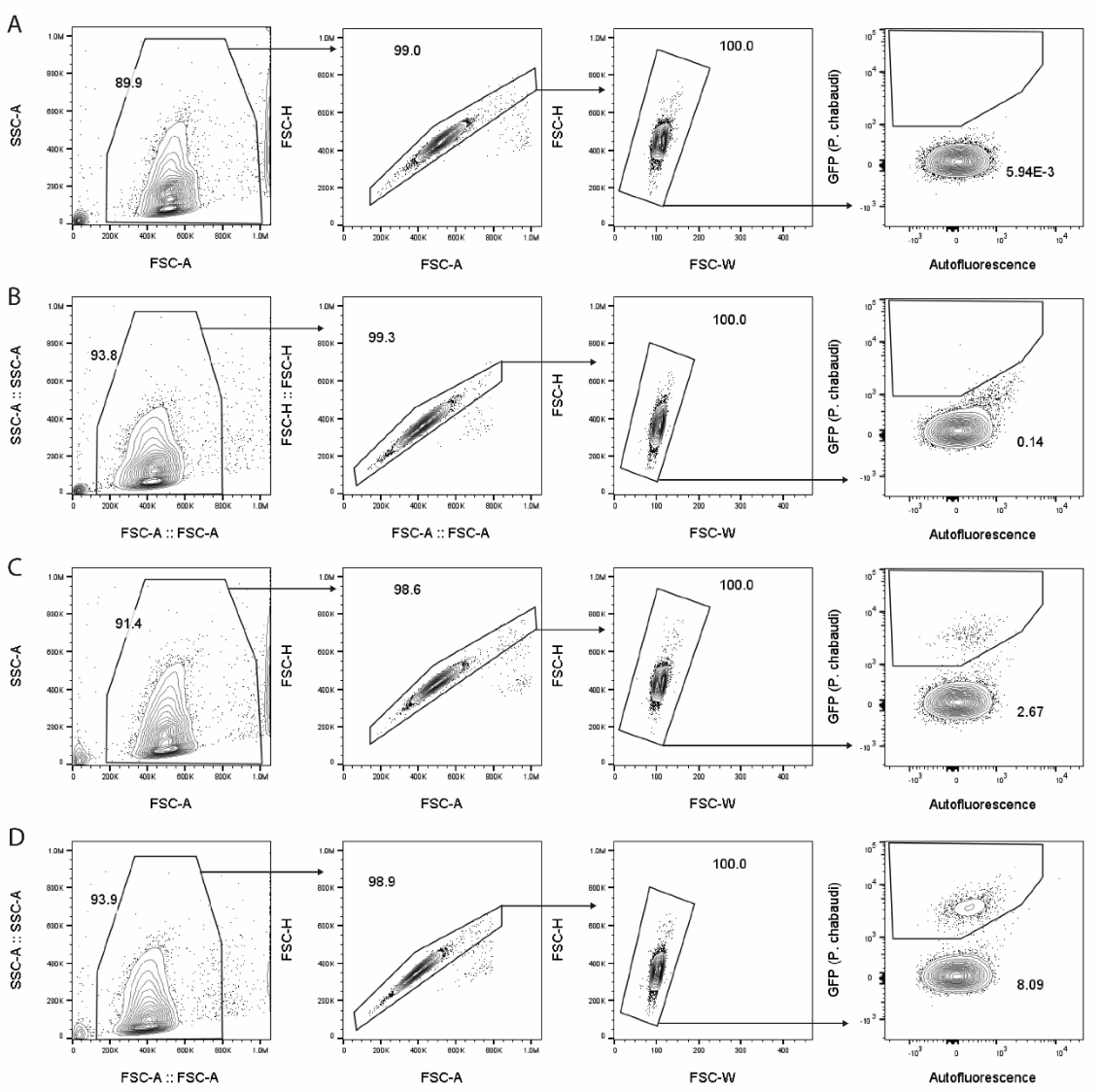




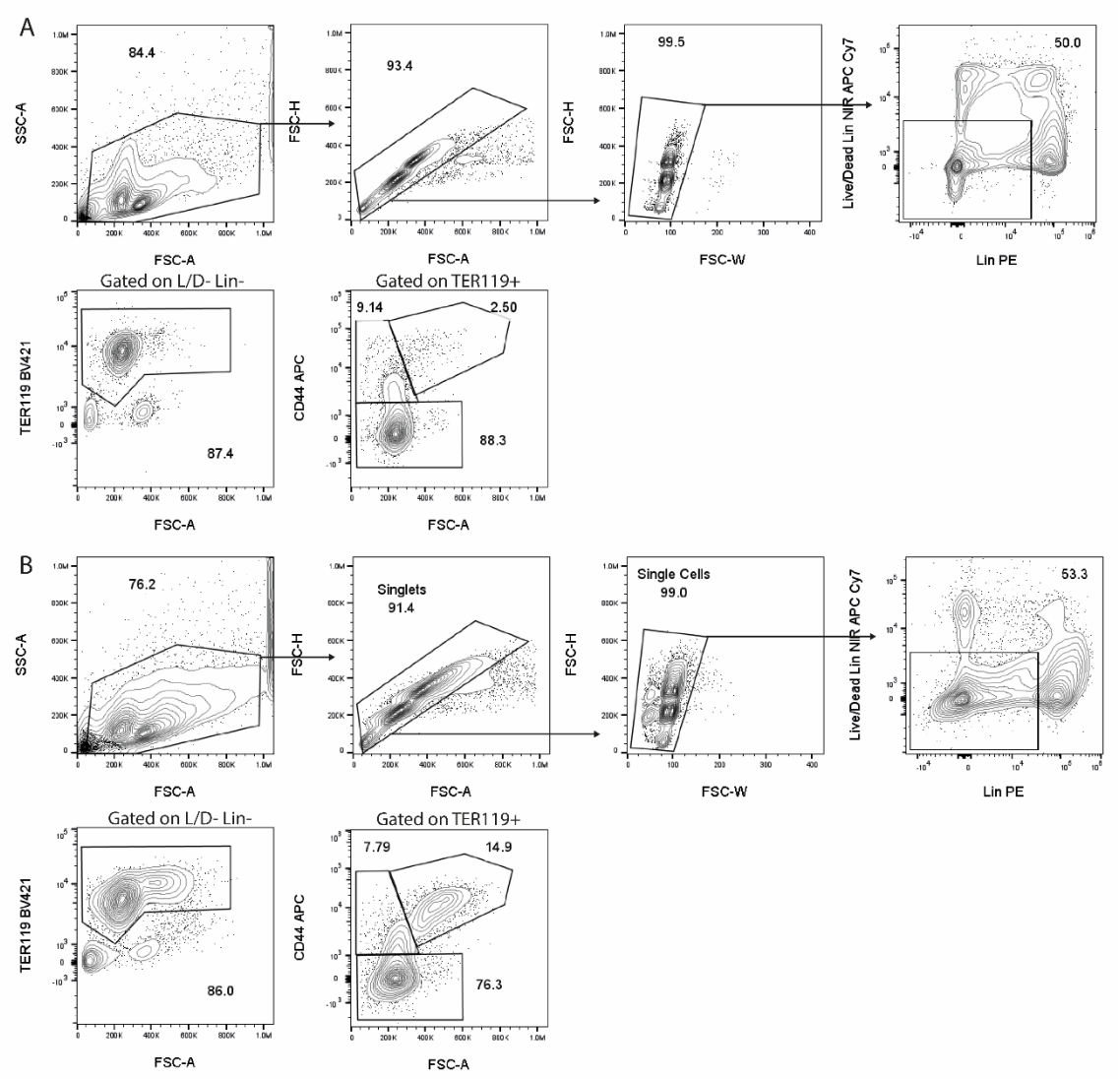
Supplemental figure S1. **Representative flow cytometry gating schemes for Chapter 3.** The immunophenotype of untreated C57BL/6 (WT) and *Tfrc*$^{Y20H/Y20H}$ (TfR) mice was analysed by flow cytometry. There were no major visually appreciable differences in WT and TfR populations. Gating from a representative WT mouse is displayed. **A)** Myeloid cell gating strategy. **B-C)** Lymphocyte gating strategy for spleen (B) and lymph node (C). An identical gating strategy was employed for vehicle and mini-hepcidin treated mice and no major differences in immune populations was observed. Hence, this figure can also be considered representative for mini-hepcidin and vehicle treated mice.



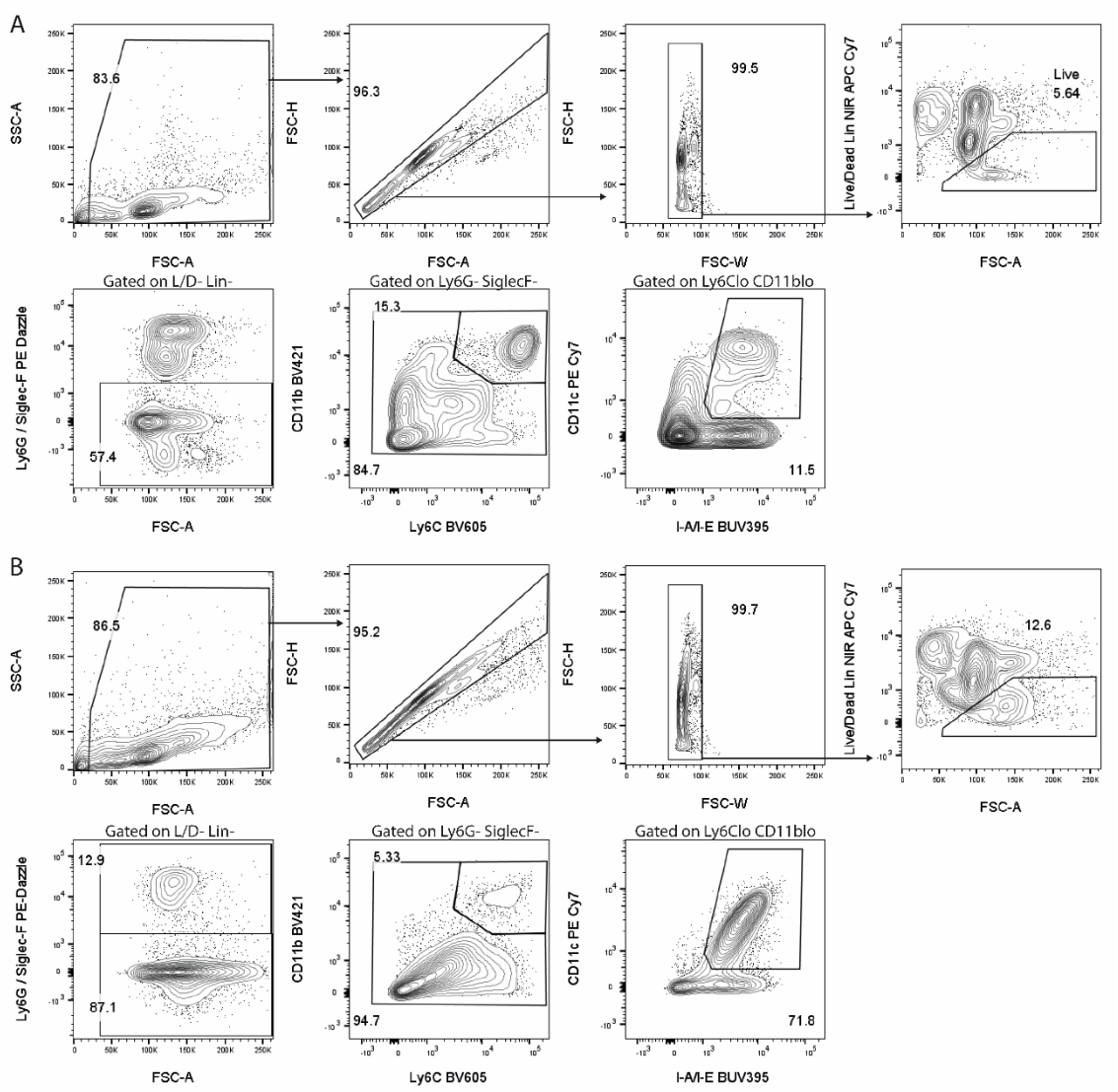
Supplemental figure S2. **Representative flow cytometry gating schemes for B cells in Chapter 3.** The B cells of untreated C57BL/6 (WT) and *Tfrc*$^{Y20H/Y20H}$ (TfR) mice was analysed by flow cytometry. There were no major visually appreciable differences in WT and TfR populations. Gating from a representative WT mouse is displayed. **A)** Bone marrow B cell gating strategy, based on Arnold et al (331). **D)** Spleen B cell gating strategy, based on Teague et al (332). CD93$^{+/-}$ gates were set according to FMO.



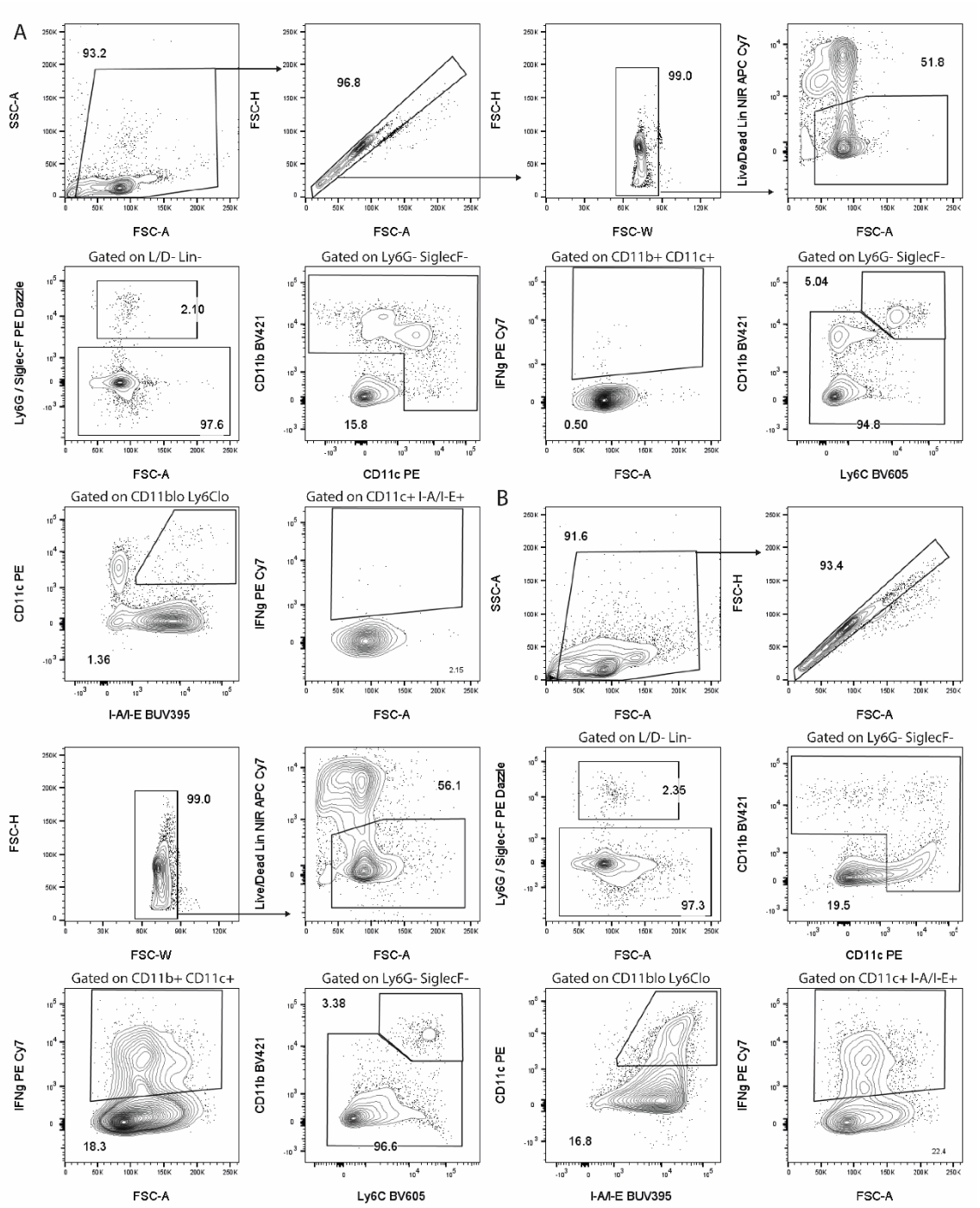
Supplemental figure S3. **Representative flow cytometry gating schemes for monitoring *P. chabaudi* infection in Chapter 4.** C57BL/6 (WT) and *Tfrc*$^{Y20H/Y20H}$ (TfR) mice were infected with *P. chabaudi* expressing GFP. Representative gating scheme for total and infected (GFP^{+}) red blood cells. The initial gate was adjusted between WT and TfR mice to adjust for TR mice having microcytic RBCs (i.e. lower FSC-A). **A)** Uninfected WT. **B)** Uninfected TfR. **C)** Infected WT. **D)** Infected TfR.



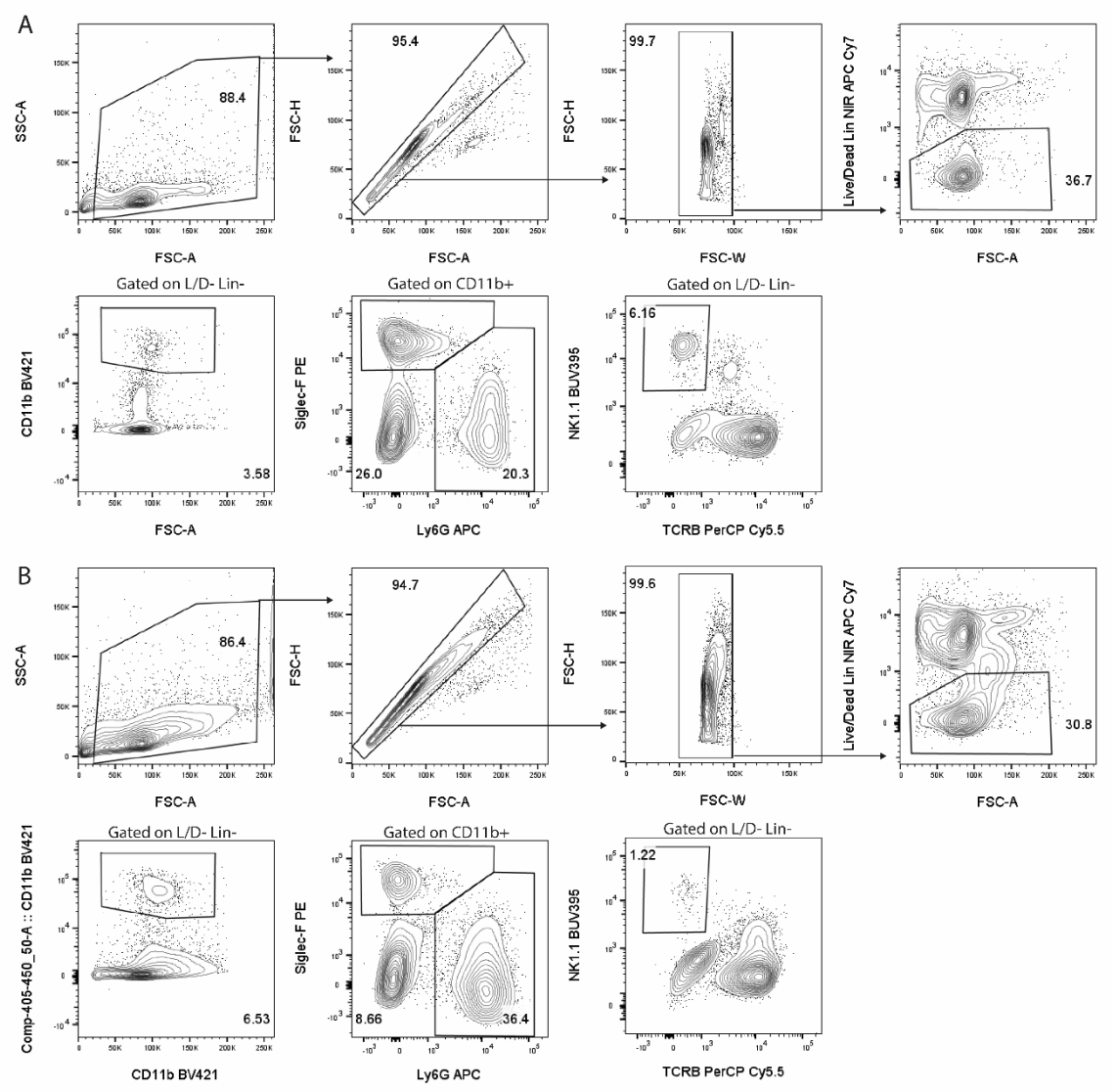
Supplemental figure S4. **Representative flow cytometry gating schemes for erythroid cells in Chapter 4.** The splenic erythroid response of C57BL/6 (WT) and *Tfrc*$^{Y20H/Y20H}$ (TfR) mice infected with *P. chabaudi* was analysed by flow cytometry. Gating scheme for splenic erythroid cells, based on Chen et al. (333). There were no major visually appreciable differences in WT and TfR populations, except for those described in the results section. Gating from a representative **A)** uninfected and **B)** infected WT mouse is displayed.



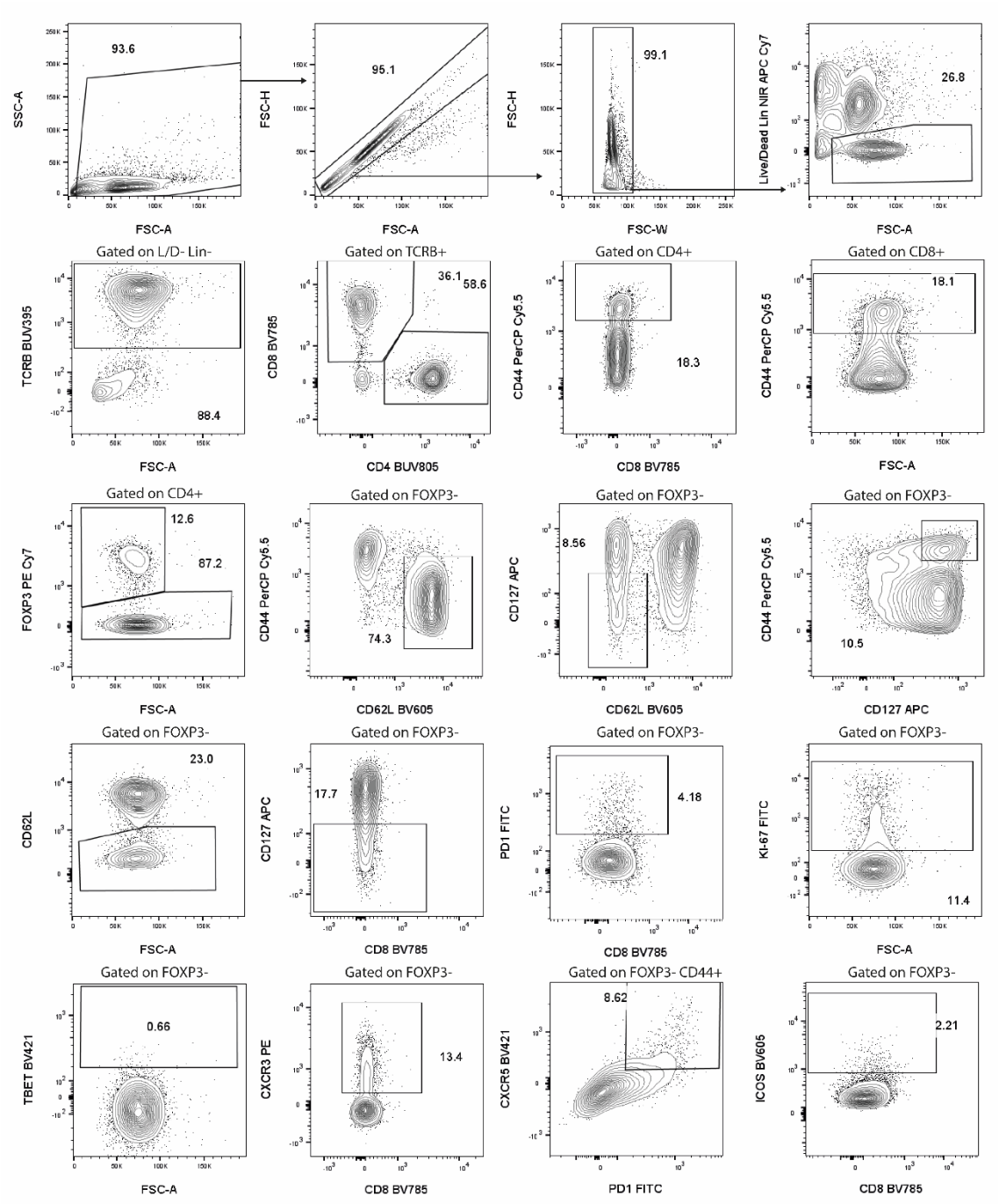
Supplemental figure S5. **Representative flow cytometry gating schemes for mononuclear phagocytes in Chapter 5.** The splenic immune response of C57BL/6 (WT) and *Tfrc*$^{Y20H/Y20H}$ (TfR) mice infected with *P. chabaudi* was analysed by flow cytometry. Mononuclear phagocyte gating strategy. There were no major visually appreciable differences in WT and TfR populations. Gating from a representative **A)** uninfected and **B)** infected WT mouse is displayed.



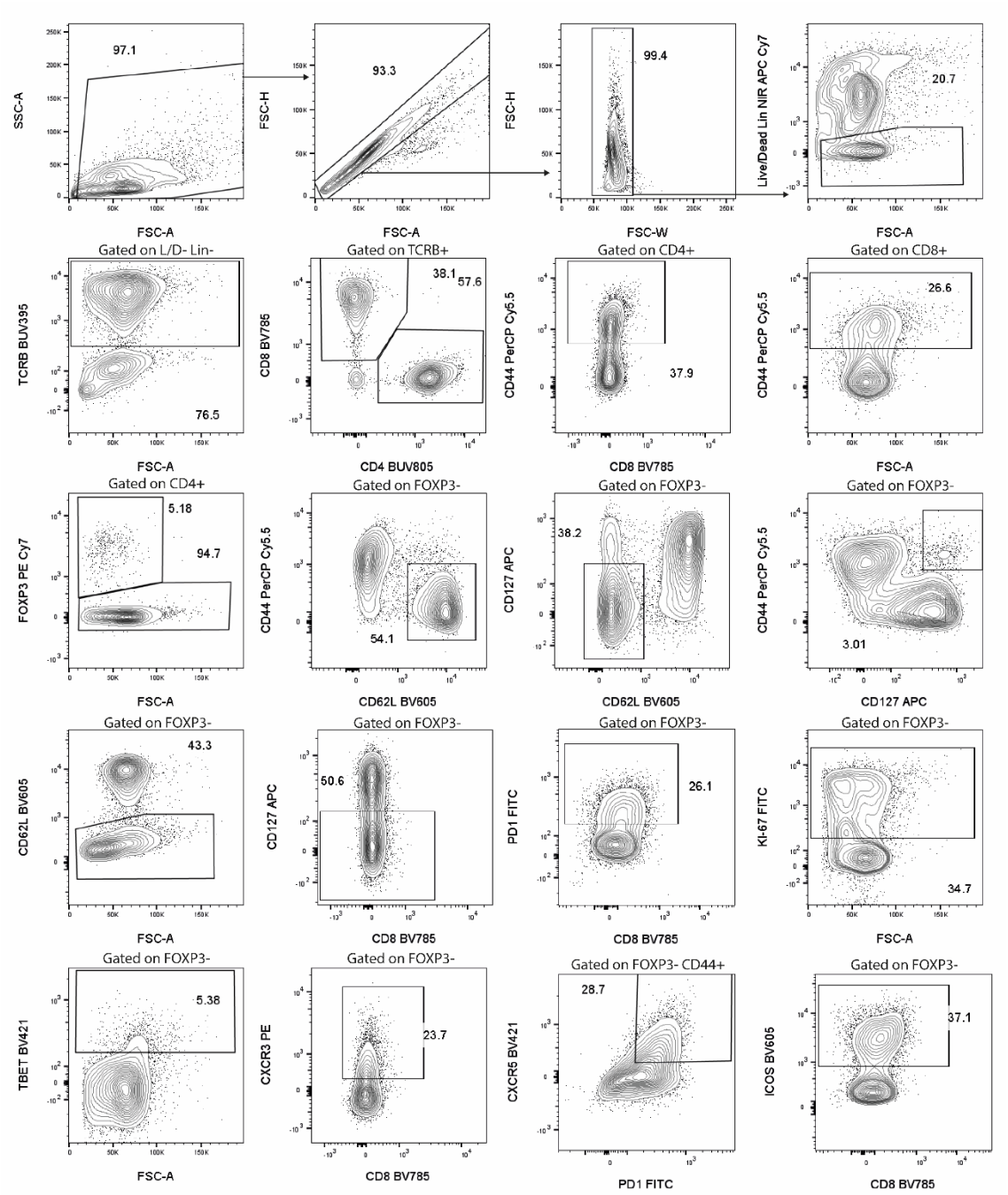
Supplemental figure S6. **Representative flow cytometry gating schemes for mononuclear phagocyte cytokine production in Chapter 5.** The splenic immune response of C57BL/6 (WT) and *Tfrc*$^{Y20H/Y20H}$ (TfR) mice infected with *P. chabaudi* was analysed by flow cytometry. Gating strategy for IFNγ producing MNPs. There were no major visually appreciable differences in WT and TfR populations. Gating from a representative **A)** uninfected and **B)** infected WT mouse is displayed.



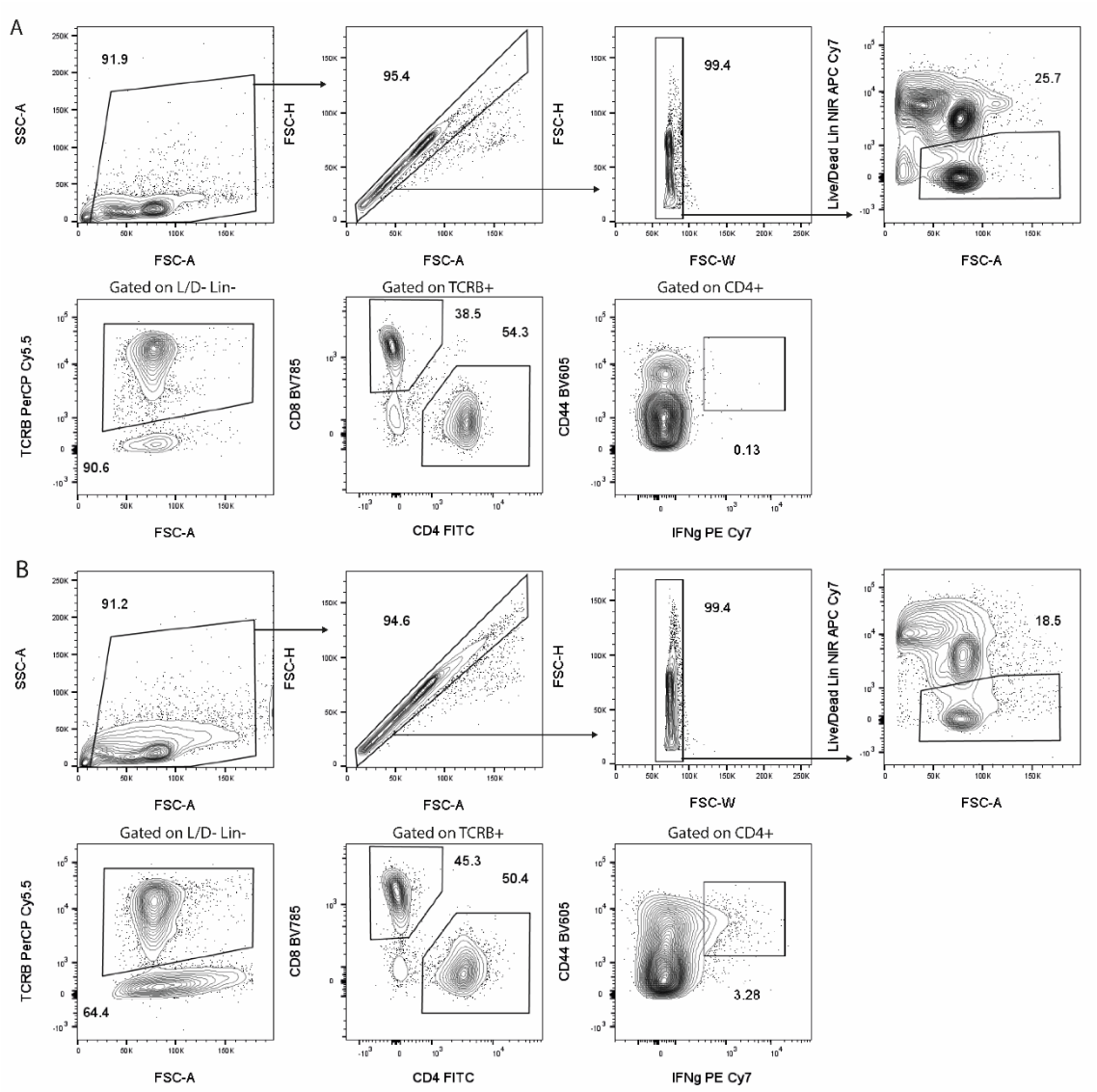
Supplemental figure S7. **Representative flow cytometry gating schemes for granulocytes and NK cells in Chapter 5.** The splenic immune response of C57BL/6 (WT) and *Tfrc*$^{Y20H/Y20H}$ (TfR) mice infected with *P. chabaudi* was analysed by flow cytometry. Gating strategy for neutrophils, eosinophils and NK cells. There were no major visually appreciable differences in WT and TfR populations. Gating from a representative **A)** uninfected and **B)** infected WT mouse is displayed.



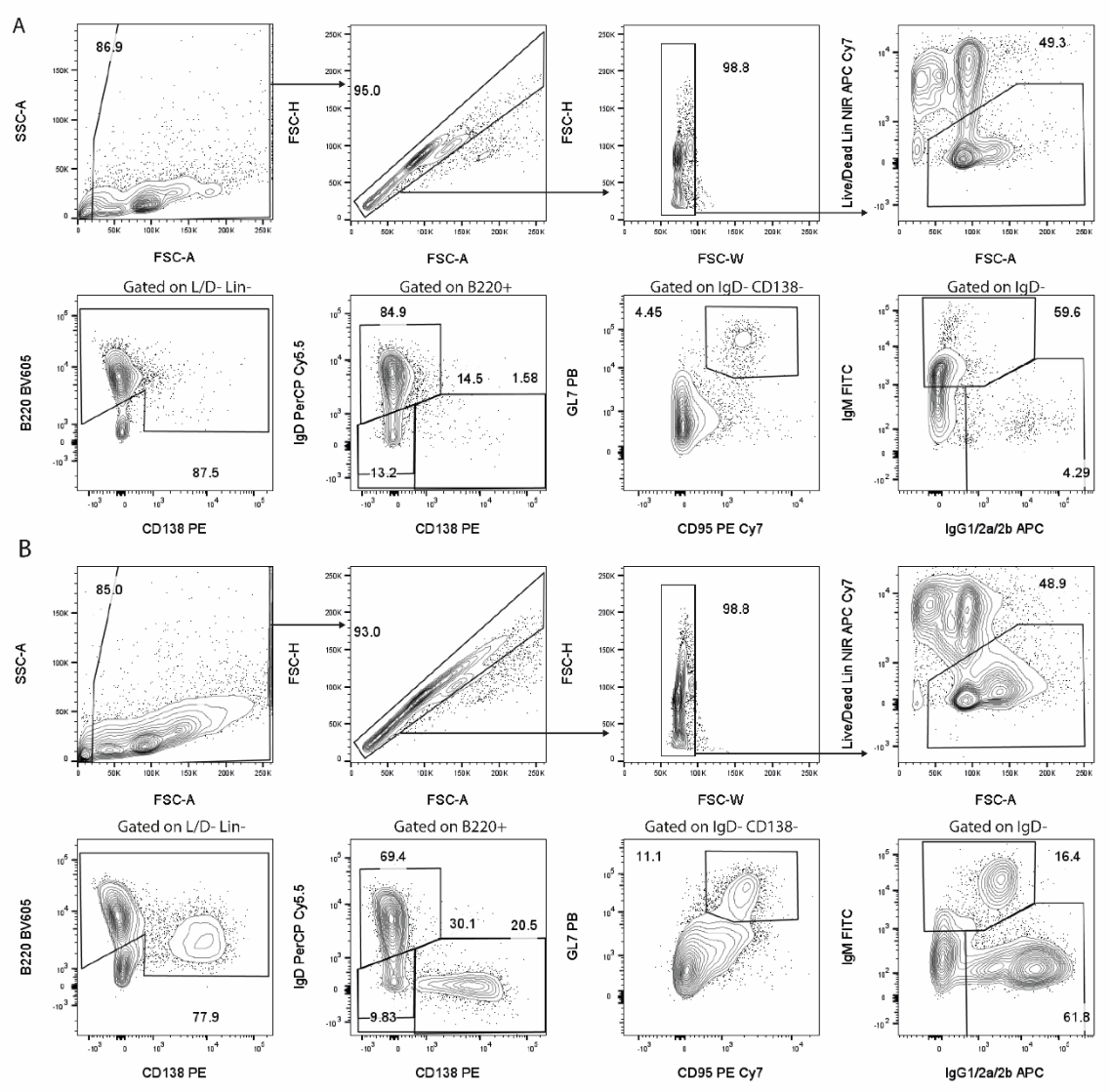
Supplemental figure S8. **Representative flow cytometry gating schemes for T cells in Chapter 5.** The splenic immune response of C57BL/6 (WT) and *Tfrc*$^{Y20H/Y20H}$ (TfR) uninfected control mice was analysed by flow cytometry. Gating strategy for T cells. There were no major visually appreciable differences in WT and TfR populations. Gating from a representative uninfected WT mouse is displayed. CD127, KI-67, TBET, CXCR5 and PD1 gates were set according to FMOs.



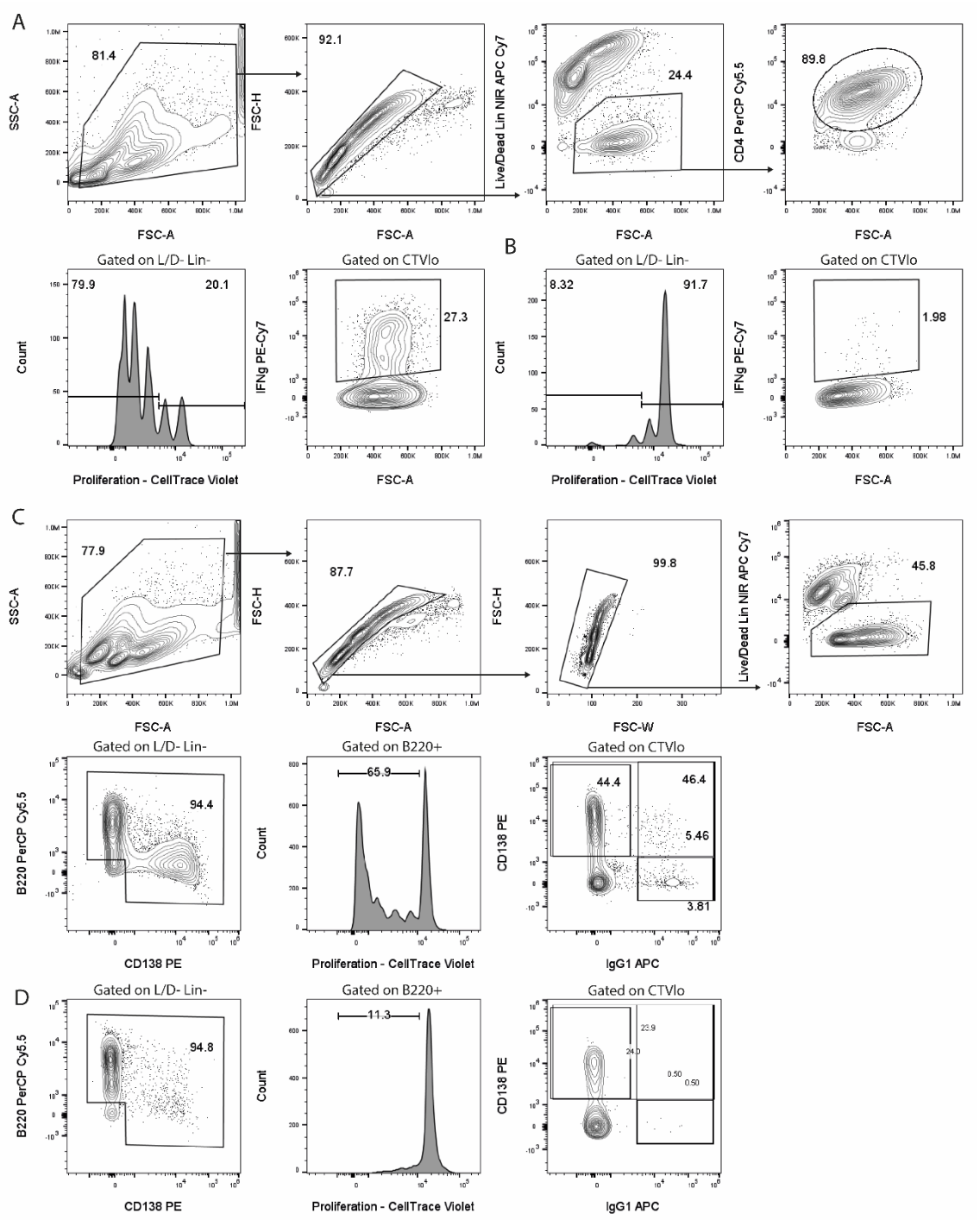
Supplemental figure S9. **Representative flow cytometry gating schemes for T cells in Chapter 5.** The splenic immune response of C57BL/6 (WT) and *Tfrc*$^{Y20H/Y20H}$ (TfR) *P. chabaudi* infected mice was analysed by flow cytometry. Gating strategy for T cells. There were no major visually appreciable differences in WT and TfR populations. Gating from a representative infected WT mouse is displayed. CD127, KI-67, TBET, CXCR5 and PD1 gates were set according to FMOs.



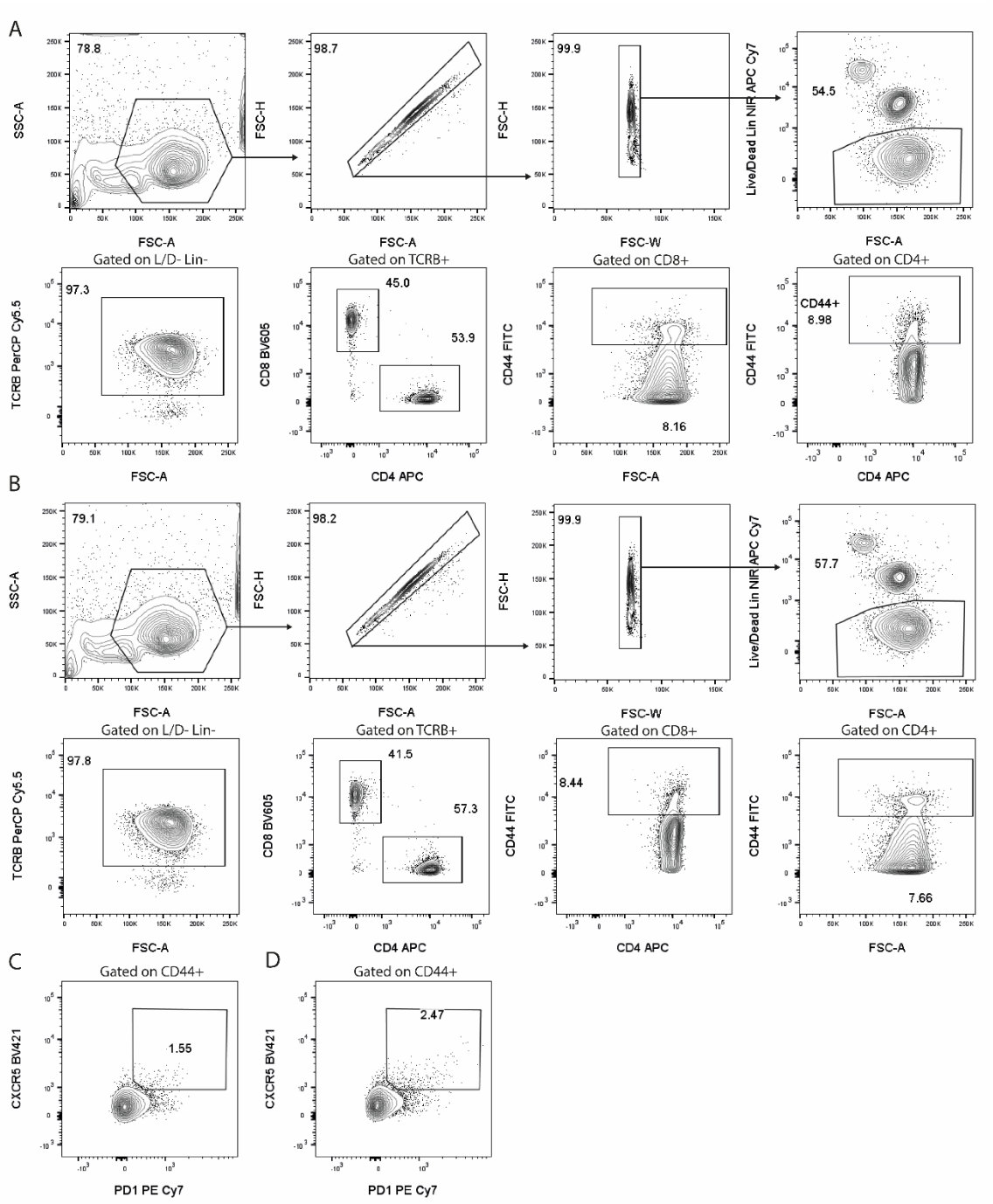
Supplemental figure S10. **Representative flow cytometry gating schemes for CD4 T cell cytokine production in Chapter 5.** The splenic immune response of C57BL/6 (WT) and *Tfrc*$^{Y20H/Y20H}$ (TfR) mice infected with *P. chabaudi* was analysed by flow cytometry. Gating strategy for IFNγ producing CD4 T cells. There were no major visually appreciable differences in WT and TfR populations. Gating from a representative **A)** uninfected and **B)** infected WT mouse is displayed.



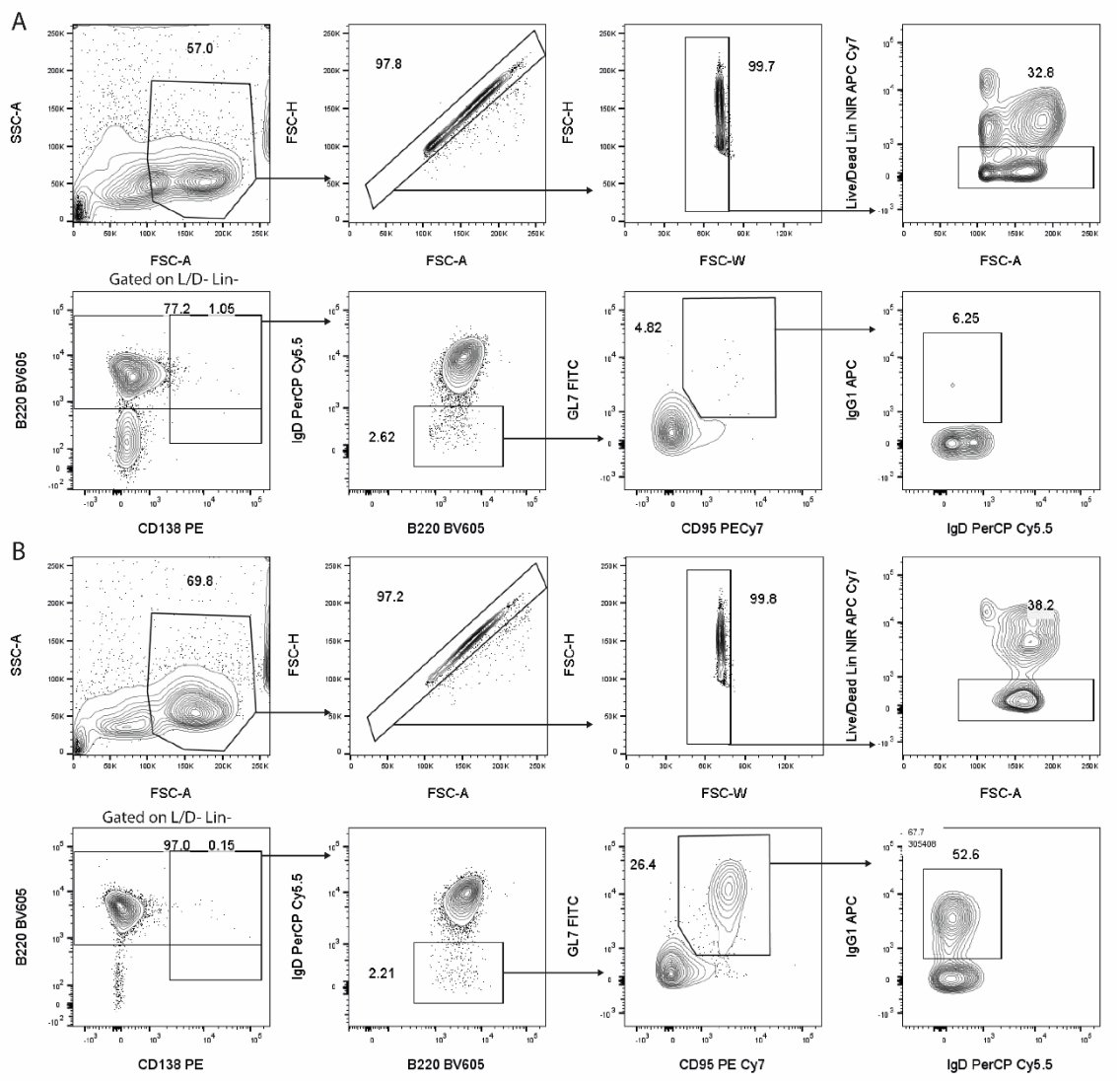
Supplemental figure S11. **Representative flow cytometry gating schemes for B cells in Chapter 5.** The splenic immune response of C57BL/6 (WT) and *Tfrc*$^{Y20H/Y20H}$ (TfR) mice infected with *P. chabaudi* was analysed by flow cytometry. B cell gating strategy. There were no major visually appreciable differences in WT and TfR populations. Gating from a representative **A)** uninfected and **B)** infected WT mouse is displayed.



Supplemental figure S12. **Representative flow cytometry gating schemes for *in vitro* cultured lymphocytes in Chapter 5.** Lymphocytes were isolated from C57BL/6 (WT) and *Tfrc*$^{Y20H/Y20H}$ (TfR) mice, cultured *in vitro*, with or without iron supplementation, and analysed by flow cytometry. **A-B)** CD4 T cell gating strategy. **C-D)** B cell gating strategy. Gating from a representative **A & C)** WT and **B & D)** TfR mouse is displayed.



Supplemental figure S13. **Representative flow cytometry gating schemes for T cells in Chapter 6.** The draining lymph node immune response of C57BL/6 (WT) and *Tfrc*$^{Y20H/Y20H}$ (TfR) mice immunised with RH5.1 was analysed by flow cytometry. Gating strategy for T cells. There were no major visually appreciable differences in WT and TfR populations. Gating from a representative **A & C)** unimmunised and **B & D)** immunised WT mouse is displayed. CXCR5 and PD1 gates were set according to FMOs.



Supplemental figure S14. **Representative flow cytometry gating schemes for B cells in Chapter 6.** The draining lymph node immune response of C57BL/6 (WT) and *Tfrc*$^{Y20H/Y20H}$ (TfR) mice immunised with RH5.1 was analysed by flow cytometry. Gating strategy for B cells. There were no major visually appreciable differences in WT and TfR populations. Gating from a representative **A)** unimmunised and **B)** mmunised WT mouse is displayd. L7 and CD95 gates were set according to FMOs

References

1. Drakesmith H, Prentice AM. Hepcidin and the Iron-Infection Axis. Science (80-). 2012 Nov 9;338(6108):768–72.
2. Andreini C, Putignano V, Rosato A, Banci L. The human iron-proteome. Metallomics. 2018;10(9):1223–31.
3. Coffey R, Ganz T. Iron homeostasis: An anthropocentric perspective. J Biol Chem. 2017;292(31):12727–34.
4. Ganz T. Systemic Iron Homeostasis. Physiol Rev. 2013;93(4):1721–41.
5. Hentze MW, Muckenthaler MU, Galy B, Camaschella C. Two to Tango: Regulation of Mammalian Iron Metabolism. Cell. 2010;142(1):24–38.
6. McKie AT, Barrow D, Latunde-Dada GO, Rolfs A, Sager G, Mudaly E, et al. An Iron-Regulated Ferric Reductase Associated with the Absorption of Dietary Iron. Science (80-). 2001 Mar 2;291(5509):1755–9.
7. Gunshin H, Mackenzie B, Berger U V., Gunshin Y, Romero MF, Boron WF, et al. Cloning and characterization of a mammalian proton-coupled metal-ion transporter. Nature. 1997 Jul;388(6641):482–8.
8. McKie AT, Marciani P, Rolfs A, Brennan K, Wehr K, Barrow D, et al. A Novel Duodenal Iron-Regulated Transporter, IREG1, Implicated in the Basolateral Transfer of Iron to the Circulation. Mol Cell. 2000 Feb;5(2):299–309.
9. Drakesmith H, Nemeth E, Ganz T. Ironing out Ferroportin. Cell Metab. 2015;22(5):777–87.
10. Slusarczyk P, Mleczko-Sanecka K. The multiple facets of iron recycling. Genes (Basel). 2021;12(9).
11. Theurl I, Hilgendorf I, Nairz M, Tymoszuk P, Haschka D, Asshoff M, et al. On-demand erythrocyte disposal and iron recycling requires transient macrophages in the liver. Nat Med. 2016;22(8):945–51.
12. Akilesh HM, Buechler MB, Duggan JM, Hahn WO, Matta B, Sun X, et al. Chronic TLR7 and TLR9 signaling drives anemia via differentiation of specialized hemophagocytes. Science (80-). 2019;363(6423).
13. Bian Z, Shi L, Guo Y-L, Lv Z, Tang C, Niu S, et al. Cd47-Sirpα interaction and IL-10 constrain inflammation-induced macrophage phagocytosis of healthy self-cells. Proc Natl Acad Sci. 2016 Sep 13;113(37).
14. Zhang Z, Zhang F, Guo X, An P, Tao Y, Wang F. Ferroportin1 in hepatocytes and macrophages is required for the efficient mobilization of body iron stores in mice. Hepatology. 2012 Sep;56(3):961–71.
15. Billesbølle CB, Azumaya CM, Kretsch RC, Powers AS, Gonen S, Schneider S, et al. Structure of hepcidin-bound ferroportin reveals iron homeostatic mechanisms. Nature. 2020;586(7831):807–11.
16. Nemeth E, Tuttle MS, Powelson J, Vaughn MD, Donovan A, Ward DMV, et al. Hepcidin regulates cellular iron efflux by binding to ferroportin and inducing its internalization. Science (80-). 2004;306(5704):2090–3.
17. Truksa J, Lee P, Beutler E. Two BMP responsive elements, STAT, and bZIP/HNF4/COUP motifs of the hepcidin promoter are critical for BMP, SMAD1, and HJV responsiveness. Blood. 2009 Jan 15;113(3):688–95.
18. Lim PJ, Duarte TL, Arezes J, Garcia-Santos D, Hamdi A, Pasricha S-R, et al. Nrf2

controls iron homoeostasis in haemochromatosis and thalassaemia via Bmp6 and hepcidin. Nat Metab. 2019 May 13;1(5):519–31.

19. Meynard D, Vaja V, Sun CC, Corradini E, Chen S, López-Otín C, et al. Regulation of TMPRSS6 by BMP6 and iron in human cells and mice. Blood. 2011 Jul 21;118(3):747–56.

20. Arezes J, Foy N, McHugh K, Sawant A, Quinkert D, Terraube V, et al. Erythroferrone inhibits the induction of hepcidin by BMP6. Blood. 2018;132(14):1473–7.

21. Armitage AE, Eddowes LA, Gileadi U, Cole S, Spottiswoode N, Selvakumar TA, et al. Hepcidin regulation by innate immune and infectious stimuli. Blood. 2011;118(15):4129–39.

22. Nemeth E, Rivera S, Gabayan V, Keller C, Taudorf S, Pedersen BK, et al. IL-6 mediates hypoferremia of inflammation by inducing the synthesis of the iron regulatory hormone hepcidin. J Clin Invest. 2004;113(9):1271–6.

23. Falzacappa Verga MV, Spasic MV, Kessler R, Stolte J, Hentze MW, Muckenthaler MU, et al. STAT3 mediates hepatic hepcidin expression and its inflammatory stimulation. Blood. 2007;109(1):353–8.

24. Young SP, Bomford A, Williams R. The effect of the iron saturation of transferrin on its binding and uptake by rabbit reticulocytes. Biochem J. 1984 Apr 15;219(2):505–10.

25. Yu B, Cheng C, Wu Y, Guo L, Kong D, Zhang Z, et al. Interactions of ferritin with scavenger receptor class A members. J Biol Chem. 2020 Nov;295(46):15727–41.

26. Shi H, Bencze KZ, Stemmler TL, Philpott CC. A Cytosolic Iron Chaperone That Delivers Iron to Ferritin. Science (80-). 2008 May 30;320(5880):1207–10.

27. Walden WE, Selezneva AI, Dupuy J, Volbeda A, Fontecilla-Camps JC, Theil EC, et al. Structure of Dual Function Iron Regulatory Protein 1 Complexed with Ferritin IRE-RNA. Science (80-). 2006 Dec 22;314(5807):1903–8.

28. Vashisht AA, Zumbrennen KB, Huang X, Powers DN, Durazo A, Sun D, et al. Control of Iron Homeostasis by an Iron-Regulated Ubiquitin Ligase. Science (80-). 2009 Oct 30;326(5953):718–21.

29. Salahudeen AA, Thompson JW, Ruiz JC, Ma H-W, Kinch LN, Li Q, et al. An E3 Ligase Possessing an Iron-Responsive Hemerythrin Domain Is a Regulator of Iron Homeostasis. Science (80-). 2009 Oct 30;326(5953):722–6.

30. Pasricha SR, Tye-Din J, Muckenthaler MU, Swinkels DW. Iron deficiency. Lancet. 2021;397(10270):233–48.

31. Lopez A, Cacoub P, Macdougall IC, Peyrin-Biroulet L. Iron deficiency anaemia. Lancet. 2016 Feb 27;387(10021):907–16.

32. Musallam KM, Taher AT. Iron deficiency beyond erythropoiesis: should we be concerned? Curr Med Res Opin. 2018;34(1):81–93.

33. Kassebaum NJ, Jasrasaria R, Naghavi M, Wulf SK, Johns N, Lozano R, et al. A systematic analysis of global anemia burden from 1990 to 2010. Blood. 2014 Jan 30;123(5):615–24.

34. Armitage AE, Agbla SC, Betts M, Sise EA, Jallow MW, Sambou E, et al. Rapid growth is a dominant predictor of hepcidin suppression and declining ferritin in Gambian infants. Haematologica. 2019;104(8):1542–53.

35. Hamad M, Bajbouj K, Taneera J. The Case for an Estrogen-iron Axis in Health and Disease. Exp Clin Endocrinol Diabetes. 2020 Apr 12;128(04):270–7.

36. Nairz M, Haschka D, Demetz E, Weiss G. Iron at the interface of immunity and

infection. Front Pharmacol. 2014;5 JUL(July):1–10.

37. Cassat JE, Skaar EP. Iron in infection and immunity. Cell Host Microbe. 2013;13(5):509–19.

38. Darton TC, Blohmke CJ, Giannoulatou E, Waddington CS, Jones C, Sturges P, et al. Rapidly Escalating Hepcidin and Associated Serum Iron Starvation Are Features of the Acute Response to Typhoid Infection in Humans. PLoS Negl Trop Dis. 2015;9(9):1–18.

39. Barber MF, Elde NC. Escape from bacterial iron piracy through rapid evolution of transferrin. Science (80-). 2014 Dec 12;346(6215):1362–6.

40. Ned RM, Swat W, Andrews NC. Transferrin receptor 1 is differentially required in lymphocyte development. Blood. 2003;102(10):3711–8.

41. Wang S, He X, Wu Q, Jiang L, Chen L, Yu Y, et al. Transferrin receptor 1-mediated iron uptake plays an essential role in hematopoiesis. Haematologica. 2020;105(8):2071–82.

42. Brekelmans P, Van Soest P, Leenen PJM, van Ewijk W. Inhibition of proliferation and differentiation during early T cell development by anti-transferrin receptor antibody. Eur J Immunol. 1994;24(11):2896–902.

43. Frost JN, Wideman SK, Preston AE, Teh MR, Ai Z, Wang L, et al. Plasma iron controls neutrophil production and function. bioRxiv. 2022;doi:10.1101/2022.03.17.484503.

44. Cronin SJF, Woolf CJ, Weiss G, Penninger JM. The Role of Iron Regulation in Immunometabolism and Immune-Related Disease. Front Mol Biosci. 2019;6(November).

45. West AP, Brodsky IE, Rahner C, Woo DK, Erdjument-Bromage H, Tempst P, et al. TLR signalling augments macrophage bactericidal activity through mitochondrial ROS. Nature. 2011 Apr 27;472(7344):476–80.

46. Murakawa H, Bland CE, Willis WT, Dallman PR. Iron deficiency and neutrophil function: different rates of correction of the depressions in oxidative burst and myeloperoxidase activity after iron treatment. Blood. 1987 May;69(5):1464–8.

47. Hassan TH, Badr MA, Karam NA, Zkaria M, El Saadany HF, Rahman DMA, et al. Impact of iron deficiency anemia on the function of the immune system in children. Medicine (Baltimore). 2016 Nov;95(47):e5395.

48. Vale-Costa S, Gomes-Pereira S, Teixeira CM, Rosa G, Rodrigues PN, Tomás A, et al. Iron Overload Favors the Elimination of Leishmania infantum from Mouse Tissues through Interaction with Reactive Oxygen and Nitrogen Species. PLoS Negl Trop Dis. 2013;7(2).

49. Collins HL, Kaufmann SHE, Schaible UE. Iron Chelation Via Deferoxamine Exacerbates Experimental Salmonellosis Via Inhibition of the Nicotinamide Adenine Dinucleotide Phosphate Oxidase-Dependent Respiratory Burst. J Immunol. 2014;168(7):3458–63.

50. Soares MP, Hamza I. Macrophages and Iron Metabolism. Immunity. 2016;44(3):492–504.

51. Recalcati S, Locati M, Marini A, Santambrogio P, Zaninotto F, De Pizzol M, et al. Differential regulation of iron homeostasis during human macrophage polarized activation. Eur J Immunol. 2010 Mar;40(3):824–35.

52. Corna G, Campana L, Pignatti E, Castiglioni A, Tagliafico E, Bosurgi L, et al. Polarization dictates iron handling by inflammatory and alternatively activated macrophages. Haematologica. 2010 Nov 1;95(11):1814–22.

53. Pagani A, Nai A, Corna G, Bosurgi L, Rovere-Querini P, Camaschella C, et al. Low hepcidin accounts for the proinflammatory status associated with iron deficiency. Blood.

2011;118(3):736–46.

54. Agoro R, Taleb M, Quesniaux VFJ, Mura C. Cell iron status influences macrophage polarization. Zissel G, editor. PLoS One. 2018 May 17;13(5):e0196921.

55. Hoeft K, Bloch DB, Graw JA, Malhotra R, Ichinose F, Bagchi A. Iron Loading Exaggerates the Inflammatory Response to the Toll-like Receptor 4 Ligand Lipopolysaccharide by Altering Mitochondrial Homeostasis. Anesthesiology. 2017 Jul;127(1):121–35.

56. Sindrilaru A, Peters T, Wieschalka S, Baican C, Baican A, Peter H, et al. An unrestrained proinflammatory M1 macrophage population induced by iron impairs wound healing in humans and mice. J Clin Invest. 2011 Mar 1;121(3):985–97.

57. Neckers LM, Cossman J. Transferrin receptor induction in mitogen-stimulated human T lymphocytes is required for DNA synthesis and cell division and is regulated by interleukin 2. Proc Natl Acad Sci U S A. 1983 Jun;80(11):3494–8.

58. Neckers LM, Yenokida G, Trepel JB, Lipford E, James S. Transferrin receptor induction is required for human B-lymphocyte activation but not for immunoglobulin secretion. J Cell Biochem. 1985;27(4):377–89.

59. Frost JN, Tan TK, Abbas M, Wideman SK, Bonadonna M, Stoffel NU, et al. Hepcidin-Mediated Hypoferremia Disrupts Immune Responses to Vaccination and Infection. Med. 2021 Feb;2(2):164-179.e12.

60. Jiang Y, Li C, Wu Q, An P, Huang L, Wang J, et al. Iron-dependent histone 3 lysine 9 demethylation controls B cell proliferation and humoral immune responses. Nat Commun. 2019;10(1):2935.

61. Teh MR, Frost JN, Armitage AE, Drakesmith H. Analysis of Iron and Iron-Interacting Protein Dynamics During T-Cell Activation. Front Immunol. 2021;12(August):1–18.

62. Wang Z, Yin W, Zhu L, Li J, Yao Y, Chen F, et al. Iron Drives T Helper Cell Pathogenicity by Promoting RNA-Binding Protein PCBP1-Mediated Proinflammatory Cytokine Production. Immunity. 2018 Jul;49(1):80-92.e7.

63. Zhao M, Li M ying, Gao X fei, Jia S jie, Gao K qin, Zhou Y, et al. Downregulation of BDH2 modulates iron homeostasis and promotes DNA demethylation in CD4+ T cells of systemic lupus erythematosus. Clin Immunol. 2018;187:113–21.

64. Klecha AJ, Salgueiro J, Wald M, Boccio J, Zubillaga M, Leonardi NM, et al. In vivo iron and zinc deficiency diminished T- and B-selective mitogen stimulation of murine lymphoid cells through protein kinase C-mediated mechanism. Biol Trace Elem Res. 2005;104(2):173–83.

65. Lametschwandtner G, Ticevic M, Kogler M, Cronin SJFF, Seehus C, Channon KM, et al. The metabolite BH4 controls T cell proliferation in autoimmunity and cancer. Nature. 2018;563(7732):564–8.

66. Yarosz EL, Ye C, Kumar A, Black C, Choi E-K, Seo Y-A, et al. Cutting Edge: Activation-Induced Iron Flux Controls CD4 T Cell Proliferation by Promoting Proper IL-2R Signaling and Mitochondrial Function. J Immunol. 2020 Apr 1;204(7):1708–13.

67. Shang C, Zhou H, Liu W, Shen T, Luo Y, Huang S. Iron chelation inhibits mTORC1 signaling involving activation of AMPK and REDD1/Bnip3 pathways. Oncogene. 2020;39(29):5201–13.

68. Shapiro J, Chang H-C, Zhao Z, Geier J, Bartom E, Chen C, et al. The Jumonji-C Histone Lysine Demethylase KDM3B Senses Cellular Iron to Regulate Anabolism Through mTORC1. Cell Press Sneak Peek. 2022;https://dx.doi.org/10.2139/ssrn.3873468.

69. Boothby M, Rickert RC. Metabolic Regulation of the Immune Humoral Response.

Immunity. 2017;46(5):743–55.

70. O'Neill LAJ, Kishton RJ, Rathmell J. A guide to immunometabolism for immunologists. Nat Rev Immunol. 2016;16(9):553–65.

71. Oppenheimer SJ. Iron and Its Relation to Immunity and Infectious Disease. J Nutr. 2001 Feb 1;131(2):616S-635S.

72. Jabara HH, Boyden SE, Chou J, Ramesh N, Massaad MJ, Benson H, et al. A missense mutation in TFRC, encoding transferrin receptor 1, causes combined immunodeficiency. Nat Genet. 2016 Jan 7;48(1):74–8.

73. Preston AE, Drakesmith H, Frost JN. Adaptive immunity and vaccination – iron in the spotlight. Immunother Adv. 2021;1(1):1–11.

74. Bagchi K, Mohanram M, Reddy V. Humoral immune response in children with iron-deficiency anaemia. BMJ. 1980 May 24;280(6226):1249–51.

75. MacDougall LG, Jacobs MR. The immune response in iron-deficient children. Isohaemagglutinin titres and antibody response to immunization. S Afr Med J. 1978 Mar 18;53(11):405–7.

76. Chandra RK, Saraya AK. Impaired immunocompetence associated with iron deficiency. J Pediatr. 1975;86(6):899–902.

77. Brussow H, Sidoti J, Dirren H, Freire WB, Brüssow H, Sidoti J, et al. Effect of malnutrition in Ecuadorian children on titers of serum antibodies to various microbial antigens. Clin Diagn Lab Immunol. 1995;2(1):62–8.

78. Stoffel NU, Uyoga MA, Mutuku FM, Frost JN, Mwasi E, Paganini D, et al. Iron Deficiency Anemia at Time of Vaccination Predicts Decreased Vaccine Response and Iron Supplementation at Time of Vaccination Increases Humoral Vaccine Response: A Birth Cohort Study and a Randomized Trial Follow-Up Study in Kenyan Infants. Front Immunol. 2020;11(July).

79. Fulop T, Wagner JR, Khalil A, Weber J, Trottier L, Payette H. Relationship Between the Response to Influenza Vaccination and the Nutritional Status in Institutionalized Elderly Subjects. Journals Gerontol Ser A Biol Sci Med Sci. 1999 Feb 1;54(2):M59–64.

80. Word Malaria Report 2021. Geneva: World Health Organisation. 2021.

81. Singh M, Suryanshu, Kanika, Singh G, Dubey A, Chaitanya RK. Plasmodium's journey through the Anopheles mosquito: A comprehensive review. Biochimie. 2021 Feb;181:176–90.

82. Cowman AF, Healer J, Marapana D, Marsh K. Malaria: Biology and Disease. Cell. 2016 Oct 20;167(3):610–24.

83. Phillips MA, Burrows JN, Manyando C, Van Huijsduijnen RH, Van Voorhis WC, Wells TNC. Malaria. Nat Rev Dis Prim. 2017;3.

84. Amino R, Thiberge S, Martin B, Celli S, Shorte S, Frischknecht F, et al. Quantitative imaging of Plasmodium transmission from mosquito to mammal. Nat Med. 2006 Feb 22;12(2):220–4.

85. Vaughan AM, Kappe SHI. Malaria Parasite Liver Infection and Exoerythrocytic Biology. Cold Spring Harb Perspect Med. 2017 Jun 1;7(6):1–22.

86. Weiss GE, Gilson PR, Taechalertpaisarn T, Tham W-H, de Jong NWM, Harvey KL, et al. Revealing the Sequence and Resulting Cellular Morphology of Receptor-Ligand Interactions during Plasmodium falciparum Invasion of Erythrocytes. Blackman MJ, editor. PLOS Pathog. 2015 Feb 27;11(2):e1004670.

87. Cowman AF, Tonkin CJ, Tham WH, Duraisingh MT. The Molecular Basis of

Erythrocyte Invasion by Malaria Parasites. Cell Host Microbe. 2017;22(2):232–45.

88. Lin CS, Uboldi AD, Epp C, Bujard H, Tsuboi T, Czabotar PE, et al. Multiple Plasmodium falciparum Merozoite Surface Protein 1 Complexes Mediate Merozoite Binding to Human Erythrocytes. J Biol Chem. 2016 Apr;291(14):7703–15.

89. Baum J, Chen L, Healer J, Lopaticki S, Boyle M, Triglia T, et al. Reticulocyte-binding protein homologue 5 – An essential adhesin involved in invasion of human erythrocytes by Plasmodium falciparum. Int J Parasitol. 2009;39(3):371–80.

90. Volz JC, Yap A, Sisquella X, Thompson JK, Lim NTY, Whitehead LW, et al. Essential Role of the PfRh5/PfRipr/CyRPA Complex during Plasmodium falciparum Invasion of Erythrocytes. Cell Host Microbe. 2016 Jul;20(1):60–71.

91. Clark MA, Goheen MM, Cerami C. Influence of host iron status on Plasmodium falciparum infection. Front Pharmacol. 2014;5(May):1–12.

92. Thomson-Luque R, Bautista JM. Home Sweet Home: Plasmodium vivax-Infected Reticulocytes—The Younger the Better? Front Cell Infect Microbiol. 2021 May 13;11.

93. Boddey JA, Cowman AF. Plasmodium nesting: Remaking the erythrocyte from the inside out. Annu Rev Microbiol. 2013;67:243–69.

94. Kafsack BFC, Rovira-Graells N, Clark TG, Bancells C, Crowley VM, Campino SG, et al. A transcriptional switch underlies commitment to sexual development in malaria parasites. Nature. 2014 Mar 13;507(7491):248–52.

95. White NJ, Pukrittayakamee S, Hien TT, Faiz MA, Mokuolu OA, Dondorp AM. Malaria. Lancet. 2014;383(9918):723–35.

96. Muriuki JM, Mentzer AJ, Webb EL, Morovat A, Kimita W, Ndungu FM, et al. Estimating the burden of iron deficiency among African children. BMC Med. 2020;18(1):1–14.

97. Van Avondt K, Nur E, Zeerleder S. Mechanisms of haemolysis-induced kidney injury. Nat Rev Nephrol. 2019;15(11):671–92.

98. Milner DA. Malaria pathogenesis. Cold Spring Harb Perspect Med. 2018;8(1):1–12.

99. Loria P, Miller S, Foley M, Tilley L. Inhibition of the peroxidative degradation of haem as the basis of action of chloroquine and other quinoline antimalarials. Biochem J. 1999 Apr 15;339 (Pt 2:363–70.

100. Birnbaum J, Scharf S, Schmidt S, Jonscher E, Maria Hoeijmakers WA, Flemming S, et al. A Kelch13-defined endocytosis pathway mediates artemisinin resistance in malaria parasites. Science (80-). 2020;367(6473):51–9.

101. Bennett A, Bisanzio D, Yukich JO, Mappin B, Fergus CA, Lynch M, et al. Population coverage of artemisinin-based combination treatment in children younger than 5 years with fever and Plasmodium falciparum infection in Africa, 2003–2015: a modelling study using data from national surveys. Lancet Glob Heal. 2017;5(4):e418–27.

102. Deroost K, Pham TT, Opdenakker G, Van den Steen PE. The immunological balance between host and parasite in malaria. Vol. 40, FEMS Microbiology Reviews. 2016. 208–257 p.

103. Tran TM, Li S, Doumbo S, Doumtabe D, Huang C-Y, Dia S, et al. An Intensive Longitudinal Cohort Study of Malian Children and Adults Reveals No Evidence of Acquired Immunity to Plasmodium falciparum Infection. Clin Infect Dis. 2013 Jul 1;57(1):40–7.

104. Offeddu V, Thathy V, Marsh K, Matuschewski K. Naturally acquired immune responses against Plasmodium falciparum sporozoites and liver infection. Int J Parasitol. 2012 May;42(6):535–48.

105. Doolan DL, Dobaño C, Baird JK. Acquired immunity to Malaria. Clin Microbiol Rev. 2009;22(1):13–36.

106. Silvie O, Amino R, Hafalla JC. Tissue-specific cellular immune responses to malaria pre-erythrocytic stages. Curr Opin Microbiol. 2017;40:160–7.

107. Draper SJ, Sack BK, King CR, Nielsen CM, Rayner JC, Higgins MK, et al. Malaria Vaccines: Recent Advances and New Horizons. Cell Host Microbe. 2018;24(1):43–56.

108. Chakravarty S, Cockburn IA, Kuk S, Overstreet MG, Sacci JB, Zavala F. CD8+ T lymphocytes protective against malaria liver stages are primed in skin-draining lymph nodes. Nat Med. 2007 Sep 19;13(9):1035–41.

109. Parmar R, Patel H, Yadav N, Parikh R, Patel K, Mohankrishnan A, et al. Infectious Sporozoites of Plasmodium berghei Effectively Activate Liver CD8α+ Dendritic Cells. Front Immunol. 2018 Feb 8;9.

110. Gazzinelli RT, Kalantari P, Fitzgerald KA, Golenbock DT. Innate sensing of malaria parasites. Nat Rev Immunol. 2014 Nov 17;14(11):744–57.

111. Doolan DL, Hoffman SL. The Complexity of Protective Immunity Against Liver-Stage Malaria. J Immunol. 2000 Aug 1;165(3):1453–62.

112. Fernandez-Ruiz D, Ng WY, Holz LE, Ma JZ, Zaid A, Wong YC, et al. Liver-Resident Memory CD8+T Cells Form a Front-Line Defense against Malaria Liver-Stage Infection. Immunity. 2016;45(4):889–902.

113. Stevenson MM, Riley EM. Innate immunity to malaria. Nat Rev Immunol. 2004;4(3):169–80.

114. Carvalho LH, Sano G, Hafalla JCR, Morrot A, de Lafaille MAC, Zavala F. IL-4-secreting CD4+ T cells are crucial to the development of CD8+ T-cell responses against malaria liver stages. Nat Med. 2002 Feb;8(2):166–70.

115. Kurup SP, Butler NS, Harty JT. T cell-mediated immunity to malaria. Nat Rev Immunol. 2019;19(7):457–71.

116. Mac-Daniel L, Ménard R. Plasmodium and mononuclear phagocytes. Microb Pathog. 2015;78:43–51.

117. McGilvray ID, Serghides L, Kapus A, Rotstein OD, Kain KC. Nonopsonic monocyte/macrophage phagocytosis of Plasmodium falciparum–parasitized erythrocytes: a role for CD36 in malarial clearance. Blood. 2000 Nov 1;96(9):3231–40.

118. Thylur RP, Wu X, Gowda NM, Punnath K, Neelgund SE, Febbraio M, et al. CD36 receptor regulates malaria-induced immune responses primarily at early blood stage infection contributing to parasitemia control and resistance to mortality. J Biol Chem. 2017;292(22):9394–408.

119. Taylor PR, Seixas E, Walport MJ, Langhorne J, Botto M. Complement contributes to protective immunity against reinfection by Plasmodium chabaudi chabaudi parasites. Infect Immun. 2001 Jun;69(6):3853–9.

120. McMorran BJ, Wieczorski L, Drysdale KE, Chan J-A, Huang HM, Smith C, et al. Platelet factor 4 and Duffy antigen required for platelet killing of Plasmodium falciparum. Science. 2012 Dec 7;338(6112):1348–51.

121. Gramaglia I, Velez J, Combes V, Grau GER, Wree M, van der Heyde HC. Platelets activate a pathogenic response to blood-stage Plasmodium infection but not a protective immune response. Blood. 2017;129(12):1669–79.

122. van der Heyde HC, Elloso MM, Chang WL, Kaplan M, Manning DD, Weidanz WP. Gamma delta T cells function in cell-mediated immunity to acute blood-stage Plasmodium chabaudi adami malaria. J Immunol. 1995;154(8):3985–90.

123. Podoba JE, Stevenson MM. CD4+ and CD8+ T lymphocytes both contribute to acquired immunity to blood-stage Plasmodium chabaudi AS. Infect Immun. 1991;59(1):51–8.

124. Mohan K, Moulin P, Stevenson MM. Natural killer cell cytokine production, not cytotoxicity, contributes to resistance against blood-stage Plasmodium chabaudi AS infection. J Immunol. 1997;159(10):4990–8.

125. Imai T, Ishida H, Suzue K, Taniguchi T, Okada H, Shimokawa C, et al. Cytotoxic activities of CD8+ T cells collaborate with macrophages to protect against blood-stage murine malaria. Elife. 2015;2015(4):1–49.

126. Giulia C, Loizon S, Guenot M, Mocan I, Halary F, De Saint-Basile G, et al. Control of Plasmodium falciparum erythrocytic cycle: γδ T cells target the red blood cell-invasive merozoites. Blood. 2011;118(26):6952–62.

127. Arora G, Hart GT, Manzella-Lapeira J, Doritchamou JY, Narum DL, Thomas LM, et al. NK cells inhibit Plasmodium falciparum growth in red blood cells via antibody-dependent cellular cytotoxicity. Elife. 2018 Jun 26;7.

128. Gonzales SJ, Reyes RA, Braddom AE, Batugedara G, Bol S, Bunnik EM. Naturally Acquired Humoral Immunity Against Plasmodium falciparum Malaria. Front Immunol. 2020;11(October):1–15.

129. Seixas E, Moura Nunes JF, Matos I, Coutinho A. The interaction between DC and Plasmodium berghei/chabaudi-infected erythrocytes in mice involves direct cell-to-cell contact, internalization and TLR. Eur J Immunol. 2009;39(7):1850–63.

130. Tiemi Shio M, Eisenbarth SC, Savaria M, Vinet AF, Bellemare M-J, Harder KW, et al. Malarial Hemozoin Activates the NLRP3 Inflammasome through Lyn and Syk Kinases. Kazura JW, editor. PLoS Pathog. 2009 Aug 21;5(8):e1000559.

131. Nahrendorf W, Ivens A, Spence PJ. Inducible mechanisms of disease tolerance provide an alternative strategy of acquired immunity to malaria. Elife. 2021;10:1–33.

132. Sponaas AM, Do Rosario APF, Voisine C, Mastelic B, Thompson J, Koernig S, et al. Migrating monocytes recruited to the spleen play an important role in control of blood stage malaria. Blood. 2009;114(27):5522–31.

133. Leisewitz AL, Rockett KA, Gumede B, Jones M, Urban B, Kwiatkowski DP. Response of the splenic dendritic cell population to malaria infection. Infect Immun. 2004;72(7):4233–9.

134. Waki S, Kurihara R, Nemoto H, Suzuki M. Effect of recombinant human colony-stimulating factor on the course of parasitaemia in non-lethal rodent malaria. Parasitol Res. 1993;79(8):703–5.

135. Riopel J, Tam M, Mohan K, Marino MW, Stevenson MM. Granulocyte-macrophage colony-stimulating factor-deficient mice have impaired resistance to blood-stage malaria. Infect Immun. 2001;69(1):129–36.

136. Guermonprez P, Helft J, Claser C, Deroubaix S, Karanje H, Gazumyan A, et al. Inflammatory Flt3l is essential to mobilize dendritic cells and for T cell responses during Plasmodium infection. Nat Med. 2013;19(6):730–8.

137. Belyaev NN, Biró J, Langhorne J, Potocnik AJ. Extramedullary Myelopoiesis in Malaria Depends on Mobilization of Myeloid-Restricted Progenitors by IFN-γ Induced Chemokines. PLoS Pathog. 2013;9(6).

138. Belyaev NN, Brown DE, Diaz AIG, Rae A, Jarra W, Thompson J, et al. Induction of an IL7-R+ c-Kithi myelolymphoid progenitor critically dependent on IFN-γ signaling during acute malaria. Nat Immunol. 2010;11(6):477–85.

139. Troye-Blomberg M, Andersson G, Stoczkowska M, Shabo R, Romero P, Patarroyo ME,

et al. Production of IL 2 and IFN-gamma by T cells from malaria patients in response to Plasmodium falciparum or erythrocyte antigens in vitro. J Immunol. 1985 Nov;135(5):3498–504.

140. Stevenson MM, Tam MF, Belosevic M, Van Der Meide PH, Podoba JE. Role of endogenous gamma interferon in host response to infection with blood-stage Plasmodium chabaudi AS. Infect Immun. 1990;58(10):3225–32.

141. Meding SJ, Cheng SC, Simon-Haarhaus B, Langhorne J. Role of gamma interferon during infection with Plasmodium chabaudi chabaudi. Infect Immun. 1990 Nov;58(11):3671–8.

142. Oakley MS, Sahu BR, Lotspeich-Cole L, Majam V, Pham PT, Banerjee AS, et al. T-bet modulates the antibody response and immune protection during murine malaria. Eur J Immunol. 2014;44(9):2680–91.

143. Su Z, Stevenson MM. IL-12 Is Required for Antibody-Mediated Protective Immunity Against Blood-Stage Plasmodium chabaudi AS Malaria Infection in Mice . J Immunol. 2002;168(3):1348–55.

144. Götz A, Tang MS, Ty MC, Arama C, Ongoiba A, Doumtabe D, et al. Atypical activation of dendritic cells by Plasmodium falciparum. Proc Natl Acad Sci U S A. 2017 Dec 5;114(49):E10568–77.

145. Fontana MF, de Melo GL, Anidi C, Hamburger R, Kim CY, Lee SY, et al. Macrophage Colony Stimulating Factor Derived from CD4+T Cells Contributes to Control of a Blood-Borne Infection. PLoS Pathog. 2016;12(12):1–26.

146. Mesin L, Ersching J, Victora GD. Germinal Center B Cell Dynamics. Immunity. 2016;45(3):471–82.

147. Pérez-Mazliah D, Nguyen MP, Hosking C, McLaughlin S, Lewis MD, Tumwine I, et al. Follicular Helper T Cells are Essential for the Elimination of Plasmodium Infection. EBioMedicine. 2017;24:216–30.

148. Oyong DA, Loughland JR, Soon MSF, Chan JA, Andrew D, Wines BD, et al. Adults with Plasmodium falciparum malaria have higher magnitude and quality of circulating T-follicular helper cells compared to children. eBioMedicine. 2022;75:103784.

149. Wikenheiser DJ, Ghosh D, Kennedy B, Stumhofer JS. The Costimulatory Molecule ICOS Regulates Host Th1 and Follicular Th Cell Differentiation in Response to Plasmodium chabaudi chabaudi AS Infection . J Immunol. 2016;196(2):778–91.

150. Pérez-Mazliah D, Ng DHL, Freitas do Rosário AP, McLaughlin S, Mastelic-Gavillet B, Sodenkamp J, et al. Disruption of IL-21 Signaling Affects T Cell-B Cell Interactions and Abrogates Protective Humoral Immunity to Malaria. PLoS Pathog. 2015;11(3):1–24.

151. Ryg-Cornejo V, Ioannidis LJ, Ly A, Chiu CY, Tellier J, Hill DL, et al. Severe Malaria Infections Impair Germinal Center Responses by Inhibiting T Follicular Helper Cell Differentiation. Cell Rep. 2016;14(1):68–81.

152. Obeng-Adjei N, Portugal S, Tran TM, Yazew TB, Skinner J, Li S, et al. Circulating Th1-Cell-type Tfh Cells that Exhibit Impaired B Cell Help Are Preferentially Activated during Acute Malaria in Children. Cell Rep. 2015 Oct;13(2):425–39.

153. Weid T von der, Langhorne J. Altered response of CD4 + T cell subsets to Plasmodium chabaudi chabaudi in B cell-deficient mice. Int Immunol. 1993;5(10):1343–8.

154. Scholzen A, Teirlinck AC, Bijker EM, Roestenberg M, Hermsen CC, Hoffman SL, et al. BAFF and BAFF Receptor Levels Correlate with B Cell Subset Activation and Redistribution in Controlled Human Malaria Infection. J Immunol. 2014;192(8):3719–29.

155. Sebina I, Fogg LG, James KR, Soon MSF, Akter J, Thomas BS, et al. IL-6 promotes CD4 + T-cell and B-cell activation during Plasmodium infection. Parasite Immunol. 2017 Oct;39(10):e12455.

156. Su Z, Stevenson MM. Central role of endogenous gamma interferon in protective immunity against blood-stage Plasmodium chabaudi AS infection. Infect Immun. 2000;68(8):4399–406.

157. Guthmiller JJ, Graham AC, Zander RA, Pope RL, Butler NS. Cutting Edge: IL-10 Is Essential for the Generation of Germinal Center B Cell Responses and Anti-Plasmodium Humoral Immunity . J Immunol. 2017;198(2):617–22.

158. Rogers KJ, Vijay R, Butler NS. Anti-malarial humoral immunity: the long and short of it. Microbes Infect. 2021;23(4–5):104807.

159. Pérez-Mazliah D, Ndungu FM, Aye R, Langhorne J. B-cell memory in malaria: Myths and realities. Immunol Rev. 2020;293(1):57–69.

160. Li C, Corraliza I, Langhorne J. A defect in interleukin-10 leads to enhanced malarial disease in Plasmodium chabaudi chabaudi infection in mice. Infect Immun. 1999;67(9):4435–42.

161. Kobayashi F, Ishida H, Matsui T, Tsuji M. Effects of in vivo Administration of Anti-IL-10 or Anti-IFN-.GAMMA. Monoclonal Antibody on the Host Defense Mechanism against Plasmodium yoelii yoelii Infection. J Vet Med Sci. 2000;62(6):583–7.

162. Omer FM, Riley EM. Transforming Growth Factor β Production Is Inversely Correlated with Severity of Murine Malaria Infection. J Exp Med. 1998 Jul 1;188(1):39–48.

163. Omer FM, de Souza JB, Riley EM. Differential Induction of TGF-β Regulates Proinflammatory Cytokine Production and Determines the Outcome of Lethal and Nonlethal Plasmodium yoelii Infections. J Immunol. 2003 Nov 15;171(10):5430–6.

164. Walther M, Tongren JE, Andrews L, Korbel D, King E, Fletcher H, et al. Upregulation of TGF-β, FOXP3, and CD4+CD25+ Regulatory T Cells Correlates with More Rapid Parasite Growth in Human Malaria Infection. Immunity. 2005 Sep;23(3):287–96.

165. Cohen J, Nussenzweig V, Nussenzweig R, Vekemans J, Leach A. From the circumsporozoite protein to the RTS, S/AS candidate vaccine. Hum Vaccin. 2010;6(1):90–6.

166. RTSS Clinical Trials Partnership. Efficacy and safety of RTS,S/AS01 malaria vaccine with or without a booster dose in infants and children in Africa: final results of a phase 3, individually randomised, controlled trial. Lancet. 2015 Jul;386(9988):31–45.

167. Moorthy VS, Newman RD, Okwo-Bele J-M, Malaria Vaccine Funders Group. Malaria Vaccine Technology Roadmap. Lancet. 2013;382(November):1700–1.

168. Collins KA, Snaith R, Cottingham MG, Gilbert SC, Hill AVS. Enhancing protective immunity to malaria with a highly immunogenic virus-like particle vaccine. Sci Rep. 2017;7(November 2016):1–15.

169. Datoo MS, Natama MH, Somé A, Traoré O, Rouamba T, Bellamy D, et al. Efficacy of a low-dose candidate malaria vaccine, R21 in adjuvant Matrix-M, with seasonal administration to children in Burkina Faso: a randomised controlled trial. Lancet. 2021;397(10287):1809–18.

170. Tiono AB, Nébié I, Anagnostou N, Coulibaly AS, Bowyer G, Lam E, et al. First field efficacy trial of the ChAd63 MVA ME-TRAP vectored malaria vaccine candidate in 5-17 months old infants and children. Borrow R, editor. PLoS One. 2018 Dec 12;13(12):e0208328.

171. Nussenzweig RS, Vanderberg J, Most H, Orton C. Protective Immunity produced by the

Injection of X-irradiated Sporozoites of Plasmodium berghei. Nature. 1967 Oct;216(5111):160–2.

172. Itsara LS, Zhou Y, Do J, Grieser AM, Vaughan AM, Ghosh AK. The Development of Whole Sporozoite Vaccines for Plasmodium falciparum Malaria. Front Immunol. 2018;9(December):1–7.

173. Sissoko MS, Healy SA, Katile A, Omaswa F, Zaidi I, Gabriel EE, et al. Safety and efficacy of PfSPZ Vaccine against Plasmodium falciparum via direct venous inoculation in healthy malaria-exposed adults in Mali: a randomised, double-blind phase 1 trial. Lancet Infect Dis. 2017 May;17(5):498–509.

174. Sissoko MS, Healy SA, Katile A, Zaidi I, Hu Z, Kamate B, et al. Safety and efficacy of a three-dose regimen of Plasmodium falciparum sporozoite vaccine in adults during an intense malaria transmission season in Mali: a randomised, controlled phase 1 trial. Lancet Infect Dis. 2021 Nov;

175. Langhorne J, Ndungu FM, Sponaas AM, Marsh K. Immunity to malaria: More questions than answers. Nat Immunol. 2008;9(7):725–32.

176. Minassian AM, Silk SE, Barrett JR, Nielsen CM, Miura K, Diouf A, et al. Reduced blood-stage malaria growth and immune correlates in humans following RH5 vaccination. Med. 2021;2(6):701-719.e19.

177. Duffy PE. Transmission-Blocking Vaccines: Harnessing Herd Immunity for Malaria Elimination. Expert Rev Vaccines. 2021 Feb 1;20(2):185–98.

178. Kirkman LA, Deitsch KW. Vive la Différence: Exploiting the Differences between Rodent and Human Malarias. Trends Parasitol. 2020;36(6):504–11.

179. Stanisic DI, McCarthy JS, Good MF. Controlled Human Malaria Infection: Applications, Advances, and Challenges. Andrews-Polymenis HL, editor. Infect Immun. 2018 Jan;86(1).

180. Wykes MN, Good MF. What have we learnt from mouse models for the study of malaria? Eur J Immunol. 2009;39(8):2004–7.

181. Langhorne J, Buffet P, Galinski M, Good M, Harty J, Leroy D, et al. The relevance of non-human primate and rodent malaria models for humans. Malar J. 2011 Dec 2;10(1):23.

182. Spence PJ, Jarra W, Lévy P, Reid AJ, Chappell L, Brugat T, et al. Vector transmission regulates immune control of Plasmodium virulence. Nature. 2013 Jun 29;498(7453):228–31.

183. Muriuki JM, Mentzer AJ, Mitchell R, Webb EL, Etyang AO, Kyobutungi C, et al. Malaria is a cause of iron deficiency in African children. Nat Med. 2021;27(4):653–8.

184. Spottiswoode N, Duffy PE, Drakesmith H. Iron, anemia and hepcidin in malaria. Front Pharmacol. 2014 May 30;5(May):1–11.

185. Raventos-Suarez C, Pollack S, Nagel RL. Plasmodium Falciparum: Inhibition of in Vitro Growth by Desferrioxamine. Am J Trop Med Hyg. 1982 Sep 1;31(5):919–22.

186. Ferrer P, Tripathi AK, Clark MA, Hand CC, Rienhoff HY, Sullivan DJ. Antimalarial Iron Chelator, FBS0701, Shows Asexual and Gametocyte Plasmodium falciparum Activity and Single Oral Dose Cure in a Murine Malaria Model. Snounou G, editor. PLoS One. 2012 May 21;7(5):e37171.

187. Smith HJ, Meremikwu MM. Iron-chelating agents for treating malaria. Cochrane Database Syst Rev. 2003 Apr 22;

188. Harvey PW, Bell RG, Nesheim MC. Iron deficiency protects inbred mice against infection with Plasmodium chabaudi. Infect Immun. 1985 Dec;50(3):932–4.

189. Koka S, Föller M, Lamprecht G, Boini KM, Lang C, Huber SM, et al. Iron deficiency influences the course of malaria in Plasmodium berghei infected mice. Biochem Biophys Res Commun. 2007;357(3):608–14.

190. Matsuzaki-Moriya C, Tu L, Ishida H, Imai T, Suzue K, Hirai M, et al. A critical role for phagocytosis in resistance to malaria in iron-deficient mice. Eur J Immunol. 2011;41(5):1365–75.

191. Nyakeriga AM, Troye-Blomberg M, Dorfman JR, Alexander ND, Bäck R, Kortok M, et al. Iron deficiency and malaria among children living on the coast of Kenya. J Infect Dis. 2004;190(3):439–47.

192. Gwamaka M, Kurtis JD, Sorensen BE, Holte S, Morrison R, Mutabingwa TK, et al. Iron deficiency protects against severe plasmodium falciparum malaria and death in young children. Clin Infect Dis. 2012;54(8):1137–44.

193. Jonker FAM, Calis JCJ, van Hensbroek MB, Phiri K, Geskus RB, Brabin BJ, et al. Iron status predicts malaria risk in Malawian preschool children. PLoS One. 2012;7(8):1–8.

194. Sazawal S, Black RE, Ramsan M, Chwaya HM, Stoltzfus RJ, Dutta A, et al. Effects of routine prophylactic supplementation with iron and folic acid on admission to hospital and mortality in preschool children in a high malaria transmission setting: community-based, randomised, placebo-controlled trial. Lancet. 2006 Jan;367(9505):133–43.

195. Ojukwu JU, Okebe JU, Yahav D, Paul M. Oral iron supplementation for preventing or treating anaemia among children in malaria-endemic areas. In: Ojukwu JU, editor. Cochrane Database of Systematic Reviews. Chichester, UK: John Wiley & Sons, Ltd; 2009.

196. Okebe JU, Yahav D, Shbita R, Paul M. Oral iron supplements for children in malaria-endemic areas. In: Paul M, editor. Cochrane Database of Systematic Reviews. Chichester, UK: John Wiley & Sons, Ltd; 2011.

197. Neuberger A, Okebe J, Yahav D, Paul M. Oral iron supplements for children in malaria-endemic areas. Cochrane Database Syst Rev. 2016 Feb 27;2016(2).

198. Vos T, Abajobir AA, Abate KH, Abbafati C, Abbas KM, Abd-Allah F, et al. Global, regional, and national incidence, prevalence, and years lived with disability for 328 diseases and injuries for 195 countries, 1990–2016: a systematic analysis for the Global Burden of Disease Study 2016. Lancet. 2017 Sep;390(10100):1211–59.

199. Arezes J, Jung G, Gabayan V, Valore E, Ruchala P, Gulig PA, et al. Hepcidin-induced hypoferremia is a critical host defense mechanism against the siderophilic bacterium vibrio vulnificus. Cell Host Microbe. 2015;17(1):47–57.

200. Petzer V, Tymoszuk P, Asshoff M, Carvalho J, Papworth J, Deantonio C, et al. A fully human anti-BMP6 antibody reduces the need for erythropoietin in rodent models of the anemia of chronic disease. Blood. 2020;136(9):1080–90.

201. Jin J, Tarrant RD, Bolam EJ, Angell-Manning P, Soegaard M, Pattinson DJ, et al. Production, quality control, stability, and potency of cGMP-produced Plasmodium falciparum RH5.1 protein vaccine expressed in Drosophila S2 cells. npj Vaccines. 2018;3(1).

202. Spence PJ, Jarra W, Lévy P, Nahrendorf W, Langhorne J. Mosquito transmission of the rodent malaria parasite Plasmodium chabaudi. Malar J. 2012;11:1–7.

203. Bushell ES, Marr EJ, Milne RM, Anar B, Girling G, Schwach F, et al. An enhanced toolkit for the generation of knockout and marker-free fluorescent Plasmodium chabaudi. Wellcome Open Res. 2020;5:1–20.

204. Miura K, Orcutt AC, Muratova O V, Miller LH, Saul A, Long A. Including a Reference Serum on Each Plate to Detect Antibodies Induced by Experimental Malaria Vaccines.

Vaccine. 2008;26(2):193–200.

205. Duarte TL, Neves J V. Measurement of Tissue Non-Heme Iron Content using a Bathophenanthroline-Based Colorimetric Assay. J Vis Exp. 2022 Jan 31;(179).

206. Livak KJ, Schmittgen TD. Analysis of Relative Gene Expression Data Using Real-Time Quantitative PCR and the 2−ΔΔCT Method. Methods. 2001 Dec;25(4):402–8.

207. MalariaGEN Resource Centre. Leucocyte depletion of 2.0mL of Plasmodium-infected whole blood using MN2100ff cellulose columns [Internet]. MalariaGEN Protocols. 2016. Available from: https://www.malariagen.net/

208. Finberg KE, Whittlesey RL, Fleming MD, Andrews NC. Down-regulation of Bmp/Smad signaling by Tmprss6 is required for maintenance of systemic iron homeostasis. Blood. 2010 May 6;115(18):3817–26.

209. Fleming MD, Trenor CC, Su MA, Foernzler D, Beier DR, Dietrich WF, et al. Microcytic anaemia mice have a mutation in Nramp2, a candidate iron transporter gene. Nat Genet. 1997 Aug;16(4):383–6.

210. Bartnikas TB, Fleming MD, Schmidt PJ. Murine mutants in the study of systemic iron metabolism and its disorders: An update on recent advances. Biochim Biophys Acta - Mol Cell Res. 2012;1823(9):1444–50.

211. Clark MA, Goheen MM, Fulford A, Prentice AM, Elnagheeb MA, Patel J, et al. Host iron status and iron supplementation mediate susceptibility to erythrocytic stage Plasmodium falciparum. Nat Commun. 2014 Dec 25;5(1):4446.

212. Jabara HH, Boyden SE, Chou J, Ramesh N, Massaad MJ, Benson H, et al. Supplamentary - A missense mutation in TFRC, encoding transferrin receptor 1, causes combined immunodeficiency. Nat Genet. 2015;48(1):74–8.

213. Manolova V, Nyffenegger N, Flace A, Altermatt P, Varol A, Doucerain C, et al. Oral ferroportin inhibitor ameliorates ineffective erythropoiesis in a model of β-thalassemia. J Clin Invest. 2019;130(1):491–506.

214. Guo S, Casu C, Gardenghi S, Booten S, Aghajan M, Peralta R, et al. Reducing TMPRSS6 ameliorates hemochromatosis and β-thalassemia in mice. J Clin Invest. 2013 Apr 1;123(4):1531–41.

215. Preza GC, Ruchala P, Pinon R, Ramos E, Qiao B, Peralta MA, et al. Minihepcidins are rationally designed small peptides that mimic hepcidin activity in mice and may be useful for the treatment of iron overload. J Clin Invest. 2011;121(12):4880–8.

216. Ramos E, Ruchala P, Goodnough JB, Kautz L, Preza GC, Nemeth E, et al. Minihepcidins prevent iron overload in a hepcidin-deficient mouse model of severe hemochromatosis. Blood. 2012 Nov 1;120(18):3829–36.

217. Thomas DW, Hinchliffe RF, Briggs C, Macdougall IC, Littlewood T, Cavill I. Guideline for the laboratory diagnosis of functional iron deficiency. Br J Haematol. 2013 Jun;161(5):639–48.

218. Prentice AM, Ghattas H, Doherty C, Cox SE. Iron metabolism and malaria. Food Nutr Bull. 2007;28(4 SUPPL.):524–39.

219. Sahu T, Boisson B, Lacroix C, Bischoff E, Richier Q, Formaglio P, et al. ZIPCO, a putative metal ion transporter, is crucial for *Plasmodium* liver-stage development. EMBO Mol Med. 2014 Nov 25;6(11):1387–97.

220. Slavic K, Krishna S, Lahree A, Bouyer G, Hanson KK, Vera I, et al. A vacuolar iron-transporter homologue acts as a detoxifier in Plasmodium. Nat Commun. 2016 Apr 20;7(1):10403.

221. Sigala PA, Crowley JR, Hsieh S, Henderson JP, Goldberg DE. Direct Tests of

Enzymatic Heme Degradation by the Malaria Parasite Plasmodium falciparum. J Biol Chem. 2012 Nov;287(45):37793–807.

222. Gabay T, Ginsburg H. Hemoglobin Denaturation and Iron Release in Acidified Red Blood Cell Lysate-A Possible Source of Iron for Intraerythrocytic Malaria Parasites. Exp Parasitol. 1993 Nov;77(3):261–72.

223. Pollack S, Fleming J. Plasmodium falciparum takes up iron from transferrin. Br J Haematol. 1984 Oct;58(2):289–93.

224. Clark M, Fisher NC, Kasthuri R, Cerami Hand C. Parasite maturation and host serum iron influence the labile iron pool of erythrocyte stage Plasmodium falciparum. Br J Haematol. 2013;161(2):262–9.

225. Peto TE, Thompson JL. A reappraisal of the effects of iron and desferrioxamine on the growth of Plasmodium falciparum “in vitro”: the unimportance of serum iron. Br J Haematol. 1986 Jun;63(2):273–80.

226. Sanchez-Lopez R, Haldar K. A transferrin-independent iron uptake activity in Plasmodium falciparum-infected and uninfected erythrocytes. Mol Biochem Parasitol. 1992 Oct;55(1–2):9–20.

227. Muckenthaler MU, Rivella S, Hentze MW, Galy B. A Red Carpet for Iron Metabolism. Cell. 2017;168(3):344–61.

228. Leong YW, Lee EQH, Rénia L, Malleret B. Rodent Malaria Erythrocyte Preference Assessment by an Ex Vivo Tropism Assay. Front Cell Infect Microbiol. 2021;11(July):1–13.

229. Zhang DL, Wu J, Shah BN, Greutélaers KC, Ghosh MC, Ollivierre H, et al. Erythrocytic ferroportin reduces intracellular iron accumulation, hemolysis, and malaria risk. Science (80-). 2018 Mar 30;359(6383):1520–3.

230. Muriuki JM, Mentzer AJ, Band G, Gilchrist JJ, Carstensen T, Lule SA, et al. The ferroportin Q248H mutation protects from anemia, but not malaria or bacteremia. Sci Adv. 2019;5(9):1–13.

231. Medzhitov R, Schneider DS, Soares MP. Disease tolerance as a defense strategy. Science (80-). 2012;335(6071):936–41.

232. Martins R, Carlos AR, Braza F, Thompson JA, Bastos-Amador P, Ramos S, et al. Disease Tolerance as an Inherent Component of Immunity. Annu Rev Immunol. 2019;37:405–37.

233. Pamplona A, Ferreira A, Balla J, Jeney V, Balla G, Epiphanio S, et al. Heme oxygenase-1 and carbon monoxide suppress the pathogenesis of experimental cerebral malaria. Nat Med. 2007;13(6):703–10.

234. Seixas E, Gozzelino R, Chora Â, Ferreira A, Silva G, Larsen R, et al. Heme oxygenase-1 affords protection against noncerebral forms of severe malaria. Proc Natl Acad Sci U S A. 2009;106(37):15837–42.

235. Ramos S, Carlos AR, Sundaram B, Jeney V, Ribeiro A, Gozzelino R, et al. Renal control of disease tolerance to malaria. Proc Natl Acad Sci U S A. 2019;116(12):5681–6.

236. Ferreira A, Marguti I, Bechmann I, Jeney V, Chora Â, Palha NR, et al. Sickle hemoglobin confers tolerance to plasmodium infection. Cell. 2011;145(3):398–409.

237. Gozzelino R, Andrade BB, Larsen R, Luz NF, Vanoaica L, Seixas E, et al. Metabolic adaptation to tissue iron overload confers tolerance to malaria. Cell Host Microbe. 2012;12(5):693–704.

238. Wu Q, Sacomboio E, Souza LV de, Rui M, Cardoso S, Ademolue TW, et al. A Protective Inter-Organ Communication Response Against Life-Threatening Malarial

Anemia. bioRxiv. 2022;doi:10.1101/2022.01.12.475857.

239. van Swelm RPL, Wetzels JFM, Swinkels DW. The multifaceted role of iron in renal health and disease. Nat Rev Nephrol. 2020;16(2):77–98.

240. Arezes J, Foy N, McHugh K, Sawant A, Quinkert D, Terraube V, et al. Erythroferrone inhibits the induction of hepcidin by BMP6. Blood. 2018;132(14):1473–7.

241. Corradini E, Meynard D, Wu Q, Chen S, Ventura P, Pietrangelo A, et al. Serum and liver iron differently regulate the bone morphogenetic protein 6 (BMP6)-SMAD signaling pathway in mice. Hepatology. 2011 Jul;54(1):273–84.

242. Gao J, Chen J, De Domenico I, Koeller DM, Harding CO, Fleming RE, et al. Hepatocyte-targeted HFE and TFR2 control hepcidin expression in mice. Blood. 2010 Apr 22;115(16):3374–81.

243. de Menezes MN, Salles ÉM, Vieira F, Amaral EP, Zuzarte-Luís V, Cassado A, et al. IL-1α promotes liver inflammation and necrosis during blood-stage Plasmodium chabaudi malaria. Sci Rep. 2019;9(1):1–12.

244. Lelliott PM, McMorran BJ, Foote SJ, Burgio G. Erythrocytic iron deficiency enhances susceptibility to Plasmodium chabaudi infection in mice carrying a missense mutation in transferrin receptor 1. Infect Immun. 2015;83(11):4322–34.

245. Fu Y, Tilley L, Kenny S, Klonis N. Dual labeling with a far red probe permits analysis of growth and oxidative stress in P. falciparum -infected erythrocytes. Cytom Part A. 2010;9999A:NA-NA.

246. Brugat T, Cunningham D, Sodenkamp J, Coomes S, Wilson M, Spence PJ, et al. Sequestration and histopathology in Plasmodium chabaudi malaria are influenced by the immune response in an organ-specific manner. Cell Microbiol. 2014;16(5):687–700.

247. Baazim H, Antonio-Herrera L, Bergthaler A. The interplay of immunology and cachexia in infection and cancer. Nat Rev Immunol. 2021;0123456789.

248. Cumnock K, Gupta AS, Lissner M, Chevee V, Davis NM, Schneider DS. Host Energy Source Is Important for Disease Tolerance to Malaria. Curr Biol. 2018;28(10):1635-1642.e3.

249. Ramos S, Ademolue TW, Jentho E, Wu Q, Guerra J, Martins R, et al. A hypometamobilc defense strategy against Plasmodium infection. bioRxiv. 2021;doi:10.1101/2021.09.08.459402.

250. Wang A, Huen SC, Luan HH, Baker K, Rinder H, Booth CJ, et al. Glucose metabolism mediates disease tolerance in cerebral malaria. Proc Natl Acad Sci U S A. 2018;115(43):11042–7.

251. Wyart E, Hsu MY, Sartori R, Mina E, Rausch V, Pierobon ES, et al. Iron supplementation is sufficient to rescue skeletal muscle mass and function in cancer cachexia. 2022;1–18.

252. Zhao H, Konishi A, Fujita Y, Yagi M, Ohata K, Aoshi T, et al. Lipocalin 2 bolsters innate and adaptive immune responses to blood-stage malaria infection by reinforcing host iron metabolism. Cell Host Microbe. 2012;12(5):705–16.

253. Azcárate IG, Sánchez-Jaut S, Marín-García P, Linares M, Pérez-Benavente S, García-Sánchez M, et al. Iron supplementation in mouse expands cellular innate defences in spleen and defers lethal malaria infection. Biochim Biophys Acta - Mol Basis Dis. 2017;1863(12):3049–59.

254. Van Den Ham KM, Shio MT, Rainone A, Fournier S, Krawczyk CM, Olivier M. Iron prevents the development of experimental cerebral malaria by attenuating CXCR3-mediated T cell chemotaxis. PLoS One. 2015;10(3):1–20.

255. Bundi CK, Nalwoga A, Lubyayi L, Muriuki JM, Mogire RM, Opi H, et al. Iron Deficiency Is Associated with Reduced Levels of Plasmodium falciparum-specific Antibodies in African Children. Clin Infect Dis. 2021;73(1):43–9.

256. Tchum SK, Sakyi SA, Adu B, Arthur F, Oppong FB, Dzabeng F, et al. Impact of IgG response to malaria-specific antigens and immunity against malaria in pre-school children in Ghana. A cluster randomized, placebo-controlled trial. PLoS One. 2021;16(7 July):1–13.

257. Deroost K, Alder C, Hosking C, McLaughlin S, Lin J-W, Lewis MD, et al. Tissue macrophages and interferon-gamma signalling control blood-stage Plasmodium chabaudi infections derived from mosquito-transmitted parasites. Curr Res Immunol. 2021;2(July):104–19.

258. del Portillo HA, Ferrer M, Brugat T, Martin-Jaular L, Langhorne J, Lacerda MVG. The role of the spleen in malaria. Cell Microbiol. 2012;14(3):343–55.

259. Guilliams M, Mildner A, Yona S. Developmental and Functional Heterogeneity of Monocytes. Immunity. 2018;49(4):595–613.

260. Hirako IC, Assis PA, Galvão-Filho B, Luster AD, Antonelli LR, Gazzinelli RT. Monocyte-derived dendritic cells in malaria. Curr Opin Microbiol. 2019;52(Who 2017):139–50.

261. Stephens R, Langhorne J. Effector memory Th1 CD4 T cells are maintained in a mouse model of chronic malaria. PLoS Pathog. 2010;6(11).

262. Saravia J, Chapman NM, Chi H. Helper T cell differentiation. Cell Mol Immunol. 2019;16(7):634–43.

263. Chen X, Bäumel M, Männel DN, Howard OMZ, Oppenheim JJ. Interaction of TNF with TNF receptor type 2 promotes expansion and function of mouse CD4+CD25+ T regulatory cells. J Immunol. 2007 Jul 1;179(1):154–61.

264. Liu T, Soong L, Liu G, König R, Chopra AK. CD44 expression positively correlates with Foxp3 expression and suppressive function of CD4+ Treg cells. Biol Direct. 2009 Dec 23;4(1):40.

265. Roco JA, Mesin L, Binder SC, Nefzger C, Gonzalez-Figueroa P, Canete PF, et al. Class-Switch Recombination Occurs Infrequently in Germinal Centers. Immunity. 2019;51(2):337-350.e7.

266. Nutt SL, Hodgkin PD, Tarlinton DM, Corcoran LM. The generation of antibody-secreting plasma cells. Nat Rev Immunol. 2015;15(3):160–71.

267. Salmerón A, Borroto A, Fresno M, Crumpton MJ, Ley SC, Alarcón B. Transferrin receptor induces tyrosine phosphorylation in T cells and is physically associated with the TCR zeta-chain. J Immunol. 1995 Feb 15;154(4):1675–83.

268. Regis G, Bosticardo M, Conti L, De Angelis S, Boselli D, Tomaino B, et al. Iron regulates T-lymphocyte sensitivity to the IFN- /STAT1 signaling pathway in vitro and in vivo. Blood. 2005 Apr 15;105(8):3214–21.

269. Scharer CD, Barwick BG, Guo M, Bally APR, Boss JM. Plasma cell differentiation is controlled by multiple cell division-coupled epigenetic programs. Nat Commun. 2018;9(1).

270. Su Z, Fortin A, Gros P, Stevenson MM. Opsonin-independent phagocytosis: An effector mechanism against acute blood-stage Plasmodium chabaudi AS infection. J Infect Dis. 2002;186(9):1321–9.

271. Orago AS, Facer CA. Cytotoxicity of human natural killer (NK) cell subsets for Plasmodium falciparum erythrocytic schizonts: stimulation by cytokines and inhibition

by neomycin. Clin Exp Immunol. 1991 Oct;86(1):22–9.

272. Kim CC, Parikh S, Sun JC, Myrick A, Lanier LL, Rosenthal PJ, et al. Experimental malaria infection triggers early expansion of natural killer cells. Infect Immun. 2008 Dec;76(12):5873–82.

273. Knackstedt SL, Georgiadou A, Apel F, Abu-Abed U, Moxon CA, Cunnington AJ, et al. Neutrophil extracellular traps drive inflammatory pathogenesis in malaria. Sci Immunol. 2019;4(40):1–18.

274. Littwitz-Salomon E, Moreira D, Frost JN, Choi C, Liou KT, Ahern DK, et al. Metabolic requirements of NK cells during the acute response against retroviral infection. Nat Commun. 2021;12(1):152–60.

275. Pfeifhofer-Obermair C, Tymoszuk P, Nairz M, Schroll A, Klais G, Demetz E, et al. Regulation of Th1 T Cell Differentiation by Iron via Upregulation of T Cell Immunoglobulin and Mucin Containing Protein-3 (TIM-3). Front Immunol. 2021;12(May):1–11.

276. Yoshimoto T, Takahama Y, Wang CR, Yoneto T, Waki S, Nariuchi H. A pathogenic role of IL-12 in blood-stage murine malaria lethal strain Plasmodium berghei NK65 infection. J Immunol. 1998;160(11):5500–5.

277. Oakley MS, Sahu BR, Lotspeich-Cole L, Solanki NR, Majam V, Pham PT, et al. The Transcription Factor T-bet Regulates Parasitemia and Promotes Pathogenesis during Plasmodium berghei ANKA Murine Malaria . J Immunol. 2013;191(9):4699–708.

278. Kurup SP, Obeng-Adjei N, Anthony SM, Traore B, Doumbo OK, Butler NS, et al. Regulatory T cells impede acute and long-term immunity to blood-stage malaria through CTLA-4. Nat Med. 2017 Oct 11;23(10):1220–5.

279. Yao Y, Chen Z, Zhang H, Chen C, Zeng M, Yunis J, et al. Selenium–GPX4 axis protects follicular helper T cells from ferroptosis. Nat Immunol. 2021;22(9):1127–39.

280. Waters LR, Ahsan FM, Wolf DM, Shirihai O, Teitell MA. Initial B Cell Activation Induces Metabolic Reprogramming and Mitochondrial Remodeling. iScience. 2018;5:99–109.

281. Jang KJ, Mano H, Aoki K, Hayashi T, Muto A, Nambu Y, et al. Mitochondrial function provides instructive signals for activation-induced B-cell fates. Nat Commun. 2015;6:1–13.

282. Zhang S, Pruitt M, Tran D, Du Bois W, Zhang K, Patel R, et al. B Cell-Specific Deficiencies in mTOR Limit Humoral Immune Responses. J Immunol. 2013;191(4):1692–703.

283. Raybuck AL, Cho SH, Li J, Rogers MC, Lee K, Williams CL, et al. B Cell–Intrinsic mTORC1 Promotes Germinal Center–Defining Transcription Factor Gene Expression, Somatic Hypermutation, and Memory B Cell Generation in Humoral Immunity. J Immunol. 2018 Apr 15;200(8):2627–39.

284. Vijay R, Guthmiller JJ, Sturtz AJ, Surette FA, Rogers KJ, Sompallae RR, et al. Infection-induced plasmablasts are a nutrient sink that impairs humoral immunity to malaria. Nat Immunol. 2020 May 18;21(7):790–801.

285. McLean E, Cogswell M, Egli I, Wojdyla D, De Benoist B. Worldwide prevalence of anaemia, WHO Vitamin and Mineral Nutrition Information System, 1993-2005. Public Health Nutr. 2009;12(4):444–54.

286. Hill DL, Carr EJ, Rutishauser T, Moncunill G, Campo JJ, Innocentin S, et al. Immune system development varies according to age, location, and anemia in African children. Sci Transl Med. 2020;12(529).

287. Bustamante LY, Bartholdson SJ, Bei AK, Theron M, Uchikawa M. Basigin is a receptor essential for erythrocyte invasion by Plasmodium falciparum. 2011;4–8.

288. Douglas AD, Williams AR, Illingworth JJ, Kamuyu G, Biswas S, Goodman AL, et al. The blood-stage malaria antigen PfRH5 is susceptible to vaccine-inducible cross-strain neutralizing antibody. Nat Commun. 2011;2(1).

289. Douglas AD, Baldeviano GC, Lucas CM, Lugo-Roman LA, Crosnier C, Bartholdson SJ, et al. A PfRH5-based vaccine is efficacious against heterologous strain blood-stage plasmodium falciparum infection in Aotus monkeys. Cell Host Microbe. 2015;17(1):130–9.

290. Payne RO, Silk SE, Elias SC, Miura K, Diouf A, Galaway F, et al. Human vaccination against RH5 induces neutralizing antimalarial antibodies that inhibit RH5 invasion complex interactions. JCI Insight. 2017;2(21).

291. Huang BW, Pearman E, Kim CC. Mouse Models of Uncomplicated and Fatal Malaria. Bio-protocol. 2015;5(13):1–14.

292. Kaslow DC, Biernaux S. RTS, S: Toward a first landmark on the Malaria Vaccine Technology Roadmap. Vaccine. 2015;33(52):7425–32.

293. Lal AA, de la Cruz VF, Welsh JA, Charoenvit Y, Maloy WL, McCutchan TF. Structure of the gene encoding the circumsporozoite protein of Plasmodium yoelii. A rodent model for examining antimalarial sporozoite vaccines. J Biol Chem. 1987 Mar 5;262(7):2937–40.

294. Arun Kumar K, Sano G, Boscardin S, Nussenzweig RS, Nussenzweig MC, Zavala F, et al. The circumsporozoite protein is an immunodominant protective antigen in irradiated sporozoites. Nature. 2006 Dec 6;444(7121):937–40.

295. Weiss WR, Mellouk S, Houghten RA, Sedegah M, Kumar S, Good MF, et al. Cytotoxic T cells recognize a peptide from the circumsporozoite protein on malaria-infected hepatocytes. J Exp Med. 1990 Mar 1;171(3):763–73.

296. Kumar S, Miller LH, Quakyi IA, Keister DB, Houghten RA, Maloy WL, et al. Cytotoxic T cells specific for the circumsporozoite protein of Plasmodium falciparum. Nature. 1988 Jul;334(6179):258–60.

297. Singh AP, Buscaglia CA, Wang Q, Levay A, Nussenzweig DR, Walker JR, et al. Plasmodium Circumsporozoite Protein Promotes the Development of the Liver Stages of the Parasite. Cell. 2007 Nov;131(3):492–504.

298. Rodrigues EG, Zavala F, Eichinger D, Wilson JM, Tsuji M. Single immunizing dose of recombinant adenovirus efficiently induces CD8+ T cell-mediated protective immunity against malaria. J Immunol. 1997 Feb 1;158(3):1268–74.

299. Hodgson SH, Ewer KJ, Bliss CM, Edwards NJ, Rampling T, Anagnostou NA, et al. Evaluation of the efficacy of ChAd63-MVA vectored vaccines expressing circumsporozoite protein and ME-TRAP against controlled human malaria infection in malaria-naive individuals. J Infect Dis. 2015;211(7):1076–86.

300. Chuang I, Sedegah M, Cicatelli S, Spring M, Polhemus M, Tamminga C, et al. DNA Prime/Adenovirus Boost Malaria Vaccine Encoding P. falciparum CSP and AMA1 Induces Sterile Protection Associated with Cell-Mediated Immunity. PLoS One. 2013;8(2).

301. Kollmann TR. Variation between populations in the innate immune response to vaccine adjuvants. Front Immunol. 2013;4(APR):1–11.

302. Tatsis N, Fitzgerald JC, Reyes-Sandoval A, Harris-McCoy KC, Hensley SE, Zhou D, et al. Adenoviral vectors persist in vivo and maintain activated CD8+ T cells: Implications for their use as vaccines. Blood. 2007;110(6):1916–23.

303. Kurosaki T, Kometani K, Ise W. Memory B cells. Nat Rev Immunol. 2015 Mar 13;15(3):149–59.

304. Weisel FJ, Mullett SJ, Elsner RA, Menk A V., Trivedi N, Luo W, et al. Germinal center B cells selectively oxidize fatty acids for energy while conducting minimal glycolysis. Nat Immunol. 2020;21(3):331–42.

305. Lam WY, Bhattacharya D. Metabolic Links between Plasma Cell Survival, Secretion, and Stress. Trends Immunol. 2018;39(1):19–27.

306. Pengo N, Scolari M, Oliva L, Milan E, Mainoldi F, Raimondi A, et al. Plasma cells require autophagy for sustainable immunoglobulin production. Nat Immunol. 2013;14(3):298–305.

307. Howden AJM, Hukelmann JL, Brenes A, Spinelli L, Sinclair L V., Lamond AI, et al. Quantitative analysis of T cell proteomes and environmental sensors during T cell differentiation. Nat Immunol. 2019;20(11):1542–54.

308. Portugal S, Carret C, Recker M, Armitage AE, Gonçalves LA, Epiphanio S, et al. Host-mediated regulation of superinfection in malaria. Nat Med. 2011;17(6):732–7.

309. Wade J, Byrne DJ, Ballentine CJ, Drakesmith H. Temporal variation of planetary iron as a driver of evolution. Proc Natl Acad Sci U S A. 2021;118(51):1–8.

310. Posey JE, Gherardini FC. Lack of a Role for Iron in the Lyme Disease Pathogen. Science (80-). 2000 Jun 2;288(5471):1651–3.

311. Bruyneel B, vande Woestyne M, Verstraete W. Lactic acid bacteria: Micro-organisms able to grow in the absence of available iron and copper. Biotechnol Lett. 1989 Jun;11(6):401–6.

312. Rametta R, Meroni M, Dongiovanni P. From Environment to Genome and Back: A Lesson from HFE Mutations. Int J Mol Sci. 2020 May 15;21(10):3505.

313. Distante S, Robson KJH, Graham-Campbell J, Arnaiz-Villena A, Brissot P, Worwood M. The origin and spread of the HFE-C282Y haemochromatosis mutation. Hum Genet. 2004;115(4):269–79.

314. Carter R, Mendis KN. Evolutionary and historical aspects of the burden of malaria. Clin Microbiol Rev. 2002;15(4):564–94.

315. Kariuki SN, Williams TN. Human genetics and malaria resistance. Hum Genet. 2020;139(6–7):801–11.

316. Loy DE, Liu W, Li Y, Learn GH, Plenderleith LJ, Sundararaman SA, et al. Out of Africa: origins and evolution of the human malaria parasites Plasmodium falciparum and Plasmodium vivax. Int J Parasitol. 2017;47(2–3):87–97.

317. White NJ. Antimalarial drug resistance. J Clin Invest. 2004 Apr 15;113(8):1084–92.

318. Smith MR, Myers SS. Impact of anthropogenic CO2 emissions on global human nutrition. Nat Clim Chang. 2018;8(9):834–9.

319. El-Sayed A, Kamel M. Climatic changes and their role in emergence and re-emergence of diseases. Environ Sci Pollut Res. 2020 Jun 28;27(18):22336–52.

320. Råberg L, Sim D, Read AF. Disentangling Genetic Variation for Resistance and Tolerance to Infectious Diseases in Animals. Science (80-). 2007 Nov 2;318(5851):812–4.

321. Gonçalves BP, Huang C-Y, Morrison R, Holte S, Kabyemela E, Prevots DR, et al. Parasite Burden and Severity of Malaria in Tanzanian Children. N Engl J Med. 2014 May 8;370(19):1799–808.

322. Gupta S, Snow RW, Donnelly CA, Marsh K, Newbold C. Immunity to non-cerebral

severe malaria is acquired after one or two infections. Nat Med. 1999;5(3):340–3.

323. Akpogheneta OJ, Duah NO, Tetteh KKA, Dunyo S, Lanar DE, Pinder M, et al. Duration of Naturally Acquired Antibody Responses to Blood-Stage Plasmodium falciparum Is Age Dependent and Antigen Specific. Infect Immun. 2008 Apr;76(4):1748–55.

324. Weiss GE, Crompton PD, Li S, Walsh LA, Moir S, Traore B, et al. Atypical Memory B Cells Are Greatly Expanded in Individuals Living in a Malaria-Endemic Area. J Immunol. 2009 Aug 1;183(3):2176–82.

325. Weiss GE, Clark EH, Li S, Traore B, Kayentao K, Ongoiba A, et al. A Positive Correlation between Atypical Memory B Cells and Plasmodium falciparum Transmission Intensity in Cross-Sectional Studies in Peru and Mali. Diemert DJ, editor. PLoS One. 2011 Jan 14;6(1):e15983.

326. Bryce J, Boschi-Pinto C, Shibuya K, Black RE. WHO estimates of the causes of death in children. Lancet. 2005;365(9465):1147–52.

327. Prendergast AJ. Malnutrition and vaccination in developing countries. Philos Trans R Soc B Biol Sci. 2015 Jun 19;370(1671):20140141.

328. Pasricha SR, Drakesmith H. Iron Deficiency Anemia: Problems in Diagnosis and Prevention at the Population Level. Hematol Oncol Clin North Am. 2016;30(2):309–25.

329. Gera T, Sachdev HPS. Effect of iron supplementation on incidence of infectious illness in children: systematic review. BMJ. 2002 Nov 16;325(7373):1142–1142.

330. Stoffel NU, Zeder C, Brittenham GM, Moretti D, Zimmermann MB. Iron absorption from supplements is greater with alternate day than with consecutive day dosing in iron-deficient anemic women. Haematologica. 2020 May;105(5):1232–9.

331. Arnold J, Murera D, Arbogast F, Fauny J-D, Muller S, Gros F. Autophagy is dispensable for B-cell development but essential for humoral autoimmune responses. Cell Death Differ. 2016 May 20;23(5):853–64.

332. Teague BN, Pan Y, Mudd PA, Nakken B, Zhang Q, Szodoray P, et al. Cutting Edge: Transitional T3 B Cells Do Not Give Rise to Mature B Cells, Have Undergone Selection, and Are Reduced in Murine Lupus. J Immunol. 2007 Jun 15;178(12):7511–5.

333. Chen K, Liu J, Heck S, Chasis JA, An X, Mohandas N. Resolving the distinct stages in erythroid differentiation based on dynamic changes in membrane protein expression during erythropoiesis. Proc Natl Acad Sci. 2009 Oct 13;106(41):17413–8.